Molecular Mediators of Mammographic Density

Submitted in partial fulfilment for the requirements of the degree of Doctor of Philosophy

Alastair J Ironside, MRes, MBBS (Hons)

Queen Mary University of London

2017

Statement of originality

I, Alastair James Ironside, confirm that the research included within this thesis is my own work or that where it has been carried out in collaboration with, or supported by others, that it is duly acknowledged below and my contribution indicated. Previously published material is also acknowledged below.

I attest that I have exercised reasonable care to ensure that the work is original, and does not to the best of my knowledge break any UK law, infringe any third party's copyright or other Intellectual Property Right, or contain any confidential material.

I accept that the college has the right to use plagiarism detection software to check the electronic version of the thesis.

I confirm that this thesis has not been previously submitted for the award of a degree by this or any other university.

The copyright of this thesis rests with the author and no quotation from it or information derived from it may be published without the prior written consent of the author.

Signature:

Date:

Details of work carried out by others:

1. Primary breast fibroblasts were isolated by Dr Jenny Gomm, Dr Linda Haywood and Mr Iain Goulding, Breast Research group, Centre for Tumour Biology, Barts Cancer Institute, London, UK

2. Paraffin embedding of collagen gels and cutting of sections was performed by Dr George Elia, Core Pathology Lab, Barts Cancer Institute, London, UK

3. Cutting of sections was performed by Dr Reema Paudel, Centre for Tumour Biology, Barts Cancer Institute, London, UK

Details of collaborations:

1. Collaboration with Professor Claude Chelala and Dr Jun Wang, Bioinformatics group, Centre for Molecular Oncology and Imaging, Barts Cancer Institute, London, UK

Professor Chelala and Dr Wang performed the differential gene expression analysis, pathway analysis and merger of the pilot and follow up RNA Seq datasets. Discussions

with the group also assisted in the RNA Seq experiment design and interpretation of the analysis.

2. Collaboration with Dr Marc Poirot and Dr Sandrine Silvente-Poirot, Sterol metabolism and therapeutic innovation group, Toulouse Centre for Cancer Research, Toulouse, France

   In conjunction with Dr Antonin Lamaziere, Laboratory of mass Spectrometry, Sorbonne University- University Pierre and Marie Curie, Paris, France

Dr Marc Poirot and Dr Sandrine Silvente-Poirot performed the mass spectrometry sterol analysis on frozen fibroblast cell pellets treated with different drug regimens, with the assistance of Dr Antonin Lemaziere.

Dr Marc Poirot and Dr Sandrine Silvente-Poirot performed transmission electron microscopy imaging of pre-fixed fibroblasts treated with different drug regimens. Discussions with the group also assisted with interpretation of the RNA Seq data and validation experiment design.

3. HB2 cells and HB2 cells overexpressing Her2 were a kind gift from Professor Valerie Speirs, University of Leeds, UK. The cells were originally obtained from Dr Fedor Berdichevski, University of Birmingham, UK

Published material contained in this thesis:

Ironside, A.J. and J.L. Jones, Stromal characteristics may hold the key to mammographic density: The evidence to date. Oncotarget, 2016 (Epub ahead of print).

This work was funded by a Medical Research Council (MRC) Clinical Research Training Fellowship MR/L002213/1

Abstract

Introduction

Mammographic density (MD), created predominantly by increased stromal tissue, is a major breast cancer risk factor, though little is known about the biological mechanisms mediating it.

Tamoxifen prevents breast cancer in a subset of high risk women via mechanisms that appear dependent on reduction of MD. Animal models suggest tamoxifen remodels the mammary stroma to a tumour-inhibitory phenotype. This study aims to analyse the effect of tamoxifen on human breast fibroblast function and identify pro-tumourigenic pathways contributing to density-associated risk.

Methods

Primary human breast fibroblasts from normal, high risk or breast cancer patients were treated with hydroxytamoxifen (100nM-5μM). Fibroblast function was analysed by measuring: proliferation, expression of stromal proteins fibronectin and collagen 1; effects on TGF-β signalling and up-regulation of myofibroblast marker SMA. Genome wide analysis was performed using RNA-Seq. Significantly deregulated pathways were validated by PCR, western blotting and mass spectrometry.

Results

Fibroblasts from 23 patients were treated with hydroxytamoxifen. All patients showed reduced proliferation with treatment. 62% of patients showed reduced fibronectin expression. TGF- β-mediated up-regulation of SMA and fibronectin were consistently inhibited by tamoxifen.

RNA-Seq analysis revealed down-regulation of Wnt signalling, an established pro-fibrogenic and pro-tumourigenic pathway. In addition, there was significant modulation of many metabolic pathways, including components of the microsomal anti-oestrogen binding site (AEBS).

Binding of tamoxifen to the AEBS inhibits cholesterol epoxide hydrolase (ChEH) enzyme activity, promoting an anti-tumourigenic phenotype. The effects of tamoxifen on fibroblasts could be partly replicated using tesmilifene, a commercially available

inhibitor of ChEH. Mass spectrometry analysis confirmed an altered cholesterol metabolite profile in tamoxifen treated fibroblasts.

Conclusion

These data indicate that tamoxifen can directly remodel the mammary stromal microenvironment, generating a less ‘reactive’ stroma. Thus, tamoxifen impacts on multiple pathways, many independent of the oestrogen receptor, to create a tumour-inhibitory microenvironment. This offers exciting potential for patient monitoring and alternative breast cancer prevention strategies.

Table of Contents

List of Figures

List of Tables

List of Abbreviations

4-OHTam	4-hydroxytamoxifen
8DHC	8-dehydrocholesterol
7DHC	7-dehydrocholesterol
ABC	ATP-binding cassette
ADAMTS1	ADAM metallopeptidase with thrombospondin type 1 motif
ADH	Atypical ductal hyperplasia
AEBS	Anti-oestrogen binding site
AI	Aromatase inhibitor
AKT	Active protein kinase B
AMH	Anti-Müllerian hormone
ANOVA	Analysis of variance
AU	Arbitrary Unit
bFGF	Basic fibroblast growth factor
BCN	Breast Cancer Now
BCI	Barts Cancer Institute
BMI	Body mass index
BMP	Bone morphogenic proteins
BSA	Bovine serum albumin
BRCA1/2	Breast cancer 1/2 gene
CAF	Cancer associated fibroblast
CAV-1	Caveolin 1
CB1/2	Cannabinoid receptor 1/2
CCL	c-c motif chemokine ligand
CDH1	E Cadherin
ChEH	Cholesterol epoxide hydrolase

COX	Cyclo-oxygenase
CRP	C-reactive protein
CT	Cholestane triol
CYP19	Aromatase
CYP2D6	Cytochrome P450 2D6
CYP3A4/5	Cytochrome P450 3A4/5
dH_20	distilled water
D8D71	3β-hydroxysteroid-Δ8Δ7-isomerase
DCIS	Ductal carcinoma in situ
DCSS	Double charcoal stripped foetal bovine serum
DDA	Dendrogenin A
DHCR7	7-dehydrocholesterol reductase
DHCR24	24-dehydrocholesterol reductase
DMSO	Dimethyl sulphoxide
DPPE	Tesmilifene
E2	17-β oestradiol
EC	Cholesterol epoxide/epoxy-cholesterol
ECM	Extra-cellular matrix
EDTA	Ethylenediaminetetraacetic acid
EMT	Epithelial to mesenchymal transition
ER	Oestrogen receptor
ERK	Extracellular signal-regulated kinase
FAK	Focal adhesion kinase
FAP	Fibroblast activation protein
FBS	Foetal bovine serum
FC	Fold change

FCM	Fibrobast conditioned media
FDM	Fibroblast derived matrix
FDR	False discovery rate
FGF	Fibroblast growth factor
FN	Fibronectin
FSP1	Fibroblast specific protein 1
GC	Gas chromatography
GDF	Growth and differentiation factors
GSEA	Gene set enrichment analysis
H+E	Haematoxylin and Eosin
Her2	Human epidermal growth factor receptor 2
HGF	Hepatocyte growth factor
HRP	Horse radish peroxidase
HRT	Hormone replacement therapy
HOXA9	Homeobox A9
IBIS	International breast cancer intervention study
IgG	Immunoglobulin
IGF	Insulin-like growth factor
IKKβ	IκB-kinase-β
IL-6	Interleukin six
LI	Lobular involution
LDL	Low density lipoprotein
LXR	Liver X receptor
JNK-1	c-Jun N-terminal kinase 1
LDH	Lactate dehydrogenase
LOX	Lysyl oxidase

LOXL	Lysyl oxidase-like
miR	Micro RNA
MD	Mammographic density
MDS	Multidimensional scaling
MLB	Multilamellar bodies
MMP	Matrix metalloproteinase
MRI	Magnetic resonance imaging
NBF	Neutral buffered formalin
NGAL	Neutrophil gelatinase-associated lipocalin
NHSBCSP	National Health Service Breast Cancer Screening Programme
NICE	National Institute for Clinical Excellence
p21	Cyclin-dependent kinase inhibitor 1
p53	Tumour protein p53
PBS	Phosphate buffered saline
PBST	Phosphate buffered saline and tween 20
PCA	Principle component analysis
PDGFRα/β	Platelet derived growth factor receptor alpha/beta
PHD2	Prolyl hydroxylase domain protein 2
PI3K	Phosphoinositide 3-kinase
PIK3CA	Phosphatidylinositol-4,5-bisphosphate 3-kinase, catalytic subunit alpha
PIP2	Phosphatidylinositol 4,5-bisphosphate
PIP3	Phosphatidylinositol (3,4,5)-trisphosphate
PPAR	Peroxisome proliferator-activated receptor
PR	Progesterone receptor
PTEN	Phosphatase and tensin homologue
qRT-PCR	Quantitative real-time polymerase chain reaction

Rho	Rho GTPase
RIPA	Radioimmunoprecipitation assay
ROCK	Rho-associated coiled-coil-containing protein kinase
ROS	Reactive oxygen species
RT	Room temperature
SARA	SMAD anchor for receptor activation
SDF-1	Stromal derived factor 1
SDS	Sodium dodecyl sulphate
SDS-PAGE	SDS-Polyacrylamide gel electrophoresis
SEER	Surveillance, Epidemiology and End Results
SERM	Selective oestrogen receptor modulator
siRNA	Small interfering RNA
SMA	Alpha smooth muscle actin
SNP	Single nucleotide polymorphism
SREBP	Steroid response element binding proteins
STK11	Serine/threonine kinase 11
TACS	Tumour associated collagen signatures
TDLU	Terminal duct lobular unit
TEM	Transmission electron microscopy
TGF-β	Transforming growth factor beta
TIMP	Tissue inhibitor of metalloproteinase
TP53	Tumour protein p53
TNF	Tumour necrosis factor
VEGF	Vascular endothelial growth factor
VEGFR	Vascular endothelial growth factor receptor

WISP1 Wnt1 inducing signalling pathway protein 1

Acknowledgements

I have many people to thank for their support, without which this work would not have been possible.

Firstly, my supervisor Professor Louise Jones has been an incredible source of support and guidance throughout my PhD. Her enthusiasm and passion for science initially inspired me to undertake a PhD and continues to inspire me to undertake academic research in my future career. Undertaking this PhD has allowed to participate in a wealth of other academic activities outside of the lab and I am extremely grateful for these opportunities. It has been an immense privilege to work with someone with such fantastic vision and whose leadership inspires such dedication and commitment amongst her team. Thank you so much for everything.

My second supervisor, Professor Claude Chelala and Dr Jun Wang have been an enormous help in analysing the sequencing data from this project. The results from their analysis have been critical in directing the entire focus of this project. I have also benefited immensely from the exposure to publically available resources for mining data and basic bioinformatics analysis.

Our colleagues in Toulouse, Dr Marc Poirot and Dr Sandrine Silvente-Poirot have been fantastic collaborators and provided invaluable expertise on the role of cholesterol metabolism in breast cancer biology. The sterol quantification analysis and electron microscopy work they completed in conjunction with Dr Antonin Lamaziere have been crucial to allowing me to complete this work.

I also owe a huge debt of gratitude to the other members of the Breast Group. Firstly thank you to my wonderful mentors in primary cell culture, Dr Jenny Gomm and Dr Linda Haywood, for such excellent training, keeping me continually stocked up with a supply of primary fibroblasts and making the tiny Cat 2 room such an enjoyable, if space limited, place to work. Many thanks also to Mr Iain Goulding for also helping to supply fibroblasts and his patience with the multiple requests for retrieving clinical data for my samples.

A big thank you to Dr Mike Allen for his advice with planning experiments, troubleshooting problems in the lab, unique analysis of current affairs and sci-fi/gaming related discussions. Many thanks to Dr Sally Dreger for her tuition in various laboratory techniques, inspirational fancy dress ideas, limitless supply of cake and impressive demonstrations on how to keep 200 first year undergraduate students under control.

Thanks to Dr Sally Smith for helping to identify suitable cases for the project, allowing me to maintain my cut up skills during my research time and for her London theatre, restaurant and holiday recommendations.

Many thanks to Miss Rachel Nelan the RNA 'guru' for her advice on RNA extraction, preparation of samples for sequencing, daily coffee shop visits and in depth insider knowledge of the UK and European festival and clubbing scenes. Thanks very much to my fellow PhD students Miss Mary Kate Hayward, Miss Natalie Allen and Dr Kathryn Hawkesford for their support following experimental failures, fashion advice, lessons in social media etiquette and wedding planning tips.

A big thanks also to Dr Reema Paudel for her assistance with cutting sections, reacquainting me with Nepalese and Tibetan momos and invaluable support with the tissue study which has allowed me to have the time to write up this thesis. Finally a big thank you to Dr Adrienne Morgan for her tuition in immunocytochemistry, introducing me to the value of patient and public involvement in research, advice on political activism and the local eating and drinking establishments of Clerkenwell.

I would also like to thank various other members of the Tumour Biology laboratory including Dr George Elia for his tuition in immunohistochemistry and support with paraffin embedding and cutting tissue sections. Many thanks to Dr Linda Hammond for training me to use the confocal and Axiophot microscopes. Thanks also to Dr Ed Carter and Miss Zareen Khan for their help with preparing collagen gels for 3D cell culture and performing the gel contraction assay.

Many thanks to Professor John Marshall and Dr John Connelly for their input discussing the project progress at my 9 and 18 month assessments. Thanks also to Professor Valerie Speirs who kindly supplied the normal HB2 cells and the HB2 cells overexpressing Her2.

Finally, a huge thank you to John for your continual support, understanding and tolerance of weekends and evenings spent in the lab over the past three years and to the rest of my friends and family for their support and encouragement.

1 Introduction

1.1 Biology of the normal breast

The adult breast is a tear shaped gland which sits anteriorly on the chest wall on top of the pectoralis major muscle. It extends horizontally from the edge of the sternum to the mid axillary line. A small portion of breast tissue extends into the axilla itself as the tail of Spence [1]. The breast shows considerable variation in size and shape between individuals.

The structure of the breast is adapted to the production of milk (lactation) following pregnancy and childbirth. The epithelial component consists of a branching network of ducts ending in a terminal duct lobular unit (TDLU) [1]. The terminal duct branches into clusters of small, highly specialised acini to form a lobule (Figure 1).

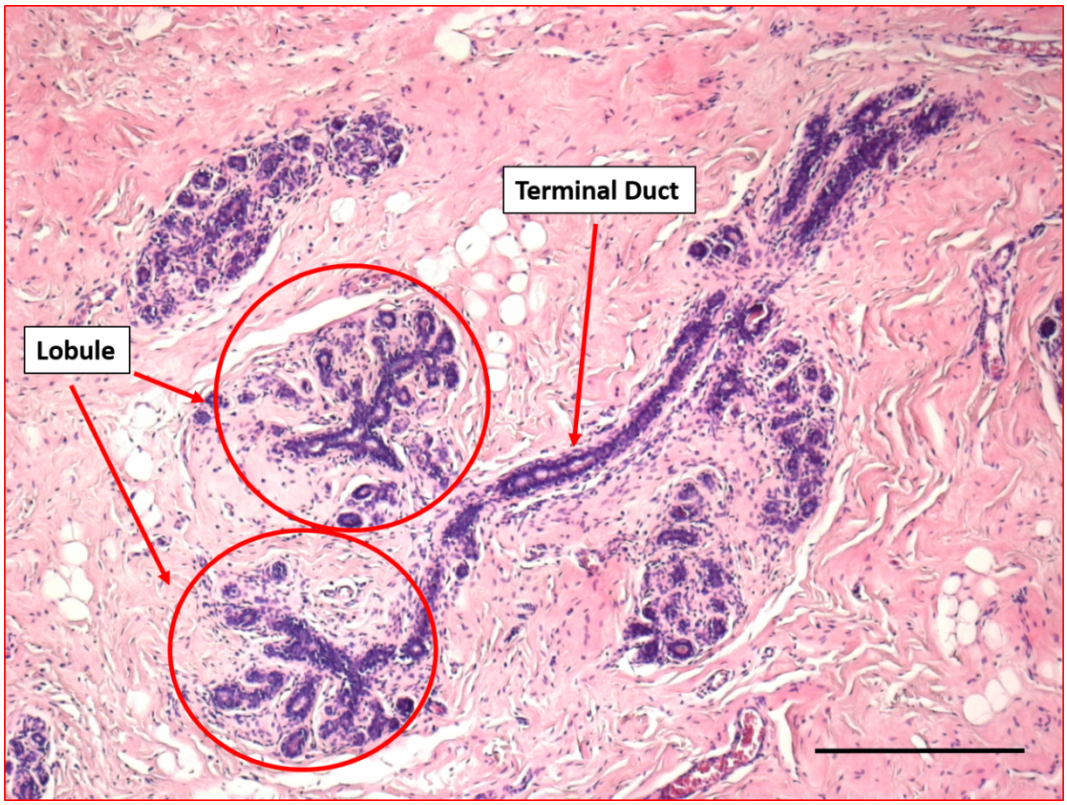

Figure 1: Terminal duct lobular unit (TDLU) of the breast. Multiple specialised lobules branch from the terminal duct. Haematoxylin and Eosin (H+E) stained section x4 objective. Scale bar = 1mm.

The ducts and lobules are lined by two types of epithelial cells; an inner luminal epithelial cell layer which secretes the milk proteins, and an outer myoepithelial cell layer with associated basement membrane [2]. The myoepithelial cells have contractile properties to facilitate milk protein secretion and synthesise the basement membrane components [2] (Figure 2).

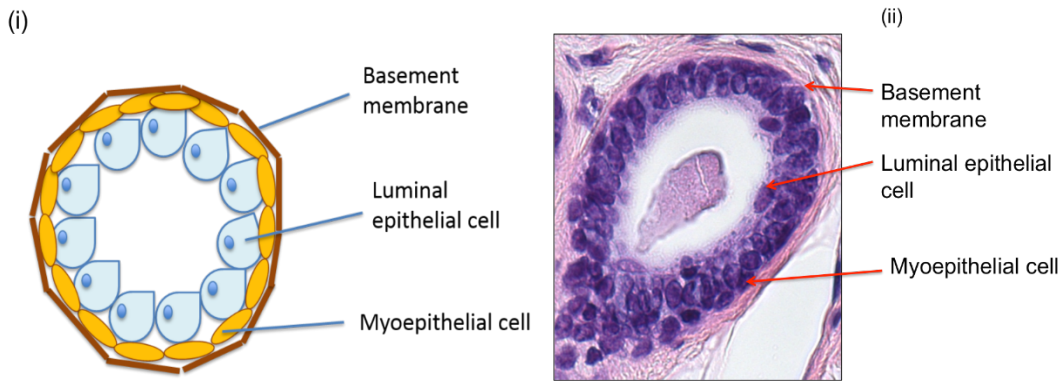

Figure 2: (i) Structure of a normal breast duct. The duct has a bilayered structure comprising an inner layer of luminal epithelial cells surrounded by an outer myoepithelial cell layer and basement membrane. (ii) High power (x20 objective) view of a normal breast duct, H+E stained section.

The ducts and lobules are embedded throughout the breast in a stroma which forms the principle tissue mass of the breast. The specialised intralobular stroma is myxoid and highly vascularised whereas the interlobular stroma comprises more collagenous fibrous tissue, adipose tissue, scattered blood vessels and mixed inflammatory cells [2]. Approximately 12-20 large ducts converge at the nipple where the milk is secreted [2] (Figure 3).

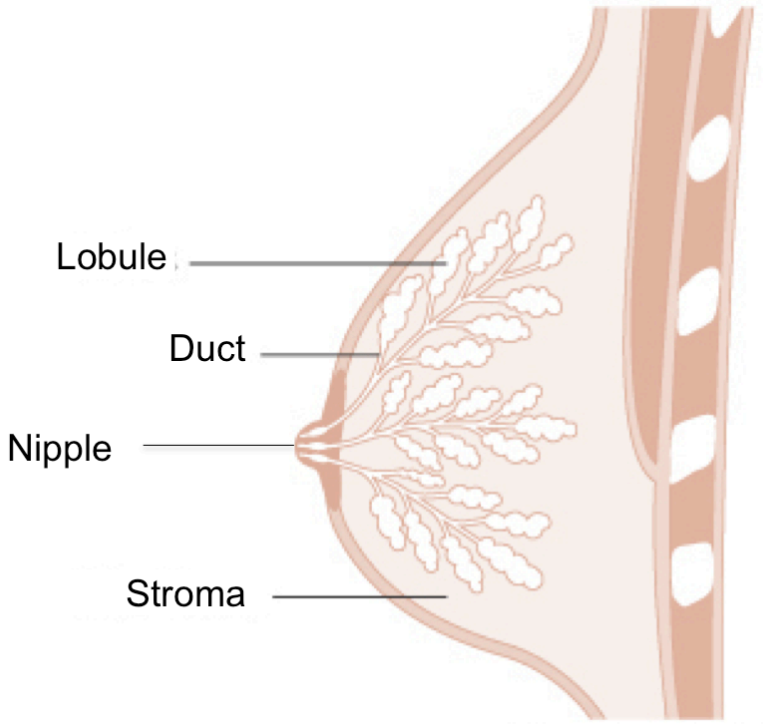

Figure 3: Anatomy of the breast. The ducts and lobules are embedded in a stroma which forms the principle tissue mass of the breast. Approximately 12-20 large ducts converge at the nipple. Adapted from www.cancerresearchuk.org

The breast undergoes dynamic changes in response to alterations in systemic hormone levels associated with the menstrual cycle. After ovulation, there is a rise in oestrogen and progesterone levels and this is accompanied by an increase in epithelial cell proliferation and an increase in the number of acini per lobule [1]. The intralobular stroma also becomes oedematous. Following menstruation, hormone levels fall, the lobules regress and the oedema resolves [1].

The onset of pregnancy results in full maturation of the breast with a marked increase in the number and size of lobules [1]. Following childbirth the lobules produce milk until the cessation of lactation when the epithelial cells undergo programmed cell death and the lobules regress [1].

With increasing age, there is a gradual involution of the lobules and the specialised intralobular stroma. The lobular involution is particularly pronounced after the menopause [1]. The interlobular stroma is also remodelled and this process is characterised by a reduction in the proportion of radiodense fibrous tissue and an increase in radiolucent adipose tissue [3].

1.2 Pathogenesis of breast cancer

The vast majority of breast cancer (>95%) is adenocarcinoma arising in the ductal/lobular system of the breast, initially as ductal carcinoma *in situ* (DCIS) [2]. DCIS refers to a clonal proliferation of neoplastic cells that is confined to the ducts and lobules by the basement membrane (Figure 4) [2]. Myoepithelial cells are preserved in involved ducts and lobules.

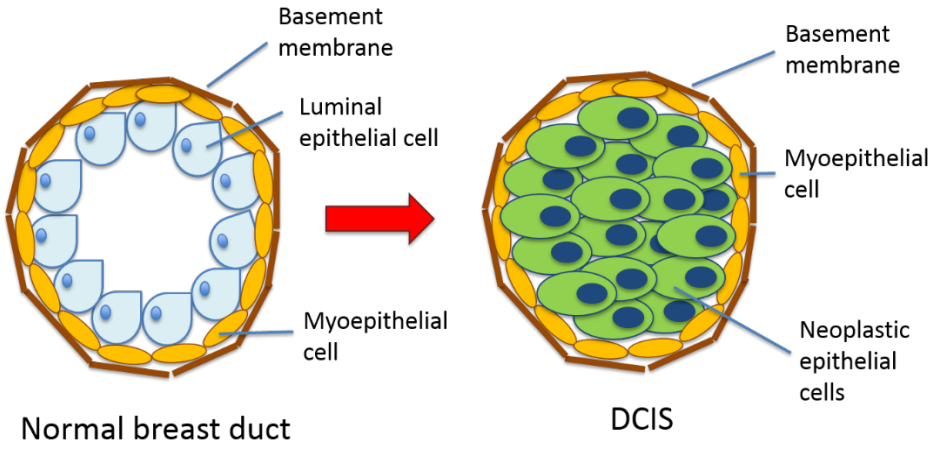

Figure 4: Comparison of a normal breast duct versus DCIS. Most breast cancer arises initially as DCIS, a clonal proliferation of neoplastic cells confined to the ducts and lobules by the basement membrane. The myoepithelial cell layer is preserved.

Invasive carcinoma is defined as the moment when the neoplastic epithelial cells in DCIS have penetrated the basement membrane and infiltrated into the surrounding stroma (Figure 5) [2]. The transition from DCIS to invasive disease is accompanied by loss of the myoepithelial cell layer [2].

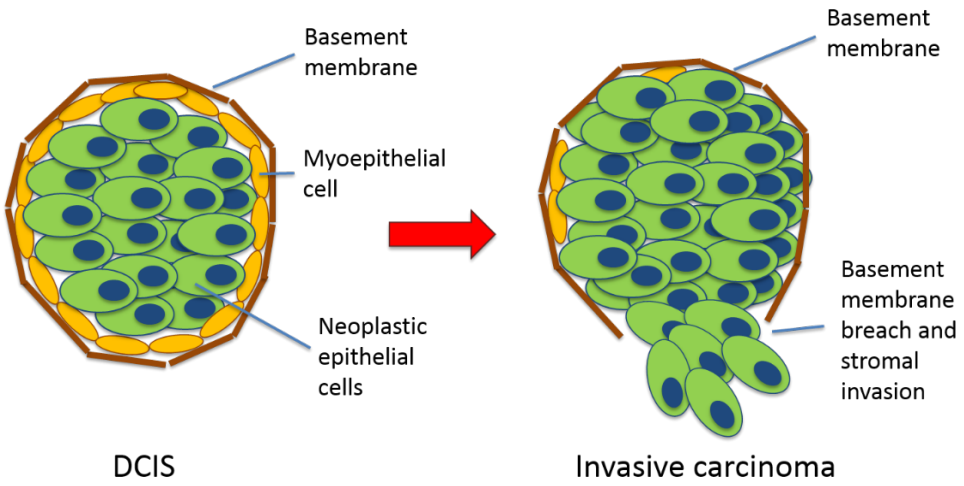

Figure 5: The progression of DCIS to invasive carcinoma. The definition of invasive carcinoma is when the neoplastic epithelial cell population in DCIS has breached the basement membrane and infiltrated the surrounding stroma. There is loss of the intact myoepithelial cell layer.

The biological and molecular events governing the initiation of DCIS, and those governing the transition from DCIS to invasive breast cancer are presently unknown.

Invasive breast carcinoma is traditionally classified based on the morphological appearance of the tumour. The advent of high throughput sequencing technologies has enhanced our understanding of the diversity of genetic mutations present in invasive breast cancer and facilitated the classification of this heterogenous disease at the molecular level.

Four distinct molecular sub groups have been identified: Luminal A, luminal B, Her2 over-expressing and basal like.

Charles Perou and colleagues first defined four breast cancer 'intrinsic' subtypes with similar gene expression patterns (Her2 over-expressing, basal like, luminal and normal breast like), based on hierarchical clustering analysis of microarray data [4]. Subsequent studies by the Sorlie group further sub-classified the luminal group into luminal A and luminal B tumours, and demonstrated that the classification of breast tumours into the various molecular subtypes is of prognostic significance [5, 6].

Clinically the four molecular categories (luminal A, luminal B, Her2 over-expressing and basal like) reflect three therapeutic groups [2, 7]. Immunohistochemistry and fluorescent *in-situ* hybridization (FISH) are used in routine clinical practice to classify tumours into one of these three groups based on tumour cell expression of oestrogen receptor (ER), and Her2.

Firstly, the ER positive group, which may also be progesterone receptor (PR) positive, includes the luminal A and luminal B subtypes (approximately 50-65% of cases). Secondly, the Her2 overexpressing tumours (20%) and finally the triple negative (ER/PR/Her2 negative) tumours (15%) which represent the basal like subtype [2, 7]. These three therapeutic groups represent the major genetic pathways of breast cancer tumourigenesis [7].

Despite the fact that basal like breast cancer is associated with negative immunohistochemical expression of ER, PR and Her2 [6], a number of studies have demonstrated that triple negative tumours are in fact a heterogeneous group of tumours encompassing a variety of molecular subtypes [8, 9]. Bertucci and colleagues examined the gene expression profile of 172 triple negative tumours and found that only 123 (71%) clustered with basal like breast cancer, suggesting not all triple negative tumours are of the basal like subtype [8]. Furthermore, of 160 tumours defined as showing a basal like pattern of gene expression, just 123 (77%) were found to be triple negative by immunohistochemistry [8].

In addition, Rakha and colleagues performed a large immunohistochemical analysis on two well defined breast cancer cohorts with clinical follow up [9]. They found that triple negative tumours were a particularly heterogeneous group of breast cancers and advocate the use of specific basal immunohistochemical markers (cytokeratin 5/6, cytokeratin 14, cytokeratin 17 and epidermal growth factor receptor) to define basal like breast cancer within triple negative tumours [9].

1.3 Breast cancer incidence and mortality

Breast cancer is a major public health burden globally, in 2008 more than 1.4 million women were diagnosed with the disease and there were 459,000 deaths [10]. The Surveillance, Epidemiology and End Results (SEER) database estimates that 246,660 American women will be diagnosed with breast cancer in 2016, with 40,450 dying of the disease [11]. It is also estimated that 12.4% of American women will be diagnosed with breast cancer at some point in their lifetime [11].

Breast cancer is the most common cancer in the UK with 50,285 new diagnoses in 2014 and 11,762 deaths in 2012. The lifetime risk for being diagnosed with breast cancer for women in the UK is 1 in 8 [12]. Breast Cancer incidence in the UK has increased significantly over the past 4 decades (Figure 6) [12].

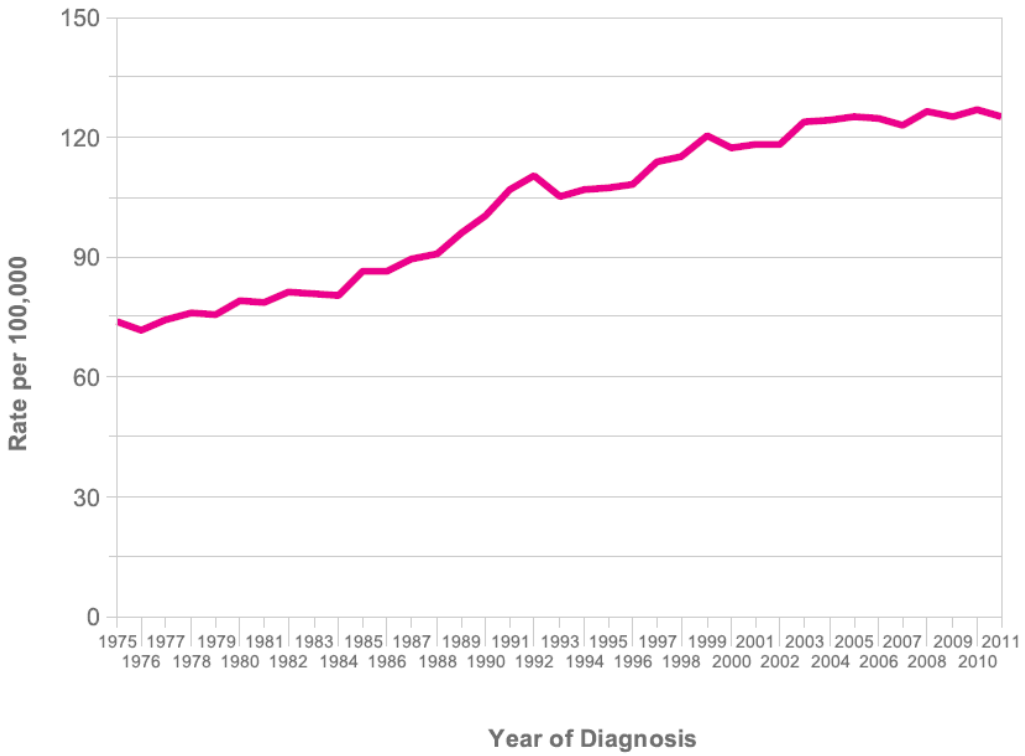

Figure 6: UK female invasive breast cancer age-standardised incidence rates per 100,000 population 1975-2011. Taken from www.cancerresearchuk.org [12]

This increase is partly attributed to the introduction of the National Health Service Breast Cancer Screening Programme (NHSBCSP) in 1988. Currently the NHSBCSP invites women aged between 50 and 70 years for mammographic screening every three years. The value of increasing the age limits for screen in currently being evaluated in England with women aged 47-73 being offered screening mammograms [12].

Mortality from breast cancer has overall progressively decreased since the early 1970s (Figure 7), this has been attributed to a variety of factors including earlier detection due to the advent of NHSBCSP and improvements in treatment with better surgical techniques, radiotherapy and adjuvant treatments including tamoxifen [13, 14].

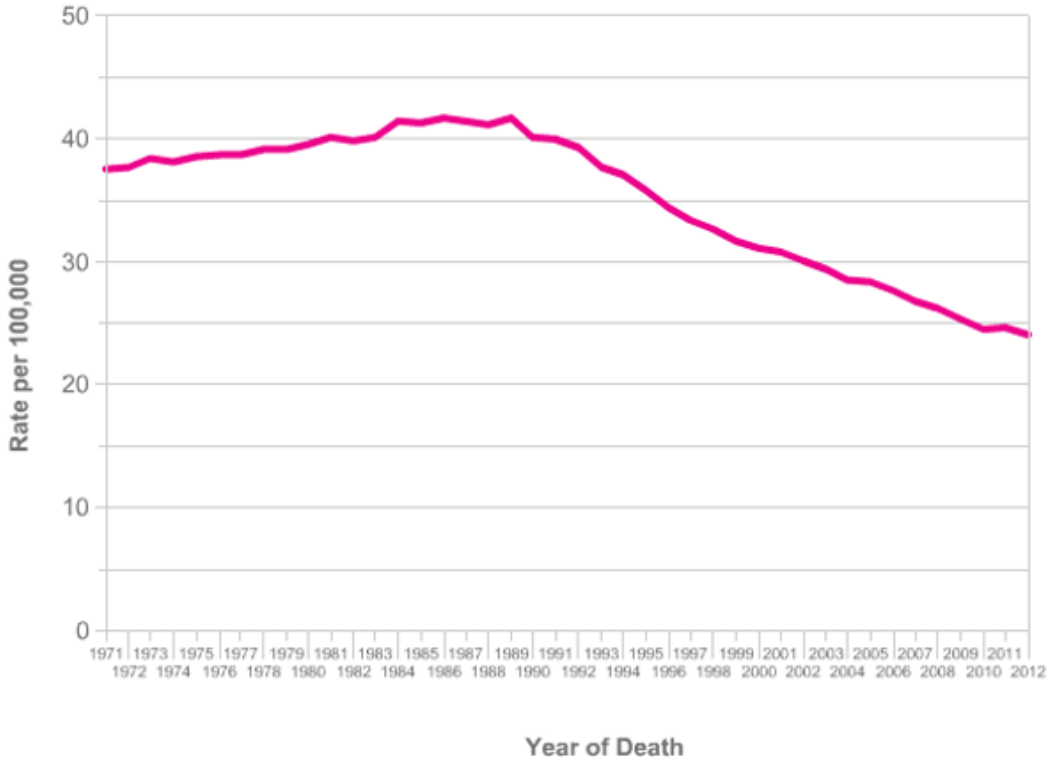

Figure 7: UK female age-standardised breast cancer mortality rates per 100,000 population 1971-2012. Taken from www.cancerresearchuk.org [12]

Earlier detection of breast cancer substantially improves survival, as demonstrated by the notable fall in 5 year survival with increasing stage of disease (Figure 8). Thus

there is considerable interest, not only in increasing detection at an earlier stage, but also in developing strategies to prevent breast cancer and to prevent breast cancer progression.

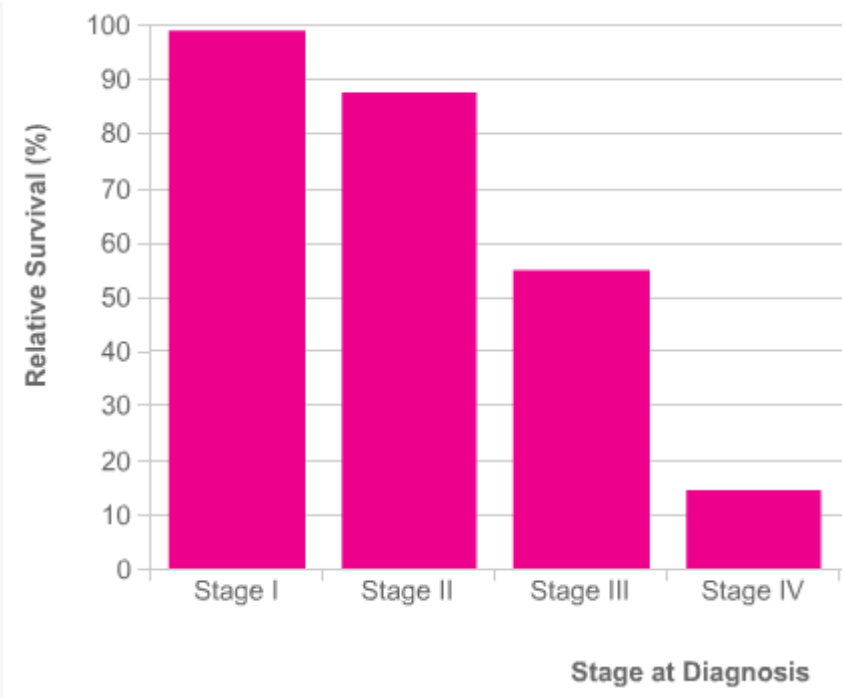

Figure 8: UK female breast cancer relative survival by stage 2002-2006. Taken from www.cancerresearchuk.org [12]

There is considerable geographic variation in the incidence of breast cancer globally with the highest rates seen in economically developed countries [15]. These differences in incidence may be partly explained by variation in exposure to the different risk factors for breast cancer. Gaining an improved understanding of these risk factors can help inform targeted breast cancer prevention strategies.

1.4 Breast cancer risk factors

Many factors have been identified as being influential in a woman's likelihood of developing breast cancer.

1.4.1 Age and family history

Increasing age is associated with the strongest relative risk of all the breast cancer risk factors [16] with the majority of tumours occurring over age 50. Women with a family history are at increased risk of developing breast cancer with an increased lifetime incidence of 5.5% for women with one affected first degree relative and 13.3% for those with two [16].

1.4.2 Genetic factors

A small proportion of breast cancers, approximately 5-10%, are due to germline mutations in breast cancer susceptibility genes [17]. These mutations can be classified as high, moderate risk or low risk based on the strength of the relative breast cancer risk they impart (Table 1).

Locus	Gene	Variant	Relative Breast Cancer Risk	Association with MD
High Risk				
17q21	BRCA1		5-45	
13q12.3	BRCA2		9-21	
17p13.1	TP53		2-10	
10p23.3	PTEN		2-10	
19p13.3	STK11		2-10	
16q22.1	CDH1		2-10	
16p12.1	PALB2		2-7	
Moderate Risk				
11q22.3	ATM		2-3	
22q12.1	CHEK2		2-3	
17q22-q24	BRIP1		2-3	
Low Risk				
1p36.22	PEX14	rs616488	1.06	
1p13.2	AP4B1	rs11552449	1.07	
1p11.2	NOTCH2/FCGR1B	rs11249433	1.09	
1q32.1	LGR6	rs11249433	1.1	
1q32.1	MDM4	rs4245739	1.14	
2p24.1	LINC01376	rs12710696	1.1	
2q14.2	INHBB	rs120487546	1.1	
2q31.1	CDCA7	rs1550623	1.06	
2q35	TNP1/IGFBP5/2/TNS1	rs13387042	1.14	
2q35	DIRC3	rs16857609	1.08	
3p26.1	ITPR1	rs6762644	1.07	
3p24	NEK10/SLC4A7	rs4973768	1.1	*
3p24.1	TGFBR2	rs12493607	1.06	
4q24	TET2	rs9790517	1.05	
4q34.1	ADAM29	rs6828523	1.11	
5p15.33	TERT	rs10069690	1.06	
5p12	FGF10AS1.MRPS30	rs4415084	1.17	
5q11	MAP3K1	rs889312	1.12	
5q11.2	RAB3C	rs10472076	1.05	
5q12.1	PDE4D	rs1353747	1.09	
5q14.3	ARRDC3	rs10474352	1.09	
5q33.3	EBF1	rs1432679	1.07	*
6p25.3	FOXQ1	rs11242675	1.06	
6p23	RANBP9	rs204247	1.05	
6q14.1	FAM46A	rs17529111	1.05	
6q25.1	TAB2	rs9485272	1.11	*
6q25.1	ESR1	rs2046210	1.16	*
7q35	ARHGEF5	rs720475	1.06	
8p12	RPL17P33	rs9693444	1.07	
8q21.13	HNF4G	rs6472903	1.1	
8q21.13	HNF4G	rs2943559	1.13	
8q24.21	MYC	rs11780156	1.07	
9p21.3	CDKN2A/2B	rs1011970	1.06	

9q31.2	KLF4	rs10759243	1.06	
9q31.2	KLF4	rs865686	1.12	
10p21.31	MLLT10	rs7072776	1.07	
10q21.2	ZNF365	rs10822013	1.12	*
10q22.3	ZMIZ1	rs704010	1.08	
10q25.2	TCF7L2	rs7904519	1.06	
10q26	FGFR2	rs2981579	1.27	
11p15	LSP1	rs3817198	1.07	*
11q13.3	CCND1	rs554219	1.27	
11q24.3	BARX2	rs11820646	1.05	
12p13.1	ATF7IP	rs12422552	1.05	
12p11.22	PTHLH	rs10771399	1.16	
12q22	NTN4	rs17356907	1.1	*
12q24.21	MED13L	rs1292011	1.09	
14q13.3	PAX9	rs2236007	1.08	
14q24.1	RAD51L1	rs999737	1.09	*
14q32.12	CCDC88C	rs941764	1.06	
15q26.1	PRC1	rs2290203	1.08	
16q12.1	TOX3	rs3803662	1.24	*
16q12.2	FTO	rs17817449	1.08	*
17q22	STXBP4	rs6504950	1.06	
18q11.2	AQP4	rs527616	1.05	
18q11.2	CHST9	rs1436904	1.04	
19p13.11	BABAM1	rs8170	1.15	
19p13.11	ELL	rs4808801	1.08	
19q13.31	KCNN4	rs3760982	1.06	
20q11.22	RALY	rs2284378	1.1	
21q21.1	NRIP1	rs2823093	1.09	
22q12.2	EMID1	rs132390	1.12	
22q13.2	MKL1	rs6001930	1.12	*

Table 1: Known cancer susceptibility gene variants and their relative breast cancer risk compared to individuals who do not possesses the variant. Taken from Mavaddat et al [17], Ziv et al [18] and Couch et al [19]. The variants also associated with MD are highlighted (*).

High risk genes such as *BRCA1* and *BRCA2* have been extensively studied with regard to their contribution to breast cancer risk and the tumour types they predispose to [17, 20]. The contribution of the lower risk genetic variants and the biological mechanisms behind the risk they impart is less well understood.

1.4.3 Reproductive and hormonal factors

Cumulative lifetime exposure to oestrogen is associated with an increased risk of breast cancer; early age of menarche and late menopause both independently increase risk [21]. Conversely, term pregnancy and, in particular, early age of first birth

reduce risk. Pregnancies which end in spontaneous or induced abortion do not appear to increase breast cancer risk [22]. Breastfeeding demonstrates a protective effect against breast cancer in addition to the effect of parity [23]. Despite the long term protective effect of parity on breast cancer risk, it has been suggested by Schedin and colleagues that there is a transient increase in risk immediately following pregnancy [24]. This increased risk falls to normal levels within a few years in younger women but may remain elevated for substantially longer in older women [24].

Combined oral contraceptive use imparts a small increase in breast cancer risk [25]; however, tumours diagnosed in women who had used oral contraceptives were found to be less advanced clinically than those who had never taken these medications [25]. Hormone replacement therapy increases the risk of breast cancer in current users and the risk increases with the duration of treatment [26]. However, the increased risk reduces after stopping treatment and largely disappears after five years following treatment cessation [26].

1.4.4 Mammographic density

Women with high mammographic density (MD) have a risk of developing breast cancer 4-6 times higher than those with very little density [27]. MD is discussed in detail in section 1.5.

1.4.5 Proliferative breast disease

Clinical studies have indicated that intraductal proliferative breast lesions are associated with varying degrees of risk for the development of invasive breast cancer based on their morphological classification [28]. This risk ranges from 1.5 times that of the background population for usual type ductal hyperplasia, to 4-5 fold for atypical ductal hyperplasia (ADH) and 8-10 fold for ductal carcinoma insitu (DCIS) [28-30]. The associated risk of ADH may be further increased in premenopausal women and in those with a family history of breast cancer [29].

1.4.6 Ethnicity

Women from different ethnic groups have varying risks of breast cancer. This is demonstrated by data from the SEER database which shows that in the USA the highest incidence of breast cancer is in white women with an age-adjusted incidence of 127.9 per 100,000. This is higher than black women (124.4 per 100,000) and substantially higher than American Indian/Alaskan native women (82.0 per 100,000) [11]. Despite having a lower incidence of breast cancer, black women have a significantly higher mortality (30.2 per 100,000) compared to white women (21.3 per 100,000) [11].

Ethnic variation in breast cancer incidence and mortality has also been noted in the UK where black women have been observed to have a higher rate of mortality from early stage tumours and present at an earlier age [31].

The underlying causes of ethnic variation in breast cancer incidence and mortality appear to be multifactorial with factors such as access to treatment, socioeconomic status and tumour biology influencing outcome [32].

1.4.7 Obesity and diet

Studies have demonstrated that obesity is a significant risk factor for breast cancer in post-menopausal women not taking exogenous hormones [33, 34]. Conversely, reduction in weight is thought to have a protective effect [35].

An Italian study observed an association with a high glycaemic load diet and breast cancer risk [36]. Diets high in fruit and vegetables and high in fibre have both been shown to have a protective effect against breast cancer [37, 38].

1.5 Mammographic density

1.5.1 Mammographic density and breast cancer risk

Mammographic density (MD) refers to the proportion of a mammogram occupied by radiologically dense fibroglandular tissue and is a major, highly heritable, independent risk factor for breast cancer (Figure 9).

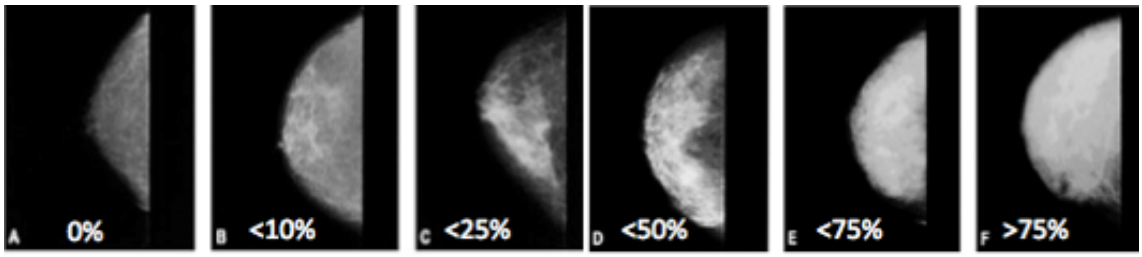

Figure 9: Series of mammogram images of increasing density from 0 – 75% density, taken from Boyd [39]

The association of dense breast tissue with increased breast cancer risk was first noted by Wolfe in 1976 [40]. Since then, there have been numerous studies that have examined this association further. A comprehensive meta-analysis of 14,000 cases observed that women with >75% breast density had 4-6 times the risk of developing breast cancer compared to women with breasts of the lowest 25% density [41]. This study also demonstrated that the increased breast cancer risk imparted by high MD was largely consistent across different types of study, encompassing different geographical populations and employing a variety of methods of MD measurement [41].

The relative risk imparted by high MD is greater than family history or menstrual and reproductive risk factors, only age and BRCA mutation status are associated with a higher relative risk (Table 2) [16].

Risk Factor	Relative Risk	At Risk Group
Age	>10	Elderly individuals
BRCA 1/2	5-45	Germline BRCA1 mutation
Mammographic Density	>5	High mammographic density
Geographical Location	5	Developed countries
Age at menarche	3	Before 11 years
Age at menopause	2	After 54 years
Age at first full pregnancy	3	First child after age 40
Family history (non-BRCA)	≥ 2	Breast cancer in first degree relative
Previous benign breast disease	4-5	Atypical hyperplasia
Cancer in other breast	>4	Previous breast cancer
Socioeconomic group	2	Groups I and II
Body mass index (BMI)	Pre-menopausal 0.7 Postmenopausal 2	High body mass index
Alcohol Consumption	1.07	7% increase with every daily drink
Exposure to ionising radiation	3	Anormal exposure to young girls after 10 years

Table 2: Comparison of relative risk imparted by high mammographic density to relative risk of other breast cancer risk factors. Adapted from Mavaddat et al [42], Boyd et al [43] and Veronesi et al [16]

Such is the strength of the association of MD with breast cancer risk that a recent study by Brentnall and colleagues found that MD alone was a slightly stronger risk factor than both the Tyler-Cuzick and Gail models of risk prediction in their univariate analysis [44]. In addition, a recent Canadian study found that MD at screening outperformed clinical risk factors (age, number of births, HRT use, first-degree family history of breast cancer and menopausal status) in predicting future cancer risk [45].

Furthermore, given the high frequency of breast density in the general population, the attributable risk is substantial and it is estimated that approximately one third of breast cancers could be explained by density in more than 50% of the breast [43]. This is a much greater attributable risk than other strong relative risks for breast cancer such as BRCA gene mutation, which accounts for just 5% of all breast cancer [43]. High MD is

also associated with increased local recurrence and risk of second primary breast cancer [46, 47].

1.5.2 Pathological correlate of dense breast tissue

MD reflects variations in the tissue composition of the breast and is positively associated with collagen, epithelial and stromal cells and negatively associated with fat [48]. Despite this, MD is not reflected by a specific histological abnormality. However, MD is associated with histological lesions associated with a significant increased risk of breast cancer such as atypical hyperplasia, columnar cell lesions and ductal carcinoma in-situ [49, 50].

MD has also been associated with reduced lobular involution (LI) - the increase in the proportion of fat and reduction in glandular tissue and collagen noted in the breasts of post-menopausal women (age related atrophy) [3]. A recent study by Gierach and colleagues found three measures of reduced LI were associated with greater area and volumetric MD in premenopausal women [51]. A study from the Mayo clinic also reported the correlation between MD and reduced LI. In addition, they found that when controlling for MD, women with reduced LI still had an increased risk of breast cancer, suggesting the two variables are independent risk factors [52].

Given that MD and reduced LI are correlated but independently associated with breast cancer risk, Gierach and colleagues investigated whether a common pathological feature linked the two variables [53]. They found serum insulin-like growth factor 1 (IGF-1) levels were elevated in women with higher TDLU counts (a marker of reduced LI) and that this association was strongest in women with high MD [53]. They propose that elevated IGF-1 levels may identify a subgroup of high risk women with both high MD and reduced LI [53].

Stroma is the major tissue component of the breast and is composed of stromal cells (fibroblasts, endothelial cells, immune cells and adipocytes) and ECM proteins, the

most abundant of which is collagen I. A number of studies have indicated that mammographic density corresponds more to alterations in stromal composition rather than epithelial changes [54-58]. Corroborative of these findings, one study has recently investigated the association of leukocyte telomere length, a surrogate marker for epithelial cell replication, with MD and found no significant association [59].

A comprehensive study by Li and colleagues examined histological features of breast tissue obtained at forensic autopsy [48]. They found that the area of stromal collagen was most strongly associated with percentage density and accounted for 29% of the variation in percentage density whereas nuclear area and glandular area accounted for between 4 and 7% of the variation [48]. Similarly, Pang et al have recently reported a significant association of increasing MD with increased proportion of fibrous stroma [60]. Representative histological images of high and low density breast tissue are displayed in Figure 10 below.

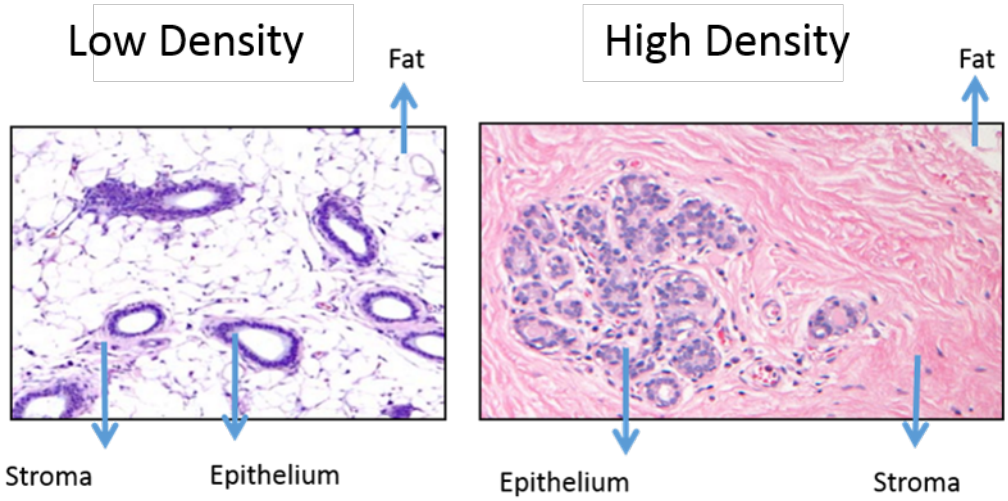

Figure 10: Representative H+E stained sections of low and high density breast tissue (x10 objective)

A recent proteomics study by McConnell and colleagues found high MD breast tissue was associated with aligned periductal collagen fibrils rather than total quantity of amorphous stromal collagen [61]. Their analysis also highlighted mediators of collagen fibril organisation (periostin and collagen XVI) as showing significantly up-regulated

expression in high MD breast tissue [61]. In addition, Huo and colleagues have reported more organised stromal collagen present in high MD breast tissue compared to low MD tissue [62]. These findings highlight the contribution of both quantitative and qualitative factors to the composition of high MD breast tissue.

MD has also been hypothesised to represent the influence of local oestrogen production on the breast [63]. However, systemic levels of oestrogen have so far only shown an inverse or no association with MD [64]. One study has reported an inverse association of serum levels of leptin, C-reactive protein (CRP) and other adipose-derived factors with MD [65].

Serum levels of prolactin and IGF-1 have been associated with MD in a number of studies [53, 66, 67]. In addition, dense breast tissue has been associated with higher immunohistochemical expression of IGF-1, IGF-1 receptor and higher levels of tissue inhibitor of metalloproteinases 3 (TIMP 3) within both the epithelium and stroma [68, 69]. Furthermore, genetic polymorphisms in several components of the insulin-like growth factor (IGF) pathway also show an association with increased MD [70]. These findings suggest that the IGF-1 pathway may have a contributory role in determining MD.

Stromal expression of cyclo-oxygenase 2 (COX-2) has been associated with MD in human tissue samples [71] and an animal model of MD [72], suggesting high MD tissue may facilitate a more pro-inflammatory microenvironment.

Stromal proteoglycans have been proposed as major contributors to MD and potentially to density-associated risk [73]. Studies investigating the association of proteoglycans and MD have been limited with inconclusive results [73]. To date, increased expression of the proteoglycans lumican, decorin, perlecan and syndecan-4 have been reported in high MD versus low MD tissues [54, 73].

Despite the association of stromal components and high MD breast tissue, there is no standardised approach to measuring MD in histological sections. This, combined with the fact that MD is often heterogenous in nature throughout the breast, poses a significant challenge to the planning to translational studies using human tissue.

1.5.3 Measurement of mammographic density

A variety of methods have been employed to assess MD and, to date, no ideal method has been developed. Initial classification systems incorporated both qualitative and quantitative measures. Wolfe described four mammographic parenchymal patterns: N1, predominantly fat, P1, ductal prominence in <25% of the breast, P2, ductal prominence in >25% of the breast and DY, extensive dysplasia [40] . These were stratified into two categories reflecting high and low risk for the subsequent development of cancer. Another example is the Tabar classification, consisting of 5 patterns (I-V) based on anatomic-mammographic correlation [74]. Four of the five Tabar patterns (II-V) largely correspond to the four patterns described by Wolfe.

The American College of Radiology has developed a qualitative and quantitative classification system for clinical purposes, known as BI-RADS, which has largely replaced the Wolfe and Tabar classifications and is categorised accordingly: (1) almost entirely fatty (<25% dense), (2) scattered fibroglandular densities (26-50%), (3) heterogeneously dense (51-74%) and (4) extremely dense (>75%). This visual assessment method is relatively quick and easy to perform however, there is a degree of both intra and inter observer variability [75].

Cumulus is a computer-assisted technique allowing purely quantitative assessment of breast density. The software allows the total breast area, absolute dense area, absolute non-dense area and percentage density to be calculated. Quantitative methods of density assessment have been observed to give a better risk prediction [76, 77]. However, there are some important limitations with Cumulus. It requires digitised

analogue films and is not yet compatible with digital images. Since many units are converting to digital images, this may prove a problem for conducting future studies. The digitisation of analogue images is also time consuming and therefore the development of high throughput, fully automated methods is a priority. Assessment methods that measure volumetric density are also being developed which will hopefully provide a more accurate estimation of the amount of fibroglandular tissue within the breast. However, surprisingly, initial results suggest that the volumetric methods do not give better risk estimations than 2D area-based measurements [78].

Most studies assessing MD in quantitative terms use the relative measure of density - percentage density. However, this does not convey any information about the absolute amounts of dense and non-dense tissues. The amount of non-dense tissue may be important, since the fatty tissue is an important source of local oestrogens, which may influence the dense tissue. The evidence to date is inconclusive as to whether relative or absolute density is a better predictor of breast cancer risk. One study by Vachon demonstrated a comparable prediction potential for both [79], whereas Stone and colleagues have suggested that, as a single parameter, the absolute dense area provides more information than percentage density on breast cancer risk [80]. Conversely, a study in an Asian population by Wong et al [81], and a recent large meta-analysis by Pettersson and colleagues, have suggested that percentage density is a better risk predictor than absolute dense area [82].

1.5.4 Modifiers of MD

A key feature of MD compared to other established risk factors for breast cancer is that it is dynamic and modifiable. This modifiability offers significant therapeutic potential in the form of cancer prevention strategies targeted to reduce breast density.

MD typically decreases with advancing age, whereas breast cancer incidence conversely increases with advancing age [43, 83]. The Pike model (Figure 11) can be

used to resolve this apparent paradox. This a theoretical model which suggests that cumulative lifetime exposure of the breast to dense tissue and associated growth factors and hormones, also referred to as 'breast tissue ageing', results in increased cell division and accumulation of genetic damage, conferring the age-related risk of developing breast cancer (equivalent to the area under the curve in Figure 11) [84]. The breast tissue ageing rate is an estimate of the number of breast cell divisions occurring during a given time period.

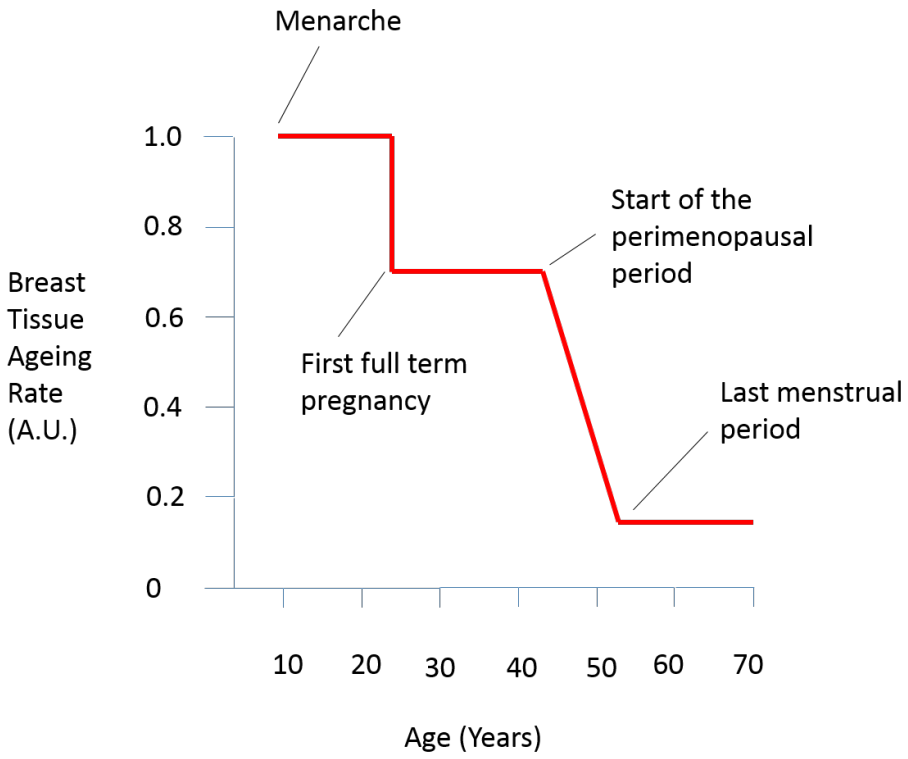

Figure 11: The Pike Model of breast tissue ageing. The red line represents the rate of breast tissue ageing (an estimate of the number of breast cell divisions occurring during a given time period) and reflects changes in breast density with age. Breast density is at its highest following the menarche, falls with each successive pregnancy and then falls sharply during the perimenopausal period. The model helps to explain the discrepancy observed when there is a high risk of breast cancer at advanced age, but breast density is at its lowest. The model suggests that the cumulative lifetime exposure to dense breast tissue, and the associated growth factors and hormones, imparts the risk (equivalent to the area under the red line) by increasing cell division and accumulation of genetic damage. Thus, at a higher age, there is a greater area under the curve and there is a higher risk of breast cancer. Adapted from Pike et al [84]. (A.U. = Arbitrary Units)

According to the model, the rate of breast tissue ageing is greatest during menarche, falls with each successive pregnancy and then falls rapidly at the onset of the

perimenopausal period [84]. The underlying assumptions of this model are that breast tissue 'ages' at a constant rate, starting at menarche and continuing to first birth. The model also assumes that cell division is proportional to the age of the individual, and that reproductive factors modify the rate of cell division after first birth and again after menopause.

This is reflected in the apparent hormonally responsive nature of MD; women with risk factors for breast cancer related to prolonged oestrogen exposure, such as late first pregnancy and early menarche, show a higher degree of MD [27]. In addition, the use of combined hormone replacement therapy (HRT) also increases MD [85, 86]. Conversely parous women have a lower degree of MD (approximately a 10% reduction per live birth [87]) and there is a significant reduction in MD following the menopause [27, 88]. Bone mineral density is a putative marker of lifetime exposure to oestrogen and has been associated with MD in obese premenopausal and postmenpausal women [89].

An important confounding factor is that MD is also negatively associated with body mass index (BMI), an independent risk factor for breast cancer [87, 90]. High BMI reduces percentage density by increasing the non-dense portion of the breast and has also been associated with reduced absolute density in some studies [91, 92], however this is not a consistent finding [93, 94]. Failure to correct for BMI may lead to a significant underestimation of risk [90].

Interestingly, a recent prospective analysis of BMI during childhood showed a significant inverse association with premenopausal MD at age 25-29 years [95]. These results suggest childhood body fatness may have a role in determining premenopausal breast density, independently of adult BMI [95].

Rather surprisingly, given the trend for inverse association of BMI with MD, a Korean study has reported components of the metabolic syndrome, a condition often

accompanied by obesity, to be associated with increased MD in premenopausal women and that blood glucose and insulin resistance were associated with MD in postmenopausal women [96]. MD has also been associated with increased birth weight in postmenopausal women in a Swedish population [97].

The influence of diet and lifestyle factors on MD have been investigated by a number of studies with mixed findings. A recent Spanish study found a lower degree of MD in postmenopausal and non-smokers adhering to the World Cancer Research Fund dietary and exercise recommendations for cancer prevention [98]. A randomised controlled trial of dietary soy supplementation was found to have no effect of MD [99], whereas a weak association with dietary animal fat and red meat intake in adolescence with MD has also been reported [100]. A Danish study has recently reported an inverse association with smoking and MD [101]. In addition, no association with long term exposure to air pollution and MD was observed within the same cohort [102].

The association of alcohol consumption and MD has also been examined by a number of studies with inconsistent findings. A positive association has recently been demonstrated in a multi-ethnic urban cohort [103] and in premenopausal women [104]. However no association was found with alcohol consumption in early adulthood and midlife with MD in two US cohorts [105].

Given the inconsistencies in many of the studies investigating determinants of MD, it is clear that further research is needed to clarify these complex associations. An International Consortium on Mammographic Density has recently been established [106] with the aim of precisely characterising the determinants of MD and analysing how these vary across different global populations [106]. The results of these analyses will help inform strategies for the identification and management of high risk individuals.

1.5.5 Pharmacological modulation of MD

As previously mentioned, combined hormone replacement therapy has been associated with increased MD and breast cancer risk [85, 86, 107], particularly among current users [108]. To date, no consistent association with MD and oral contraceptive use has been demonstrated [107].

Tamoxifen is a selective oestrogen receptor modulator (SERM), demonstrated in the first International Breast Cancer Intervention Study (IBIS I) to reduce MD and breast cancer risk [109]. A further nested case control study within the IBIS I cohort revealed that, in those women taking tamoxifen, those who showed a >10% reduction in MD had a 63% lower risk of developing breast cancer [110]. Furthermore, those women who showed a poor response to tamoxifen treatment (<10% reduction in MD) showed no associated risk reduction. Thus the protective effect of tamoxifen appears associated with a reduction in MD.

This has been further highlighted in a recent retrospective study of breast cancer patients who received adjuvant tamoxifen for 15 years [111]. A 20% relative reduction in MD was reported for women who took tamoxifen, and this reduction was associated with a 50% risk reduction in breast cancer mortality [111]. In addition, Czene and colleagues found that women who experienced a >10% reduction in MD in the contralateral breast following adjuvant therapy for breast cancer had a 55% less likelihood of contralateral recurrence [112].

Intriguingly, on-going follow up from the IBIS I study has shown that the 5 years of tamoxifen treatment given as per the trial protocol have long lasting benefits, with a protective effect still evident at 15 years [113].

Presently the mechanisms conferring susceptibility to the protective effect of tamoxifen treatment remain unknown, however, an association of cytochrome P450 2D6

(CYP2D6) metaboliser status with MD change in response to tamoxifen has recently been reported [114].

In an animal model of breast cancer, tamoxifen treatment initiated remodelling of the mammary stroma to a tumour inhibitory phenotype with lower levels of fibronectin and reduced extra-cellular matrix (ECM) turnover [115]. Furthermore, a recent study utilising a xenograft model of high MD human tissue maintained in murine biochambers showed that tamoxifen treatment resulted in a reduction in radiographic tissue density characterised histopathologically by a decrease in stromal tissue and increase in adipose tissue [116]. The evidence from these studies suggest that tamoxifen may modulate density and breast cancer risk by modifying the stromal microenvironment of the breast.

Raloxifene, another SERM found to be effective at preventing breast cancer (to a lesser degree than tamoxifen, but with an improved side effect profile [117]) has also been investigated in two small studies for ability to modulate MD, however no significant change in density with treatment was observed [118, 119].

Overall there have been nine randomised controlled trials of SERMs for the prevention of breast cancer. A recent meta-analysis incorporating data from over 83,000 participants found a 38% reduction in breast cancer incidence with tamoxifen [120]. On the basis of these findings, the National Institute for Clinical Excellence (NICE) approved tamoxifen and raloxifene for breast cancer prevention in high risk individuals in 2013 [121].

Aromatase inhibitors (AI) are another class of drug which have demonstrated superior efficacy to SERMs in breast cancer prevention in two randomised clinical trials [122, 123]. The IBIS II trial of anostrazole versus placebo in 3,864 post-menopausal women reported a 53% reduction in breast cancer incidence [122].

A limited number of small studies have examined the effect of the AIs letrozole and examestane on MD and have yielded inconsistent results [124-128]. One study has reported a decrease in MD in 11 out of 16 postmenopausal women treated for one year with letrozole [126] and a recent phase II trial of examestane for high risk women showed a reduction in MD at one year [128]. Conversely, other studies have demonstrated no change in MD with AI treatment [127] [124, 125]. The inconsistencies in these findings may be explained by the small study sizes and variation in methods for assessing MD.

A gonadotrophin-releasing hormone agonist has also been reported to reduce MD after one year's treatment in a single, small study of premenopausal women [129]. Statins are another group of drugs that have been extensively investigated for their influence on breast cancer risk and prognosis [130]. One study has investigated the influence of statin use on MD and found no significant association [131].

1.5.6 Genetic contribution to MD

MD appears to be highly heritable; studies of twins have attributed up to 65% of the variation in MD to genetic factors [132, 133] with the remaining 35% being modifiable.

The majority of studies investigating the genetic contribution to MD have focused on investigating the single nucleotide polymorphisms (SNPs) associated with increased breast cancer risk and their relationship with MD. So far SNPs in the region of ESR1, CCDC170, EBF1, LSP1, MIR1972-2:FTO, RAD51L1, ZNF365, MKL1, TNRC9/TOX 3, NTN4, NEK10, TAB2 and loci at 2p24.1 and 12q24 [134-140] have all been identified as having a significant association with MD. Most of these studies were conducted in women of European descent. Recently Mariapun et al compared the association of these previously described SNPs with MD in an Asian population and found a similar association of SNPs in the 6q25.1 region near to ESR1 with MD [141]. The findings

suggest there is a shared heritability of MD and breast cancer risk across different global populations with varying levels of breast cancer incidence [141].

One study has investigated SNPs that can modify the increase in MD seen with current use of HRT, however no significant interactions were identified after adjustment for multiple testing [142].

In addition, a recent meta-analysis of 10,727 women found that 18% of breast cancer susceptibility variants were associated with at least one MD measure [140]. Despite this, these SNPS are thought to account for only a small percentage of the variance in breast density with the remainder attributed to genes that are currently unknown [135].

Vachon and colleagues have investigated the association of germline copy number variations and MD across two patient cohorts [143]. In one cohort they found five chromosomal regions (3q26.1 (2 regions), 8q24.22, 11p15.3 and 17q22) that were significantly associated with MD [143]. The locus at 3q26 demonstrated the strongest association and interestingly there are no known SNPs in this region. Despite demonstrating these significant associations with MD, the findings were unable to be replicated in the second patient cohort [143].

Studies investigating more established genetic mutations known to confer a strong risk for breast cancer have focused on BRCA1 and BRCA2, and have demonstrated no significant association with MD [144-146]. To date, no studies have investigated other established genetic risk factors such as phosphastase and tensin homolog (PTEN), tumour protein 53 (TP53), E-Cadherin (CDH1) or serine/threonine kinase 11 (STK11) for association with MD.

Studies investigating candidate genes involved in oestrogen metabolism, oestrogen receptors, COMT enzyme and the insulin like growth factor (IGF) pathway have shown a positive association with MD [147, 148]. In addition, variants of the prolactin gene were associated with MD in a Norwegian population currently taking HRT [149].

However, not all findings are consistent; a recent study investigating SNPs in hormone metabolism genes in an Asian population found no association with MD [150]. A comprehensive study of over 2000 SNPs in genes involved in the regulation of mitosis also found no association with MD [151].

Given the strong heritability of MD, the inconsistencies reported between candidate gene studies, and the small proportion of the variation in MD that can be attributed to SNPs, it is clear that much of the remaining genetic contribution to MD remains to be elucidated.

1.5.7 Mammographic density and breast tumour characteristics

It is uncertain whether high MD predisposes to the development of a particular tumour type, for example, a more aggressive tumour phenotype than those found in non-dense breasts. Therefore, a number of studies have investigated the association of percentage density and breast cancer sub-type. Overall these studies report largely inconsistent findings which are most likely a reflection of the wide variation present in study design, size, method of MD measurement, and whether other confounding factors were controlled for.

Given that MD appears to be a hormonally responsive trait, one might expect high MD to predispose to the development of tumours that are ER positive. Of those studies which made adjustments in their analysis to control for confounding factors, two groups have found an increased risk for the development of ER positive tumours only [152, 153]. However, several studies have found an increased risk for the development of both ER positive and ER negative tumours [154-157].

A recent Swedish study, controlling for possible confounding factors, found no association of MD with hormone receptor status, histological tumour type or lymph node status [158]. A significant association was seen with tumour size; however this may be due, in part, to the masking effect of high density breast tissue. More recently, a Norwegian study has also reported an association of tumour size and lymph node involvement with MD [159] and a North American study has reported association of MD with larger tumour size and higher tumour grade [157].

A North American case-control study has reported an increased risk for the development of Her2 negative, luminal A and triple negative tumours [155]. However, another larger North American study has reported no association with Her2 status [157].

Given the degree of inconsistency in the findings of studies which have investigated the association of MD with tumour subtype, McCormack and dos Santos Silva have recently performed a systematic meta-analysis incorporating over 24,000 cases. Their extensive analysis found a similar magnitude of association with ER+ and ER- tumours and no difference in the association with Her2 status [160]. This comprehensive analysis suggests that MD increases the risk of all breast tumour types.

1.5.8 High MD breast tissue fosters a tumour-promoting stromal microenvironment

Whilst there is a strong clinical correlation, MD has not yet been causally linked to tumour formation and there have been a limited number of studies investigating the biological pathways mediating MD. Given that the stroma forms the major constituent component of dense breast tissue, the pathways contributing to the density-associated breast cancer risk are likely to involve the stromal cells, ECM proteins, and their interaction with the epithelial component.

There has been much more focus on the role of the stromal microenvironment in established breast cancer than the role of stroma in the regulation of normal breast function, and clues as to the function of the stroma may be gleaned from this body of work, which is briefly summarised below.

1.5.8.1 Cancer associated fibroblasts

Cancer associated fibroblasts (CAFs) display an activated phenotype and share many similarities with activated myofibroblasts found at sites of wound healing and inflammation [161]. CAFs have been shown to contribute to the progression and outcome of many other solid tumours, in addition to breast cancer [162] through both common and distinct pathways depending on the tumour type [163].

At present, there is no single universal marker capable of reliably identifying all CAFs. Instead, a variety of different markers have been employed, often in combination. The

most commonly used are: high expression of alpha smooth muscle actin (SMA), fibroblast specific protein 1 (FSP1), fibroblast activation protein (FAP), platelet derived growth factor alpha receptor (PDGFRα) and beta receptor (PDGFRβ) [164]. The lack of a single marker for CAFs reflects the heterogeneity that exists between CAFs located within the same tumour microenvironment.

1.5.8.2 Activation of CAFs

The molecular events mediating the activation of CAFs are not fully understood. Tumour-cell derived TGF-β and SDF-1 are thought to be the principal activators of fibroblasts in the local tumour microenvironment via an autocrine signalling loop [165]. Other tumour derived factors which have been demonstrated to induce activation of fibroblasts include PDGFα/β [166], basic fibroblast growth factor (bFGF) [167] and interleukin 6 (IL-6) [168].

Recently Clare Isacke and colleagues have identified Wnt7a as a key factor secreted by aggressive breast tumour cells capable of inducing the CAF phenotype and triggering ECM remodelling to facilitate tumour cell invasion [169]. The authors propose Wnt7a acts to potentiate TGF-β signalling rather than activating the canonical Wnt signalling pathway [169].

Another crucial molecular event in the activation of CAFs appears to be down-regulation of tumour suppressor genes such as PTEN, p53, p21 and CAV-1. Levels of CAV-1 protein have been found to be lower in CAFs compared to normal fibroblasts [170] and this has been proposed to be a consequence of oxidative stress signalling / autophagy [171]. In addition, the absence of stromal CAV-1 expression has been repeatedly correlated with poor prognostic factors, resistance to therapy and reduced survival in breast cancer patients [172-174].

Gene expression profiling studies comparing CAFs to normal fibroblasts have attempted to further dissect the mechanisms involved in fibroblast activation and

crosstalk with the epithelial cells. Bauer et al found up-regulation of Wnt1 inducing signalling pathway protein 1 (WISP1), Collagen X and TGF-β isoforms in CAFs [175]. They proposed that WISP1 expression in CAFS could activate Wnt signalling in tumour cells in a paracrine manner [175].

Whether fibroblast activation can occur at an early stage in tumourigenesis, even before epithelial transformation, remains unclear.

1.5.8.3 CAFs and breast cancer initiation and progression

The ability of CAFs to facilitate tumourigenesis has been demonstrated in animal models where normal fibroblasts within the host animal were pre-irradiated before implanting premalignant epithelium. The irradiated hosts developed tumours much faster and displayed a more aggressive phenotype [176]. TGF-β was implicated as a key signalling pathway affecting the tumour latency [176].

CAFs are also reported to enhance tumour growth via the production of growth factors such as hepatocyte growth factor (HGF), bFGF, and insulin-like growth factor (IGF) [177, 178]. It has been reported by one group that the tumour cells act in a paracrine manner to stimulate HGF production by CAFs [179], resulting in a positive feedback loop promoting tumour growth. CAFs have also been suggested to fuel tumour growth by increasing local oestrogen production via amplified stromal aromatase activity [180].

Recent evidence also suggests a key role for CAFs in breast cancer cell invasion and metastasis. CAFs from the tumour/stroma interface have been proposed to be potent inducers of EMT [181] - the process by which tumour cells lose polarity and epithelial markers such as E-cadherin and gain a more invasive mesenchymal phenotype. In addition, CAFs are known to produce a number of MMPs [182], which not only facilitate invasion by degrading ECM, but have also been proposed to have a role in enhancing EMT [183]. CAFs have also been proposed to promote the transition of DCIS to

invasive carcinoma [184] via a mechanism involving COX-2, vascular endothelial growth factor (VEGF) and MMP9 [185].

1.5.8.4 CAFs and ECM remodelling

The proteases secreted by CAFs degrade and facilitate remodelling and reorganisation of the ECM, a process which is associated with cancer progression [186]. This process may be facilitated by high expression of syndecan-1 in CAFs, which has been reported to have a role in mediating collagen fibre alignment [187]. In addition, CAFs may aberrantly secrete proteins such as collagen, fibronectin and tenascin C, which could contribute to an altered ECM composition [178].

1.5.8.5 CAFs and inflammation

Infiltration of immune cells into the tumour microenvironment is observed in many solid tumours including breast cancer and is associated with tumour progression [188]. Cytokines and chemokines secreted by CAFs are potent recruiters of inflammatory cells to the tumour microenvironment [188]. The chemokine c-c motif chemokine ligand 2 (CCL2) has been reported to promote the infiltration of monocytes/macrophages into both the primary tumour and metastatic site in a mouse model [189]. Other inflammatory mediators secreted by CAFs include IL-6, tumour necrosis factor (TNF) and SDF-1, which are capable of recruiting a diverse array of inflammatory cells to the tumour microenvironment [190].

1.5.8.6 CAFs and epigenetic changes

Data regarding the role of epigenetic changes within the breast cancer microenvironment to breast cancer progression is limited. CAFs have been demonstrated to have different methylation patterns when compared to normal fibroblasts [191]. The CYP19 gene encoding aromatase has been found to be hypomethylated in stromal fibroblasts with enhanced aromatase activity [192]. Histone H3K27 has also been found to be hypomethylated in CAFs, resulting in increased

ADAM metallopeptidase with thrombospondin type 1 motif (ADAMTS1), which correlated with a more invasive phenotype [193].

1.5.8.7 CAFs and tumour metabolism

Recently, the contribution of CAFs to the metabolic reprogramming of the breast cancer microenvironment has been elucidated. Tumour cells display a complex, altered glucose metabolism where they utilise aerobic glycolysis to form lactate from glucose, a process known as the 'Warburg Effect' [194]. In addition, intra-tumoural hypoxia is also common, resulting in the activation of hypoxia inducible factor 1 alpha (HIF1α) signalling and the production of lactate and pyruvate via anaerobic glycolysis. Furthermore, tumour cells can also generate energy via oxidative phosphorylation [194].

The influence of CAFs on the tumour cell metabolism is known as the 'Reverse Warburg effect'. In this recently described model, CAFs undergo aerobic glycolysis and 'feed' the tumour cells with high energy metabolites pyruvate and lactate [195]. This altered fibroblast metabolism is proposed to be due to oxidative stress induced by reactive oxygen species (ROS), such as hydrogen peroxide, generated by intra-tumoural hypoxia [195, 196]. Oxidative stress results in reduction of CAV-1 and lysosomal activation and autophagy/mitophagy, inducing a shift to glycolytic metabolism [195]. Activated CAFs themselves produce ROS, which further activates more fibroblasts in the local environment.

The generation of ROS by CAFs is proposed to contribute to genomic instability and aneuploidy in the cancer cells, driving co-evolution of the tumour and stroma [171]. Eventually the tumour cells switch to metabolism predominantly via oxidative phosphorylation and ROS continue to be generated only by the stroma [171].

A recent study by Janine Erler and colleagues has suggested that the activated CAF phenotype may be reversible [197]. Chronic hypoxia resulted in CAF deactivation, less

contractile force and reduced ECM remodelling [197]. The authors propose a mechanism involving inhibition of prolyl hydroxylase domain protein 2 (PHD2), leading to HIF1α stabilisation and gradually reduced expression of SMA [197]. This study challenges the accepted notion of hypoxia being a tumour promoting factor within the microenvironment and suggests that there may be variations in response to hypoxia depending on the cell type involved [197].

A summary of the various mechanisms by which CAFs promote breast cancer progression is displayed in Figure 12.

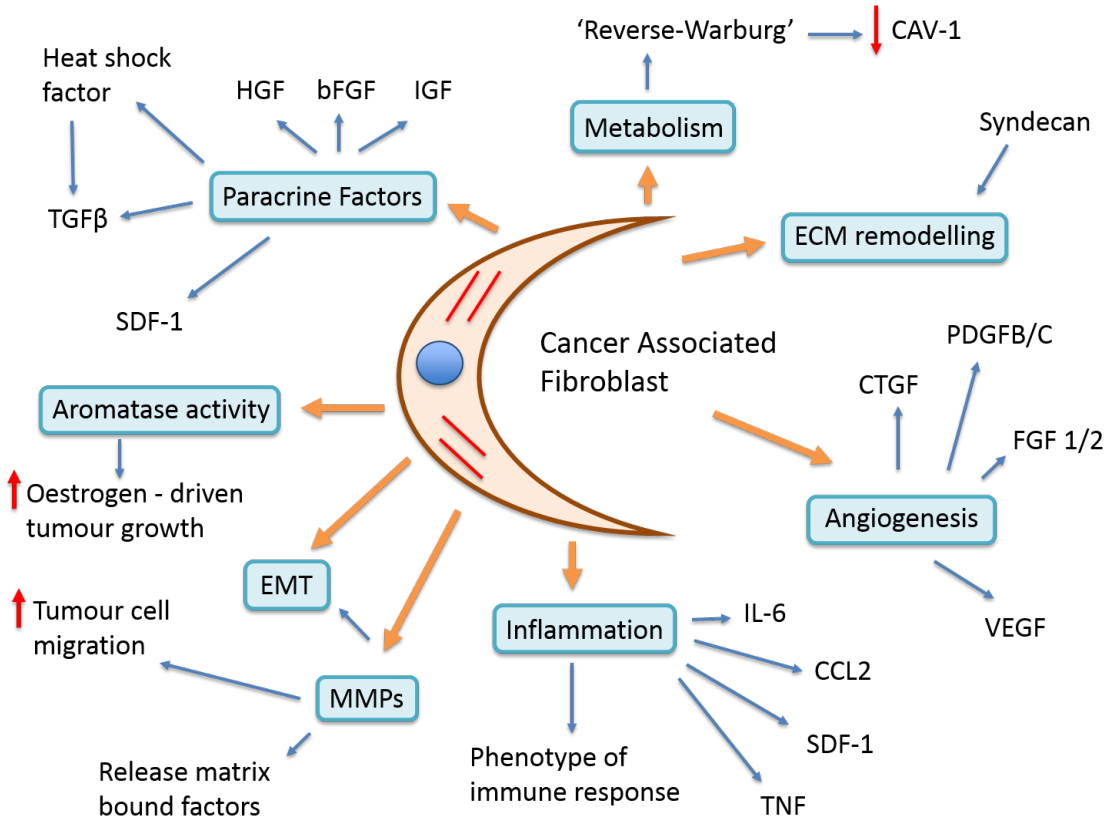

Figure 12: Summary of the multiple mechanisms by which CAFs contribute to breast tumour progression

In addition to CAFs, the tumour microenvironment consists of a diverse array of cell types including inflammatory cells, endothelial cells, adipocytes and ECM proteins which have been investigated for their potential contribution to the progression of breast cancer. These will not be covered in detail here.

1.5.9 Biological mechanisms contributing to density-associated risk

As discussed above, the stromal microenvironment is known to have an important role in the progression of established invasive breast cancer [198], acting via multiple diverse mechanisms including the influence of growth factors secreted by cancer associated fibroblasts and remodelling of the ECM [198, 199]. In addition, ECM gene expression levels are also associated with breast cancer prognosis [200], response to neo-adjuvant chemotherapy [201] and endocrine therapy [202]. Similar stromal mechanisms may also have a role in promoting tumourigenesis in breast tissue of high MD; the evidence for this is reviewed below.

1.5.9.1 Paracrine factors

It has been hypothesised that in areas of high MD, abundant stromal fibroblasts may aberrantly secrete growth factors and hormones/cytokines that stimulate epithelial cell proliferation [68, 203]. One study has suggested that local oestrogen production in the breast may be responsible for determining density [63]. Local oestrogen is synthesised from androgens in the breast by aromatase enzyme activity. Studies from Vachon et al and Huo et al have both reported increased aromatase immunoreactivity in the stromal cells of mammographically dense regions of the breast compared to non-dense regions [62, 63].

Increased stromal aromatase activity could result in sufficient local oestrogen production to stimulate epithelial cell proliferation and drive tumourigenesis. These findings are supported by in-vitro work from another group who have observed that cell density, shape and ECM proteins are capable of inducing stromal aromatase expression [204], thus providing a potential mechanistic link. This study also highlighted a role for IκB-kinase-β (IKKβ) as a key messenger in mediating this response. Figure 13 summarises the potential contribution of paracrine and mechanical factors to the induction of stromal cell aromatase activity.

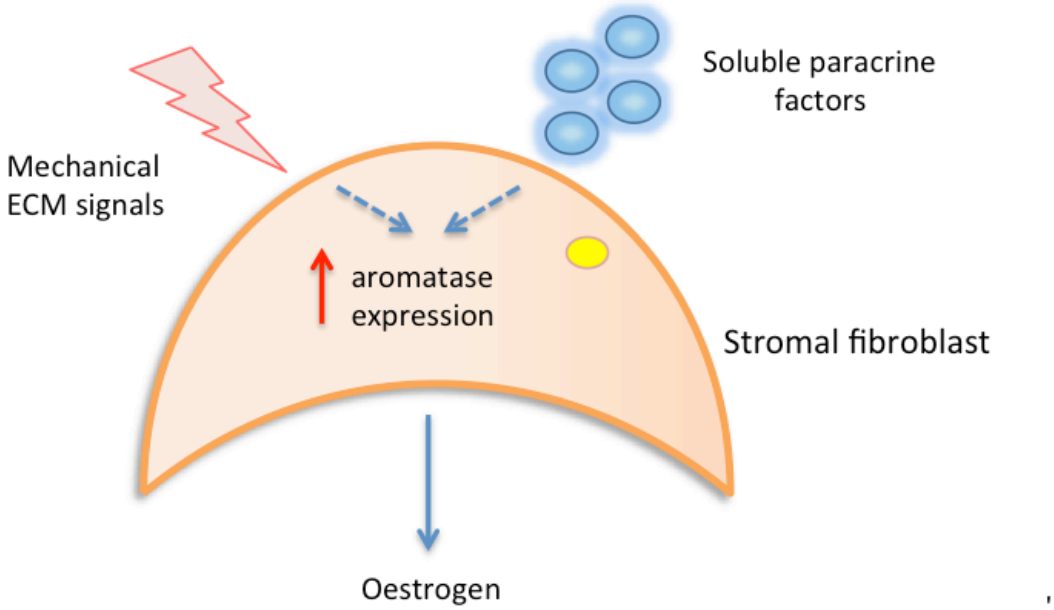

Figure 13: Local paracrine and mechanical signals may contribute to increased stromal aromatase expression, leading to increased oestrogen production and epithelial cell proliferation.

1.5.9.2 Collagen density, force and ECM stiffness

It has been suggested that increased collagen production by stromal fibroblasts contributes to a stiffer ECM. The inability of normal breast epithelium to contract stiff matrix causes a tensional imbalance, reflected by altered signalling pathways that have the potential to induce epithelial cell proliferation [205].

Patricia Keely and colleagues developed a bi-transgenic mouse to model high breast density, utilising the Col1a1^{tmJae} transgene which reduces collagen proteolysis, and examined the propensity for tumour formation with increased mammary collagen. They observed that higher stromal collagen density in mouse mammary tissue resulted in a threefold increase in tumour number and that the tumours which developed displayed a more invasive phenotype with greater local invasion and metastasis. The authors

propose a functional link between increased stromal collagen density and breast cancer initiation and progression [206].

Two possible mechanisms are suggested by which increased collagen density might promote tumour development. The first is a direct effect of increased matrix stiffness, resulting in a higher mechanical force and resistance to contractility on the epithelial cells. These forces might alter focal adhesion and Rho GTPase (Rho) signalling, resulting in increased proliferation [206]. The second proposed mechanism is more indirect and suggests that collagen density modulates the behaviour of mammary fibroblasts, resulting in altered secretion of soluble growth factors and chemokines such as TGF-β, epidermal growth factor (EGF) and IGF, which in turn influence epithelial cell behaviour [206], as summarised in Figure 14.

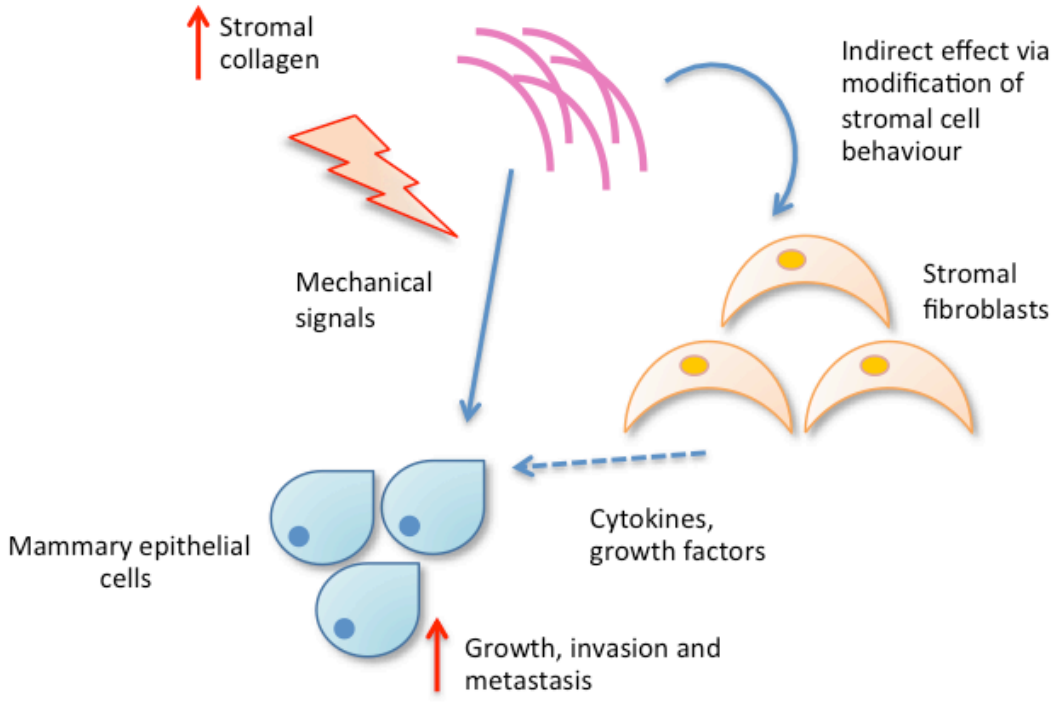

Figure 14: Increased collagen density may influence mammary epithelial cell behaviour directly *via* mechanistic signals or indirectly *via* modifying stromal cell behaviour.

Further work by this group examined whether collagen density alone, in the absence of fibroblasts, could alter mammary epithelial cell behaviour in 3D culture models. Supporting this hypothesis, greater collagen density alone increased matrix stiffness and promoted epithelial cell proliferation and invasion [207]. They showed that mammary epithelial cells formed clustered 3D matrix-adhesions containing activated focal adhesion kinase (FAK) in response to matrices of high stiffness. FAK, Rho and ERK were all found to be necessary for successful mechanotransduction of mammary epithelial cells, and inhibition of ERK or the Rho/Rho-associated protein kinase (ROCK) pathway reverted the invasive phenotype promoted by high density matrices [207].

The authors propose that continued mechanical stimulation from a dense stromal matrix results in sustained activation of FAK-Rho signalling which, in turn, up-regulates other pathways such as Ras- MAPK. ERK acts as a crucial bottleneck, regulating the response and inducing transcription of proliferation associated genes.

The significance of the Rho/ROCK pathway in mediating mechanotransduction has been further highlighted in a mouse model of tissue stiffness with sustained ROCK activation. ROCK increased tissue stiffness by increasing collagen deposition in mouse skin and stabilised epithelial nuclear beta catenin expression, leading to transcriptional activation of pro-proliferative pathways and epidermal thickening [208]. Inhibition of ROCK or actomyosin contraction inhibited these responses [208].

Soon et al examined the effect of high density collagen matrices on mammary epithelial cell behaviour. They found that high density matrices up-regulated the expression and activity of Rho-associated coiled-coil-containing protein kinase 1 (ROCK 1) via inhibition of notch homolog 1 (NOTCH1) [209]. ROCK- 1 is proposed to have a key role in cell contractility and facilitating epithelial cell migration in conjunction with MMP proteolytic activity, thus providing an alternative mechanism for density modulation of cell behaviour.

As well as collagen density, the significance of collagen fibre alignment within the ECM in facilitating mammary tumour cell invasion has also been investigated by the Keeley group [210]. Collagen changes at the tumour/stroma boundary termed 'Tumour associated collagen signatures' (TACS) have been classified and used as markers of malignant progression. TACS-3, where the collagen fibres are orientated perpendicular to the tumour boundary, has been shown to correspond to sites of focal invasion in mouse models [206, 210] and in an analysis of human tissue samples is also associated with poor disease-specific and disease-free survival [211].

The precise biological mechanisms mediating alignment of the ECM remain unclear though it has been suggested that syndecan signalling, cyclooxygenase-2 (COX-2) signalling, stromal immune cells and other glycoproteins such as neutrophil gelatinase-associated lipocalin (NGAL) may play a role [205].

The Schedin group has also recently examined the contribution of collagen fibre architecture within the ECM to mammary tumourigenesis [212]. They found that ECM from parous rats decreased tumour growth compared to ECM from nulliparous rats. Proteomic analyses revealed that, surprisingly, the parous matrix contained a greater quantity of collagen I than the nulliparous matrix [212]. Crucially, second-harmonic generation imaging revealed the collagen fibres in the parous matrix were significantly less linearised and aligned than those in the nulliparous ECM. Furthermore, using 3D cell culture models, they demonstrated that linearised collagen 1 induced cell phenotypes associated with invasive behaviour compared to non-linearised collagen [212].

These data once again emphasise the importance of assessing both qualitative and quantitative elements of the stroma when considering the impact of mammographic density.

1.5.9.3 Collagen cross-linking, integrin signalling and ECM stiffness

Weaver and colleagues have investigated how collagen cross-linking mediated by lysyl oxidase (LOX), a family of ECM cross-linking enzymes, can influence mammary epithelial cell behaviour. They used the MMTV-Neu mouse model of breast cancer to show that fibroblasts overexpressing LOX form a stiffer mammary fat pad and promote the growth and invasion of premalignant mammary epithelial cells. Similarly, inhibition of LOX resulted in a less stiff matrix and reduction in tumourigenesis [213]. LOX-mediated collagen cross-linking resulted in a stiff matrix characterised by increased focal adhesions, integrin clustering and subsequent increase in integrin signalling, increased FAK activity and enhanced PI3-K signalling. PI3-K signalling has been suggested to promote invasion of mammary epithelial cells in-vitro and tumourigenesis in-vivo [214]. Thus it is proposed that LOX may have a pivotal role in modulating breast tumour progression by stiffening the ECM and initiating integrin-mediated mechanotransduction of mammary epithelial cells. In keeping with these findings, LOX expression is also elevated in many cancers [215], has been associated with prognosis [216] and is proposed to have a key role in facilitating tumour metastasis [217].

The Weaver group has also conducted a biophysical study of human breast tissue stiffness at the epithelial-stromal border in adjacent normal, in-situ and invasive disease [218]. They found the histological progression from normal to in-situ to invasive disease was accompanied by progressive tissue stiffening characterised by increased collagen fibre deposition, linearisation and fibre thickening [218]. TGF-β signalling and immune cell infiltration also correlated with tissue stiffness, which was greatest in the more aggressive molecular tumour subtypes (basal-like and Her2 over-expressing) [218]. This study further demonstrates the association of breast tissue stiffening and cancer initiation and progression.

The same group have also studied the molecular determinants of mammary epithelial cell mechanotransduction, and have highlighted a crucial role for the focal adhesion

component vinculin in translating the mechanical cues from a stiff ECM into tumour promoting intracellular signalling pathways [219].

It is suggested that a stiff ECM drives integrin binding and activation, forming focal adhesions. At the focal adhesion, vinculin is activated and binds talin and actin forming a stable talin-vinculin-actin complex. The stabilisation of this complex facilitates PI3-K conversion of phosphatidylinositol 4,5-bisphosphate (PIP2) to phosphatidylinositol (3,4,5)-trisphosphate (PIP3), phosphorylation of FAK and AKT, and up-regulation of pro-tumourigenic signalling pathways [219]. Thus, common mechanisms for mammographic density signalling, centering around focal adhesions and the cytoskeleton, are becoming apparent, as summarised in Figure 15.

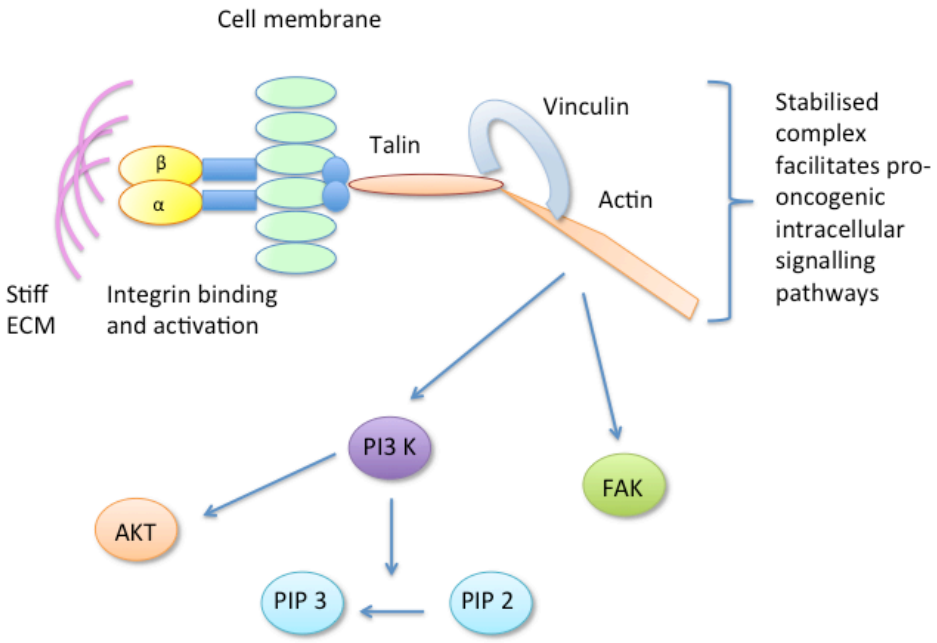

Figure 15: The focal adhesion component vinculin is activated in response to stiff ECM, forming a stable talin-vinculin-actin complex which promotes pro-oncogenic signalling pathways.

The Weaver group have also reported that changes in ECM stiffness can modulate micro RNA expression [220]. They demonstrated that increased matrix stiffness in both human and mouse mammary tissue induces expression of micro RNA-18a (miR-

18a) via integrin-dependent activation of beta catenin and MYC. miR-18a subsequently interacts and inhibits expression of the tumour suppressor gene PTEN, which itself is a negative regulator of PI3-K activity – previously demonstrated as a key pathway promoting mammary epithelial cell malignant progression [213].

miR-18a was also noted to indirectly inhibit PTEN expression via decreasing levels of homeobox A9 (HOXA9) (Figure 16). Interestingly, loss of PTEN expression in breast CAFs has also been implicated in mammary tumourigenesis [221], acting via a mechanism involving down-regulation of micro RNA 320 [222]. Whether this response can be modulated by tissue/ECM stiffness is unknown.

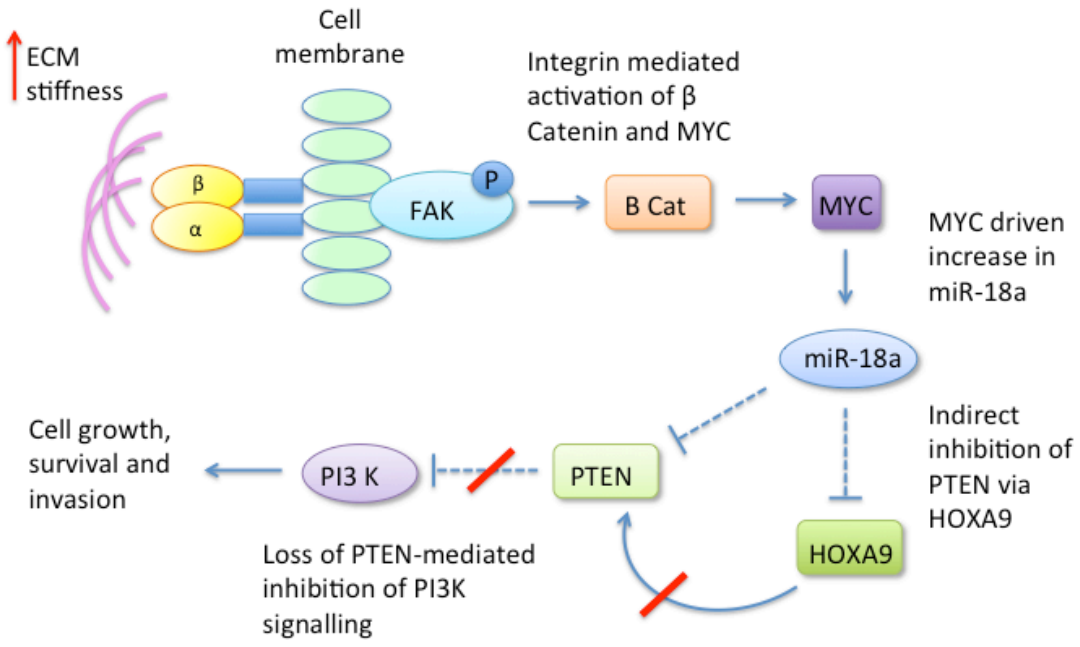

Figure 16: Dense ECM induces expression of micro RNA 18a via activation of MYC and beta catenin. miR-18a inhibits PTEN both directly and indirectly via HOXA9, resulting in up-regulation of PI3-K signalling.

In the Weaver study, miR-18a levels were able to distinguish luminal A from luminal B tumours and high miR-18a expression was predictive of poor outcome in tissue

biopsies of patients with luminal breast cancers, suggesting that this pathway could be utilised clinically. Whether this could be used to monitor patient response to chemopreventive measures remains to be determined.

1.5.9.4 Reduced expression of CD36

One of the key features of high mammographic density is the change in balance of adipose tissue to fibrous stroma, and it might be anticipated that factors determining adipose differentiation may be altered. A recent study from Tlsty and colleagues has suggested a critical role for the transmembrane receptor CD36 in mediating MD by controlling two key density-determining factors: stromal adipocyte content and ECM accumulation [223].

Gene expression profiling was used to determine differentially expressed genes in fibroblasts from high and low density disease-free breast tissue and cancer associated fibroblasts. CD36 expression was repressed in a range of stromal cell types (fibroblasts, adipoytes, endothelial cells) in both tissues of high MD and in tumour stroma. Loss of stromal CD36 expression in-vitro and in-vivo resulted in less fat accumulation and greater ECM accumulation, a phenotype shared by tissues of high MD and desmoplastic tumour stroma [223].

The authors suggest that reduced CD36 expression across multiple stromal cell types results in a complex, co-ordinated set of signalling pathways which increases the risk of tumour development via a variety of mechanisms including adipocyte differentiation, angiogenesis, cell-ECM interaction and immune signalling. In addition, clinically more aggressive tumours were associated with a greater degree of CD36 repression [223]. These findings highlight the potential importance of CD36 as a targetable stromal biomarker of MD-associated risk in the cancer prevention setting.

Further work by this group has demonstrated that epithelial cells in high MD tissue show more DNA damage signalling, shorter telomeres and increased activin A

secretion compared to low density tissue [224]. In addition, epithelial expression of activin A and telomere dysfunction were capable of reducing CD36 expression in the surrounding stromal fibroblasts, suggesting a potential pathway by which high MD tissue might arise. Whether the initiating DNA damage event occurs in the epithelial or stromal compartment of the breast remains to be elucidated, but these studies highlight the dynamic interaction between stromal and epithelial compartments.

1.5.9.5 JNK-1 stress signalling and the myofibroblast phenotype

Further interrogating gene expression array data from low and high density fibroblasts, Lisanti et al focused on genes that were transcriptionally up-regulated by at least 1.5 fold in high compared to low density fibroblasts [225]. They performed gene-set enrichment analysis and found that high density fibroblasts demonstrated up-regulation of several cellular processes including stress signalling, stemness, angiogenesis, inflammation and fibrosis. These processes are similar to those observed in the wound healing response and could potentially mediate a pro-inflammatory and pro-fibrotic microenvironment, with high density fibroblasts sharing similar characteristics to activated myofibroblasts.

In addition, when the high density fibroblast gene signature was compared to the profile of tumour stroma, c-Jun N-terminal kinase 1 (JNK-1) stress signalling emerged as the most significant biological process shared between the two data sets [225]. The authors postulate that the stromal JNK-1 activation occurs via stressors in the microenvironment such as reactive oxygen species, TGF-β and fibroblast growth factor (FGF) signalling. The activated JNK-1 stress signalling mediates the onset of a 'myofibroblast' phenotype characterised by ongoing inflammation and fibrosis, resulting in pro-tumourigenic, high density stroma (summarised in Figure 17) [225].

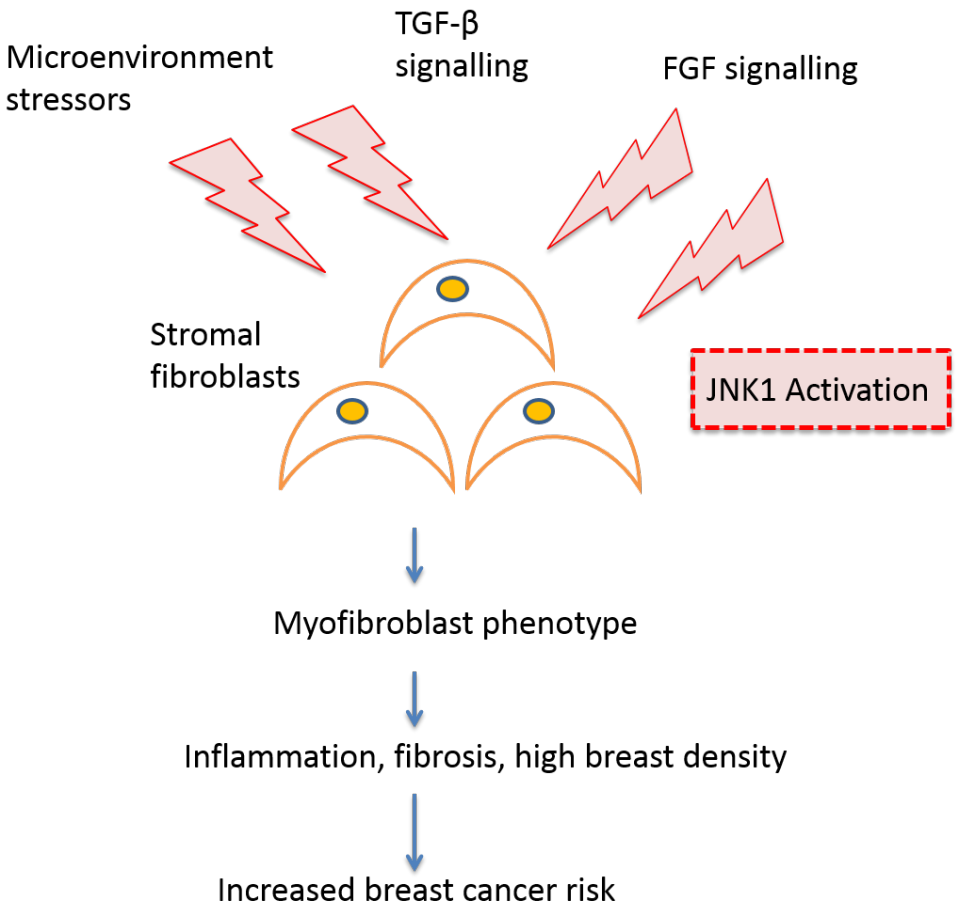

Figure 17: Microenvironment stressors induce activation of JNK-1 signalling in breast stromal cells. JNK-1 signalling confers a pro-inflammatory, pro-fibrotic 'myofibroblast' phenotype, leading to increased breast density and cancer risk. Adapted from Lisanti et al [225]

The authors also highlight a potential role for JNK-1 inhibitors as a cancer prevention strategy by inhibiting the development of the high density fibroblast phenotype. Whether such markers of an activated stroma could be used to measure patient risk and as indicators of response to treatment strategies is an intriguing possibility.

1.5.9.6 Mitogenesis, mutagenesis and the 'inactive' stromal microenvironment gene signature

Martin and Boyd have proposed that the combined effects of cell proliferation (mitogenesis) and genetic damage to proliferating cells by mutagens (mutagenesis) may account for the increased risk of breast cancer with high MD [226]; a hypothesis similar to the concept of 'breast tissue ageing' proposed by Pike [84].

The Martin and Boyd model has been further adapted by Sun and colleagues, who examined stromal gene expression signatures from non-neoplastic breast tissue adjacent to invasive carcinoma in a series of breast cancer patients. They found that high MD was particularly associated with an 'Inactive' stromal microenvironment signature [57]. This inactive subtype was associated with increased stromal composition, higher expression of cellular adhesion genes, increased oestrogen response gene expression and reduced TGF-β signalling. Interestingly, the observation of reduced TGF-β signalling in high MD stroma is somewhat contradictory to the model proposed by Lisanti et al, discussed in the previous section. A possible explanation for this discrepancy is that the morphologically normal tissue adjacent to invasive carcinoma sampled in the study by Sun et al may be displaying aberrant gene expression, due to the proximity to the tumour. Therefore, it may not be representative of truly non-neoplastic breast tissue.

These data further emphasise the importance of stromal biology in mediating MD. The revised Martin and Boyd model incorporates and highlights the role of the stromal microenvironment in breast tumourigenesis.

Reduced TGF-β signalling in dense breast tissue has also been observed by Yang and colleagues who compared gene expression in high and low density non-tumour breast tissue taken 5cm away from invasive carcinoma [71]. A number of genes implicated in TGF-β signalling showed decreased expression in dense tissue (TGFBR2, SOS, SMAD3, CD44 and TNFRSF11B). Immunohistochemical analysis of the same tissues showed higher stromal expression of COX-2 and proliferation marker Ki67 [71]. Inhibition of TGF-β by COX has previously been reported in other organ systems [227] and loss of TGF-β ligand-mediated inhibition of mammary epithelial cell proliferation is proposed as a potential mechanism for density-associated breast cancer risk.

The authors also suggest a potential role for COX-2 inhibitors as a breast cancer prevention strategy for high risk individuals. This is somewhat counter-intuitive, given the established pro-fibrogenic role of TGF-β. Furthermore, of note, the increased stromal Ki67 expression observed in this study is inconsistent with data from other groups who have reported no association of Ki67 with MD [62, 228, 229].

Chew and colleagues have also reported increased COX-2 expression in the stromal and (to a lower degree of significance) epithelial cells of high MD breast tissue in both human samples and a xenograft model of MD [72]. Furthermore, tumours developing in a mouse model of high collagen density breast tissue were found to express more COX-2 than those developing in wild type mammary stroma [230]. When the transgenic mice were treated with COX-2 inhibitors, the tumours which developed were smaller and displayed a less aggressive phenotype [230]. Furthermore, the stromal microenvironment of these tumours showed reduced recruitment of neutrophils and macrophages and fewer SMA expressing activated fibroblasts [230].

The contribution of neutrophils to tumour initiation in high density stroma was further explored by the same group [231]. They found enhanced neutrophil cytokine signalling in tumours developing in high collagen density stroma compared to wild type stroma [231]. In addition, when neutrophils were depleted, the number of tumours developing in high density stroma was significantly reduced [231]. No effect of neutrophil depletion was observed in tumours developing in wild type stroma [231].

This study further highlights the potential significance of COX-2 in mammary tumourigenesis within a high collagen density microenvironment and once again highlights a potential therapeutic role for COX-2 inhibitors. Furthermore, the findings once again allude to the pro-inflammatory nature of high MD stroma with a key potential tumour-promoting role of neutrophils.

A summary of our current understanding of the complex stromal biological pathways conferring MD-associated breast cancer risk is displayed in Figure 18 below.

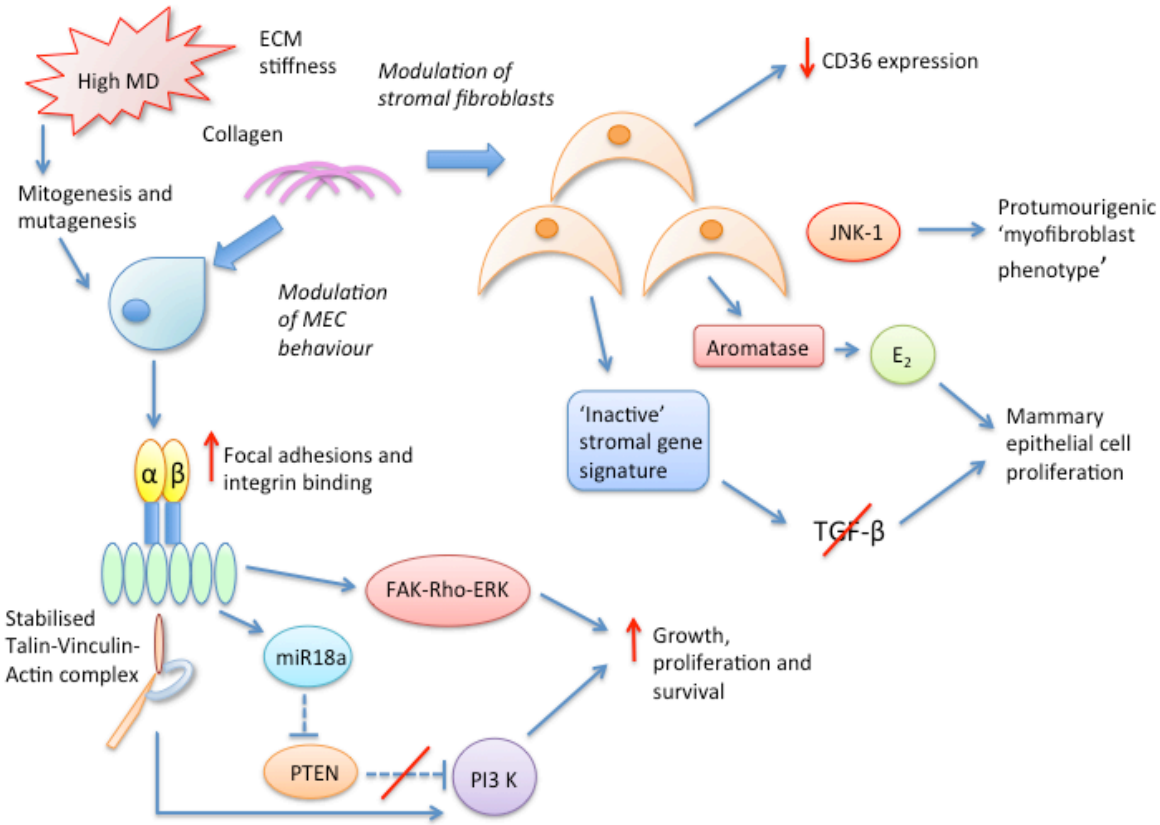

Figure 18: Potential stromal molecular pathways mediating the density-associated cancer risk conferred by high MD breast tissue.

Despite the progress made in these preclinical studies towards identifying potential stromal markers and signalling pathways contributing to breast density, this has not readily translated into clinically relevant markers or targets. Further clinically applicable approaches are needed to identify the key stromal molecules driving density-associated risk in humans.

1.6 Clinical implications

The influence of MD on breast cancer risk has a number of important clinical implications, particularly with regard to identification of high risk individuals, screening and prevention. Currently MD is not routinely measured as part of the NHS Breast Cancer Screening Programme in the UK.

A number of studies have investigated whether including a measure of MD improves risk estimation compared to standard risk models [232-235], with some additionally incorporating SNPs associated with breast cancer risk into their prediction models [236]. All of these studies found a small but consistent improvement in risk estimation with the addition of MD measures. Furthermore, a recent prospective study of over 50,000 women in the UK found that MD alone was a stronger univariate risk factor for breast cancer than both the Tyrer-Cuzick and Gail models [44], and in their full analysis added accuracy to both models [44]. These findings serve to emphasise the potential clinical power of MD to accurately identify populations at increased risk of breast cancer.

Screening at more frequent intervals with more than one imaging modality may be appropriate for women with dense breasts due to their increased risk of developing cancer and their increased risk of tumour 'masking'. A recent analysis of personalised mammographic screening according to MD, age, family history and history of breast biopsy was found to be cost effective [237].

The investigators of the Predicting Risk at Screening (PROCAS) study in the UK have proposed that the first mammographic screening appointment as an ideal opportunity to assess an individual's future breast cancer risk using a model which incorporates MD and educate them regarding relevant lifestyle modifications and, if appropriate, chemoprevention [238]. The same group also report that the majority of study participants wished to receive risk information and that this had no detrimental effect on

their attendance for screening [239]. Introduction of risk assessment to the initial screening appointment could facilitate the development of risk-stratified screening to closely monitor those at higher risk whilst those at low risk may not need to attend as frequently. Currently the NHSBCSP only provides additional screening with magnetic resonance imaging (MRI) for those at very high risk of breast cancer with BRCA1/2 or TP53 gene mutations.

In order for chemopreventive strategies for high risk individuals to have an impact on breast cancer incidence, there would need to be a substantial increase from the uptake of tamoxifen reported in the IBIS I trial of just 10% [240]. Barriers to increased uptake include concern regarding the potential risks of thromboembolic events and endometrial cancer and, in particular, the anti-oestrogenic side effects of tamoxifen including debilitating hot flushes and sexual dysfunction [241, 242]. It has been estimated that up to 50% of breast cancers could be prevented in the subgroups of women at high and moderate risk if there was maximal uptake of current chemoprevention [243].

It has been postulated that change in MD could be used as a marker of response in clinical trials evaluating breast cancer prevention strategies [244]. This could reduce the need for long observation periods currently required to evaluate the likelihood of developing breast cancer following an intervention. Interestingly, a number of studies have suggested that reduction in MD can be used as a prognostic marker of response to tamoxifen in the adjuvant setting [111, 245]. Li and colleagues reported that postmenopausal women taking adjuvant tamoxifen showing a greater than 20% reduction in MD had a 50% reduced risk of death from breast cancer [111]. In addition, Ko et al found reduction in MD with adjuvant tamoxifen was associated with a reduced risk of recurrence in ER positive breast cancer patients [245]. Furthermore, Nyante et al found a reduced risk of breast cancer with a substantial reduction in MD following adjuvant tamoxifen in both pre- and postmenopausal women, though the protective

effect was only seen in those women with a moderate to high baseline level of MD [246].

Subsequent work from this group found that the majority of MD reduction with adjuvant tamoxifen occurs after the first year of treatment with very little further reduction after the fifth year [247]. A further subset analysis, limited by statistical power, demonstrated that patients who showed a ≥10% reduction in MD at one year had a non-significant improvement in disease free survival [248]. These data suggest that a single measurement of MD after one year of treatment may be sufficient to identify those individuals likely to respond well to treatment in both the preventive and adjuvant settings. Importantly, non-responders can also be identified and potentially switched to an alternative treatment regime.

Brentnall and colleagues recently investigated whether SNPs in the regions of ZNF423 and CTSO could predict response to tamoxifen in the preventive setting. However, no significant predictive value for SNPs in either gene region was identified [249].

MD is more strongly associated with breast cancer risk than other variables such as family history and reproductive factors. Therefore, understanding the biology of MD may allow individual risk prediction for breast cancer. MD also offers the advantage over other breast cancer risk factors of being modifiable, which provides exciting potential for targeted therapeutic intervention to reduce both MD and breast cancer risk.

Targeting components of the microenvironment is already an established strategy in the adjuvant treatment setting for a number of different tumour types [250, 251]. The most advanced of these strategies are agents targeting VEGF signalling in the tumour vasculature with a number agents now licenced for use in several metastatic cancers in combination with cytotoxic therapies [251, 252]. Beyond VEGF there are several other

anti-angiogenic agents in preclinical trials targeted against PDGF and FGF signalling pathways [253, 254].

Components of tumour-associated inflammation are also a focus of new agents targeted against the microenvironment. An IL-6 neutralising antibody is currently undergoing evaluation in clinical trials [255], and neutralising antibodies against human chemokines have shown promising results in preclinical models of prostate and breast cancer [256]. Disrupting tumour-stroma crosstalk via integrin inhibition is also the subject of clinical trials with agents showing limited anti-tumour efficacy at present [257, 258]. Specifically targeting cancer associated fibroblasts, utilising their expression of fibroblast activation protein α, remains at the preclinical stage of development. Such strategies involve; the development of anti-FAP antibodies conjugated to cytotoxic drugs [259], utilising the enzymatic activity of FAP to activate pro-drugs in the vicinity of the tumour [260], and vaccines targeted against FAP [261].

Harnessing similar approaches in the preventive setting to target the stromal molecules and pathways mediating MD could provide an effective cancer prevention strategy. Thus, further work to dissect the complex biological pathways mediating MD is urgently needed to identify novel, clinically relevant, biomarkers driving the density-associated risk.

1.7 Exploiting the modifiability of MD by tamoxifen

The drug tamoxifen has been demonstrated to reduce both MD and breast cancer risk in a proportion of high risk women. Thus, the ability to exploit the modifiability of MD with tamoxifen could prove of significant clinical value.

1.7.1 Pharmacology of tamoxifen

Tamoxifen is a member of the selective oestrogen receptor modulator (SERM) family of drugs. It is described as a SERM due to its complex pharmacology, displaying a variety of tissue-specific actions at the oestrogen receptor (ER) [262, 263]. This family of drugs contain a hydrophobic core that mimics the steroid backbone of oestrogens, grafted to a dialkylaminoalkyl side chain [264].

In mammary epithelial cells the classical mechanism of action of tamoxifen is as a competitive antagonist at oestrogen receptor alpha (ERα). Binding of tamoxifen to ERα blocks the pro-proliferative effects of oestrogen (17-β oestradiol) on neoplastic ERα-positive mammary epithelial cells [265, 266].

The binding of 17-β oestradiol to ERα up-regulates the expression of c-MYC and cyclin D1 and promotes cell cycle progression from G1 to S phase in mammary epithelial cells [267]. Hence the binding of oestrogen to ER and subsequent target gene stimulation is considered the predominant mechanism responsible for oestrogen-driven mammary tumour initiation and progression [268].

The diverse functions of oestrogens are mediated via specific oestrogen receptors (ER). Currently there are two identified ER isoforms – ERα and ERβ which share a common structural architecture and function as ligand-dependent transcription factors that stimulate target gene expression [269].

Expression of both ERα and ERβ has been demonstrated in mouse skin fibroblasts [270]. The expression of ER in human breast fibroblasts remains uncertain.

1.7.2 Tamoxifen metabolism

Tamoxifen itself has weak affinity for ER [265] however, undergoes extensive first pass metabolism in the liver to two active metabolites: N-dimethyltamoxifen (subsequently metabolised to α-hydroxytamoxifen, N-didesmethyl-tamoxifen and 4-hydroxy-N-desmethyl-tamoxifen (endoxifen)) and 4-hydroxy-tamoxifen (4-OHTam) [271], a small proportion of which also undergoes further metabolism to endoxifen. These active metabolites have substantially higher affinity for ER (30-100 fold) than tamoxifen [265].

Several enzymes are known to regulate the metabolism of tamoxifen [272] (Figure 19). The conversion of tamoxifen to N-dimethyltamoxifen, and of 4-OHTam to endoxifen is predominantly regulated by the activity of hepatic cytochrome P450 3A4/5 (CYP3A4/5) [272]. Whereas, the conversion of tamoxifen to 4-OHTam, and of N-dimethyltamoxifen to endoxifen is predominantly regulated by activity of hepatic cytochrome P450 2D6 (CYP2D6) [272].

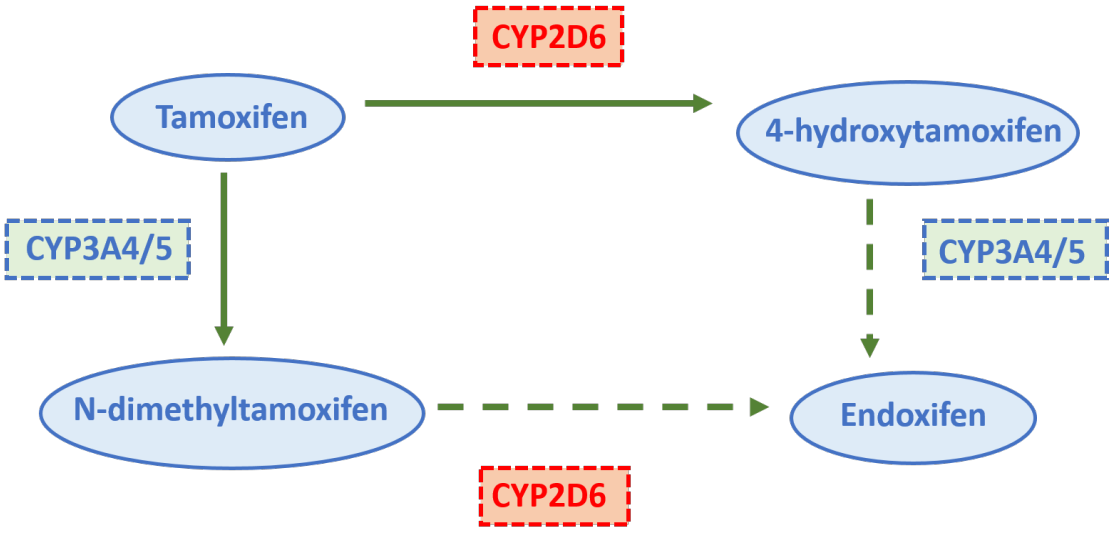

Figure 19: Metabolism of tamoxifen. Tamoxifen undergoes first pass metabolism in the liver to N-dimethyltamoxifen and 4-Hydroxytamoxifen which both can be further metabolised to endoxifen. The cytochrome P450 enzymes CYP2D6 and CYP3A4/5 have important roles in regulating the metabolism of tamoxifen.

Recent attention has focused on genetic variants (polymorphisms) in CYP2D6, which have been proposed to alter the activity of the enzyme, and potentially influence how

patients respond to tamoxifen treatment [273]. The potential therapeutic significance of CYP2D6 genotype is unclear and a recent meta-analysis of 25 studies failed to find an association between CYP2D6 genotype and tamoxifen response for all-cause mortality or overall survival in breast cancer patients [274]. However, an association of CYP2D6 genotype with change in MD with tamoxifen treatment has been reported in the preventive setting [114].

The concentration of tamoxifen and its metabolites within breast tissue is hugely variable due to the variation in individuals' ability to metabolise the drug [275] and the fact that the drug accumulates in tissue with treatment [276, 277]. One study has investigated the concentration of tamoxifen, endoxifen and 4-OHTam after 28 days treatment and found that all three showed substantial tissue accumulation, with 4-OHTam showing the greatest accumulation (up to 1411 fold the serum concentration, equivalent of up to 10μM) in cancer tissue [278]. In addition, there was significant variation in the tissue concentrations of all metabolites between individuals, emphasising the complex nature of tamoxifen metabolism.

This substantial variability in tissue concentration may contribute towards the differences seen in patient response to tamoxifen in the preventive and adjuvant settings.

1.7.3 Clinical use of tamoxifen

Tamoxifen has been used as a treatment for established breast cancer since the 1970s. A meta-analysis of 20 randomised clinical trials demonstrated that five years adjuvant tamoxifen for ERα positive breast cancer reduced both recurrence (RR 0.53, 95% CI: 0.47-0.59) and mortality (RR 0.71, 95% CI: (0.61-0.81) [279]. Furthermore, the benefit of tamoxifen persists if treatment is continued for 10 years [279].

In clinical practice, the level of expression of the ERα isoform is the principle marker used to predict response to tamoxifen. Tumours which are designated ER-negative may not be completely devoid of ER and may still express very low levels of ERα.

Despite the reported benefits of tamoxifen, a proportion of ERα positive breast cancer patients develop resistance to treatment [280, 281]. The mechanisms governing tamoxifen resistance are presently unknown. As discussed previously, tamoxifen has also shown efficacy in the prevention of breast cancer in high risk individuals [282] (which appears to be related to a corresponding decrease in breast density, as mentioned above) and as a treatment for DCIS [283].

The long term safety of tamoxifen is a subject of controversy due to significant treatment-related toxicities including increased risk of endometrial cancer and thrombo-embolic events [284]. Furthermore, patient adherence to medication is also a significant challenge due to the debilitating anti-oestrogen side effects [241, 242]. Thus, there is significant interest in dissecting the mechanisms by which tamoxifen exerts its cancer protective effect, so that these pathways might be specifically targeted and undesirable toxicities and side effects avoided.

Interestingly, 5-10% of ERα negative breast tumours have been reported to show a degree of sensitivity to tamoxifen therapy [285, 286]. A number of studies have suggested that expression of the oestrogen receptor beta (ERβ) isoform may explain sensitivity to treatment in patients with ERα negative tumours [287-289], however there are inconsistencies in findings between studies. Saal and colleagues found that ERβ protein levels were predictive of response to tamoxifen treatment with a strong positive correlation reported for patients with ERβ +/ ERα – tumours and disease free survival [287]. Conversely, a recent study from the Mayo clinic found that expression of ERβ1 was associated with improved outcome following tamoxifen treatment in patients with co-expression of ERα [288].

1.7.4 ER-Independent mechanisms of action

In addition, there is emerging evidence of alternative mechanisms of action, independent of the ER [290, 291]. Tamoxifen has been found to have a variety of non-genomic effects at therapeutic doses [292].

1.7.4.1 Effect on cholesterol and sphingolipid metabolism

After the ER, tamoxifen has another high affinity binding site in the endoplasmic reticulum known as the microsomal anti-oestrogen binding site (AEBS) [293]. Recent work by Poriot and colleagues has suggested that the binding of tamoxifen and other SERMs to the AEBS inhibits cholesterol epoxide hydrolase (ChEH) enzyme activity, resulting the in the accumulation of cholesterol precursors [294, 295]. This mechanism has been proposed to contribute to the anti-cancer effects of tamoxifen in breast tumour cells [296].

In addition, tamoxifen and its metabolites have been found to influence sphingolipid metabolism [297]. This mechanism has been proposed to have clinical significance by enhancing the pro-apoptotic properties of ceramide-based chemotherapy regimens. In addition, a direct effect on neutrophil behaviour by tamoxifen has been observed and attributed to modulation of intracellular ceramide [298].

Reddel and colleagues reported in 1985 that tamoxifen was capable of inhibiting proliferation and inducing apoptosis in a number of ER negative breast cancer cell lines [299]. Since then there have been significant interest in trying to delineate the ER-independent, pro-apoptotic, mechanisms of action of tamoxifen.

1.7.4.2 Rises in intracellular calcium

A number of studies have reported that tamoxifen significantly increases intracellular calcium levels in a variety of ER negative tumour cell lines, and this is associated with

increased apoptosis [300-302]. However, the precise mechanism leading to enhanced intracellular calcium has yet to be determined.

Recently, it has been reported that tamoxifen has low micromolar affinity for cannabinoid 1 and 2 (CB1 and CB2) receptors and demonstrates an inverse agonist effect upon binding [303]. Normally agonists of CB1 and CB2 induce the inhibition of intracellular calcium influx [304], suggesting that the inverse agonist of tamoxifen at these receptors may explain the observed rise in intracellular calcium levels.

The induction of oxidative stress by tamoxifen has also been proposed to modulate JNK-1 signalling [305], a pathway proposed to initiate apoptosis via increasing the activity of caspase 8 [305] and up-regulating the expression of Fas-ligand [306]. Tamoxifen has also been reported to induce apoptosis in the triple negative breast cancer cell line MDA-MB-231 by reducing AKT phosphorylation when used in combination with the phosphoinositide-dependent kinase-1 (PDK1) inhibitor OSU-03012, however suppression of AKT phosphorylation was also noted with PDK1 inhibitor treatment alone [307]. Thus it is not clear whether the reported induction of apoptosis can truly be attributed to the effect of tamoxifen treatment.

1.7.4.3 Effect of tamoxifen on the stromal microenvironment

The ability of tamoxifen to directly modulate the stromal microenvironment is a novel concept, contrary to the classical rationale for tamoxifen prescription as a targeted therapy against ER expressed in neoplastic breast epithelial cells. Nevertheless, there is emerging data to support a direct effect on the mammary stroma.

Much of this work has focused on the ability of tamoxifen to modulate TGF-β signalling. TGF-β is a pro-fibrotic cytokine up-regulated in the wound healing response and is the most potent known inducer of fibroblast activation to the myofibroblast phenotype [308]. As discussed in the earlier section, gene expression studies have highlighted up-

regulation of TGF-β signalling in high density mammary stroma [225]. Thus it is plausible that tamoxifen may modulate density by inhibiting the pro-fibrotic actions of TGF-β.

TGF-β signalling is mediated either via the canonical pathway involving phosphorylation of SMAD proteins or via a variety of non-canonical routes [309]. The canonical signalling pathway involves one of the TGF-β superfamily of ligands (including TGF-βs, bone morphogenic proteins (BMPs), growth and differentiation factors (GDFs), Anti-Müllerian hormone (AMH) and activins) binding to a TGF-β type II receptor dimer (Figure 20A) [310]. The type II receptor is a serine/threonine receptor which recruits a type I receptor dimer forming a hetero-tetrameric complex (Figure 20B). The type II receptor phosphorylates serine residues on the type I receptor, activating it (Figure 20B) [310].

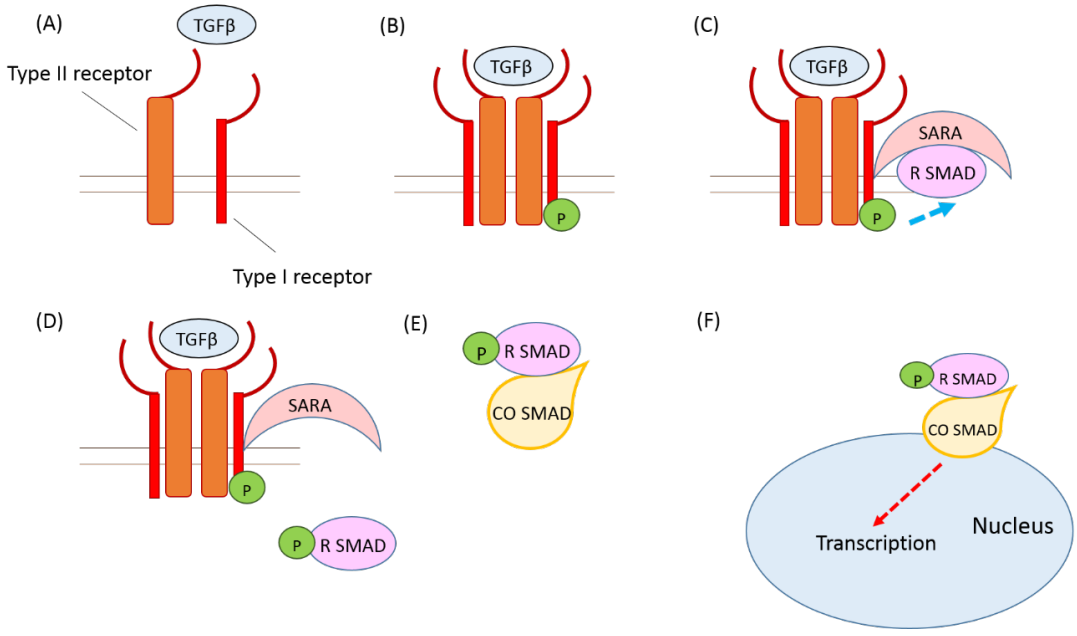

Figure 20: The canonical TGF-β signalling pathway. TGF-β ligands bind to a type II receptor (A) which recruits a type I receptor to form a hetero-tetrameric complex (B). The type II receptor phosphorylates serine residues on the type I receptor and activates it (B). One of five R-SMAD proteins binds to the activated type I receptor via interaction with the SARA protein (C). The type 1 receptor phosphorylates the R-SMAD, inducing a conformational change and subsequent dissociation of the R-SMAD from the receptor and SARA (D). The phosphorylated R-SMAD associates with a CO-SMAD (E) and translocates to the nucleus, binds to transcription factors, facilitating transcription of target genes (F).

One of five receptor regulated SMAD proteins (R-SMAD) binds the type I receptor via an interaction with the SMAD anchor for receptor activation (SARA) protein (Figure 20C) [311]. In the case of the TGF-β ligands, intracellular signalling is mediated via SMAD 2 and SMAD3 [311]. The type I receptor subsequently phosphorylates the R-SMAD, inducing a conformational change resulting in the dissociation of the R-SMAD from the receptor complex and SARA (Figure 20D) [311]. The phosphorylated R-SMAD then associates with a CO-SMAD such as SMAD 4 (Figure 20E). The R-SMAD/CO-SMAD complex translocates to the nucleus, binds transcription factors resulting in the transcription of target genes (Figure 20F) [311].

TGF-β can also signal through a variety of non-canonical (non-SMAD) pathways to mediate changes in gene transcription and cellular function [312]. These pathways include branches of the MAP kinase pathways, Rho-like GTPase pathways and PI3-K/AKT pathways [312].

A recent study from Carthy and colleagues found that tamoxifen inhibited TGF-β-mediated activation of primary skin and breast fibroblasts. They reported no effect on canonical TGF-β signalling but reported inhibition of non-SMAD signalling via ERK1/2 and transcription factor FRA2 [313]. Conversely, Kim and colleagues found that tamoxifen inhibited canonical TGF-β signalling in a mouse renal fibroblast cell line and inhibited renal fibrosis in a mouse model [314]. Thus, whilst a consistent inhibitory effect on TGF-β signalling has been observed in both of these studies, the precise mechanism of action remains to be elucidated and it is possible that differing tissue-specific mechanisms of action may exist.

The antifibrotic properties of tamoxifen have also been utilised clinically as a treatment for disorders of fibrosis such as chronic renal disease [315], dupytrens contracture [316], desmoid tumours [317] and idiopathic retroperitoneal fibrosis [318]. These

antifibrotic properties may contribute to remodelling of the mammary stroma and the observed reduction in MD with tamoxifen treatment [110].

A recent study by Shim and colleagues reports an anti-angiogenic effect of tamoxifen and other SERMs on endothelial cells by disrupting cholesterol trafficking, leading to an abnormal distribution of vascular endothelial growth factor receptor 2 (VEGFR2) [319]. In addition, an anti-angiogenic effect of tamoxifen has been reported in ER negative in-vitro and animal models of angiogenesis [320]. Therefore, tamoxifen may be able to influence the stromal microenvironment through diverse, ER-independent mechanisms.

2 Introduction and aims of the study

There is now robust epidemiological data demonstrating the protective effect of tamoxifen for women at high risk of breast cancer [113]. Furthermore, this protection is associated with a reduction in MD [110].

Recent studies consistently report that high density breast tissue corresponds predominantly to increased stromal tissue [54, 55]. This suggests that tamoxifen may be acting directly on the mammary stroma to reduce density and breast cancer risk. In addition, there is evidence from a variety of models that tamoxifen can directly modify stromal cell behaviour [115, 321].

These observations form the hypothesis for this study:

Tamoxifen protects the breast through a direct effect on stromal fibroblast function, modifying key biological pathways, reflected as a decrease in MD.

The biological mechanisms mediating density-associated breast cancer risk are poorly understood. Thus, the aim is to exploit the effects of tamoxifen on MD to elucidate the pathways involved in determining stromal density.

Knowledge of such pathways could be utilised clinically in the form of risk prediction and personalised screening regimens, prediction of response to chemopreventive agents such as tamoxifen, and the in development of novel targeted cancer prevention strategies.

To investigate this hypothesis, the aims are:

(i) *To use in-vitro models of primary human breast fibroblasts to dissect the effect of tamoxifen on stromal cell function.*

Initially, a cohort of patients' fibroblasts will be screened for response to tamoxifen. Data from Cuzick and colleagues suggest that 46% of high risk women show a significant reduction in MD (>10%) with tamoxifen [110], therefore it is anticipated that not all patients will respond. Target genes will be those implicated in generating stromal density and assays will be performed to measure fibroblast proliferation, migration, markers of activation and effect on TGF-β signalling.

(ii) To use RNA Seq to carry out a whole transcriptome analysis on the effect of tamoxifen on fibroblast gene expression.

The genome wide analysis will be undertaken to compare the transcriptome of tamoxifen treated vs vehicle control treated fibroblasts. The samples selected for this part of the analysis will be those demonstrating a significant response to tamoxifen in part (i).

(iii) Validation of selected pathways modulated by tamoxifen and investigation of the role of the ER in these pathways.

Significant changes in gene expression will be validated by quantitative real-time polymerase chain reaction (qRT-PCR) or western blotting.

Several of the 'top hit' genes modulated by tamoxifen are involved in cholesterol and lipid metabolism, therefore analysis of fibroblast phenotype and differentiation will also be undertaken.

(iv) To explore the impact of tamoxifen-modified fibroblasts on epithelial cell behaviour.

Data from in-vitro and in-vivo models suggests that a dense stroma promotes epithelial cell proliferation and, in pre-malignant cells, can promote tumorigenic behaviour, including invasion [213].

Fibroblasts pre-treated with tamoxifen or vehicle control will be cultured in 3D with epithelial cells. The effect on epithelial cell behaviour will be analysed by measuring proliferation (Ki67), colony size and morphology. The effect of fibroblast-derived matrix and conditioned media from fibroblasts pre-treated with tamoxifen and vehicle control, on epithelial cell proliferation, will also be assessed.

3 Methods and Materials

3.1 Fresh breast tissue acquisition

Fresh human breast tissue was obtained from samples donated to the Breast Cancer Now Breast (BCN)/ Barts Cancer Institute (BCI) tissue bank (Ethical Approval Reference 10/H0308/49, Cambridgeshire Ethics Committee October 2010). Following surgery, the tissue was examined by a pathologist and samples of fresh and snap frozen tissue were taken which would not compromise the diagnostic work up of the specimen.

3.2 Tissue definitions and abbreviations

Tissue samples were classified into the following categories (Table 3)

Tissue Type	Abbreviation	Definition
Normal Reducing Mammoplasty	N	Breast tissue removed purely for cosmetic reasons. No past history or family history of breast cancer.
Tumour	T	Tissue taken from within a tumour
Adjacent	A	Non-tumour tissue taken within 2cm of a tumour
Dense Surround	DS	Non-tumour tissue taken from more than 5cm from the tumour in an apparently dense area of breast tissue (macroscopic assessment by pathologist).
Non Dense Surround	NDS	Non-tumour tissue taken from more than 5cm from the tumour in an apparently non-dense area of breast tissue (macroscopic assessment by pathologist).
Prophylactic Mastectomy	PM	Non tumour breast tissue removed prophylactically due to high risk (Family history or BRCA mutation status).
Contralateral Prophylactic	CP	Non-tumour breast tissue removed prophylactically following tumour diagnosis in the opposite breast due to high risk of recurrence.
Contralateral	CM	Non-tumour breast tissue removed following tumour diagnosis in the opposite breast for cosmetic reasons/ breast asymmetry.

Table 3: Tissue sample definitions

3.3 Cell Culture

3.3.1 Isolation of primary human breast fibroblasts from breast tissue

Primary breast fibroblasts were isolated using an adapted protocol from Gomm et al [322] (summarised in Figure 21). The fresh breast tissue was briefly washed in 70% ethanol, then three successive washes in RPMI (Sigma, R5886) supplemented with gentamycin (10µg/ml) (Sigma, G1397). The tissue was then chopped and digested overnight at 37^{o}C with collagenase (1mg/ml, Sigma, C2674) and hyaluronidase (1mg/ml, Sigma, H3506) on a roller mixer. This process separates the tissue into three components: fat, organoids and stromal cells/fibroblasts. The following day the fat layer was separated by decanting and the organoids and stromal cells/fibroblasts were washed three times in RPMI followed by three sedimentation steps at room temperature (RT) to isolate the stromal/fibroblast component. After 30 minutes of sedimentation, the supernatant (stromal/fibroblast) component was removed and placed into culture or frozen for later use. The organoid component underwent further processing to isolate single epithelial and myoepithelial cells, which did not form part of this study.

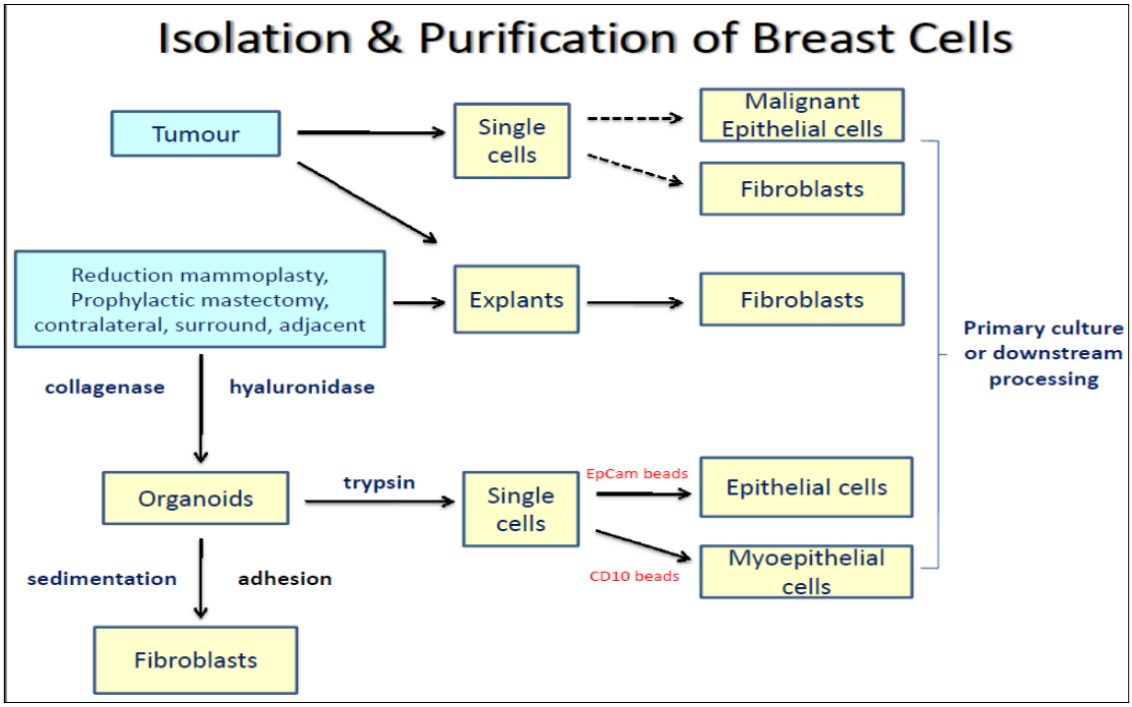

Figure 21: Summary of the steps to isolate purified cell types from primary human breast tissue, adapted from Gomm et al [322].

3.3.2 Cell types and media requirements

Primary human breast fibroblasts were cultured for a limited number of passages in Dulbecco's Modified Eagles Medium with HAM F-12 (DMEM F12, Sigma, D8437) supplemented with 10% foetal bovine serum (FBS, Invitrogen, 10500), penicillin/streptomycin (100µg/ml, Sigma, P4333) and amphotericin B (2.5µg/ml, Sigma, A2942).

The ERα positive cell line (MCF 7) utilised in this study was previously available in the laboratory. Cells were cultured in Dulbecco's Modified Eagles's Medium (DMEM, Sigma, D6429) supplemented with 10% FBS and penicillin/streptomycin (100µg/ml).

The normal mammary epithelial cell line HB2 and Her2 overexpressing HB2 cells were a gift from Professor Valerie Speirs, University of Leeds. These cells were originally obtained from Dr Fedor Berditchevski, University of Birmingham. The cells were

cultured in DMEM supplemented with 10% FBS, hydrocortisone (5µg/ml, Sigma, H0888) and human insulin (2µg/ml, Sigma, I9278).

3.3.3 Cell culture in experiments using tamoxifen, 4-OHTam, 17-β oestradiol, fulvestrant and tesmilifene

Tissue culture media supplemented with phenol red has been shown to have oestrogenic properties [323, 324] and FBS is known to harbour small quantities of endogenous hormones [325, 326].

In order to ensure the cells under investigation were completely deprived of any hormonal stimulation prior to treatment with Tamoxifen (Sigma, T5648) 4-OHTam (Sigma, H7094), 17-β oestradiol (E2, Sigma, E2257), Fulvestrant (Sigma 14409) and Tesmilifene (DPPE, Sigma, D2571) cells were cultured in phenol red free DMEM F12 (Sigma, D64134) supplemented with 5% double charcoal stripped foetal bovine serum (DCSS, First Link, 02-46-850) and L-glutamine (2mM, Sigma, G7513) for at least 24 hours before drug treatment.

3.3.4 Propagation and subculture

Cells were grown in T175 flasks (Fisher Scientific) and incubated at 37^{o}C in 5% CO_2. The cells were monitored using an inverted phase contrast microscope. Culture media was changed every 3-4 days.

Once cells had reached confluence, the cells were passaged by removing and discarding the media and washing with phosphate buffered saline (PBS). 5ml of Trypsin/Ethylenediaminetetraacetic acid (EDTA) solution (Hyclone, SV30031.01) was added at a concentration of 0.05% trypsin and 0.02% EDTA. The flask was placed at 37^{o}C for 3 minutes until they started to detach. The cells were then washed with media, scraped and spun down in a centrifuge for 3 minutes at 1500 rpm. The supernatant

was discarded and the pellet re-suspended in fresh media before being seeded into a new flask.

HB2 cells and HB2 cells overexpressing Her2 were passaged by washing with PBS then adding 10ml of 0.1% EDTA (Fisher Chemical, D065053) for 5 minutes at 37^{o}C. The EDTA was then removed and 5ml of trypsin/EDTA solution at a concentration of 0.25% trypsin and 0.1% EDTA was added for a further 3 minutes at 37^{o}C until the cells started to detach. The cells were then washed with media, scraped and spun down in a centrifuge for 3 minutes at 1500 rpm. The supernatant was discarded and the pellet re-suspended in fresh media before being seeded into a new flask.

3.3.5 Preservation and de-frosting

Cells were preserved in liquid nitrogen in freezing media comprising 54% DMEM F12, 40% FBS and 6% dimethyl sulphoxide (DMSO, Sigma, D2650). Cells were re-suspended in 1ml of freezing medium per cryovial. For reconstitution, frozen cells were rapidly thawed until semi-solid and then added to 5ml DMEM F12 in a 15ml tube. The DMSO was removed by centrifuging at 1500 rpm for 3 minutes, removing the supernatant and re-suspending the pellet in fresh media and adding to new T175 flask.

3.4 Western blotting

3.4.1 Cell lysis

When harvesting cells for protein analysis, culture medium was removed and the flask rinsed with cold PBS, before adding cold radioimmunoprecipitation assay (RIPA) buffer (50mM Tris-HCl pH 8.0, 150mM NaCl (Fisher, 358-1), 1mM EDTA (Fisher, BP 118-500), 1% Igepal CA-630 (NP-40; Calbiochem, 490216), 0.1% sodium dodecyl sulphate (SDS)) mixed with a cocktail of protease inhibitors (Calbiochem, 539131) at 1:100, activated sodium orthovanadate at 1:100 and sodium fluoride at 1: 20. The plate was scraped and the suspension was placed in an eppendorf tube and incubated on ice for 15 minutes. The eppendorf was then centrifuged at 10000 rpm at 4^{o}C for 5 minutes. The pellet was discarded and the supernatant transferred to a new eppendorf.

3.4.2 Protein quantification

Protein concentration was estimated with a Bio-Rad DC protein Assay (Bio Rad Laboratories, 500-0114, 114, 115). Cell lysates and BSA (bovine serum albumin, Sigma, A9418) standards (diluted in distilled water) were added at 5µl volumes to a 96 well plate in triplicate, before adding 25µl of solution A/S (1000µl reagent A and 20µl reagent S) per well followed by 200µl of reagent B per well. The reagents were left to incubate for 10 minutes at room temperature before reading on a 96 well plate reader at 620nm. An absorbance versus concentration curve was plotted using the BSA standards and this was used to estimate the sample protein concentration. Samples were frozen at -20^{o}C until required.

3.4.3 SDS gel electrophoresis

An SDS-Polyacrylamide gel electrophoresis (SDS-PAGE) gel was prepared with component volumes adjusted depending on the molecular weight of the protein of interest. The resolving gel solution (4.6ml distilled water (dH_2O), 2.7ml 30% acrylamide

mix (National Diagnostics, EC 890), 2.5ml 1.5M Tris (pH 8.8), 100µl 10% SDS (National Diagnostics EC 874), 100µL 10% ammonium persulphate (APS, National Diagnostics, EC 504) and 8µl TEMED (Flowgen, H17459)) was dispensed into a 1mm thick gel cassette (Invitrogen, NC2010) and 1ml of dH_20 was overlaid to allow sample diffusion. After the gel was set (approximately 10 minutes), the dH_20 was poured off. A 5% SDS-PAGE stacking gel solution (2.1ml dH20, 500µl 30% acrylamide, 380µl 1M Tris (pH6.8), 30µl 10% SDS, 30µl 10% APS and 3µl TEMED) was added to the cassette, a 1mm 10 well comb was inserted and the gel left to set for about 10 minutes. The comb was removed and the cassette placed in a gel tank containing 500ml of running buffer (50ml tris-glycine/SDS (Amresco, 0307) in 450ml dH_20).

Once the stacking gel had set, 10-30µg of each protein sample was added to 4X sample loading buffer (5% SDS, 20% buffer (0.5M tris, 0.2M NaH_2PO_4, pH 7.8), 5% β-mercaptoethanol (Sigma, M7522), 50% glycerol (Fisher, G/0600/17), 0.01% bromophenol blue (Sigma, B8026) and 20% dH_20) to give a final concentration of 1X. Samples were then boiled for 5 minutes at 95^oC before being loaded into the gel along with 5µl of PageRuler pre-stained protein ladder (Generon, SM0671) and run for 80 minutes at 150V, RT.

A non-reducing protocol was utilized when blotting for collagen I. This involved omitting β-mercaptoethanol from the x4 sample loading buffer and not boiling the samples prior to loading into the gel.

Transfer buffer (50ml tris-glycine buffer (Severn Biotech, 20-6400-10) in 450ml 80% dH_20/ 20% MeOH) was prepared. Transfer sponges and a 0.45µM nitrocellulose membrane (Amersham, RPN2030) were soaked in transfer buffer while the cassette was removed from the gel tank and the stacking gel separated. A sandwich was created within the transfer apparatus, containing wet sponges, filter paper, the gel and presoaked nitrocellulose membrane with the membrane immediately adjacent to the

gel. Any air bubbles were removed by gently rolling a glass tube along the sandwich, prior to sealing the lid and placing the apparatus into the inner chamber of the gel tank. Transfer buffer was added to the top of the inner chamber and dH_2O added to the outer chamber. The whole tank was then placed in ice and run at 30V for 90 minutes at 4°C.

After transfer, the membrane was blocked in 5% skimmed milk powder (Sigma, 70166)/ PBST (0.1% Tween 20 (Applichem, A4974) in PBS) for 1 hour with gentle rocking. The membrane was inserted into a 50ml tube containing 5ml of primary antibody diluted 1:1-2000 in 5% milk/PBST (depending on primary antibody used (Table 4)) and incubated overnight at 4°C on a roller mixer. The membrane was then washed in PBST three times for 5 minutes each time, after which the membrane was placed in 5ml of horse radish peroxidase (HRP)-conjugated secondary antibody (anti-mouse/rabbit IgG HRP, 1: 2000, Dako, P0488, P0260) and incubated for 1 hour RT on a roller mixer. The membrane was washed three times in PBST (5 minutes each) and the protein was visualised by developing in ECL detection (Amersham, RPN 2106) reagent.

Antibody	*Dilution*	*Species*	*Manufacturer*
FN-IST 4	1: 2000	Mouse monoclonal	Sigma (F0196)
pSMAD 2	1: 1000	Rabbit polyclonal	Cell Signalling (3101S)
SMAD 2	1: 1000	Rabbit polyclonal	Cell Signalling (8657)
pSMAD 3	1: 1000	Rabbit polyclonal	Cell Signalling (9520S)
SMAD 3	1: 1000	Rabbit polyclonal	Cell Signalling (9523S)
pERK 1/2	1:1000	Rabbit polyclonal	Cell Signalling (9101S)
Total ERK	1:1000	Rabbit polyclonal	Cell Signalling (9102)
LOX	1:1000	Rabbit polyclonal	Novus Biologicals (NB100-2527)
Collagen 1	1:1000	Rabbit polyclonal	AbCam (ab34710)
SMA	1: 5000	Mouse monoclonal	Sigma (M0581)
ER-Beta	1: 1000	Rabbit polyclonal	AbCam (ab3576)
DHCR7	1: 500	Rabbit polyclonal	AbCam (ab103296)
ER-Alpha	1: 1000	Rabbit polyclonal	Cell Signalling (8644S)
Her-2/ErbB2	1: 1000	Rabbit monoclonal	Cell Signalling (2165S)
HSC70	1: 5000	Mouse monoclonal	Santa Cruz (sc-7298)

Table 4: Primary antibodies used for Western Blotting

3.5 Immunocytochemistry

Cells were fixed in 10% neutral buffered formalin (NBF, Cell Path Ltd, BAF-0010-25A) for 10 minutes at RT and washed twice with PBS. Cells were then permeabilised by incubating with 0.1% Triton for 15 minutes at RT, washed with PBS and blocked with 5% normal horse serum (NHS, Sigma, 12449C)/ 3% BSA for 15 minutes at RT. Cells were then incubated overnight at 4^{o}C with the appropriate primary antibody diluted in 5% NHS/ 3% BSA (Table 5). Cells were then washed three times in PBS, incubated with biotinylated secondary anti-mouse or anti-rabbit secondary antibody (Vector Laboratories, 1:200 in 1% BSA) for 40 minutes at RT, washed in PBS a further three times before incubating with avidin-biotinylated peroxidase complex (Vectastain ABC kit, Vector Laboratories, PK 6101, 6102) for 30 minutes at RT. Cells were washed with PBS three more times before developing using a DAB kit (Vectastain, Vector Laboratories, SK 4100). Cells were then washed twice with PBS and counterstained with Haematoxylin for 2 minutes, rinsed in tap water and then stored in PBS at 4^{o}C.

Antibody	Species	Dilution	Manufacturer
Ki67	Mouse monoclonal	1:100	Dako (T7240)
ER-Alpha (EP1)	Rabbit monoclonal	1:100	Cell Marque/Sigma Aldrich (AC-0015EU)
ER-Beta	Rabbit polyclonal	1:100	Abcam (ab3576)

Table 5: Primary antibodies used for immunocytochemical staining

3.5.1 Ki67 quantification

10 randomly selected fields were examined at x10 objective and the number of positive cells were counted and expressed as a percentage of the total number of cells present per field.

3.6 Statistical analysis

Statistical significance was determined by two tailed Student's *t*-test using Prism (Graphpad software). A p-value <0.05 was regarded as significant in all statistical analysis.

4 Effect of tamoxifen on fibroblast proliferation

4.1 Introduction

Epidemiological data suggest that tamoxifen can reduce MD in a proportion of women at high risk for breast cancer [109]. A significant (>10%) reduction in MD following treatment appears crucial to receive the protective effect of the drug [110]. Numerous studies have observed that high density breast tissue is characterised by increased stromal content [54, 55]. Thus tamoxifen may act directly on stroma to reduce density.

Studies investigating a direct effect of tamoxifen on stromal cells are limited, however there is emerging evidence of significant ER-independent mechanisms of tamoxifen action at therapeutic doses [298, 313, 315, 319].

The effect of tamoxifen on the proliferation of primary breast fibroblasts was examined to determine if a direct effect on stromal cell function could be observed.

4.2 Methods and materials

4.2.1 MTS and Alamar Blue cell proliferation assays

Cell proliferation was measured using CellTiter 96 Aqueous One Solution Cell Proliferation Assay (MTS, Promega, G350) and CellTiter-Blue Cell Viability Assay (Alamar Blue, Promega, G8081). Both assays use the metabolic activity of cells as a surrogate measure for cell viability. The indicator dye reagents act as intermediate electron acceptors and are reduced by viable cells, resulting in a colour change. The MTS assay reagent is a tetrazolium salt (yellow colour) which is reduced to coloured formazan (brown/red colour). The Alamar Blue reagent is resazurin (blue colour) which is reduced to resofurin (pink colour).

Indicator dye reagent (70µl) was added to one well of cultured cells with 350µl fresh media (5:1 media: reagent v/v ratio). After incubation for 2 hours at 37^{o}C, 100µl aliquots were removed in triplicate and dispensed into a 96 well plate. Absorbance at 492nm (MTS) or 550nm and 600nm (Alamar Blue) was determined using a 96 well plate reader.

4.2.1.1 Fibroblast proliferation assay

Individual patient's fibroblasts were optimised for seeding in 24 well plate format. Cells were treated with 4-OHTam (100nM-25µM), E2 (100pM – 100nM), or 4-OHTam and E2 in combination for 10 days with fresh drug and media changes every 2-3 days. The cells were cultured in phenol red free medium and charcoal stripped serum (as described in section 3.3.3). Proliferation was measured immediately prior to treatment (Time 0) and at 2-3 day intervals. Values were normalised to Time 0.

4.2.1.2 MCF7 proliferation assay

Cells were seeded at 5x 10^4 cells per well in 24 well plate format and serum starved for 24 hours. Cells were treated with E2 (100pM-100nM), 4-OHTam (5μM) and Fulvestrant (5μM) for up to 10 days with fresh drug and media changes every 2-3 days. The cells were cultured in phenol red free medium and charcoal stripped serum (as described in section 3.3.3). Proliferation was measured as described above.

4.2.2 LDH cytotoxicity assay

Cell toxicity was measured using the CytoTox 96 Non-Radioactive Cytotoxicity Assay (Promega, G1780). Lysed cells release lactate dehydrogenase (LDH), a stable cytosolic enzyme. LDH in conditioned media is measured using a coupled enzymatic assay resulting in the conversion of a tetrazolium salt to a red formazan product. The amount of colour formed is proportional to the number of lysed cells.

50μl aliquots of conditioned media from fibroblasts treated with vehicle control or 4-OHTam for three days were removed in triplicate and dispensed into a 96 well plate. 50μl of substrate mix was added to each well and incubated at room temperature for 30 minutes in the dark. 50μl of stop solution was then added to each well and absorbance at 492nm determined using a 96 well plate reader. To calculate percentage cytotoxicity, lysis solution was added to triplicate wells of vehicle control treated fibroblasts to give a measurement of the maximum possible cell lysis per well. The absorbance values obtained in the remaining experimental wells were normalised as a percentage of the maximal lysis value.

4.3 Results

4.3.1 Fibroblast patient cohort

4.3.1.1 Cohort characteristics

Fibroblasts from 24 patients were isolated and cultured successfully from a variety of different tissue types. The patient characteristics of the cohort with regard to age and tissue type are displayed in Table 6 below:

Patient ID	Tissue Type	Age (Years)	Menopausal Status
1004	Normal reducing mammoplasty	27	Pre-menopausal
1024	Dense surround	51	Peri-menopausal
1203	Dense surround	43	n/a
1247	Dense surround	51	n/a
1299	Dense surround	77	Post-menopausal
1299	Non dense surround	77	Post-menopausal
1513	Normal reducing mammoplasty	21	Pre-menopausal
1567	Prophylactic mastectomy	44	Pre-menopausal
1621	Prophylactic mastectomy	21	Pre-menopausal
1681	Dense Surround	44	Pre-menopausal
1890	Non dense surround	60	Post-menopausal
1923	Prophylactic mastectomy	45	Pre-menopausal
1989	Normal reducing mammoplasty	33	Pre-menopausal
1991	Prophylactic mastectomy	41	Pre-menopausal
2090	Dense surround	48	Pre-menopausal
2093	Contralateral prophylactic	53	Post-menopausal
2124	Prophylactic mastectomy	41	Pre-menopausal
2182	Normal reducing mammoplasty	25	Pre-menopausal
2204	Prophylactic mastectomy	46	Pre-menopausal
2266	Contralateral prophylactic	48	Peri-menopausal
2585	Normal reducing mammoplasty	24	Pre-menopausal
3078	Normal reducing mammoplasty	58	Post-menopausal
3137	Normal reducing mammoplasty	49	Pre-menopausal
3353	Normal reducing mammoplasty	25	Pre-menopausal

Table 6: Characteristics of patient fibroblast cohort

The total number of patient samples from each tissue type and the mean age of these groups are displayed in Table 7 below.

Tissue Type	Total Patient Number	Mean Age (Years)
Normal reducing mammoplasty	8	32.8
Dense surround	6	52.3
Non-dense surround	2	68.5
Prophylactic mastectomy	6	39.6
Contralateral prophylactic	2	50.5

Table 7: Mean patient age by tissue type

Patients in the normal reducing mammoplasty and prophylactic mastectomy groups have a lower mean age than those in the other groups.

4.3.1.2 Fibroblast morphology

Significant variation in the morphology of fibroblasts between patient samples was noted. Some patients' cells showed a prominent spindled morphology whereas other cells were more plump and flattened. Examples of these are displayed in Figure 22 below.

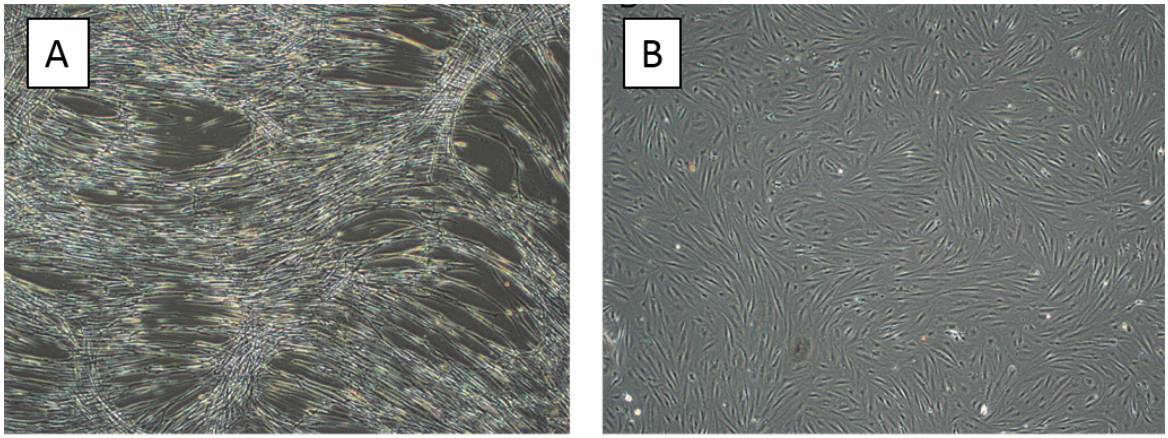

Figure 22 Variation in primary breast fibroblast morphology. The morphology of fibroblasts from different patients varied significantly. Representative examples (A) Prophylactic mastectomy with prominent spindled morphology (B) Normal reducing mammoplasty.

4.3.2 Effect of 4-OHTam on fibroblast proliferation

The ranges of 4-OHTam concentration assessed in these experiments were determined from previous studies [278, 313, 314]. Primary fibroblasts from all patients

in the cohort consistently showed a dose dependent response to 4-OHTam; increasing 4-OHTam concentration had a negative effect on proliferation. A toxic effect was seen at concentrations greater than 6μM. These observations were consistently demonstrated using both the MTS and Alamar Blue assays, displayed in Figures 23 + 24 below.

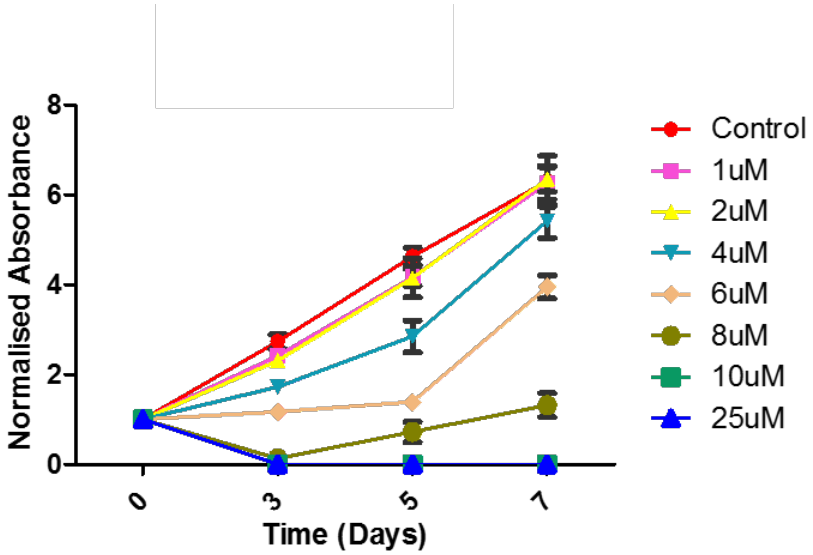

Figure 23: Effect of increasing 4-OHTam concentration (1-25μM) on fibroblast proliferation using MTS assay. Fibroblasts show a dose dependent response of reduced proliferation with increasing 4-OHTam concentration. Absorbance values are normalised to Day 0. This is an example of patient 1004. Data points represent the mean of three assays.

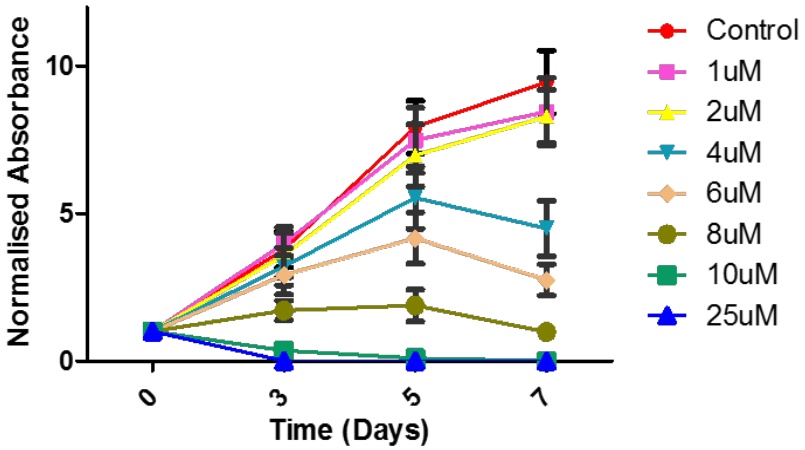

Figure 24: Effect of increasing 4-OHTam concentration (1-25μM) on fibroblast proliferation using Alamar Blue assay. Fibroblasts show a dose dependent response of reduced proliferation with increasing 4-OHTam concentration. Absorbance values are normalised to Day 0. This is an example of patient 1004. Data points represent the mean of three assays.

The negative effect of 4-OHTam on fibroblast proliferation was consistently observed in the presence of 17-β oestradiol (E2, Figure 26). E2 alone had no effect on fibroblast proliferation (Figure 25).

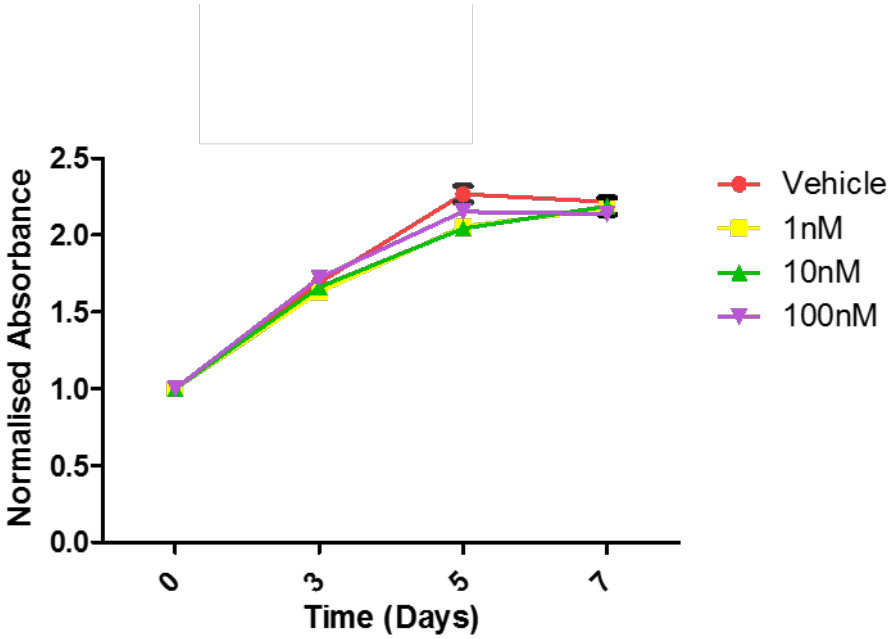

Figure 25: Effect of increasing 17-β oestradiol (E2) concentration (100pM-100nM) on fibroblast proliferation using Alamar Blue assay. No significant effect on proliferation is seen with increasing E2 concentration. Absorbance values are normalised to Day 0. This is an example of patient 1004. Data points represent the mean of three assays.

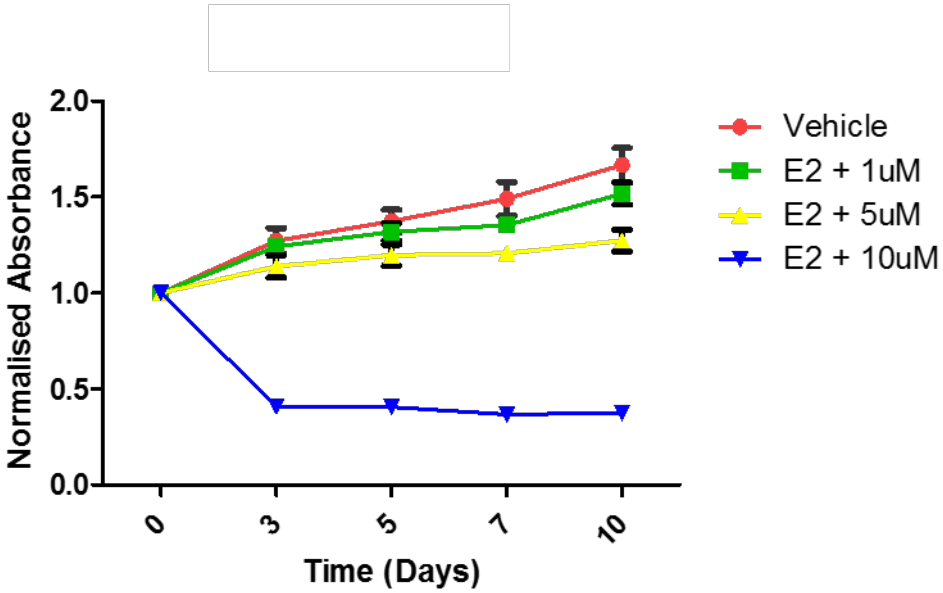

Figure 26: Effect of increasing 4-OHTam concentration (1-10μM) on fibroblast proliferation in the presence of E2 (10nM) using Alamar Blue assay. A decrease in proliferation is seen with increasing 4-OHTam concentration. Absorbance values are normalised to Day 0. This is an example of patient 1004. Data points represent the mean of three assays.

As a positive control, MCF7 cells were treated in triplicate with E2 (1nM, Figure 27). E2 substantially increased MCF7 proliferation compared to vehicle and 4-OHTam (5μM) treated cells.

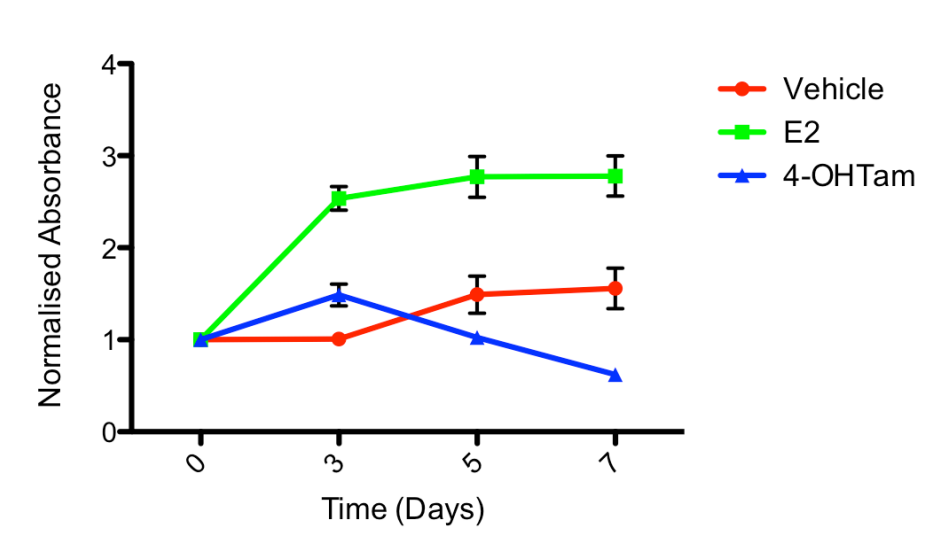

Figure 27: Effect of E2 (1nM) and 4-OHTam (5μM) on MCF7 cell proliferation using Alamar Blue assay. E2 markedly increases proliferation whereas 4-OHTam has an overall negative effect on proliferation. Absorbance values are normalised to Day 0. Data points represent the mean of three assays.

4.3.3 Comparison of Alamar Blue and MTS Assay sensitivity

To compare the sensitivities of both MTS and Alamar blue assays, a standard curve was prepared for each assay using a range of dilutions (1:1) with known numbers of cells in each well (Tables 8 + 9, Figures 28 + 29)

Cell Number	Absorbance
200000	1.932
100000	1.212
50000	0.806
25000	0.532
12500	0.368
6250	0.296
3125	0.245
1563	0.198
781	0.187
391	0.178
195	0.171
98	0.181

Table 8: Standard curve data for MTS assay. The assay loses sensitivity for accurately quantifying cell number at a concentration of around 400 cells per well.

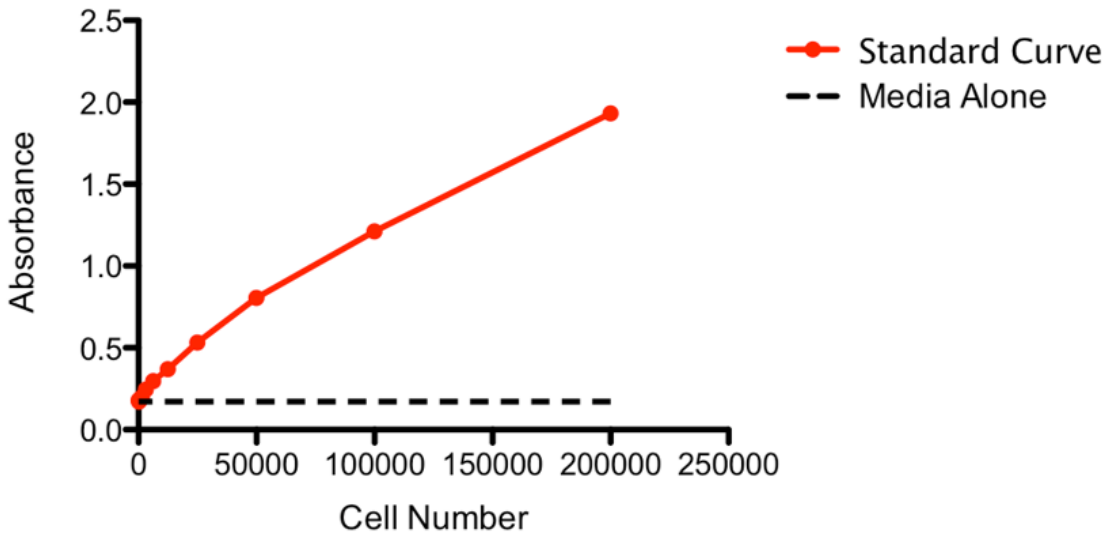

Figure 28: MTS Assay standard curve. The assay has a lower limit of detection at around 400 cells per well.

Cell Number	Absorbance
200000	0.726
100000	0.352
50000	0.133
25000	0.014
12500	-0.068
6250	-0.121
3125	-0.155
1563	-0.150
781	-0.180
391	-0.195
195	-0.255
98	-0.294

Table 9: Standard curve data for AB assay. The assay continues to have sensitivity for detecting cell number to a concentration of less than 100 cells per well.

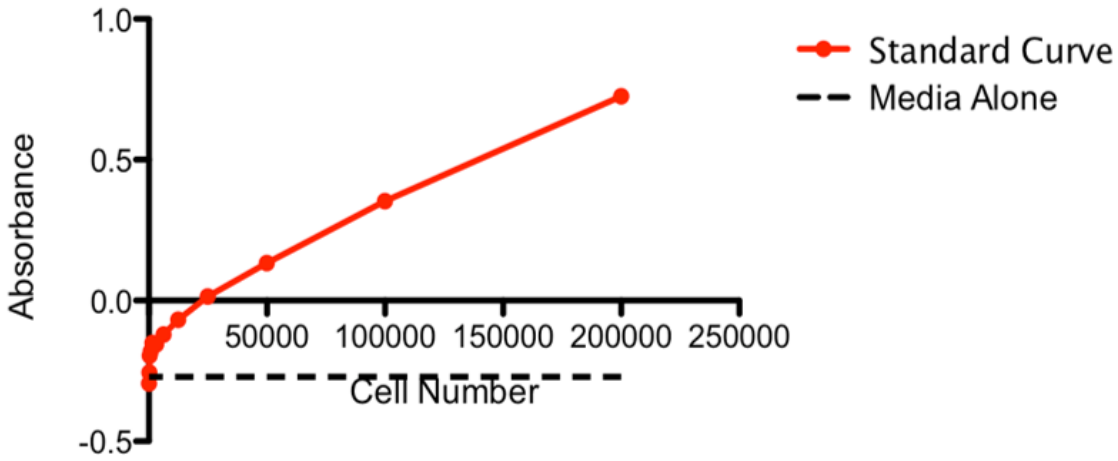

Figure 29: Alamar Blue assay standard curve. The assay has a lower limit of detection of less than 100 cells per well.

The MTS assay had a lower limit of detection of around 400 cells per well, whereas the Alamar Blue assay had a lower limit of detection of around 100 cells per well.

Given the enhanced sensitivity of the Alamar Blue assay for detecting small changes in cell number, this was adopted as the preferred assay. A negative absorbance value is seen for lower cell numbers in the Alamar Blue assay since the absorbance ratio is

calculated by subtracting the absorbance of the substrate of the reaction from the absorbance of the product. Thus, when fewer cells are present, less product is formed and the ratio becomes negative in value.

4.3.4 Effect of 4-OHTam on fibroblast proliferation using Ki67

Given that both the MTS and Alamar blue assays use cell metabolism as a surrogate measure for proliferation, Ki67 immunocytochemistry was performed on primary fibroblasts from two patients treated with vehicle control and 4-OHTam (5μM) for one week, to analyse the proportion of cells in the cell cycle (Figure 30).

(i)

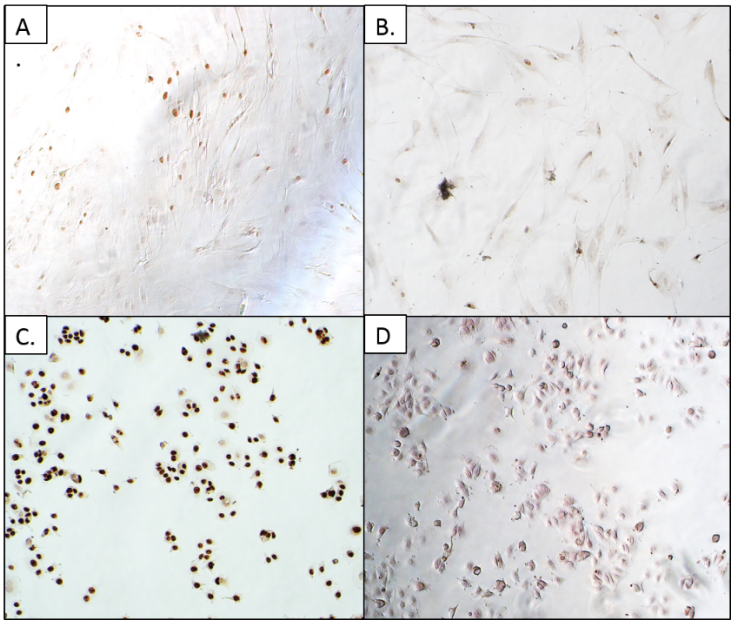

(ii)

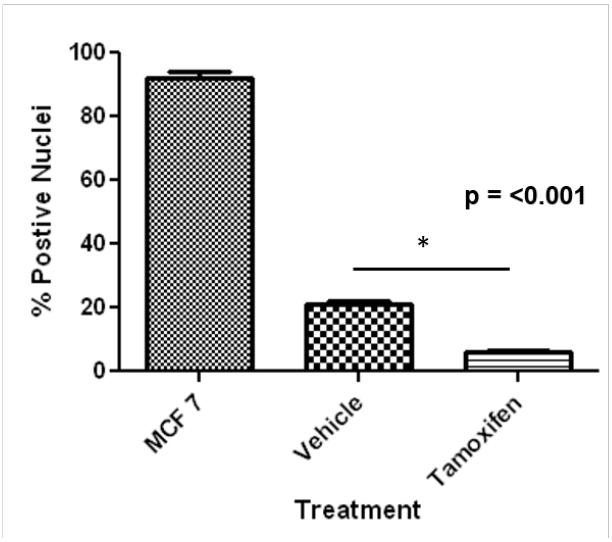

Figure 30: (i) Representative images of Ki67 immunocytochemistry staining (X10 magnification) of (A) vehicle control treated fibroblasts (B) 4-OHTam (5μM) treated fibroblasts. (C) MCF7 cells (positive control). (D) MCF 7 cells (negative control with mouse immunoglobulin, Haematoxylin staining of nuclei only). (ii) Graph showing % positive staining cells per total number of cells per x10 objective field (n = 10).

Significantly more cells in the cell cycle (Ki67 positive) were present in the vehicle control treated fibroblasts compared to those treated with 4-OHTam ($p<0.001$, Figure 30).

4.3.5 Effect of 4-OHTam on fibroblast proliferation by direct cell counts

To further evaluate the effect of 4-OHTam on fibroblast proliferation, T175 flasks were seeded with 4 x10^5 cells from three patients, hormone deprived for 24 hours and treated with vehicle control, 4-OHTam (5μM), 4-OHTam and E2 (10nM), or E2 for 7 days. Viable cells were counted using trypan blue (Sigma, T8154). Fibroblasts treated with 4-OHTam (+/- E2) were significantly reduced in number after 7 days compared to those treated with vehicle control or E2 alone (p <0.001, Figure 31).

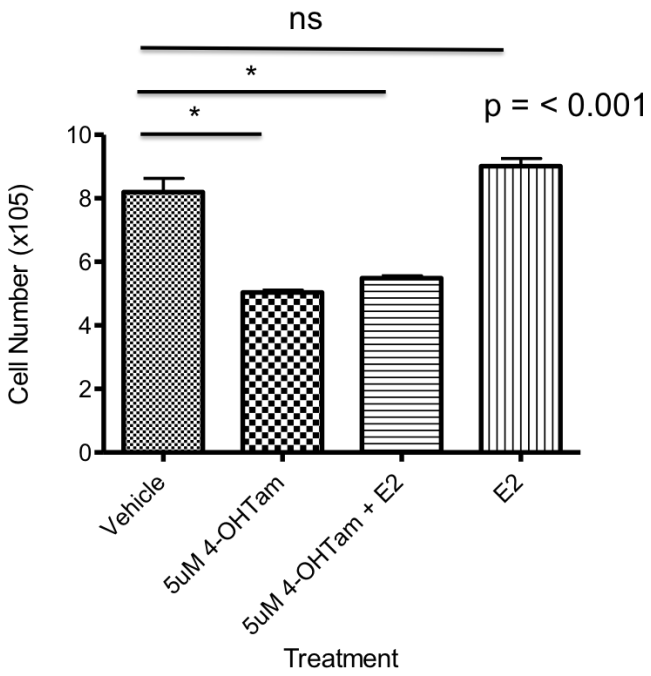

Figure 31: Number of viable cells present after one week treatment with vehicle control, 4-OHTam (5μM), 4-OHTam + E2 (10nM) or E2. Cells treated with 4-OHTam or 4-OHTam + E2 showed significantly less growth than vehicle or E2 treated cells. Example of patient 1004 (n=3).

4.3.6 Effect of 4-OHTam on fibroblast toxicity

To confirm the observed effect on proliferation was not simply due to a toxic effect causing cell death, the LDH assay was performed using three patients' primary fibroblasts treated with increasing concentrations of 4-OHTam (1-25μM). Significant toxicity was only seen in concentrations of 4-OHTam >6μM, suggesting the effect on proliferation noted at lower concentrations is not merely a toxic effect (Figure 32).

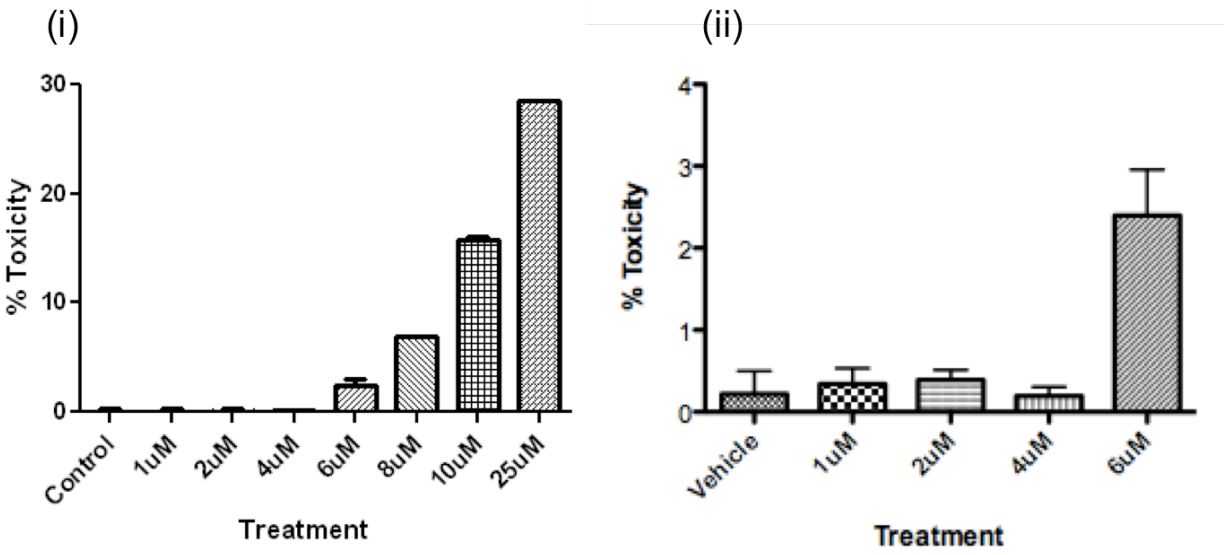

Figure 32: (i) and (ii): Effect on increasing 4-OHTam concentration on cell toxicity using the LDH assay. Significant toxicity is only seen at concentrations of 6μM and above. (i) Overall results, (ii) Enhanced view concentrations up to 6μM. This is an example of patient 1004 (n =3).

4.3.7 Effect of 4-OHTam on fibroblast phenotype

Fibroblasts treated with concentrations of 4-OHTam of 200nM and above displayed a consistent phenotype characterised by the accumulation of small perinuclear cytoplasmic vesicles (Figure 33). This was observed in fibroblasts from all patients in the cohort.

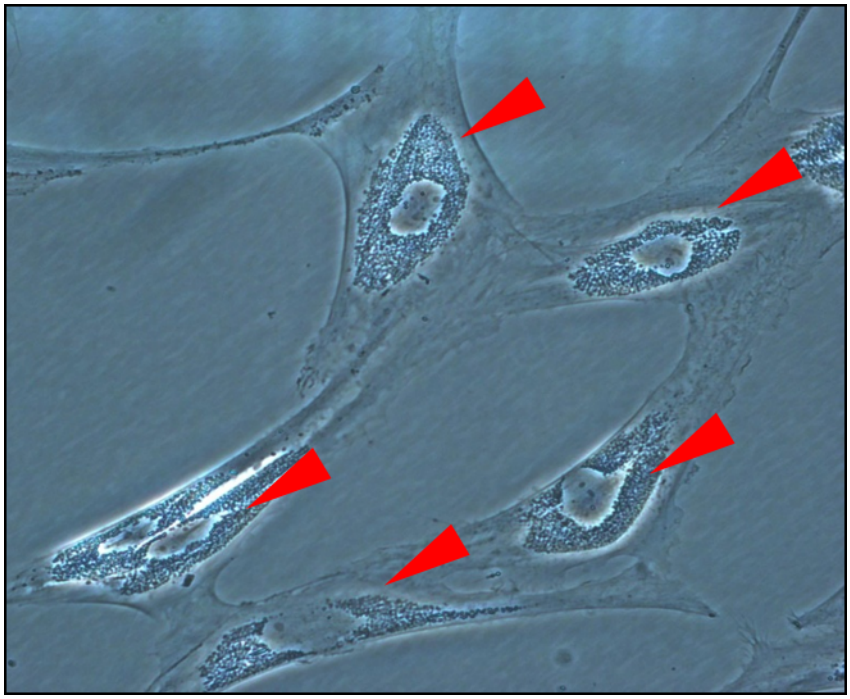

Figure 33: Phase contrast image of primary fibroblast phenotype following one week treatment with 5μM 4-OHTam (x40 objective, Red arrows = perinuclear cytoplasmic vesicles).

4.3.8 Reversibility of 4-OHTam treated fibroblast phenotype

Primary fibroblast proliferation was measured following 4-OHTam treatment for 5 days and then again after switching back to control media, to determine if the observed negative proliferative effect of 4-OHTam was retained after removal of the drug from the culture media (Figures 34 + 35).

The negative effect of 4-OHTam on fibroblast proliferation showed a degree of recovery after switching back to control media following 5 days of 4-OHTam (Figure 34). In addition, a partial reversal of the morphological 4-OHTam phenotype (reduced numbers of perinuclear cytoplasmic vesicles) was seen once the culture media was changed to vehicle control (Figure 35).

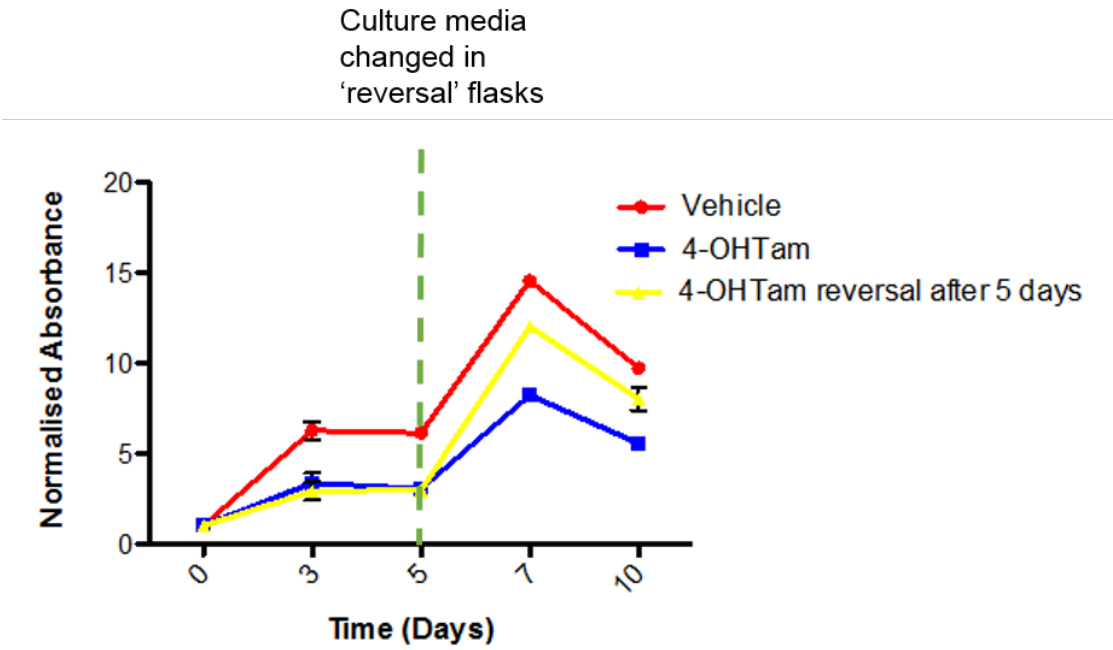

Figure 34. Reversibility of 4-OHTam (5μM) effect on cell proliferation using Alamar Blue assay. The negative effect of 4-OHTam on cell proliferation shows a degree of recovery once 4-OHTam is removed from the culture media after day 5. Example of patient 2182. Datapoints represent the mean of three assays.

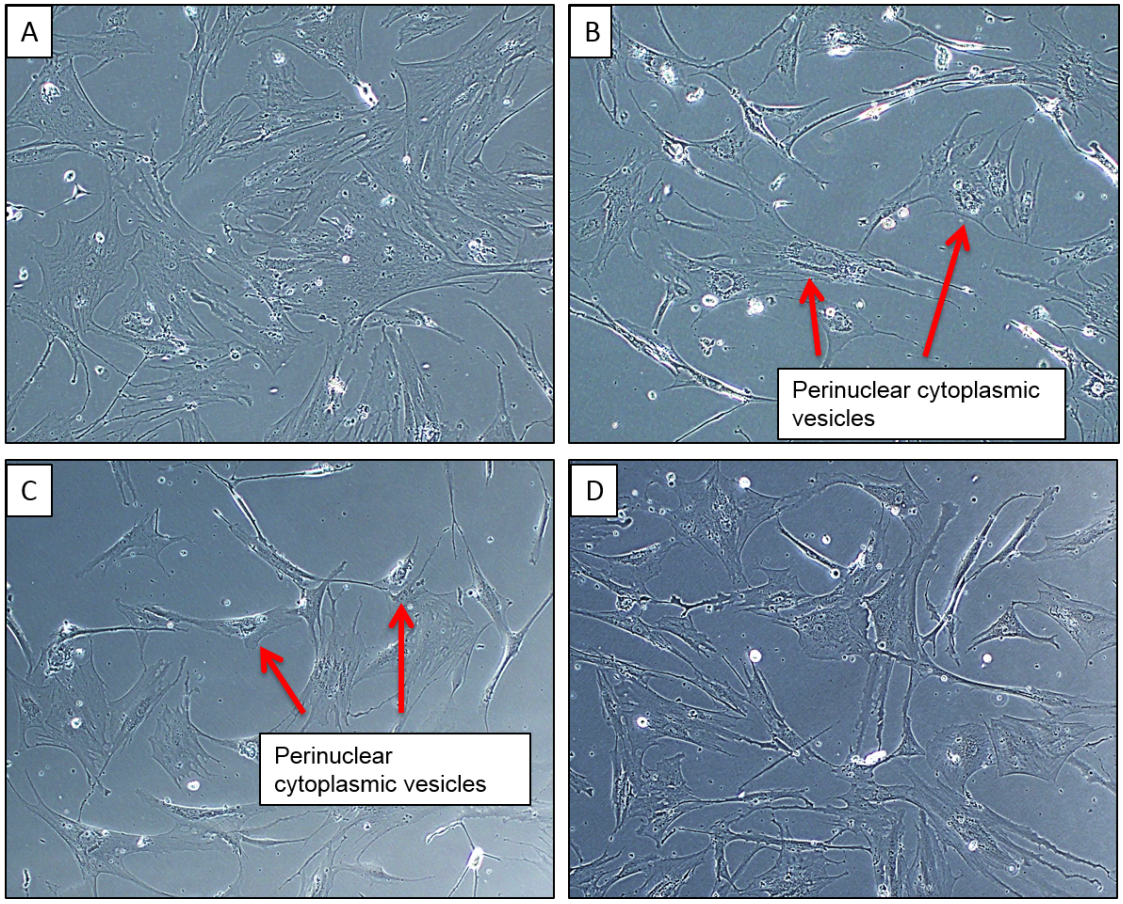

Figure 35: Reversibility of 4-OHTam fibroblast phenotype. Fibroblasts treated with 4-OHTam (5μM) for 5 days showed some reversibility of the 4-OHTam treatment phenotype, with gradual loss of perinuclear cytoplasmic vesicles when the culture media was switched to vehicle control. (A) Vehicle control treated fibroblasts (B) 4-OHTam treated fibroblasts displaying characteristic phenotype (C) 4-OHTam treated fibroblasts 2 days after switching to vehicle control media, showing some loss of perinuclear cytoplasmic vesicles. (D) 4-OHTam treated fibroblasts 5 days after switching to vehicle control media with few remaining perinuclear cytoplasmic vesicles.

4.4 Discussion

4.4.1 Fibroblast patient cohort

The cohort of primary fibroblasts were isolated from patients with a wide age range (21-77 years) and a range of non-tumour breast tissue type (Table 6). The fibroblasts isolated from reduction mammoplasty and prophylactic 'risk reducing' mastectomy tissue were from younger patients (mean 32.8 years and 39.6 years respectively), in keeping with the clinical need for intervention at an earlier age (Table 7). Cells isolated from surround tissue were from older patients (mean 50.6 years) who have a higher incidence of breast cancer. The inter-patient variation in the cohort was reflected by variation in the morphology of the cultured fibroblasts (Figure 22). Capturing the heterogeneity that exists between individual patients by using primary cell cultures is a strength of this study. Unfortunately, due to constraints of time, radiological data regarding the MD of these patients was not available.

4.4.2 Effect of 4-OHTAM on fibroblast proliferation

A consistent negative, dose dependent, effect on fibroblast proliferation was observed with 4-OHTam treatment in fibroblasts from the entire patient cohort (Figures 23 +24). This effect on proliferation was accompanied by a characteristic phenotype where the 4-OHTam treated fibroblasts accumulated small perinuclear cytoplasmic vesicles (Figure 33). At present it is unclear what these vesicles represent.

The negative effect on proliferation was observed at 4-OHTam concentrations of 100nM and above, within the range detected in the breast tissue of breast cancer patients treated with tamoxifen for one month [278]. Reduced proliferation was measured using two independent cell viability assays utilising cell metabolism as an indirect measure of proliferation (MTS and Alamar Blue, Figures 23 + 24). Alamar Blue was found to have greater sensitivity (Figures 28 + 29) and thus was adopted as the

preferred assay for the remainder of the experimental work. Direct cell counting confirmed reduced fibroblast proliferation following 4-OHTam treatment, as significantly fewer cells were present after treatment for 7 days with 4-OHTam compared to vehicle control ($p<0.001$, Figure 31).

In order to ensure these observations were physiologically relevant, co-treatment with E2 was also performed. Reduced proliferation with 4-OHTam was still observed in the presence of E2 both by direct cell counting (Figure 31) and the indirect metabolic based assays (Figure 26). Treatment with E2 alone had no significant effect on proliferation assessed via direct counting or the indirect assays (Figures 25 +31). The fact that E2 did not increase proliferation suggests the mechanisms underlying the observed effects on fibroblast proliferation may not be mediated via the agonist/antagonist functions of 4-OHTam and E2 at ER.

To further investigate the negative effect of 4-OHTam on fibroblast proliferation using an indirect assay not related to cell metabolism, Ki67 immunocytochemistry was performed. Positive Ki67 staining highlights cells actively entering the cell cycle. 4-OHTam treated fibroblasts showed significantly less Ki67 positivity than those treated with vehicle control ($p<0.001$, Figure 30), further highlighting the negative effect of 4-OHTam on fibroblast proliferation. The LDH assay confirmed that significant toxicity was only seen at 4-OHTam concentrations greater than 6μM (Figure 32), suggesting the reduced proliferation observed was not merely a result of cell toxicity.

In order to investigate whether the negative proliferative effect of 4-OHTam on fibroblasts was reversible, cells were treated with the drug for 5 days before switching back to control media. A significant recovery of cell proliferation was noted after 5 days of treatment with normal media (Figure 34). This suggests that 4-OHTam treatment does not result in irreversible changes to fibroblast function, and that regular drug dosing is needed to maintain the 4-OHTam- treated phenotype.

5 Effect of Tamoxifen on fibroblast activation

5.1 Introduction

Having observed a direct effect of 4-OHTam on the proliferation of primary breast fibroblasts, a more detailed analysis of the fibroblast response to 4-OHTam was undertaken, focused on key candidate stromal markers.

Data from Hattar and colleagues suggest that, in animal models, tamoxifen can remodel the mammary ECM to a tumour inhibitory phenotype, characterised by reduced levels of fibronectin (FN) [115]. The same study also reported modulation of expression of collagen I, the most abundant mammary ECM protein, by tamoxifen. This has also been observed in animal models of renal fibrosis [314].

Lysyl oxidase (LOX) is a collagen cross-linking enzyme implicated in driving tumour progression within a stiff ECM via enhanced integrin signalling and FAK activity [213]. Currently no data exists on the ability of tamoxifen to modulate LOX expression.

An anti-fibrotic effect of tamoxifen is well recognised [315] and it has been proposed that tamoxifen may affect the transformation of fibroblasts to the activated myofibroblast phenotype, in response to stimulation from the pro-fibrogenic cytokine TGF-β [313, 314]. However, to date, studies are limited and report contrasting findings.

Expression of ER has been reported in mouse skin fibroblasts [270], however ER expression in primary human breast fibroblasts is not known. The pure ER-antagonist fulvestrant (ICI 182780) was used to assess if tamoxifen interaction with fibroblast ER could be responsible for the observed effects on fibroblast function.

5.2 Methods and materials

5.2.1 Fibroblast scratch assay

Primary fibroblasts were seeded in 6 well plates at 4 x10^5 cells per well, allowed to adhere to plastic overnight then changed to phenol-red free media and DCSS. Once confluent, cells were serum starved for 24hours. Two perpendicular scratches were made across the diameter of the wells with a 200µl pipette tip forming a central cross for reference. The media was aspirated and cells washed with PBS three times. Cells were then incubated with vehicle control, 10% DCSS (positive control), 4-OHTam (2µM), recombinant TGF-β1 (5ng/ml, Peprotech, 100-21B) + vehicle control or TGF-β + 4-OHTam. Images of the scratch were captured using a phase contrast microscope at x4 objective immediately after scratching (Time 0), and after 8 hours. The area of the scratch was measured using Image J at Time 0 and 8 hours and the percentage decrease in area compared for each treatment condition (Figure 36).

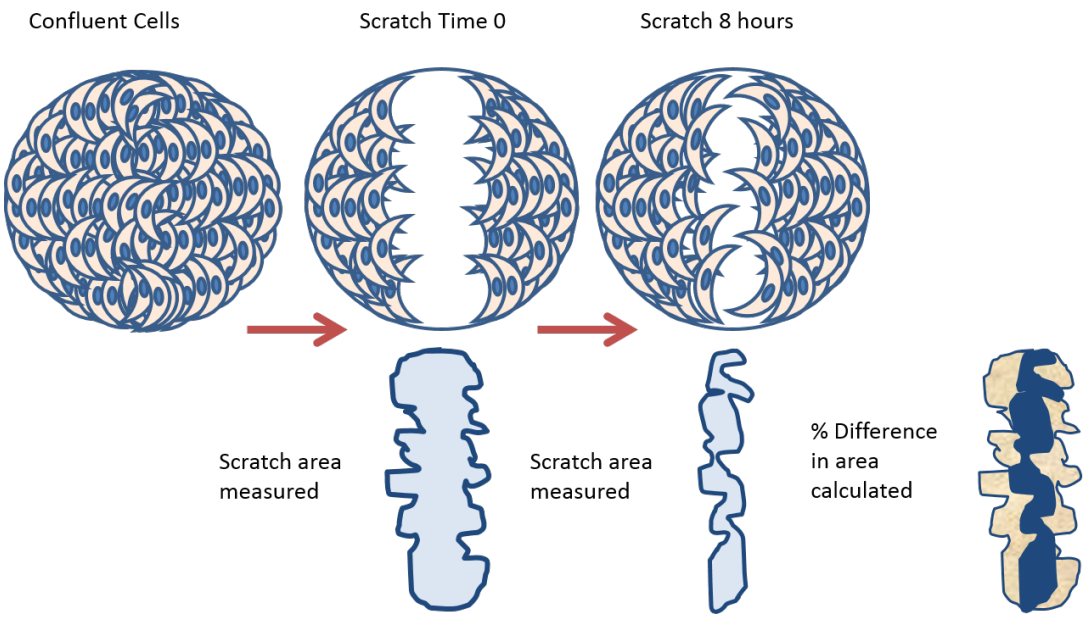

Figure 36: Scratch assay analysis method

5.2.2 Collagen gel contraction assay

An eight part collagen gel mixture (8 parts collagen 1 (rat tail, BD, 354236), 1 part phenol red-free DMEM F12, 1 part filtered DCSS, 1 part 10X DMEM (Sigma, D2429) was prepared on ice then neutralised with successive additions of 90µl 0.1M NaOH until the mixture changed colour from yellow to bright pink. The gel mixture was then dispensed in triplicate to a 24 well plate (500µl per well) and allowed to set for 2 hours at 37°C. 4 x 10^4 primary fibroblasts were seeded onto each gel in 500µl phenol red free DMEM with 5% DCSS and either vehicle control or 4-OHTam (5µM). Gels were then left overnight at 37°C before being carefully removed from the sides of the well using a needle. The media was then aspirated and replaced with fresh media containing vehicle control, 4-OHTam (5µM), TGF-β (5ng/ml) + vehicle control or TGF-β + 4-OHTam. Gels were photographed using a dissecting microscope (Carl Zeiss) immediately afterwards (Time 0) and then again at 48 hours. The area of the gel at Time 0 and 48 hours was measured using Image J and the percentage reduction in gel area calculated for each treatment condition (Figure 37).

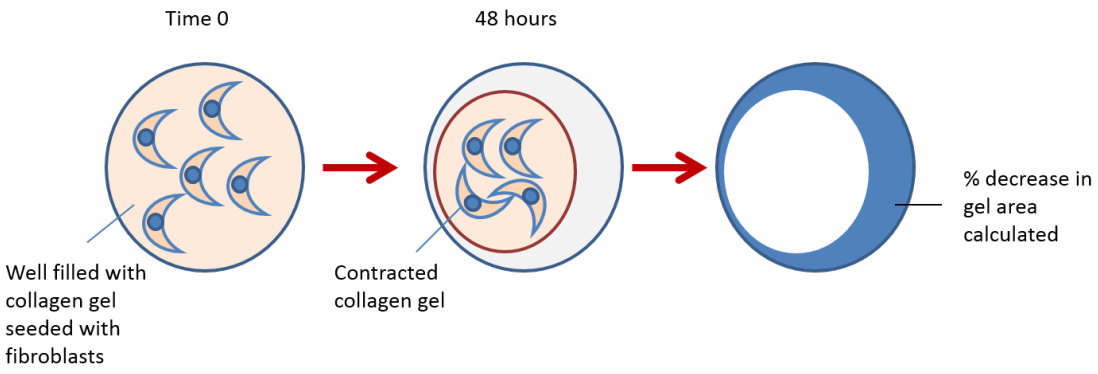

Figure 37: Collagen gel contraction assay

5.2.3 Fibroblast derived matrices (FDM)

5.2.3.1 Preparation of glass coverslips, chamber slides and culture plates for fibroblast derived matrix generation

Culture plates (24 well, 12 well and 6 well) were coated in 0.2% gelatin (Sigma, G1393) for 1 hour at 37^{o}C to prepare them for FDM generation. 13mm^{2} glass coverslips and 8 well chamber slides (Lab-Tek Fisher Scientific, TKY-210-916Y) were coated in sterile 0.2% gelatin for 1 hour at 37^{o}C then washed with PBS and incubated with sterile 1% glutaraldehyde (Sigma, G6257) for 25 minutes at RT, washed again with PBS and incubated with sterile 1M glycine (Fisher Scientific, BP381-1) for 20 minutes at RT. Coverslips, chamber slides and culture plates were then washed with PBS and incubated with DMEM F12 for 30 minutes at 37^{o}C.

5.2.3.2 Generation of fibroblast derived matrices

Primary fibroblasts from three patients were seeded at high density in DMEM F12, switching to phenol-red free media after 12 hours. Once confluent, the media was changed and replaced with fresh media supplemented with L-ascorbic acid (50µg/ml, Sigma, A4403) and either vehicle control or 4-OHTam (5µM). Ascorbic acid increases collagen production and helps to stabilise the matrix. The matrix generating media was replenished every other day for one week.

5.2.3.3 Decellurising the FDM

After one week the media was removed and the cells washed gently in sterile PBS containing 1mM $CaCl_2$ and 0.5mM $MgCl_2$ (Sigma, D8662). Cells were then lysed using warm extraction buffer (10mM Ammonium hydroxide (Sigma, 221228) and 0.1% Triton X-100 (Alfa Aesar, A16046)) and incubated at 37^{o}C for 5 minutes. Following cell lysis, FDM were carefully washed in sterile PBS twice then incubated for half an hour with DNase 1 (10µg/ml, C10104159001, Boehringer/Roche Diagnostics). FDM were

carefully washed in PBS twice, examined under phase contrast to ensure the matrix was intact, and then stored at 4°C in sterile PBS until required, for up to 1 week (Figure 38).

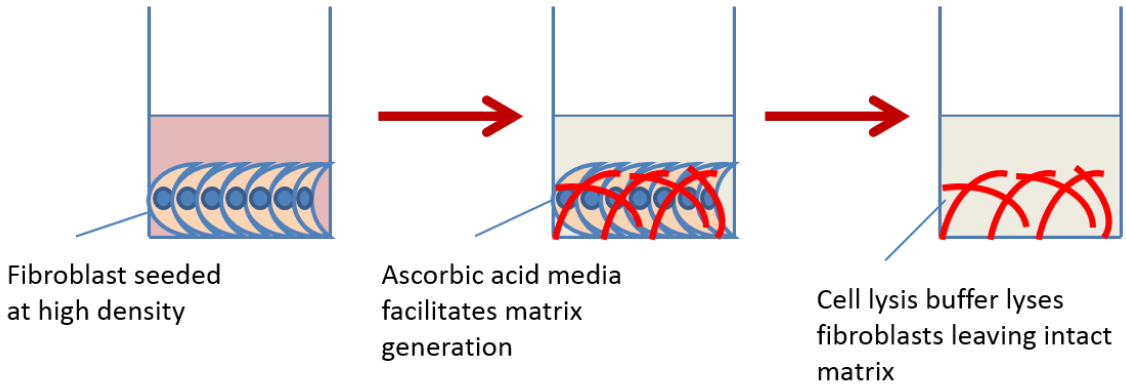

Figure 38: Preparation of fibroblast derived matrix (FDM)

5.2.3.4 Immunofluorescent staining of FDM

FDM on glass coverslips or chamber slides were fixed in 10% NBF for 20 minutes at RT, washed in sterile PBS then blocked with 5% bovine serum albumin (BSA, Sigma, A8022) overnight at 4°C. The 5% BSA was then removed and replaced with 5% BSA with anti-fibronectin IST4 antibody (1:100 dilution, Sigma, F0916) for 1 hour at RT. FDM were then washed three times with PBS and incubated for 1 hour with Alexafluor anti-mouse 488 secondary antibody (Invitrogen, A11059) in 1% BSA for 1 hour at RT. FDM were then washed four times in PBS before mounting in Prolong Gold anti-fade mounting medium with DAPI (Invitrogen, P36391).

5.2.3.5 Imaging of FDM

Images were acquired on confocal microscope LSM510 (Carl Zeiss). 488 dye was excited with the argon laser at 488nm (green fluorescence). Images were captured at 1024 x 1024 resolution. A z-stack series was taken through the thickness of the FDM with x20 objective. The serial Z stack images were merged as one maximal intensity

image for analysis. 4 measurements of FDM thickness were taken in each of the triplicate samples by subtracting the distance between the top and bottom sections of the fluorescently stained fibronectin matrix.

5.2.4 SirCol soluble collagen assay

The collagen content of fibroblast conditioned media (FCM) and FDM was determined using the SirCol soluble collagen assay (Biocolor, S1000) as per manufacturer's instructions. The assay utilises the binding of Sirius Red dye to quantify the amount of collagen present in solution – the greater the amount of red colour present, the greater the amount of collagen present.

5.2.4.1 Sample preparation

Fibroblast conditioned media (FCM) was harvested as described in Chapter 8. 1ml was transferred to triplicate eppendorf tubes along with 200µl of collagen isolation and concentrating reagent (Biocolor, S1000). The tubes were inverted several times before incubating overnight at 4^{o}C in a rack filled with ice and water. The following morning the tubes were centrifuged at 12000 rpm to pellet the concentrated collagen and the supernatant carefully removed.

FDM were prepared as described above in triplicate format on 12 well plates. The collagen within the matrices was solubilised by incubating overnight at 4^{o}C with 2ml pepsin (0.1mg/ml, Invitrogen, 00-3009)/ acetic acid (0.5M, Sigma, A6283). The extraction solution was then concentrated using the method described above with the addition of 100µl acid neutralising agent per sample, prior to the addition of collagen isolation and concentration reagent and overnight incubation.

5.2.4.2 Collagen detection and quantification

1ml of SirCol dye reagent (Biocolor, S1000) was added to each sample. Each tube was inverted several times and then placed on a rotating wheel for 30 minutes. The samples were then centrifuged at 12,000 rpm for 10 minutes and the supernatant carefully removed. 750µl ice cold acid-salt wash (Biocolor, S1000) was then carefully added on to the pellet to remove unbound collagen from the surface. The samples were then centrifuged again at 12,000 rpm for 10 minutes and the supernatant removed. 250µl alkali reagent (Biocolor, S1000) was then added to each sample and the collagen-bound dye solubilised by placing the tubes on a vortex mixer for 5 minutes.

100µl per sample was transferred to an individual well of a 96 well plate and absorbance measured at 555nm on a plate reader.

5.3 Results

5.3.1 Effect of 4-OHTam on fibronectin expression

Data from animal models suggests that fibronectin (FN) may contribute to a pro-tumourigenic mammary stroma [115]. To assess whether tamoxifen can modulate expression of total FN in human stromal cells, fibroblasts were treated with 4-OHTam (5μM) for one week (Figure 39). The entire cohort of fibroblasts was assessed.

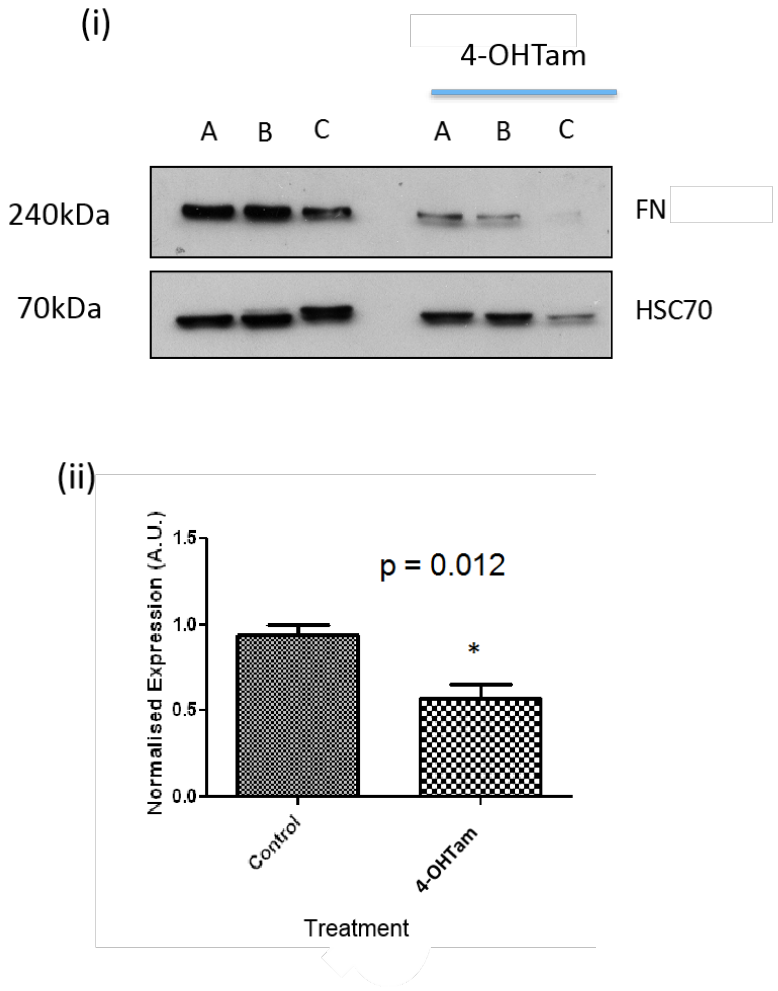

Figure 39: Fibronectin (FN) expression in three patients (A-C) treated with 4-OHTam (5μM) for one week. Significantly reduced expression of FN was observed in in 4-OHTam treated fibroblasts (p = 0.012) (i) Representative western blot image (ii) Densitometry analysis, expression normalised to loading control. (1.0 = equal protein expression level as HSC70 in 20μg sample). Representative data from patient 1004 (n=3). (A.U.= Arbitrary Units)

Fibroblasts treated with 4-OHTam showed significantly reduced expression of FN (p= 0.012, Figure 39), in a proportion of the cohort (Table 10). Primary breast fibroblasts from three patients (1513, 1004, 2090) also showed reduced expression of FN when treated with both 4-OHTam and E2 ($p<0.01$, Figure 40). No significant effect on FN expression was observed with E2 alone (Figure 40).

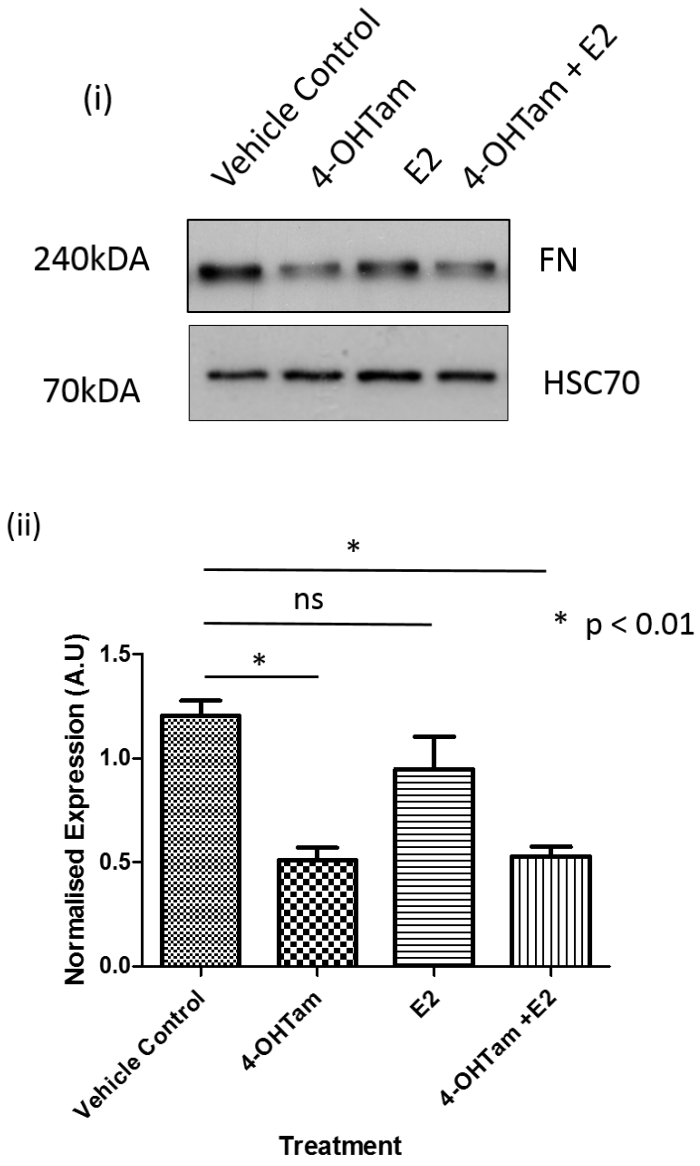

Figure 40: Effect of treatment with 4-OHTam (5μM) +/- E2 (10nM) on fibroblast expression of FN. 4-OHTam and combined 4-OHTam and E2 treatment resulted in a significant reduction in FN expression ($p<0.01$). No effect was observed with E2 alone. (i) Representative western blot image (ii) Densitometry analysis, example of patient 1513 (n=3), expression normalised to loading control (1.0 = equal protein expression level as HSC70 in 20μg sample). (A.U. = Arbitrary Units)

In contrast to the consistent effect on fibroblast proliferation, a reduction in fibronectin expression was not observed in all patients. 62% of 23 patients showed a reduction in FN expression with 4-OHTam. Those patients who did show a change in FN expression were classified as 'responders' (Table 10). Any reduction in FN expression was regarded as a positive response to 4-OHTam. Reduction in FN expression with 4-OHTam treatment was used as a screening tool to select patient samples for the whole transcriptome (RNA-Seq) pilot analysis (Chapter 6).

Patient ID	Tissue Type	Age (Years)	Reduction in FN (Y/N)
1004	Normal reducing mammoplasty	27	Y
1024	Dense surround	51	Y
1203	Dense surround	43	N
1247	Dense surround	51	Y
1299	Dense surround	77	N
1299	Non dense surround	77	N
1513	Normal reducing mammoplasty	21	Y
1567	Prophylactic mastectomy	44	N
1621	Prophylactic mastectomy	21	N
1681	Dense Surround	44	N
1890	Non dense surround	60	Y
1923	Prophylactic mastectomy	45	Y
1989	Normal reducing mammoplasty	33	Y
1991	Prophylactic mastectomy	41	N
2090	Dense surround	48	Y
2093	Contralateral prophylactic	53	Y
2124	Prophylactic mastectomy	41	Y
2182	Normal reducing mammoplasty	25	Y
2204	Prophylactic mastectomy	46	N
2266	Contralateral prophylactic	48	Y
2585	Normal reducing mamoplasty	24	Y
3078	Normal reducing mammoplasty	58	Y
3137	Normal reducing mammoplasty	49	N
3353	Normal reducing mammoplasty	25	Y

Table 10: Fibroblast cohort and response to 4-OHTam

Responders and non-responders had a similar mean age (Table 11). The majority (75%) of normal reducing mammoplasty patients showed a reduction in FN expression with 4-OHTam treatment (Table 12). A smaller proportion of prophylactic mastectomy patients (33%) showed a response to 4-OHTam treatment (Table 12).

Mean age (years)	
Responders	Non Responders
41.8	46.6

Table 11: Mean age of 4-OHTAM responders and non-responders

Tissue Type	Total Patient Number	% Responders
Normal reducing mammoplasty	8	75
Dense surround	6	50
Non-dense surround	2	50
Prophylactic mastectomy	6	33
Contralateral prophylactic	2	100

Table 12: Response to 4-OHTam and tissue type

5.3.2 Effect of 4-OHTam on fibroblast expression of lysyl oxidase (LOX)

The collagen cross-linking enzyme lysyl oxidase (LOX) has been proposed to contribute to high density mammary stroma and increased stromal LOX activity is associated with tumour progression [213]. LOX expression was assessed in primary breast fibroblasts from three patients, who had previously shown a reduction in FN expression (1004, 2090, 2093), following treatment with 4-OHTam (5μM) for one week (Figure 41).

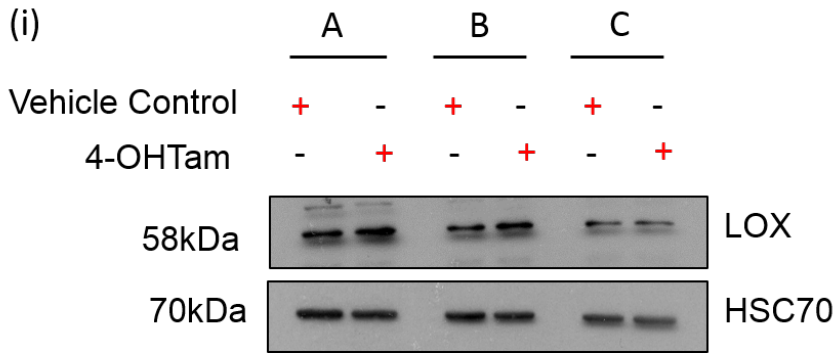

(ii)

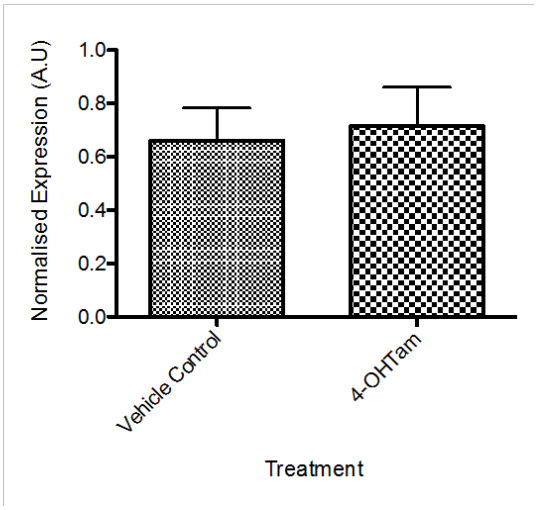

Figure 41: LOX expression in three patients' (A-C) fibroblasts treated for one week with 4-OHTam (5μm). No significant effect on LOX expression was seen with 4-OHTam treatment. (i) Representative western blot image. (ii) Densitometry analysis, representative data from patient 2090 (n=3). Expression normalised to loading control.

No significant effect on LOX expression was seen with 4-OHTam treatment in any of the three patients' fibroblasts.

5.3.3 Effect of 4-OHTam on fibroblast expression and secretion of collagen

Increased collagen density is associated with mammary tumour progression in-vitro and in-vivo [206, 207]. Collagen I expression was assessed in primary breast fibroblasts from three patients (1004, 2090, 2585), who had previously shown a reduction in FN expression, following treatment with 4-OHTam (5μM) for one week.

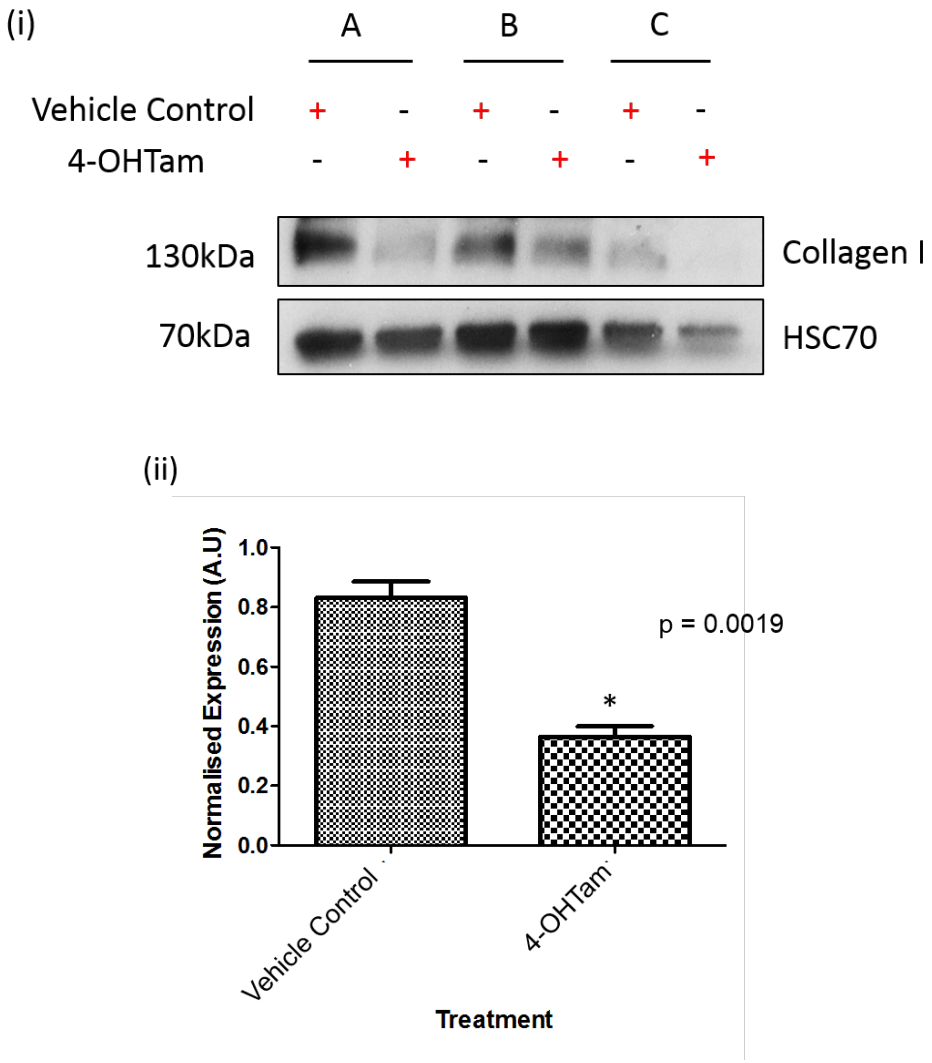

Figure 42: Collagen I expression in three patients' (A-C) fibroblasts treated with 4-OHTam (5μm) for one week. Patients A and B showed a significant reduction in collagen I expression with 4-OHTam treatment, whilst little response was observed in Patient C. (i) Representative western blot image (ii) Densitometry analysis, expression normalised to loading control. Representative data from patient 2585 (Patient A, n=3).

Two of the three patient fibroblasts examined showed a significant decrease in expression (Patients A and B), whereas the third (Patient C) showed minimal response (Figure 42), once again demonstrating inter-patient variability.

The SirCol soluble collagen assay was performed to assess whether 4-OHTam treatment influenced the secretion of soluble collagen into conditioned media by three patients' primary breast fibroblasts (2090, 2093, 2585, Figure 43).

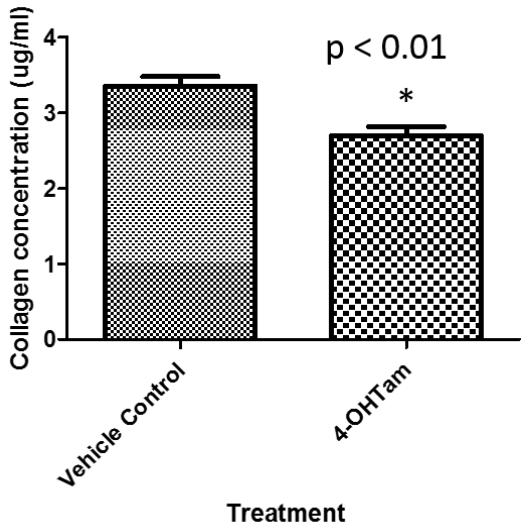

Figure 43: Total collagen concentration in conditioned media following one week treatment with 4-OHTam (5μM). Significantly less ($p < 0.01$) collagen was present in the conditioned media from 4-OHTam treated fibroblasts compared to those treated with vehicle control. Representative data from patient 2585 (n=3).

Significantly less ($p < 0.01$) collagen was present in the conditioned media from 4-OHTam treated fibroblasts compared to those treated with vehicle control (Figure 43).

Fibroblast derived matrices (FDM) generated from three patients primary fibroblasts (2093, 2182, 2266) in the presence of vehicle control or 4-OHTam (5μM) were solubilised and analysed for total collagen using the SirCol assay (Figure 44).

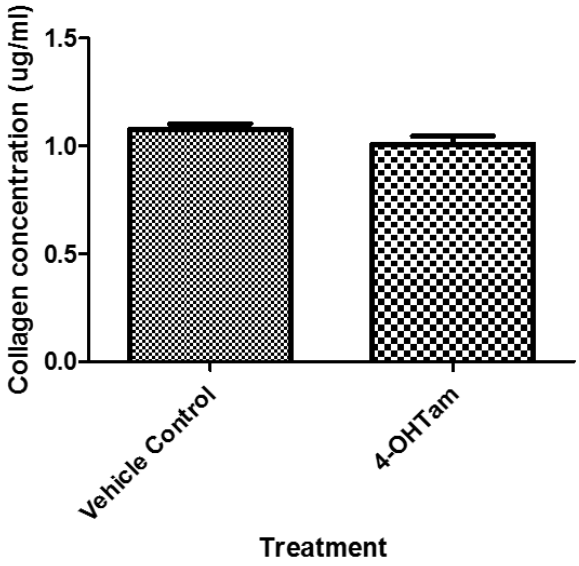

Figure 44: Collagen concentration of fibroblast derived matrices (FDM) generated from three patients primary fibroblasts in the presence of vehicle control or 4-OHTam (5μM). No significant difference is seen in the collagen content of FDM generated under the different treatment conditions. Representative data from patient 2266 (n=3).

No significant difference was seen in the collagen content of FDM generated by vehicle control or 4-OHTam treated fibroblasts (Figure 44).

5.3.4 Effect of 4-OHTam on fibroblast derived matrix thickness

FDM were generated from three patients primary fibroblasts (2090, 2182, 2266) concurrently treated with vehicle control or 4-OHTam (5μM). Immunofluorescent staining for FN was performed to assess FDM thickness (Figures 46 + 47). No significant difference was observed in the thickness of FDM generated in the presence of vehicle control or 4-OHTam (Figure 45).

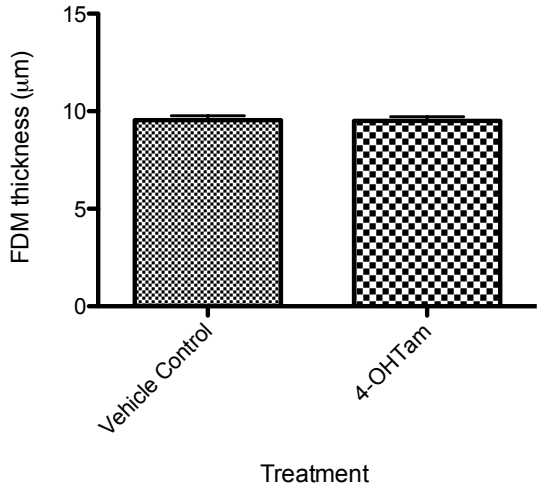

Figure 45: Thickness of FDM generated in the presence of vehicle control or 4-OHTam. No difference in FDM thickness was observed between the two treatment conditions. Representative data from 2266 (n=12).

Z stack images were taken at regular intervals (approx. 1.2µm) through the FDM

(Figure 46)

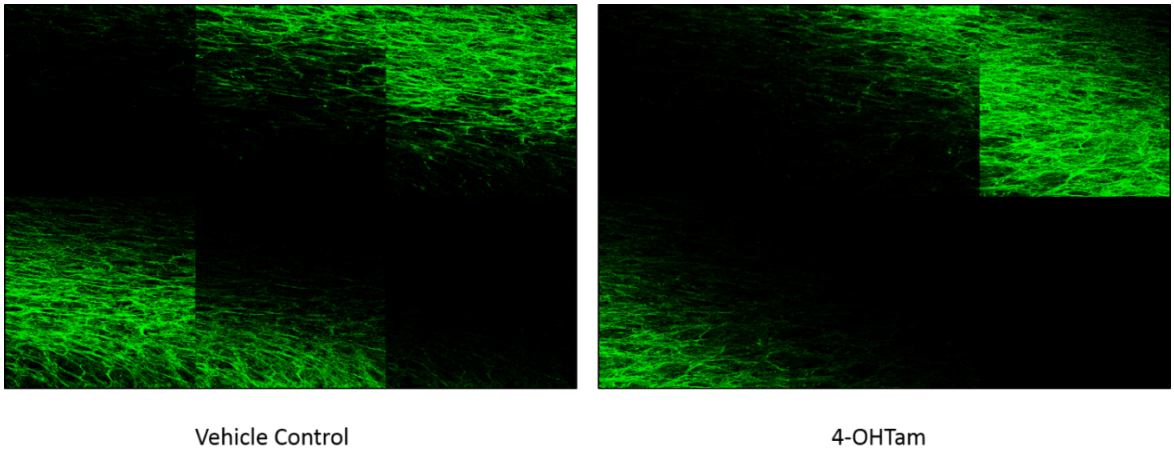

Figure 46: Serial z stack images through FDM stained with FN, generated in the presence of vehicle control or 4-OHTam.

A maximal intensity projection was generated from these images (Figure 47).

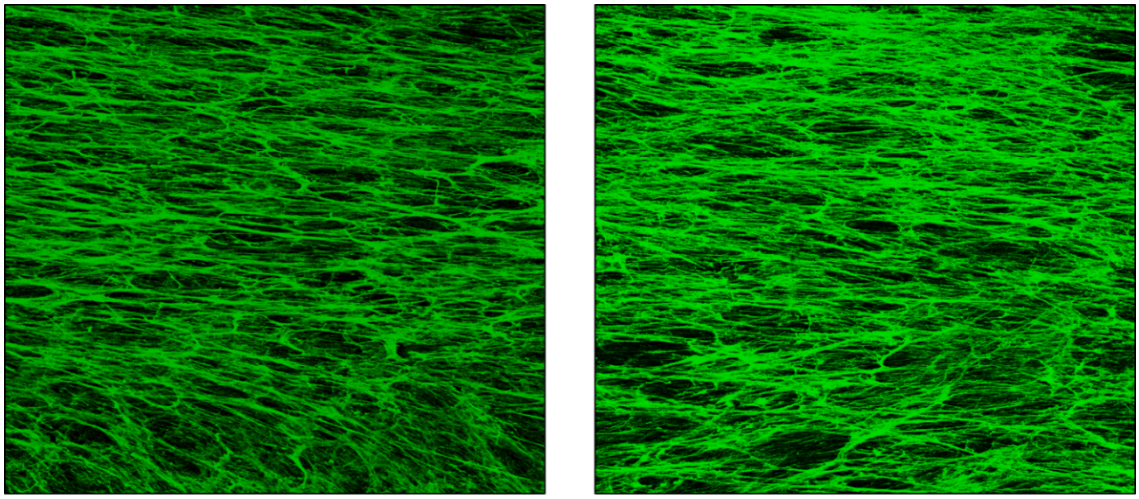

Figure 47: Maximum intensity projection of Z stack images through FDM stained for FN, generated in the presence of vehicle control or 4-OHTam (5μM). Representative images from patient 2266.

5.3.5 Effect of 4-OHTam on fibroblast activation by TGF-β

Primary breast fibroblasts were treated with 4-OHTam and stimulated with recombinant TGF-β1 to determine the effect of tamoxifen on fibroblast activation by TGF-β. Protein expression of SMA was used as a marker of fibroblast activation.

5.3.5.1 Effect of 4-OHTam on fibroblast expression of SMA

Primary fibroblasts from all patients in the cohort were treated with 4-OHTam (5μM) for three days and expression of SMA was assessed (Figure 48)

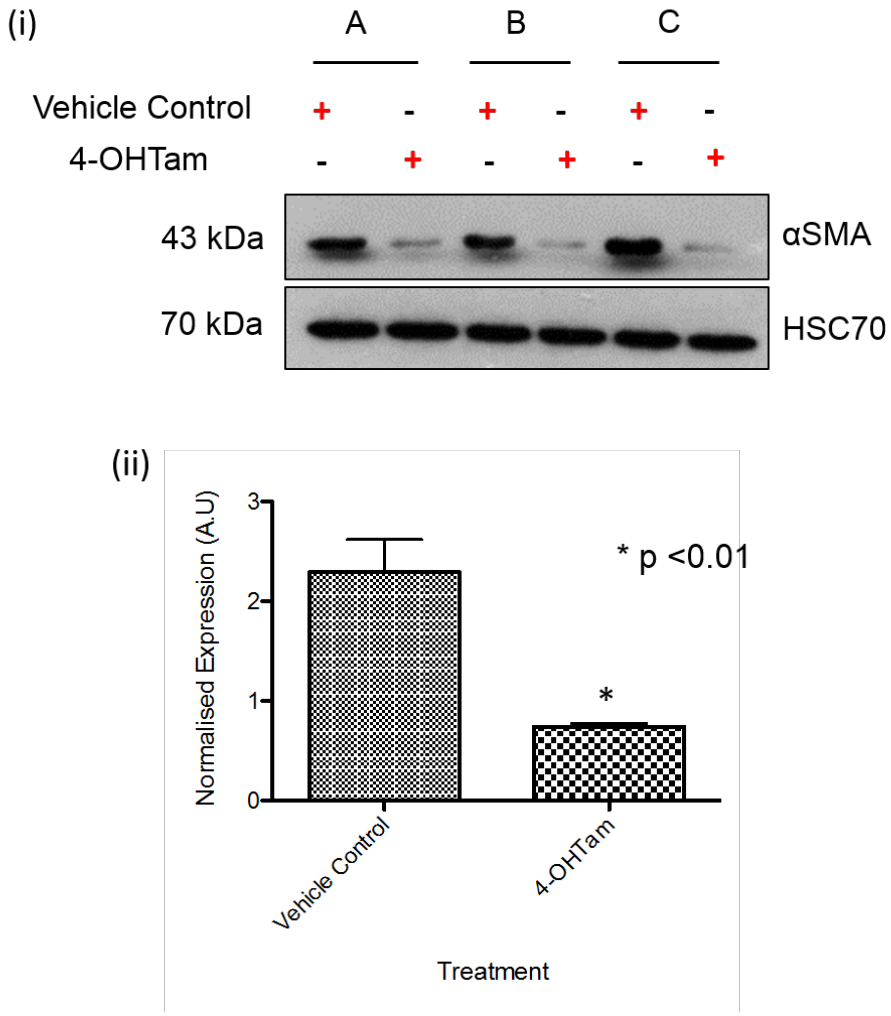

Figure 48: Effect of 4-OHTam (5μM) on fibroblast expression of SMA. A significant reduction in SMA expression was consistently seen in all three patients (p <0.01). (i) Western blot image (ii) Densitometry analysis, expression normalised to loading control. Representative data from patient 3078 (n=3).

4-OHTam treatment consistently resulted in a significant reduction (p <0.01) in SMA expression across all patients in the cohort (Figure 48).

5.3.5.2 Effect of 4-OHTam on TGF-β-mediated up-regulation of SMA

Primary breast fibroblasts from three patients (1004, 2090, 3078) stimulated with TGF-β (5ng/ml) showed significant up-regulation of SMA expression (p<0.05, Figure 49). This response was consistently inhibited in the presence of 4-OHTam (5μM, p<0.05, Figure 49)

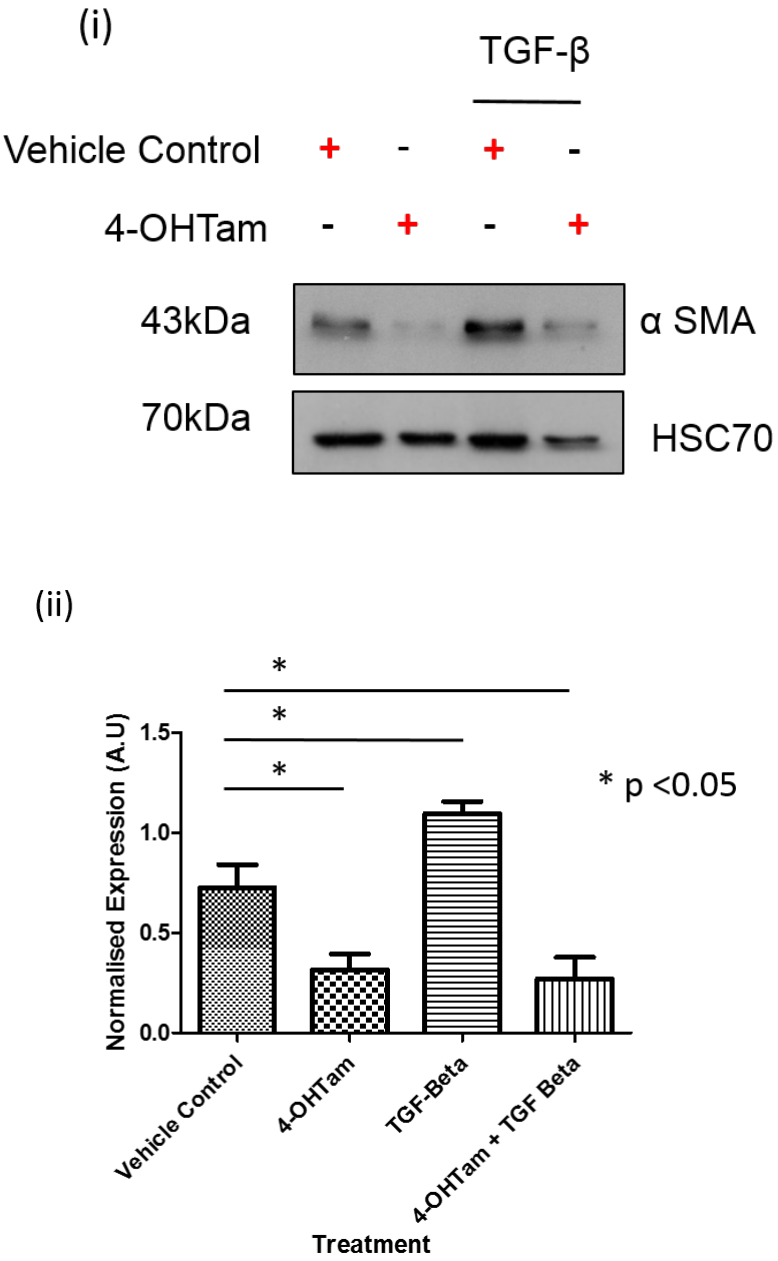

Figure 49: Effect of 4-OHTam (5μM) on fibroblast reponse to TGF-β1 (5ng/ml).TGF- β stimulation resulted in significant up-regulation of SMA expression ($p<0.05$). In the presence of 4-OHTam, this response was consistently inhibited in all patients ($p<0.05$, n=3). (i) Representative western blot image (ii) Densitometry analysis, expression normalised to loading control. Representative data from patient 3078 (n=3).

5.3.5.3 Effect of 4-OHTam on TGF-β stimulated fibroblast contraction of collagen gels

Collagen gels were seeded with primary fibroblasts from two patients (1004, 3078) and then stimulated with TGF-β1 (5ng/ml) in the presence of either vehicle control or 4-OHTam (5μM). Reduced contraction was seen in gels stimulated with TGF-β in the presence of 4-OHTam compared to TGF-β in the presence of vehicle control (p = 0.0085, Figure 50).

(i)

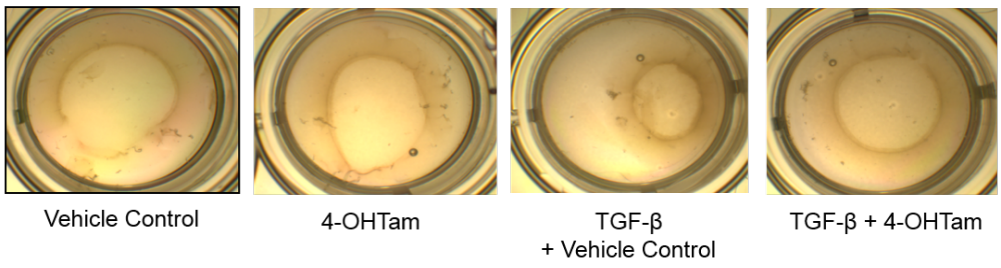

(ii)

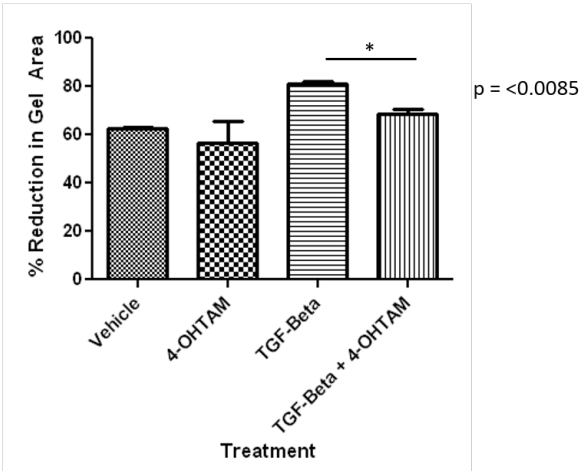

Figure 50: Effect of 4-OHTam (5μM) on TGF-β stimulated fibroblast contraction of collagen gels. The enhanced gel contraction demonstrated by stimulation with recombinant TGF-β1 (5ng/ml) is inhibited by treatment with 4-OHTam (p = 0.0085). (i) Representative images 48 hours after gel release (ii) Quantification of reduction in gel area for each treatment condition, representative data from patient 1004 (n=6).

5.3.5.4 Effect of 4-OHTam on TGF-β stimulated fibroblast migration

Scratch assays were used to assess the effect of 4-OHTam (2μM) on TGF-β (5ng/ml) stimulated fibroblast migration using cells from two patients (2090, 2266). TGF-β in the presence of vehicle control significantly increased fibroblast migration after 8 hours compared to vehicle control and 4-OHTam treated cells ($p = 0.0135$). TGF-β stimulated cell migration was reduced in the presence of 4-OHTam although the difference did not reach statistical significance ($p = 0.1789$) (Figure 51).

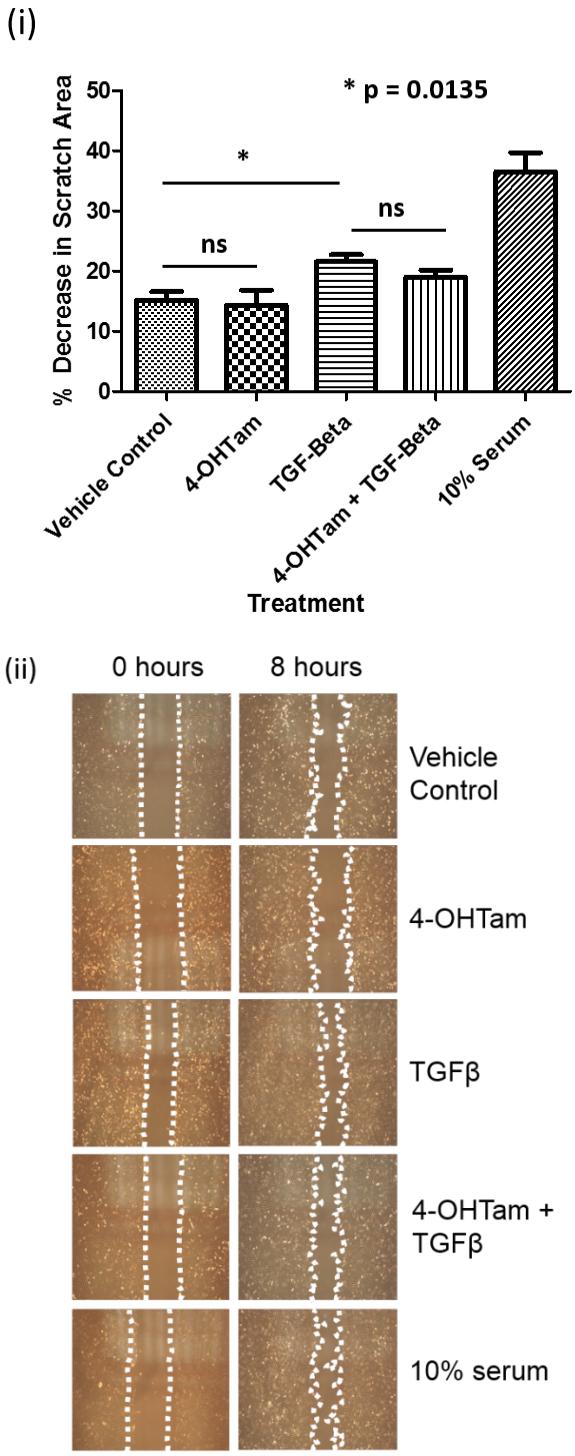

Figure 51: Effect of 4-OHTam (2μM) and TGF-β (5ng/ml) on fibroblast migration assessed by scratch assay. TGF-β in the presence of vehicle control significantly increased migration after 8 hours compared to vehicle control and 4-OHTam treated cells (p = 0.0135). TGF-β induced migration was lower in the presence of 4-OHTam however this did not reach statistical significance (p = 0.1789). (i) Graph quantifying percentage reduction in scratch area (ii) representative images at time 0 and 8 hours with scratch area outlined for each treatment condition. Representative data from patient 2090 (n=4)

5.3.5.5 Effect of 4-OHTam on SMAD signalling

Having observed a consistent inhibition of TGF-β mediated up-regulation of SMA, inhibition of fibroblast-collagen gel contraction and fibroblast migration with 4-OHTam treatment (Figures 49 - 51), primary breast fibroblasts from three patients (2090, 2182, 3353) were stimulated with recombinant TGF- β1 (5ng/ml) and expression of phosphorylated SMAD proteins analysed to determine if 4-OHTam modulated canonical TGF-β signalling.

A time course stimulation assay was initially performed using one patient's fibroblasts (3353) to determine the optimum time point to assess phosphorylation of SMAD proteins following stimulation with recombinant TGF-β1 (5ng/ml, Figure 52)

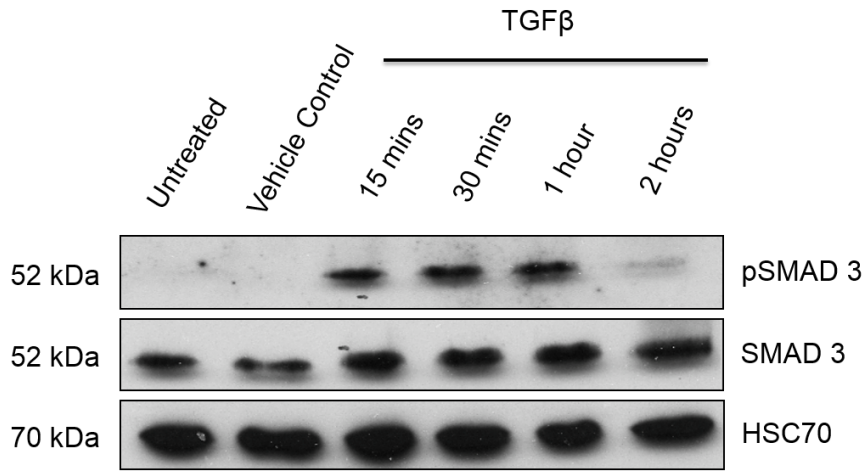

Figure 52: TGF-β stimulation assay. Primary fibroblasts were stimulated with TGF-β1 (5ng/ml) and cells harvested at sequential time points for analysis of SMAD3 protein phosphorylation. Phosphorylation of SMAD3 protein peaked after 15 minutes and remained high until 2 hours when the signal intensity fell. Representative data from patient 3353.

Based on the stimulation assay findings, a time-point of 20 minutes was selected to harvest cells for assessment of SMAD protein phosphorylation. No significant effect on the phosphorylation of SMAD 2 or SMAD3 proteins was observed in the presence of either 4-OHTam (5μM) or E2 (10nM) following TGF-β stimulation (Figures 53 + 54).

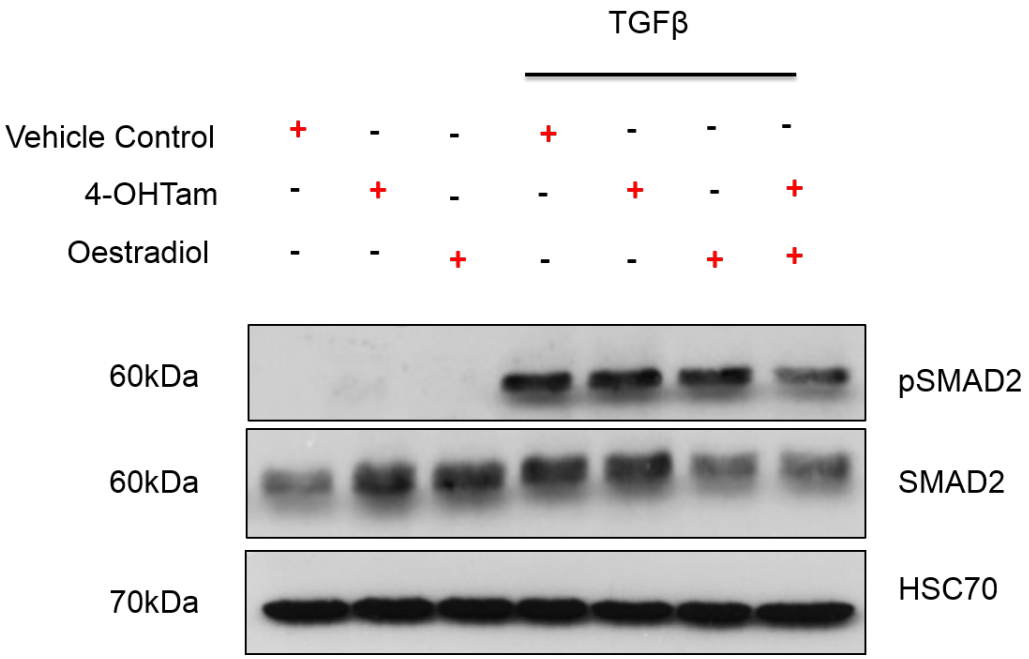

Figure 53: Effect of 4-OHTam (5μM) and 10nM E2 (10nM) on SMAD2 protein phosphorylation following stimulation with recombinant TGF-β1 (5ng/ml). No significant effect on SMAD2 phosphorylation was observed in the presence of either 4-OHTam or E2. Representative data from patient 3353.

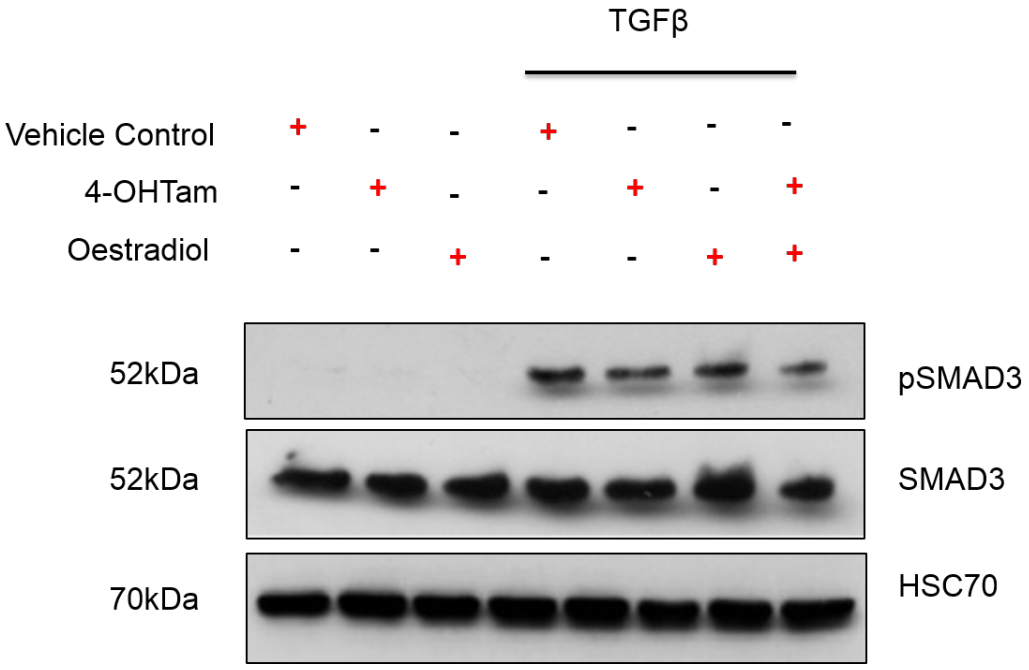

Figure 54: Effect of 4-OHTam (5μM) and 10nM E2 (10nM) on SMAD3 protein phosphorylation following stimulation with recombinant TGF-β1 (5ng/ml). No significant effect on SMAD3 phosphorylation was observed in the presence of either 4-OHTam or E2. Representative data from patient 3353.

5.3.5.6 Effect of 4-OHTam on non-canonical TGF-β signalling through ERK1/2

Having observed a significant modulation of primary fibroblast response to TGF-β by 4-OHTam (Figures 49 - 51), yet no apparent effect on canonical (SMAD) signalling (Figures 53 + 54), the effect of 4-OHTam on non-canonical TGF-β signalling through ERK1/2 was assessed. The TGF-β stimulation assay was repeated as described in section 5.3.5.5 using fibroblasts from patient 2585 and demonstrated phosphorylation of ERK1/2 after 2 minutes (Figure 55).

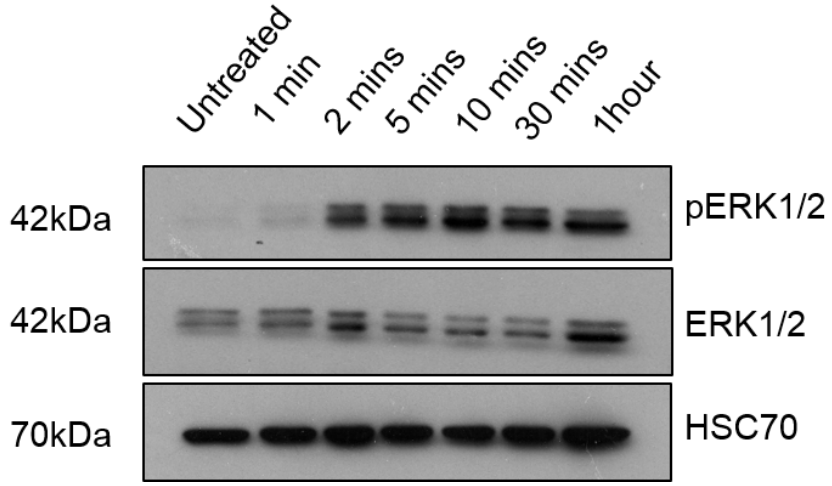

Figure 55: TGF-β stimulation assay. Significant phosphorylation of ERK1/2 was evident after two minutes and remained high up to one hour. Representative data from patient 2585.

Based on these findings, cells were harvested 5 minutes after TGF-β stimulation to assess ERK phosphorylation. Primary fibroblasts from three patients (1923, 2182, 2585) were stimulated with TGF-β with and without 4-OHTam, and the effect on ERK1/2 phosphorylation assessed.

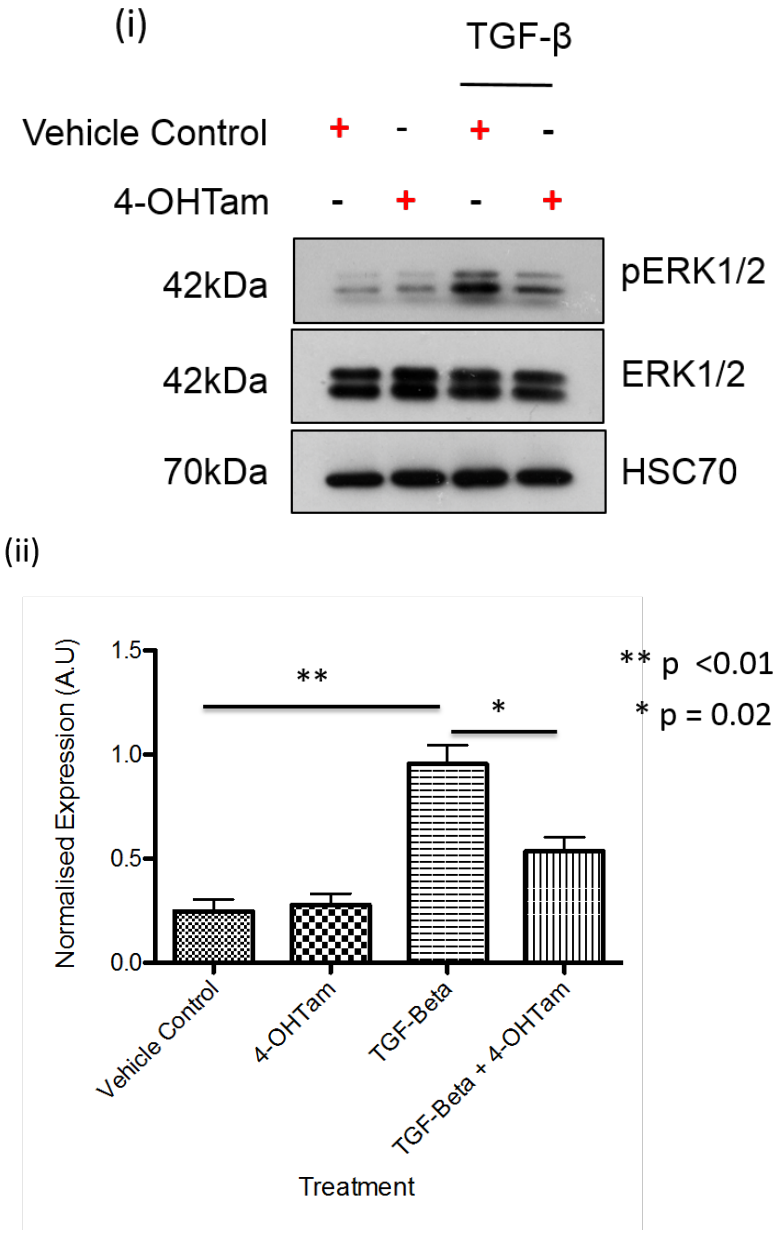

Figure 56: Effect of 4-OHTam (5μM) on non-canonical TGF-β signalling through ERK1/2. TGF-β stimulation (5mg/ml) alone resulted in significant up-regulation of ERK1/2 phosphorylation ($p < 0.01$). This response was significantly inhibited by the presence of 4-OHTam ($p = 0.02$) in all three patients' fibroblasts. (i) Western blot image (ii) Densitometry analysis, expression normalised to loading control. Representative data from patient 2585 (n=3).

TGF-β stimulation in the presence of vehicle control resulted in significant ERK1/2 phosphorylation ($p < 0.01$). Treatment with 4-OHTam significantly inhibited ERK1/2 phosphorylation following TGF-β stimulation ($p = 0.02$, Figure 56). This was seen consistently in all three patients.

5.3.6 ERα and ERβ protein expression in primary fibroblast cohort

Protein expression of ERα was not detected in any of the fibroblasts (Figure 57). Low level ERβ expression was consistently detected in all of the cohort (Figure 58). There was no association with ERβ expression and reduction in FN expression with 4-OHTam treatment (patients who showed reduced FN expression with 4-OHTam marked with * in Figure 58).

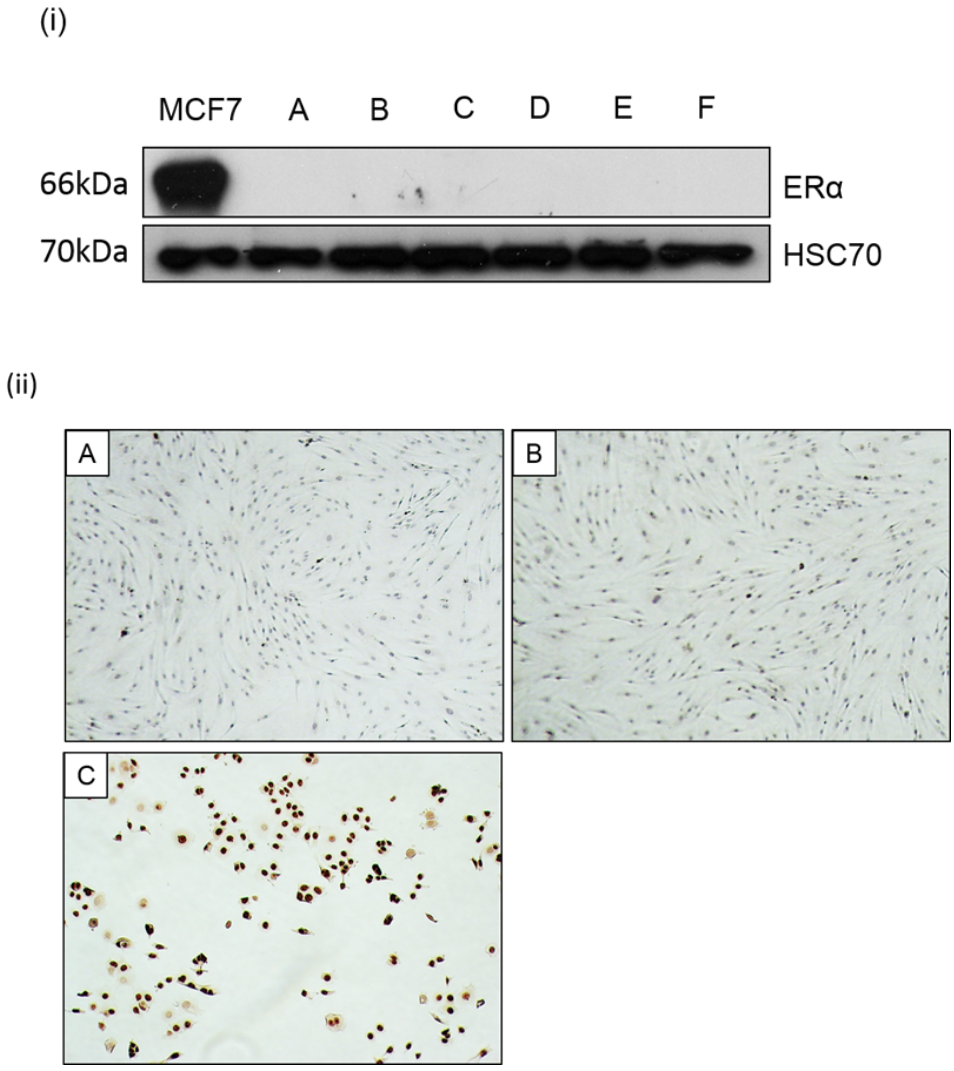

Figure 57: Oestrogen receptor alpha (ERα) expression in primary breast fibroblasts (i) Western blot image of ERα expression in six patient fibroblast samples (A-F) and MCF7 cells (positive control). No ERα expression in seen in any of the fibroblast samples. (ii) Immunocytochemical staining for ERα (x20 objective). (A) No ERα seen in primary fibroblasts (B) Rabbit immunoglobulin negative control (C) Strong ERα expression in MCF7 cells (positive control)

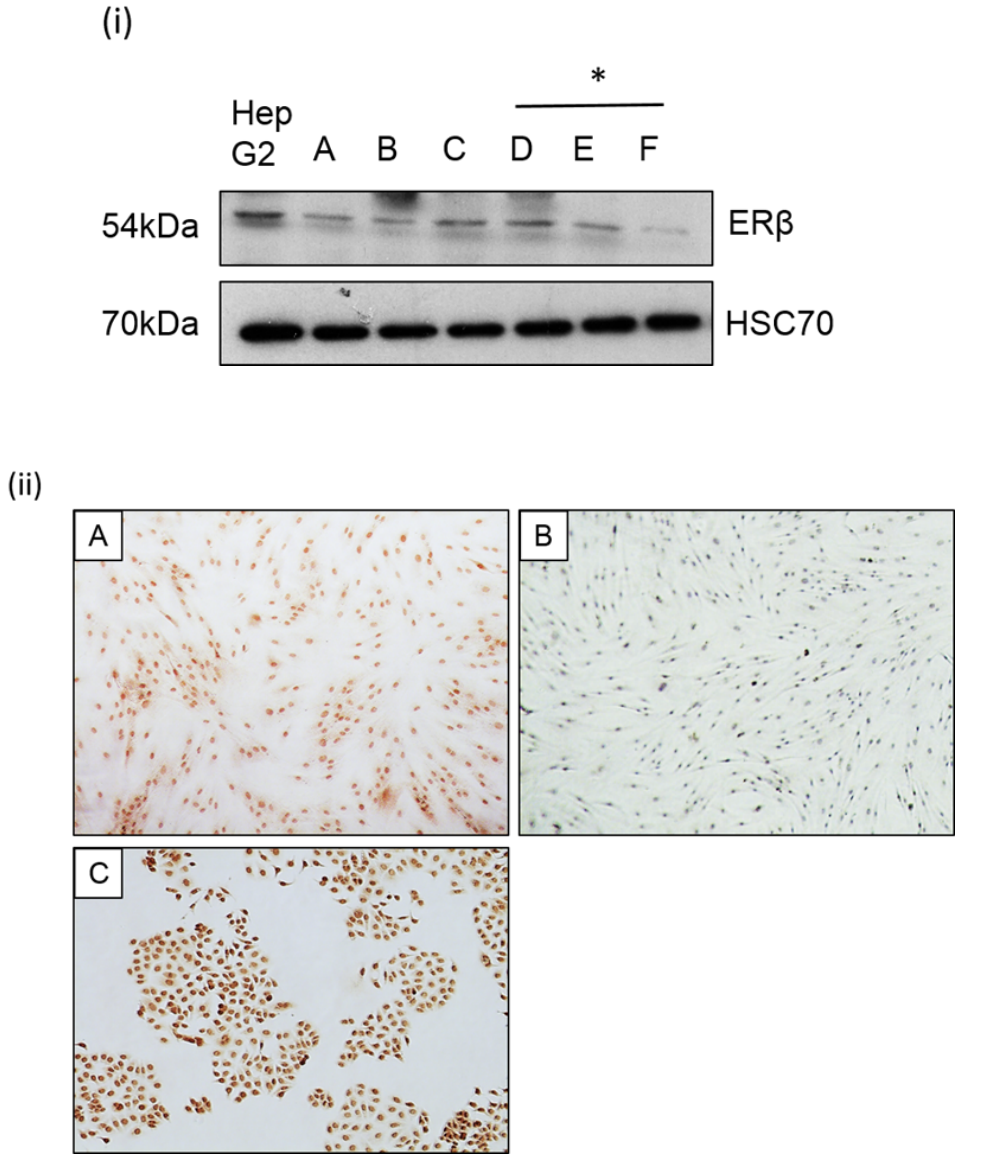

Figure 58: Oestrogen receptor beta (ERβ) expression in primary fibroblasts. (i) Western blot image of ERβ expression in six patients (A-F) primary fibroblasts (* - patients who showed a reduction in fibronectin expression with 4-OHTam) and HepG2 cell lysate (positive control). (ii) Immunocytochemical staining for ERβ (x20 objective) (A) weak nuclear and cytoplasmic expression in primary fibroblasts (B) Rabbit immunoglobulin (negative control) (C) weak to moderate nuclear expression in MCF7 cells.

5.3.7 Effect of fulvestrant on fibroblast expression of fibronectin and SMA

Fulvestrant showed a minimal effect on FN expression and no effect on SMA expression, whereas 4-OHTam substantially decreased FN expression and consistently reduced SMA expression, even in the presence of TGF-β (Figure 59). Three patients fibroblasts were assessed (2090, 2093, 2585).

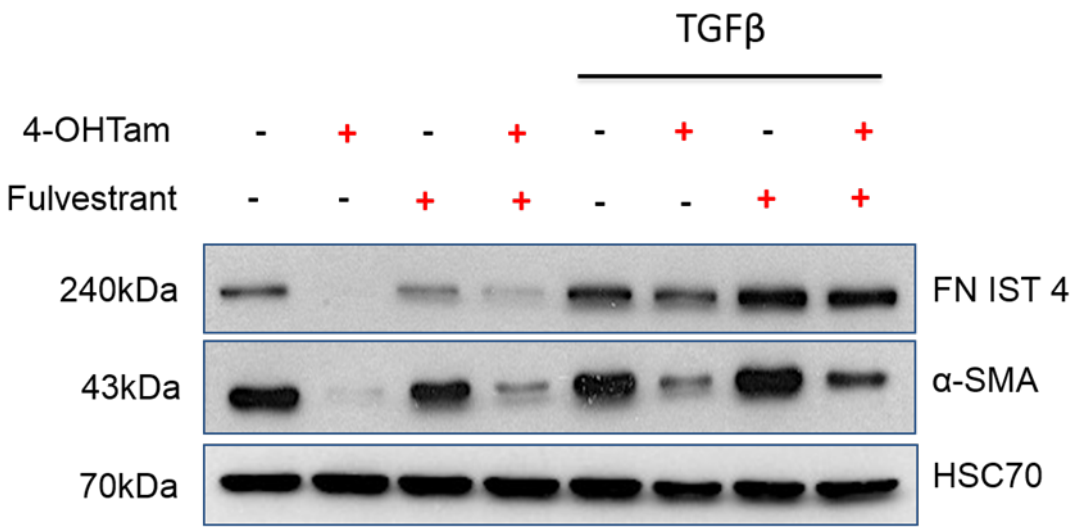

Figure 59: Effect of Fulvestrant (5μM) and 4-OHTam (5μM) on fibroblast expression of FN and SMA. Fulvestrant had a minimal effect on FN expression and no effect on TGF-β1 (5ng/ml) mediated up-regulation of FN or SMA. 4-OHTam had a substantial effect on FN expression and consistently inhibited TGF-β mediated up-regulation of FN and SMA. Example data from patient 2093

5.3.8 Effect of Fulvestrant on MCF7 Proliferation

The effect of fulvestrant on MCF7 cell proliferation was analysed, as a positive control for the drug. MCF7 cells were treated with vehicle control, E2 (10nM), fulvestrant (5μM) and E2 plus fulvestrant using phenol red free media and charcoal stripped serum (as described is sections 3.3.3 and 4.2.1.2). E2 treatment markedly increased MCF7 proliferation (Figure 60). Fulvestrant significantly decreased MCF7 cell proliferation, even in the presence of E2 (Figure 60).

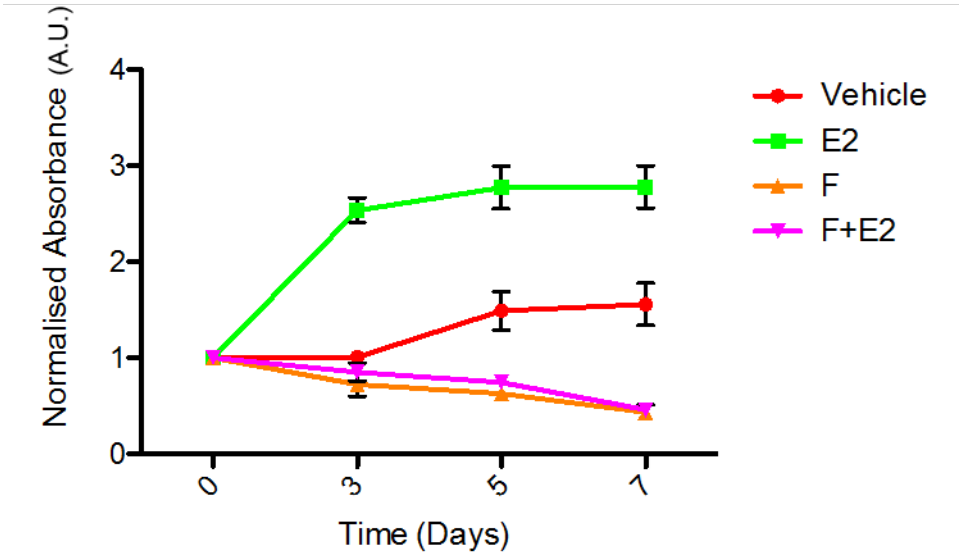

Figure 60: Effect of E2 (10nM) and Fulvestrant (F, 5μM) on MCF7 cell proliferation. E2 markedly increases MCF7 cell proliferation. Fulvestrant has a negative effect on cell proliferation, even in the presence of E2.

5.4 Discussion

5.4.1 Effect of 4-OHTam on FN expression

Almost two thirds (62%) of the primary mammary fibroblast cohort showed reduced expression of FN with 4-OHTam treatment (Figure 39, Tables 10 - 12). The variability in fibroblast response to 4-OHTam is intriguing, as it parallels the variability in response to tamoxifen observed clinically in both the preventive and adjuvant settings. Cuzick and colleagues reported just under half of women from a high risk population demonstrated a significant (>10%) reduction in MD with tamoxifen and were protected from breast cancer [110]. In addition, Li and colleagues reported just 11% of women treated with tamoxifen in the adjuvant setting showed a significant (>10%) reduction in MD [114].

This group also investigated the association of individuals who demonstrated a significant reduction in MD with polymorphisms of the CYP2D6 gene, which facilitates the metabolism of tamoxifen to 4-OHTam, a metabolite with far greater affinity for the ER. They found that individuals with a less functional CYP2D6 gene were significantly less likely to experience a significant reduction in MD (Ptrend = 0.021) [114]. This suggests an individual's ability to metabolise tamoxifen may determine whether they will respond well to treatment and receive the protective effect.

4-OHTam was used as the drug treatment in this study, which assumes extensive metabolism of tamoxifen. This may explain why the majority (62%) of our cohort of primary fibroblasts showed a response to 4-OHTam, a figure much greater than the percentage of responders from the clinical studies detailed above. Interestingly, not all patients showed a reduction in FN expression despite using pure 4-OHTam, this suggests there may be other biological factors involved in determining susceptibility to the protective effect of tamoxifen other than simply the ability to metabolise the drug.

In our fibroblast cohort, reduction in FN expression with 4-OHTam treatment did not appear to be related to patient age as both non-responder and responders had a similar mean age (41.8 vs 46.6). The type of tissue the cells were derived from did not appear to determine ability to respond to 4-OHTam as responders were present in cells derived from all tissue types. Reduction mammoplasty and contralateral prophylactic mastectomy samples had a greater proportion of responders (75% and 100%) however, the numbers present in each tissue type group are small and therefore the differences are unlikely to be significant.

Our findings of reduced FN expression with tamoxifen treatment are supportive of findings reported by a number of recent studies. Carthy and colleagues found tamoxifen reduced FN expression in primary fibroblasts from the skin and breast [313]. In addition, Kim and colleagues observed reduced FN expression in mouse model of renal fibrosis following tamoxifen treatment [314]. Furthermore, Hattar and colleagues reported reduced FN expression in the mammary ECM isolated from rats treated with tamoxifen [115].

The study by Hattar et al also highlights the potential role of FN in contributing to a pro-tumourigenic mammary stroma. Cancer cell lines injected into rats with ECM harvested from tamoxifen treated rats developed smaller tumours compared to those developing in ECM harvested from control rats [115]. Crucially, when exogenous FN was added to the ECM harvested from tamoxifen treated rats, this re-established its pro-tumourigenic activity and the tumours that developed were larger [115].

Thus tamoxifen-mediated reduction in FN expression in mammary stroma may play an important role in generating a microenvironment less permissive to tumour formation.

Primary breast fibroblasts were also treated with 4-OHTam in the presence of E2 to create a more physiologically relevant model. Reduction in FN expression was still observed in the presence of E2, to a similar degree ($p<0.01$, Figure 40). E2 alone did

not affect FN expression. This suggests there may be more complex mechanisms involved in influencing FN expression in fibroblasts rather than simply agonist or antagonist interaction at an oestrogen receptor, and that 4-OHTam may be influencing a unique pathway which E2 does not affect.

Aida-Yasuoka and colleagues reported an increase in FN expression in primary skin fibroblasts following treatment with E2 [327], in contrast to our findings. However, they observed this response to be dependent on fibroblast expression of ERα. No expression of ERα was seen in any of the primary breast fibroblasts in this study (Figure 57), which could account for these differences in response.

5.4.2 Effect of 4-OHTam on LOX Expression

LOX is a collagen cross linking enzyme which Weaver and colleagues reported to contribute to a stiff ECM, enhance focal adhesion formation, integrin signalling and facilitate the invasion of premalignant epithelial cells in-vitro and in-vivo [213]. To date, there are no reports of whether tamoxifen can modulate LOX activity.

No effect of 4-OHTam on expression of LOX was seen in three patients' primary fibroblasts (Figure 41). These three patients cells were selected as they had previously shown a response to 4-OHTam with a reduction in FN expression and thus considered 'responders'.

Despite not observing an effect on LOX expression, the functional activity of the enzyme may still be affected, thus future work could focus on addressing this. Furthermore, the LOX family has several other members (LOX-like 1-4) with similar functional activity. Therefore it is possible that tamoxifen may modulate the expression or activity of these members.

5.4.3 Effect of 4-OHTam on fibroblast collagen expression and secretion

Reduced expression of collagen I with 4-OHTam treatment was seen in three patients' fibroblasts that had previously demonstrated reduced FN expression (Figure 42). The degree of reduction in collagen expression showed significant variation between the three patients.

This heterogeneity in response to 4-OHTam, in terms of collagen I expression, is intriguing as it further highlights the complexity and variability in response seen between patients. All these three patients had previously shown reduced FN expression with 4-OHTam, highlighting that the change in expression of a single protein is no guarantee of response in all other proteins of interest. Once again this emphasises that there are complex pathways determining how patients respond to tamoxifen beyond simply the ability to metabolise the drug.

Reduced secretion of soluble collagen into the culture media was also observed in the fibroblasts treated with 4-OHTam compared to those treated with vehicle control ($p<0.01$, Figure 43) suggesting that collagen synthesis and turn over may also be affected. However, there was no difference in the collagen content of FDM generated by vehicle control or 4-OHTam treated fibroblasts (Figure 44). This may be due to the use of ascorbic acid in the matrix generation protocol. The ascorbic acid up-regulates the activity of the collagen synthesis enzymes prolyl-4-hydroxylase and lysyl hydroxylase and this may have masked any effect of 4-OHTam.

Particia Keeley and colleagues have reported that increased collagen density in the mammary ECM had tumour promoting properties with a threefold increase in tumour burden observed in an animal model of high MD [206]. Thus, reduction of collagen I expression by tamoxifen is in keeping with a tumour inhibitory effect.

Modulation of collagen by tamoxifen has been reported by a number of studies. Our findings are supported by Kim and colleagues found that tamoxifen reduced collagen I expression in a mouse model of renal fibrosis [314]. Conversely, Hattar and colleagues reported increased collagen I in the mammary ECM of tamoxifen treated rats [115]. These findings appear contradictory given the association of increased collagen density and tumourigenesis reported by the Keeley group [206]. However, increased total collagen within a mammary stroma less permissive to tumour formation has also been reported by Pepper Schedin and colleagues [212]. This group reported that mammary stroma from parous rats had tumour inhibitory properties and an increased collagen content compared to non-parous stroma [212].

A crucial feature of the collagen present in the anti-tumourigenic parous stroma was that it was significantly less organised and fibrillar in nature [212]. These observations highlight both quantitative and qualitative aspects of the mammary ECM may contribute to tumour development. The importance of collagen fibre alignment and organisation within high MD stroma has been highlighted in a proteomics study by Streuli and colleagues [61]. They found that high MD stroma was characterised by increased periductal fibrillar collagen and up-regulation of periostin and collagen XVI - mediators of fibril structure and alignment [61].

The influence of collagen fibre orientation within the mammary ECM on the propensity for tumour formation may indicate that, whilst not all patients' primary fibroblasts showed a reduction in collagen I expression with 4-OHTam treatment (Figure 42), there may have been an effect on fibre orientation that could contribute to the anti-tumour effects of tamoxifen.

Given these data indicating the importance of ECM fibre organisation and in contributing to high MD stroma, FDM were generated from cells treated with vehicle control or 4-OHTam to determine if 4-OHTam treatment influenced ECM fibre organisation. Due to constraints of time, a full analysis of ECM fibre directionality was

not undertaken. No significant difference was seen in the FDM thickness in either treatment condition (Figure 45). Despite this lack of difference between the two conditions, it is possible that tamoxifen may still influence mammary ECM fibre organisation in the body through interactions with other stromal cell types, such as immune cells, not present in our limited system. A more sophisticated 3D model system incorporating a variety of primary stromal cell types may need to be employed to appreciate subtle changes in matrix organisation.

5.4.4 Effect of 4-OHTam on fibroblast activation

Smooth muscle actin (SMA) is considered a key marker of activation [308]. Primary fibroblast treatment with 4-OHTam resulted in a significant reduction in SMA expression ($p < 0.01$, Figure 48). Given the degree and consistency of response, the entire fibroblast cohort were treated with 4-OHTam and a consistent reduction in SMA expression was seen, even in those cells who did not show a reduction in FN expression. These findings are supported by Carthy and colleagues who found reduced expression of SMA and other myogenic markers, Calponin and Sm22alpha, in primary skin and breast fibroblasts with tamoxifen treatment [313]. In addition Kim and colleagues found that tamoxifen treatment reduced SMA expression in the renal tissue of a mouse model of renal fibrosis [314].

The consistency of the response of reduced SMA expression following 4-OHTam treatment, in contrast to other markers such as FN and collagen I, which have demonstrated a degree of variability, further suggests that 4-OHTam may be acting via multiple mechanisms to effect fibroblast function.

Fibroblast expression of SMA is indicative of transformation to an activated myofibroblast phenotype [308]. This occurs physiologically in the body as part of the wound healing process. Myofibroblasts aberrantly secrete growth factors and cytokines and have contractile properties to assist with wound healing and closure [308]. The

baseline expression of SMA noted in the cultured primary cells (Figure 48) may be due to growing the cells on plastic, a material they would not normally be exposed to in the body.

SMA is also a marker used to identify CAFs which are believed to behave in a similar manner to activated myofibroblasts, secreting growth factors and cytokines to promote tumour growth [162].

The most potent factor known to transform fibroblasts to the activated myofibroblast phenotype is the pro-fibrotic cytokine TGF-β [308]. To determine whether tamoxifen could influence this response, primary breast fibroblasts were stimulated with TGF-β with and without 4-OHTam.

Stimulation with TGF-β alone consistently resulted in an increase in SMA expression ($p < 0.01$, Figure 49). In the presence of 4-OHTam, this response was consistently inhibited ($p<0.01$, Figure 49). These data suggest that tamoxifen may be able to prevent the transformation of fibroblasts to an activated myofibroblast-like phenotype and thus generate a more quiescent breast microenvironment less permissive to tumour formation.

5.4.5 Effect of 4-OHTam on canonical and non-canonical TGF-β signalling pathways

Having observed that 4-OHTam is capable of inhibiting primary breast fibroblast activation following stimulation with TGF-β, fibroblasts were stimulated with TGF-β with and without 4-OHTam to determine if inhibition of canonical (SMAD) TGF-β signalling by 4-OHTam was the mechanism involved.

TGF-β stimulation alone increased phosphorylation of SMAD 2 and SMAD3 (Figures 52 - 54). The presence of 4-OHTam or E2 had no effect on SMAD2 or SMAD3 protein phosphorylation following stimulation with TGF-β (Figures 53 + 54). These findings

suggest 4-OHTam may affect fibroblast activation via non-canonical signalling pathways.

Carthy and colleagues also observed no effect of tamoxifen on SMAD phosphorylation in primary skin and breast fibroblasts following TGF-β stimulation [313]. However, they did observe inhibition of non-canonical TGF-β signalling through the ERK1/2 MAP kinase pathway [313].

In contrast to our findings, Kim and colleagues reported inhibition of SMAD signalling by tamoxifen in a rat renal fibroblast cell line [314]. However, this response was dependent upon expression of ERα in the fibroblast cell line. No protein expression of ERα was observed in any of the primary breast fibroblasts (Figure 57), which may account for these differences [314].

Given the data from Carthy and colleagues regarding inhibition of non-canonical TGF-β signalling through ERK1/2 [313], fibroblasts were stimulated with TGF-β with and without 4-OHTam, to analyse the effect on phosphorylation of ERK1/2. TGF-β stimulation increased phosphorylation of ERK1/2 (Figures 55 + 56) and this response was consistently inhibited by the presence of 4-OHTam ($p=0.02$, Figure 56).

These data further suggest that 4-OHTam inhibits fibroblast activation via non-canonical pathways, in particular through ERK1/2. Carthy and colleagues observed, in addition to ERK1/2 phosphorylation, the transcription factor FRA2 was also inhibited by tamoxifen and this was a critical event preventing fibroblast expression of myogenic proteins following stimulation with TGF-β [313]. Further exploration of these mechanisms in primary breast fibroblasts could be a focus of future work.

5.4.6 Effect of 4-OHTam on fibroblast function

To determine the functional effect of 4-OHTam treatment, fibroblasts were seeded into collagen gels, treated with vehicle control or 4-OHTam, and then stimulated with TGF-

β. The gels with vehicle control treated fibroblasts stimulated with TGF-β showed substantial contraction (Figure 50). Treatment with 4-OHTam significantly inhibited gel contraction following TGF-β stimulation (p= 0.0085, Figure 50). Carthy and colleagues also observed reduced contraction of collagen gels seeded by tamoxifen treated fibroblasts from the skin and breast [313].

To further evaluate the effect of 4-OHTam on fibroblast function, scratch assays were performed to determine any effects on cell migration. TGF-β treated fibroblasts showed enhanced migration compared to those treated with vehicle control (p = 0.0135, Figure 51) and this effect was inhibited by the presence of 4-OHTam, although the difference did not reach statistical significance (p = 0.1789), Figure 51). These findings are supported by Kim and colleagues who also found inhibition of TGF-β stimulated migration by tamoxifen in a mouse renal fibroblast cell line [314].

These results demonstrate that the inhibition of primary breast fibroblast activation by 4-OHTam results in functional alterations in cell behaviour. The primary breast fibroblasts were less contractile and less migratory following TGF-β stimulation. This further suggests that tamoxifen treated breast stroma will be less 'reactive' and potentially less conducive to tumour formation.

Overall these data have demonstrated significant alterations in fibroblast phenotype by tamoxifen, characterised by reduced expression of ECM proteins FN and collagen 1, reduced expression of the activation marker SMA and functional alterations in cell behaviour. The combined effect of these alterations suggests the generation of a less activated breast stroma, less permissive to tumour development.

Not all of these effects were observed consistently across the fibroblast cohort, suggesting multiple mechanisms may be involved. One pathway that appears to be modulated by tamoxifen is non-canonical TGF-β signalling through ERK1/2. Carthy and colleagues observed similar effects and suggest that mechanistically, tamoxifen inhibits

the effects of TGF-β via a blockade of non-canonical signalling through ERK1/2 MAP kinase and the downstream transcription factor FRA2 [313]. They demonstrated that inhibition of MAP kinase signalling using either a specific inhibitor of the MAP kinase pathway, siRNA for FRA2 or tamoxifen was sufficient to prevent the expression of myofibroblast marker proteins in primary fibroblasts stimulated with TGF-β [313]. A focus of future work could be to determine if tamoxifen modulates FRA2 expression in the primary breast fibroblasts used in this study.

Further elucidation of the pathways by which tamoxifen generates a less reactive mammary stroma will be crucially important, in order to generate a molecular signature with the potential to predict individuals likely to respond well to treatment and be protected from developing breast cancer.

5.4.7 ERα and ERβ protein expression in primary fibroblast cohort

Having observed a variety of effects of 4-OHTam on primary breast fibroblast function, the mechanisms by which 4-OHTam exerted these effects was investigated.

Tamoxifen is classically thought to act as a competitive antagonist at ERα in the context of the treatment of an ERα positive breast tumour. The mechanism of tamoxifen action in fibroblasts is presently unknown. Mammary and skin fibroblasts have been reported to express ERβ [270, 328] and occasional studies report expression of ERα in fibroblasts [58].

Characterisation of the primary breast fibroblast cohort for protein expression of ERα and ERβ showed low level expression of ERβ but no expression of ERα in any of the patients' fibroblasts (Figures 57 + 58). The level of expression of ERβ did not correlate with reduction in FN expression with 4-OHTam treatment (Figure 58).

Therefore, interaction of tamoxifen with ERβ in primary breast fibroblasts could be a potential mechanism by which the observed effects of fibroblast function are mediated.

In order to investigate this hypothesis, primary fibroblasts were treated with the pure ER antagonist fulvestrant, a drug with high affinity for ER and little known ER-independent actions [329], to see if similar effects were observed and thus attribute these to interaction with ERβ.

The ability of fulvestrant to target ER-β has been reported in a number of studies. Peekhaus and colleagues observed that both fulvestrant and tamoxifen were capable of preventing E2-induced degradation of ER-β in MCF7 and HeLa cells [330]. More recently, Raza et al observed that 27-hydoxycholesterol was able to drive proliferation of prostate cancer cells in an ER-β dependent manner, and that both fulvestrant and the specific ER-β inhibitor PHTPP inhibited this response [331].

In addition, Fan and colleagues observed that ER-β expression promoted metastasis in a mouse model of non-small cell lung cancer, and that treatment with fulvestrant (in vitro and in vivo) or knock-down of ER-β using siRNA reduced the aggressiveness of lung cancer cells [332]. Wang et al also investigated ER-β in a cell line model of non-small cell lung cancer [333]. They found that transfection of ER-β into lung cancer cells, resulting in nuclear and cytoplasmic expression of ER-β, conferred resistance to tyrosine kinase inhibitor therapy. Treating these cells with fulvestrant re-sensitised them to tyrosine kinase inhibitor therapy [333].

Furthermore, Mishra and colleagues observed that fulvestrant treatment resulted in a negative proliferative effect on triple negative breast cancer cell lines expressing ER-β in vitro and in vivo [334]. The effect of fulvestrant was less pronounced in those cell lines with an intrinsically lower level of ER-β expression. In addition, when ER-β was knocked-in or knocked-down in the cells, their response to fulvestrant changed accordingly [334]. They also observed that fulvestrant enhanced the anti-tumour effect of tamoxifen on breast cancer cells expressing both ER-α and ER-β by preventing ER-β degradation. When ER-β expression was increased further by knock-in experiments, this further potentiated the effect of fulvestrant [334]. The authors conclude that

fulvestrant is an ER-β targeted therapy and suggest a potential therapeutic role in the treatment of ER-α negative breast cancers which express ER-β.

5.4.8 Effect of fulvestrant on fibroblast expression of fibronectin and SMA

Fulvestrant treatment had minimal effect on FN expression and no effect at all on SMA expression, with or without TGF-β stimulation (Figure 59). Conversely, 4-OHTam treatment resulted in a substantial reduction in FN expression and consistent inhibition of SMA expression (Figure 59). Given these vastly differing effects on fibroblast protein expression between the two drugs, this implies that the effects of 4-OHTam may be mediated, at least in part, by ER-independent mechanisms.

The ability of fulvestrant to act as an ER antagonist was suggested by measuring MCF7 cell proliferation in response to E2 (Figure 60). Treatment of MCF7 cells with E2 results in a significant increase in proliferation, however this response is blocked by concurrent treatment with fulvestrant (Figure 60).

Given that fulvestrant appears to act as an ER antagonist, the ability of 4-OHTam to reduce FN and SMA expression in the presence of fulvestrant suggests that 4-OHTam may be acting via ER-independent mechanisms. In this treatment condition the ER could be occupied by fulvestrant, suggesting that 4-OHTam may be acting via alternative mechanisms to modulate fibroblast protein expression.

Use of siRNA to knock down the expression of ERβ in the primary fibroblasts was attempted but unfortunately was not successful due to technical difficulties. Future work could investigate alternative ways to knock down the expression of ERβ to demonstrate that the effects of 4-OHTam are mediated via ER-independent mechanisms.

6 Whole transcriptome analysis of pathways modulated by tamoxifen using RNA-Seq

6.1 Introduction

Having identified a direct effect of 4-OHTam on primary breast fibroblast function, with an indication that the mechanisms involved may be independent of the ER, RNA-Seq was performed to gain a global perspective on the pathways modulated by 4-OHTam and further dissect potential mechanisms of action.

A pilot experiment was conducted in the first instance to determine the optimum concentration of 4-OHTam to use and to assess the quality of data obtained with the initial sequencing parameters. Following analysis of the pilot data, a second follow up batch of samples were sequenced, the data from the follow up batch was analysed separately before being merged with the pilot data and a combined analysis undertaken.

6.2 Methods and Materials

6.2.1 RNA Seq Pilot Batch

6.2.1.1 Patient sample selection

Fibroblasts from two reduction mammoplasty patients (1004 and 3078) which demonstrated a reduction in FN expression with 4-OHTam treatment were selected for the pilot batch RNA-Seq experiment.

6.2.1.2 Primary fibroblast culture and drug treatment

Primary fibroblasts were treated with vehicle control or 4-OHTam at either low dose (100nM) or high dose (5μM) for one week. Cells were then trypsinised and centrifuged at 12000 rpm for 2 minutes to form a pellet. Triplicate samples were prepared for each treatment condition, giving a total of 9 samples per patient.

6.2.1.3 RNA extraction

RNA was extracted from the cell pellets using the RNeasy Plus mini kit (Qiagen, 74134) as per manufacturer's instructions.

Briefly, the pellet was re-suspended and vortexed for 30s in 600μl Buffer RLT Plus to lyse the cells. The homogenised lysate was then transferred to a gDNA Eliminator spin column in a 2ml collection tube and centrifuged at 10000 rpm for 30 seconds. 600μl of 70% ethanol was added to the flow through, mixed by pipetting, transferred to an RNeasy spin column in a 2ml collection tube and then centrifuged for 15 seconds at 10000 rpm. The flow through was discarded, then 700μl Buffer RW1 was added to the spin column and centrifuged at 10000 rpm for 15 seconds. The flow through was discarded, 500μl Buffer RPE added to the spin column and centrifuged at 10000 rpm for 15 seconds. The flow through was discarded, a further 500μl Buffer RPE added and

spun at 10000 rpm for 2 minutes. The spin column was then added to a fresh 2ml collection tube and spun empty for 1 minute at 13000 rpm to dry the tube membrane. The RNeasy spin column was then transferred to a 1.5ml eppendorf tube and 30µl of RNase-free water added directly onto the membrane before centrifuging at 10000 rpm to elute the RNA. The final step was repeated using the RNA eluate to maximise the RNA yield.

Following RNA elution, samples were frozen at -80^{o}C. RNA quantity was estimated using the Nanodrop system. A minimum total RNA yield of 1ug was required for each sample.

6.2.1.4 Library Preparation

Library preparation was performed by Vertis Biotech, Freising, Germany using the NuGEN Ovation RNA-Seq System V2 (NuGEN, 7102) according to manufacturer's instructions.

6.2.1.5 Sequencing

Sequencing was performed by Beckman Coulter Genomics, Danvers, MA, USA using the Illumina HiSeq 2500 platform (100bp paired end reads) with three samples per HiSeq lane, aiming to achieve ~50-60million reads per sample.

6.2.1.6 Bioinformatics Analysis

Bioinformatics analysis was performed by Dr J Wang and Professor C Chelala, Bioinformatics Group, Centre for Molecular Oncology, Barts Cancer Institute, London, UK. Raw data reads were aligned to the reference genome hg19 using Tophat2. The number of uniquely aligned reads (q>10) aligned to the exonic region of each gene were counted using HTSeq based on the Ensembl annotation (version 74). Only genes that achieved at least one million reads (CPM) in at least three samples were kept.

Read numbers were further normalised using the CQN method, accounting for gene length and GC content.

Differential expression analysis was performed using the edgeR R package, employing the generalised linear model (GLM) approach, for each treatment vs control pair-wise comparison as well as ANOVA analysis across the three groups, adjusting for baseline differences between the two patients.

6.2.2 Follow up batch

6.2.2.1 Patient sample selection

Primary fibroblasts from three reduction mammoplasty patients (2585, 3137, 2182) and one BRCA1 mutation carrier (2093) contralateral prophylactic mastectomy were used for the second RNA Seq batch. These patients were selected to be a close age match to the pilot batch samples (Table 13). One patient (3137) did not show a reduction in FN expression with 4-OHTam treatment.

Patient ID	Tissue Type	Age (Years)	Ethnicity	Menopausal Status	Parity	Smoking	Reduction in FN (Y/N)
1004	Reduction mammoplasty	27	n/a	Pre-menopausal	n/a	n/a	Y
3078	Reduction mammoplasty	58	White British	Post-menopausal	2	Non smoker	Y
3137	Reduction mammoplasty	49	White British	Pre-menopausal	3	Current smoker, 10/day	N
2585	Reduction mammoplasty	24	Black British	Pre - menopausal	0	n/a	Y
2182	Reduction mammoplasty	25	White British	Pre-menopausal	2	Non smoker	Y
2093	Contralateral prophylactic mastectomy (BRCA1 mutation carrier)	53	White British	Post-menopausal	n/a	Non smoker	Y

Table 13: Clinical details of primary fibroblast samples used for the RNA Seq experiments

6.2.2.2 Sample Preparation

Primary fibroblasts were treated with vehicle control or 4-OHTam (5μM) for one week. In addition, two of the four patients were also treated with fulvestrant (5μM) for one week. Cells were then trypsinised and centrifuged at 12000 rpm for 2 minutes to form a pellet. Triplicate samples were prepared for each treatment condition, giving a total of 6 samples per patient (9 samples for those additionally treated with fulvestrant). RNA was extracted and quantified as described previously (Section 6.2.1.3)

6.2.2.3 Library Preparation

Library preparation was performed by the Wellcome Trust Centre for Human Genetics in Oxford, United Kingdom using the Tru Seq Stranded Total RNA Library Prep Kit (Illumina, RS-122-2202) according to manufacturer's instructions. Depletion of ribosomal RNA was performed using Ribo-Zero (Illumina).

6.2.2.4 Sequencing

Sequencing was performed by the Wellcome Trust Centre for Human Genetics in Oxford, United Kingdom using the Illumina HiSeq 4000 platform (100bp paired end reads) with five samples per HiSeq lane, aiming to achieve ~50-60million reads per sample.

6.2.2.5 Bioinformatics analysis

Bioinformatics analysis was performed by Dr J Wang and Professor C Chelala, Bioinformatics Group, Centre for Molecular Oncology, Barts Cancer Institute, UK. The same analysis pipeline was used as per the pilot batch (Section 6.2.1.6)

In addition, pathway analysis was performed using the gene set enrichment analysis (GSEA) tool in conjunction with the KEGG and REACTOME biological pathway databases.

6.3 Results

6.3.1 RNA Seq Pilot Batch

6.3.1.1 Data Quality Control

The pilot batch was sequenced by Beckman Coulter Genomics, achieving on average 28M reads per sample. The read alignment data for all samples is displayed in Appendix 1. Unexpectedly, a significant proportion of reads (range 29.9% - 45.2%) mapped to the mitochondrial genome (Table 14). Fortunately this did not affect the overall analysis.

Sample	Mitochondrial Counts	Total Mapped Counts	% Mitochondrial Counts
1004 C1	22537318	49811420	45.2
1004 C2	20317021	52192895	38.9
1004 C3	20762493	51046616	40.6
1004 Low T1	22672281	56578263	40.0
1004 Low T2	16670387	45785890	36.4
1004 Low T3	24834516	69698915	35.6
1004 High T1	19572427	50664546	38.6
1004 High T2	18047157	55810896	32.3
1004 High T3	9830853	30900244	31.8
3078 C1	16091988	49613100	32.4
3078 C2	16066074	52369081	30.6
3078 C3	15551013	51953928	29.9
3078 Low T1	18347529	52247522	35.1
3078 Low T2	14943004	46009384	32.4
3078 Low T3	17843236	50805865	35.1
3078 High T1	16407265	52003071	31.5
3078 High T2	14573007	44785140	32.5
3078 High T3	18394273	51790860	35.5

Table 14: Number and percentage (highlighted in red) of HiSeq reads per pilot batch sample mapping to the mitochondrial genome.

13,396 genes achieved at least 1 million reads and were filtered to the next stage of the analysis.

6.3.1.2 Preliminary analysis of differential gene expression

The multidimensional scaling (MDS, Figure 61) plot shows the significant heterogeneity in the baseline gene expression between the two pilot batch patients (Tissue Bank IDs 1004 and 3078), indicated by the clear separation of their respective samples, clustering together at opposite sides of the plot.

Both patients show a similar response to the higher dose 4-OHTam treatment, with significant changes in gene expression compared to vehicle control and low dose 4-OHTam treated samples - indicated by the higher dose 4-OHTam samples clustering together on the plot, distinctly separated from the other treatment groups (highlighted by blue circles).

There was no significant difference in the gene expression of low dose 4-OHTam treated fibroblasts and vehicle control fibroblasts, indicated by the overlapping clustering of samples between these groups on the plot (Figure 61).

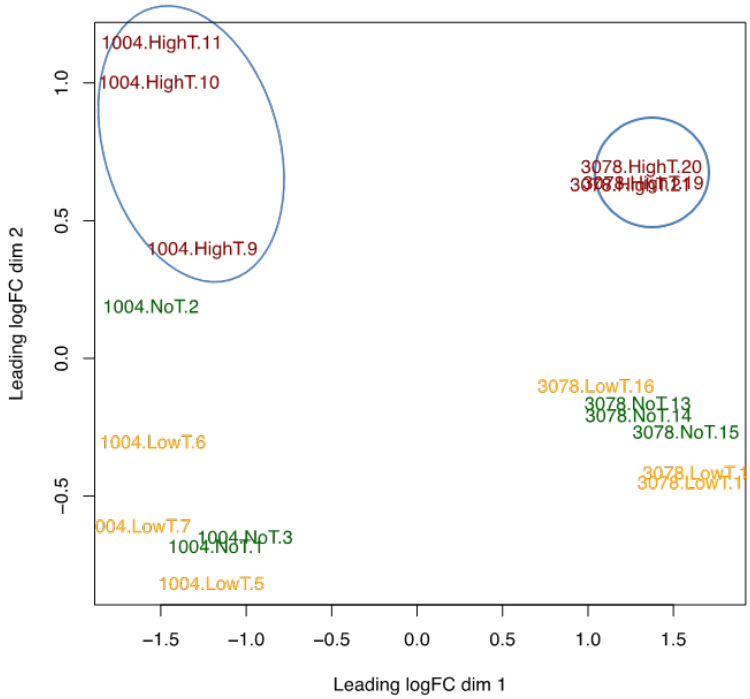

Figure 61: Multidimensional scaling (MDS) plot of global gene expression using all 13,396 filtered genes. Clear evidence of heterogeneity is seen between the two patients (3078 and 1004) with samples respectively clustering at opposing sides of the plot. In both patients, the samples treated with the higher 4-OHTam (HighT, red colour) dose cluster distinctly separate from the other treatment conditions (circled in blue). This indicates significant changes in gene expression between the samples treated with the higher dose of 4-OHTam and both the samples treated with the lower dose 4-OHTam (LowT, yellow colour) and those treated with vehicle control (NoT, green colour). No separation is seen between the samples treated with the lower dose of 4-OHTam and those treated with vehicle control, indicating no significant changes in gene expression between these conditions.

6.3.1.3 ANOVA analysis of differential gene expression

Analysis of variance (ANOVA) was performed to compare the gene expression between the three treatment groups and once again there were significant differences in the gene expression of the higher dose 4-OHTam treated groups compared to lower dose treatment and untreated groups. Using false discovery rate (FDR) <0.001, 904 differentially expressed genes were identified and using FDR <0.0001 513 differentially expressed genes were identified, displayed in the heat map below (Figure 62). There was no significant difference in gene expression between the low dose 4-OHTam treatment and untreated groups.

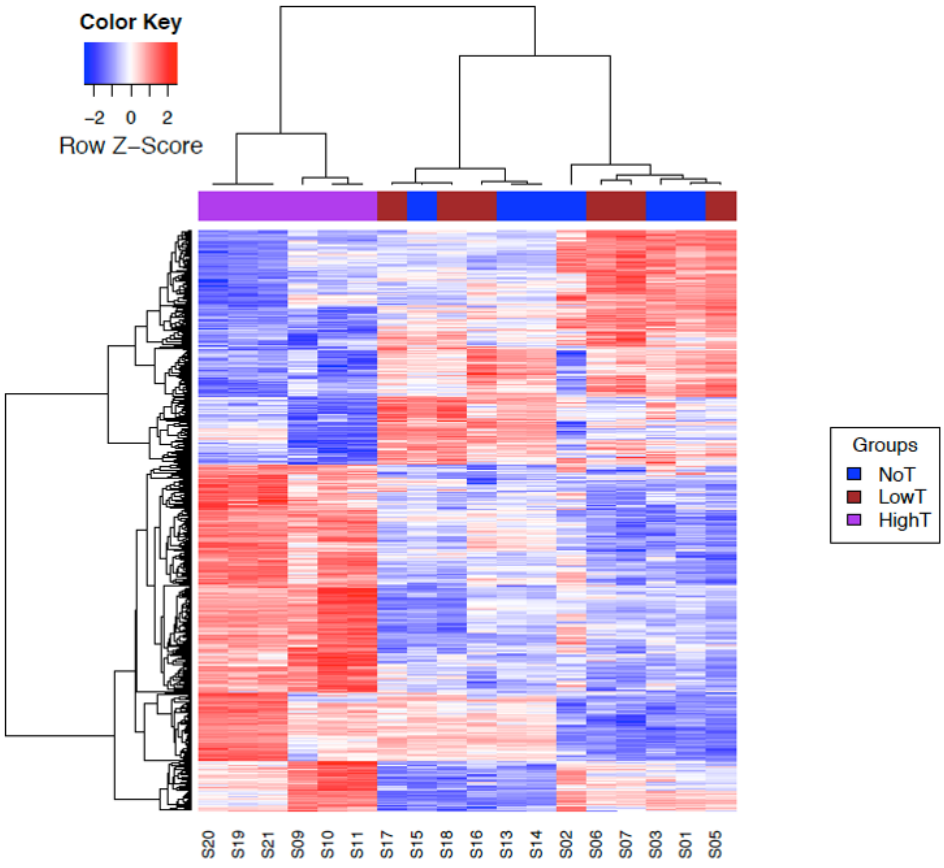

Figure 62: Heat map of 508 differentially expressed genes identified with ANOVA using FDR <0.0001. There is clear clustering of the higher dose treatment samples on the left side of the plot (HighT- pink colour) from the lower dose treatment (LowT- red colour) and vehicle control (NoT – blue colour) samples, clustered towards the right side.

The baseline heterogeneity in gene expression between the two patient samples is once again evident from the variation in position of the vehicle control treated samples on the heat map, they are not uniformly clustered together. One sample in particular (S02) shows a notable difference in gene expression from the other vehicle control treated samples.

The most significantly differentially expressed genes identified by ANOVA are displayed in Appendix 2. The top differentially expressed genes showed a 'metabolic' signature with many involved in cholesterol and lipid synthesis and metabolism. The top genes were investigated for potential mechanisms by which they might contribute towards a tumour-inhibitory mammary stroma.

6.3.2 RNA-Seq Follow up Batch

6.3.2.1 Experimental Considerations and data quality control

Having observed significant changes in gene expression only between vehicle treated samples and those treated with the higher tamoxifen dose (5μM), this dose was selected as the tamoxifen treatment condition for the follow up batch.

In order to further substantiate our hypothesis that tamoxifen may be acting via ER-independent mechanisms, a fulvestrant treatment condition was added in two of the four patient samples from the follow up batch.

A different sequencing provider – the Wellcome Trust Centre for Human Genetics in Oxford - was selected to perform the library preparation and sequencing given the issues experienced with the pilot batch data quality where many reads mapped to the mitochondrial genome. The read alignment data is displayed in Appendix 1. A greater proportion of sequencing reads for each sample of the follow up batch was successfully aligned to the genome (range 65.1% - 78.78%) compared to sequencing reads from samples in the pilot batch (range 46.69% – 60.56%).

6.3.2.2 Preliminary analysis of differential gene expression

14,311 genes were filtered to the stage of differential expression analysis. A principle component analysis (PCA) plot was constructed to visualise the differences in gene expression between the different treatment conditions (Figure 63)

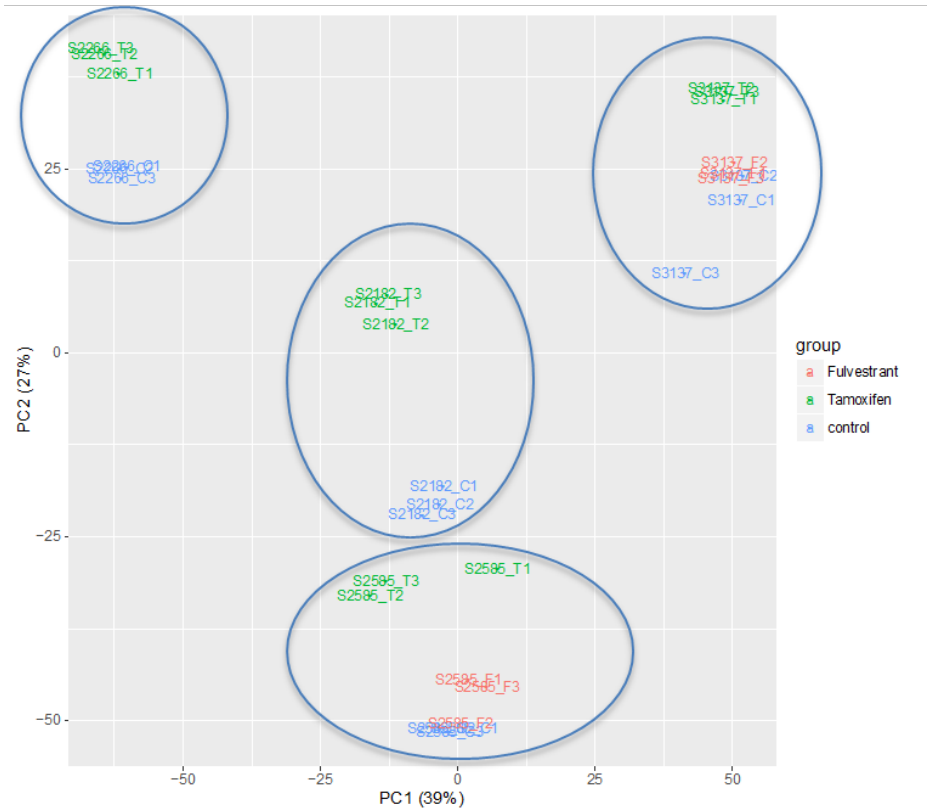

Figure 63: PCA plot of the overall gene expression of the four patient samples in the follow up batch (Vehicle control treated samples – blue, 4-OHTam treated samples – green, Fulvestrant treated samples – red). There is clear heterogeneity in the baseline gene expression between the four patients. The samples from each patient cluster in distinct regions of the plot (each blue circle contains all the samples from a particular patient).

Once again, there was clear evidence of heterogeneity in the baseline gene expression between patients, demonstrated by the clustering of the same patient's samples together in distinct regions of the plot (Figure 63, each blue circle represents one patient's samples).

In addition to the significant inter-patient heterogeneity, there were clear differences in gene expression in the 4-OHTam treated samples of all four patients compared to the samples treated with vehicle control and the two patients' samples treated with fulvestrant. This is highlighted by the distinct clustering of the green (4-OHTam) samples away from the blue (vehicle control) and red (fulvestrant) samples on the PCA plot (Figure 64). No significant differences in gene expression were noted between

fulvestrant and vehicle control samples, highlighted by the overlapping of the blue and red samples on the PCA plot (circled in red in Figure 64 below).

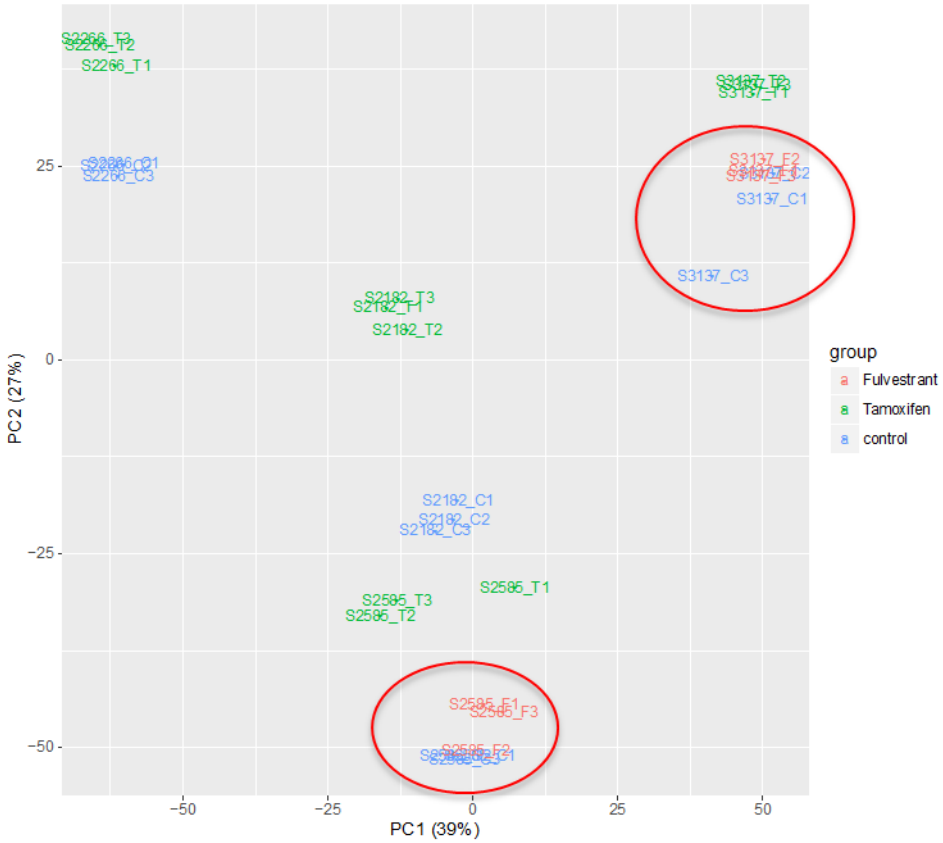

Figure 64: PCA plot of follow up RNA Seq batch showing clear differences in gene expression in the 4-OHTam (green) treated samples of all four patients compared to those treated with vehicle control (blue) and fulvestrant (red). The green samples cluster distinctly separate on the plot. No significant difference in gene expression was seen between the vehicle control and fulvestrant treated samples, highlighted by overlapping red and blue samples on the plot (highlighted in red circles).

6.3.2.3 ANOVA analysis of differential gene expression

Across the four patients from the follow up batch 184 genes were identified to be differentially expressed between the 4-OHTam treated and vehicle control groups at FDR <0.05 and absolute fold change in expression >2.

When comparing the vehicle control and fulvestrant treated samples, only two genes showed significant differential expression – *TPPP3* and *ADAMTS8.* A heat map of the differential gene expression across the samples is displayed in Figure 65.

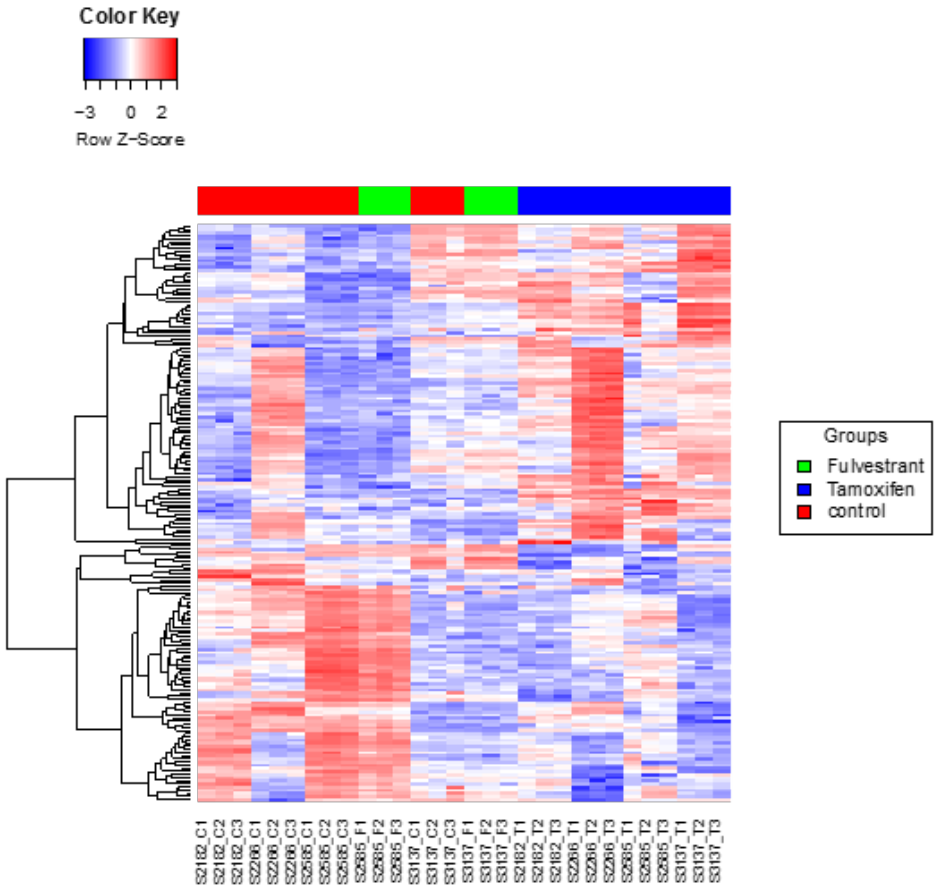

Figure 65: Heat map based on 184 differentially expressed genes across the four patient samples in the follow up batch at FDR<0.05 and absolute fold change >2. The baseline heterogeneity between the four patients is evident from the variation in gene expression in the vehicle control (red) samples. The 4-OHTam treated samples (blue) cluster together at the right side of the heat map. The vehicle control and fulvestrant (green) samples show less distinct separation from each other and cluster together on the left side.

The top differentially expressed genes from the follow up batch are displayed in Appendix 3. Once again, the list of top differentially expressed genes showed a 'metabolic' gene signature, with many genes involved in cholesterol and lipid synthesis and metabolism. Many of the top genes from the pilot batch also featured in the extended list of all 184 differentially expressed genes, using FDR<0.05 and absolute fold change >2, including the two top hits from the pilot batch - *DHCR7* and *DHCR24*.

The top differentially expressed gene in the follow up batch was leptin, which showed significantly down-regulated expression.

6.3.2.4 Comparison and merging of the pilot and follow up batch datasets

The two datasets were compared for similarities in differential gene expression between the vehicle control and 4-OHTam treated samples. Similar genes were significantly differentially expressed in both batches (eg *DHCR7, DHCR24* and cholesterol/lipid metabolic genes). In addition, there was good correlation in the log2 fold changes for commonly differentially expressed genes between the pilot and follow up batches (Figure 66). This correlation improved when the thresholds of FDR <0.05 and absolute fold change >2 were applied (Figure 67 + Figure 68).

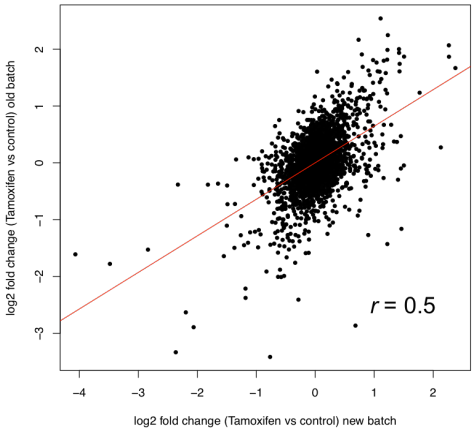

Figure 66: Plot of log2 fold change for commonly differentially expressed genes in the pilot and follow up batches. A good correlation is seen (r = 0.5).

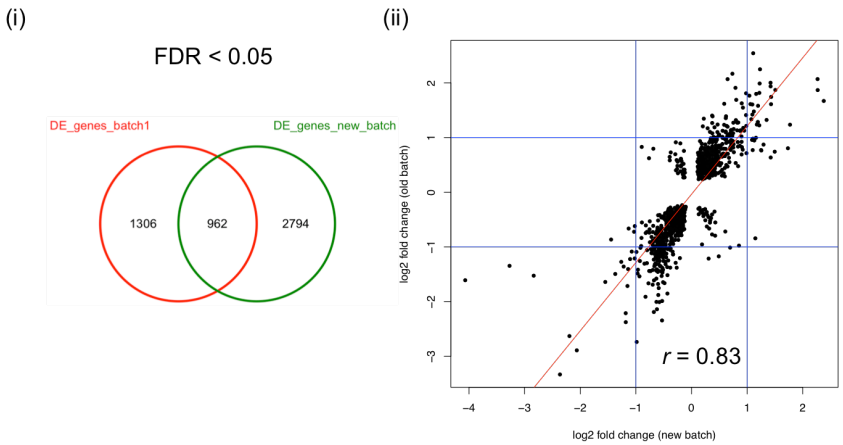

Figure 67: (i) Venn diagram of shared differentially expressed genes (n = 962) between the pilot (red circle) and follow up batches (green circle) at FDR < 0.05. (ii) Plot of log2 fold change for the 962 commonly differentially expressed genes in the pilot and follow up batches at FDR < 0.05. A good correlation is seen (r = 0.83).

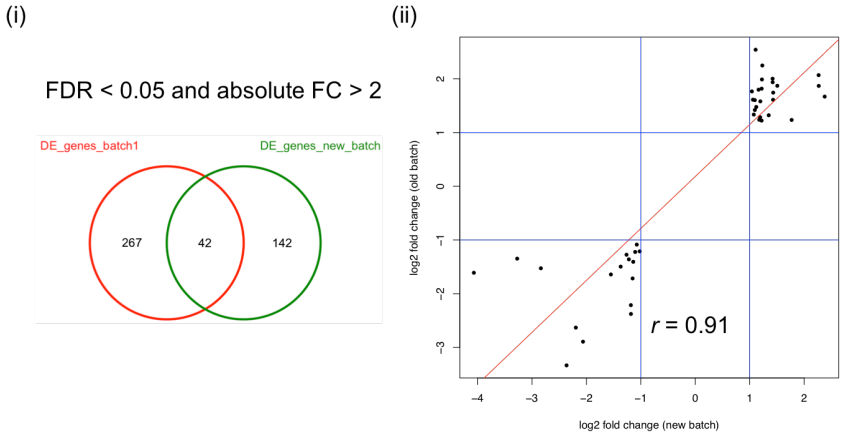

Figure 68: (i) Venn diagram of shared differentially expressed genes (n=42) between the pilot (red) and follow up (green) batches at FDR <0.05 and absolute fold change > 2. (ii) Plot of log2 fold change for the 42 commonly differentially expressed genes in the pilot and follow up batches at FDR < 0.05 and absolute fold change > 2.

The data from all 48 samples in the pilot and follow up batches was then merged. 14,960 genes were sufficiently profiled across all the merged samples to be filtered to the differential expression analysis. There was clear evidence of batch effect between the pilot and follow up samples on the initial PCA plot (Figure 69). All the samples from the pilot batch clustered distinctly on the right side of the plot whilst all samples from the follow up batch were clustered on the left.

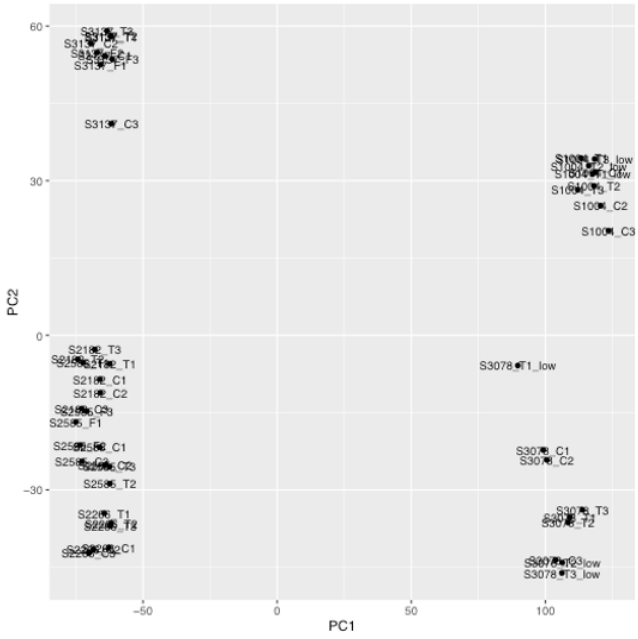

Figure 69: Initial PCA plot of the overall gene expression of samples from the pilot and follow up batches. There is clear batch effect between the pilot batch (samples clustered on right hand side of the plot) and follow up batch (samples clustered on left side of the plot).

The bioinformatics tool Combat was used to successfully remove the batch effect (Figure 70). Combat uses an extended empirical Bayes method to 'borrow information' across genes and experimental conditions between batches to achieve stable inferences for gene expression estimates. Combat includes a parametric prior method (ComBat_p) and a non-parametric method (ComBat_n), based on the prior distributions of the estimated parameters. The method is robust to outliers in small sample sizes and performs comparable to existing methods for large samples.

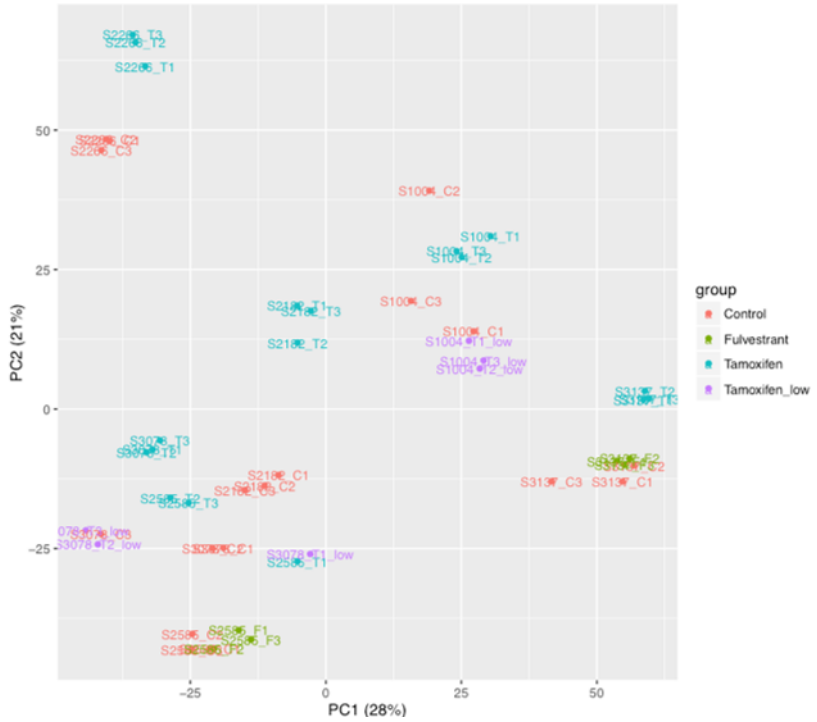

Figure 70: PCA plot of overall gene expression of all 6 patient samples from the pilot and follow up batches. The bioinformatics tool Combat successfully removed the batch effect present between the two cohorts.

The corrected plot maintained the previously observed inter-patient heterogeneity as the samples clustered together on the plot by patient of origin (Figure 71 – each blue circle contains the sample from one patient, BRCA1 mutation carrier circled in red).

Clear overlapping of the fulvestrant treated samples (green) with vehicle control samples (red) once again demonstrated a lack of significant differential gene expression between these treatment groups (Figure 71). A smaller degree of overlapping was seen with the low dose 4-OHTam and vehicle control treated samples from the pilot batch (Figure 71). Distinct separation of the higher dose 4-OHTam treated samples (aqua blue) was seen in all patients, demonstrating significant changes in gene expression (Figure 71).

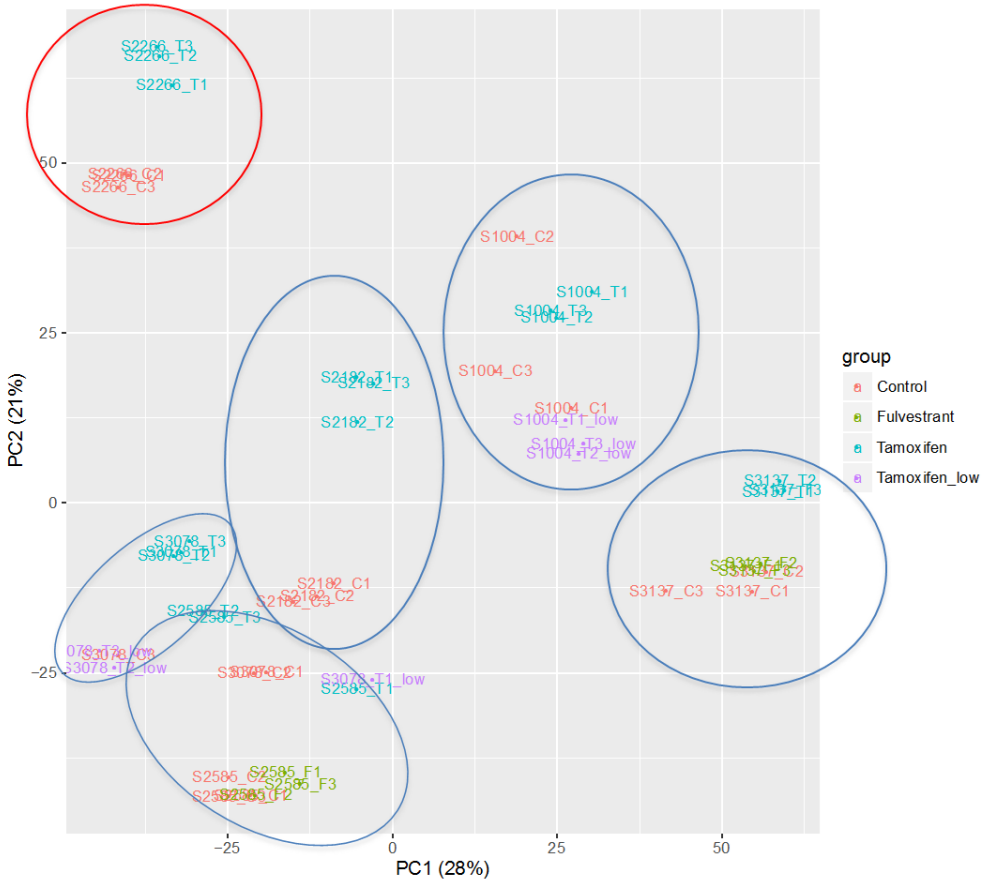

Figure 71: PCA plot of overall gene expression from all 6 patients from the pilot and follow up batches following a correction for batch effect. Each of the six patients' samples are highlighted within a separate blue circle. Note BRCA1 mutation carrier circled in red.

6.3.2.5 Differential gene expression analysis of the merged dataset

Differential gene expression analysis was performed using ANOVA on the merged dataset of six patients. At the FDR < 0.05 level, there were no significantly differentially expressed genes between the fulvestrant and vehicle control treated samples. 4,332 differentially expressed genes were identified between the higher dose 4-OHTam and vehicle control treated samples. 59 differentially expressed genes were identified between the low dose 4-OHTam and vehicle control treated samples.

When double thresholds of FDR < 0.05 and absolute fold change > 2 were applied, 149 differentially expressed genes remained between the higher dose and vehicle control treated samples. In addition, 12 differentially expressed genes remained between the

low dose 4-OHTam and vehicle control treated samples. A heat map of the 149 differentially expressed genes is shown in Figure 72. Clear evidence of heterogeneity across the six patients is seen (samples from patient with BRCA1 mutation highlighted in green box), however a consistent change in gene expression with 4-OHTam is seen across all the samples despite the baseline inter-patient variability.

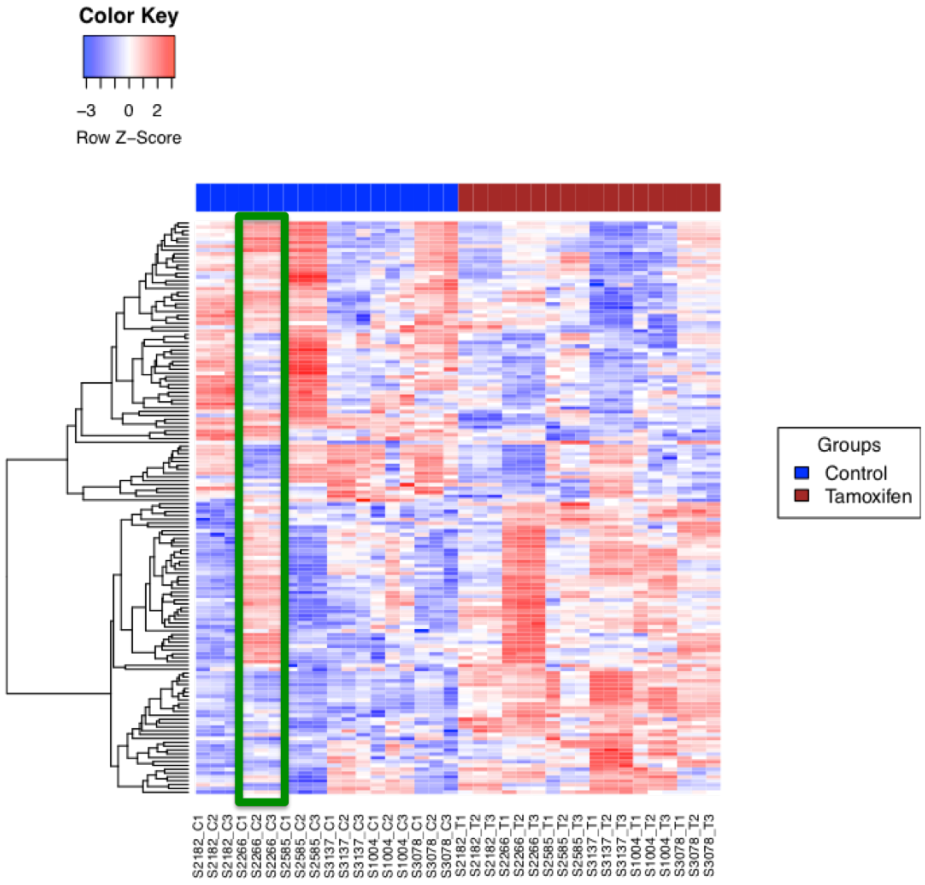

Figure 72: Heat map of 149 differentially expressed genes between higher dose 4-OHTam and vehicle control samples from the six patients at FDR < 0.05 and absolute FC > 2. Clear evidence of heterogeneity in gene expression is seen between the six patients, however they all show a consistent switch in expression with 4-OHTam treatment. Green box highlights samples from BRCA1 mutation carrier.

The top differentially expressed genes are displayed in Appendix 4. The differential gene expression analysis from the merged dataset comparing higher dose 4-OHTam and vehicle control samples once again showed a metabolic signature. Many of the top hits are involved in metabolism, in particular metabolism and synthesis of cholesterol

and lipids. The two most differentially expressed genes from the pilot batch – *DHCR7* and *DHCR24* were also in the top ten most differentially expressed genes from the merged dataset (Appendix 4).

6.3.2.6 Pathway analysis

The Gene Set Enrichment Analysis (GSEA) tool was used along with the KEGG and REACTOME biological pathway resources to identify deregulated pathways in the 4-OHTam treated fibroblasts compared to those treated with vehicle control, based on the merged dataset.

6.3.2.6.1 Up-regulated pathways

The pathways identified to be up-regulated in the 4-OHTam treated fibroblasts reflected the metabolic 'signature' seen in the differential gene expression analysis. The vast majority of the up-regulated pathways identified using REACTOME involved cholesterol and lipid synthesis and metabolism (displayed in Appendix 5). The remaining up-regulated pathways involved other aspects of metabolism, highlighting the metabolic 'signature' of gene expression

The KEGG biological pathways resource also identified up-regulated pathways involved in metabolism (Appendix 6).

6.3.2.6.2 Down-regulated pathways

The pathways identified to be down-regulated in the 4-OHTam treated fibroblasts involved a more diverse array of processes than the up-regulated pathways which were predominantly metabolic processes.

Selected down-regulated pathways identified using REACTOME are displayed Appendix 7. Many of the significantly down-regulated pathways identified using REACTOME involve the cell cycle, DNA replication and mRNA processing. Many other

cellular processes also feature including; protein synthesis and collagen formation, inflammatory cell signalling, muscle contraction and integrin signalling.

The down-regulated pathways identified using KEGG also reflected a wide variety of cellular processes including; DNA replication and cell cycle, mismatch repair, Wnt signalling, Hedgehog signalling, cytoskeleton regulation, ECM- receptor interaction and focal adhesion signalling (displayed in Appendix 8).

6.4 Discussion

6.4.1 Pilot batch data quality control

A significant proportion of sequencing reads from the pilot batch (range 29.9 - 45.2% of reads per sample) mapped to the mitochondrial genome. Such a high proportion of reads mapping to mitochondrial regions was unexpected. Data regarding the ability of tamoxifen to modulate transcription of mitochondrial genes is limited. One study has observed that 4-OHTam and E2 can modulate the transcription of nuclear respiratory factor 1 (NRF-1) in mouse mammary gland and uterine tissue [335]. NRF-1 in turn, is reported to stimulate the transcription of nuclear-encoded genes that regulate mitochondrial gene transcription [335].

Sequencing data from an unrelated project obtained from the same sequencing provider was also found to show significant over-representation of reads mapping to the mitochondrial genome. This study did not involve any treatment of samples with tamoxifen or 4-OHTam. Following discussion with our Bioinformatics colleagues, it was felt the over-representation of these reads was most likely due to the fact that the samples in both these projects had not undergone ribosomal RNA depletion prior to sequencing. This was supported by the fact that the data from the follow up batch, (where the samples did undergo ribosomal RNA depletion) did not show any over-representation of reads mapping to the mitochondrial genome.

6.4.2 Batch effect between pilot and follow up data

A significant batch effect was observed between the sequencing data obtained from the pilot and follow up batches. For each batch, the cells were cultured and treated with vehicle/4-OHTam/fulvestrant at differing times, however all the RNA was extracted and frozen at the same time. The cells used in each batch were also all at the same culture passage. The pilot and follow up batch samples were prepared approximately 9

months apart using the same RNA extraction kit. Despite using the same preparation conditions and bioinformatics analysis pipeline, a significant batch effect was still observed between the pilot and follow up datasets. This difference may therefore be due to the sensitivity and innate variability encountered when using primary cells. Small variations in culture conditions and environmental conditions in the laboratory at the time of RNA extraction may also have contributed to the batch effect. In addition, ribosomal RNA depletion was undertaken in the follow up batch but not the pilot and this may also have contributed to the variation between the two datasets.

6.4.3 Heterogeneity in the primary fibroblast cohort

In both the pilot and follow up RNA Seq experiments significant inter-patient heterogeneity in baseline fibroblast gene expression was observed (Figure 71 +Figure 72). This clearly demonstrates the value of using primary cell culture models to capture the variability and complexity of gene expression that exists between individual patients.

There are a number of clinical factors which could account for the variability in gene expression between patients. Five (Tissue bank ID 1004, 3078, 3137, 2182, 2585) of the six patients are from reduction mammoplasty cases however, one patient is a known BRCA1 mutation carrier (Tissue Bank ID 2093) who underwent prophylactic mastectomy. The samples from the BRCA1 mutation carrier cluster distinctly in the top right region of the merged dataset PCA plot (Figure 71 - red circle) and show a conspicuous pattern of gene expression on the merged dataset heat map (Figure 72 – green box).

These data suggest that the breast microenvironment in BRCA1 mutation carriers may display a unique biology and could potentially contribute to the aggressive behaviour and early age of onset of tumours in these patients. Loss of BRCA1 expression in an

immortalised fibroblast cell line has been shown to promote the growth of tumours in a mouse model of triple negative breast cancer [336]

A significant degree of heterogeneity was also observed in the gene expression between the five reduction mammoplasty patients' fibroblasts. There was a wide variation in age between these patients (24-58 years). This could account for some of the inter-individual differences in gene expression. Other clinical factors that may also have contributed to the variation include ethnicity, parity, menopausal status and smoking history. The variation in these clinical factors between the six patients is displayed in Table 13.

6.4.4 Effect of fulvestrant on fibroblast gene expression

No significant differential gene expression was seen between the fibroblasts treated with fulvestrant and those treated with vehicle control (Figure 65 + Figure 71). The lack of response of the fibroblasts to the pure ER antagonist correlates with experimental work showing no effect of fulvestrant on fibroblast activation (Figure 59), and suggests that 4-OHTam could be working via unique ER-independent mechanisms to affect primary fibroblast gene expression.

6.4.5 Up-regulated pathways in 4-OHTam treated fibroblasts

6.4.5.1 Metabolic gene signature of 4-OHTam treated fibroblasts

A 'metabolic' gene signature was observed in the analysis of RNA Seq data from the pilot, follow up and merged datasets. The majority of the up-regulated pathways in the 4-OHTam treated fibroblasts, compared to those treated with vehicle control, involve cholesterol and lipid synthesis and metabolism (Appendices 5 + 6). The most significantly up-regulated pathways using REACTOME included; cholesterol biosynthesis (NOM p = 0, FDR q = 0), glycosphingolipid metabolism (NOM p = 0, FDR q = 0), metabolism of lipids and lipoproteins (NOM p= 0, FDR q = 0), sphingolipid

metabolism (NOM p= 0, FDR q = 0), phospholipid metabolism (NOM p = 0, FDR q = <0.001), triglyceride biosynthesis (NOM p = 0, FDR q = 0.003) and fatty acyl coA biosynthesis (NOM p = 0.004, FDR q = 0.050). Significant up-regulation of sphingolipid metabolism was also identified using the KEGG biological pathway resource (NOM p = 0.002, FDR q = 0.017).

These data are supported by findings from Morad and colleagues who have observed tamoxifen to be a potent regulator of acid ceramidase activity and sphingolipid metabolism in a variety of cancer cell types [297, 337]. Furthermore, Corriden and colleagues have reported that modulation of sphingolipid metabolism by tamoxifen can affect neutrophil behaviour [298], suggesting that tamoxifen may be capable of altering immune cell activity in the breast microenvironment. Hattar and colleagues observed alteration in immune cell content of mammary stroma from tamoxifen treated rats [115]. In addition, neutrophil activity has been proposed to contribute to the pro-tumourigenic activity of high collagen density mammary stroma in a mouse model [231]. Therefore modulation of stromal immune cell activity could play an important role in tumour inhibitory activity of tamoxifen.

The up-regulation of cholesterol biosynthesis and metabolism pathways in response to breast cancer endocrine therapy has also recently been reported by Martin and colleagues [338]. They propose that the cholesterol metabolites 25- and 27-hydroxycholesterol (HC) might contribute to the development of resistance to endocrine treatments in ER positive breast cancer [338]. They observed that levels of 25- and 27-HC were elevated in a cell line model of ER positive breast cancer treated with long term oestrogen deprivation therapy [338]. In addition, 25- and 27-HC were capable of inducing the recruitment of the ER to the promoter regions of two oestrogen-regulated genes (*TTF1* and *GREB1*) and were found to be capable of binding to the ligand binding domain of the ER [338]. The authors suggest that 25- and 27-HC may be

capable of substituting for oestradiol in the setting of long term oestrogen deprivation therapy [338].

In addition to the many up-regulated pathways involving cholesterol and lipid metabolism, up-regulation of alternative metabolic processes was also observed. Significant up-regulation of iron uptake and transport was identified using REACTOME (NOM p = 0, FDR q = 0) and KEGG identified drug (NOM p = 0.002, FDR q = 0.002) and xenobiotic cytochrome P450 metabolic pathways (NOM p = 0, FDR q = 0.003)

6.4.5.2 Cholesterol metabolism and cancer biology

Reflecting the up-regulation of cholesterol biosynthesis in the pathway analysis, two of the top differentially expressed genes between 4-OHTam and vehicle control treated fibroblasts were *DHCR7* (p = <0.001) and *DHCR24* (p = <0.001, Appendix 4). The products of both these genes are enzymes involved in the terminal (post lanosterol) stages of cholesterol synthesis [339].

Enhanced cholesterol biosynthesis has been reported as a key feature of cancer cell biology [340]. Malignant cells require high levels of cholesterol in order to synthesise new cell membranes and are the principle component of 'lipid rafts' which help to activate membrane bound receptor signalling pathways [340]. Cancer cells demonstrate a number of adaptations in order to maintain high intracellular cholesterol levels including; accelerated endogenous production of cholesterol via steroid response element binding proteins (SREBP); reduced efflux via ATP-binding cassette (ABC) class A transporters and increased uptake of low density lipoprotein particle (LDL) [340].

This study is focused on the fibroblasts within the tumour microenvironment rather than the tumour cells. Unlike the tumour cells, fibroblasts do not demonstrate the same propensity for invasion and metastasis. Instead, activated fibroblasts within the local tumour microenvironment facilitate tumour growth via secretion of paracrine growth

factors and ECM proteins, as discussed in Chapter 1. Currently the role of cholesterol biosynthesis in mediating fibroblast activation in cancer is uncertain. Outside of the cancer biology field, modulation of cholesterol biosynthesis in cardiac fibroblasts by statins has been suggested to inhibit myofibroblast differentiation [341], fibroblast proliferation [342] and alter ECM production [343].

Given that enhanced cholesterol synthesis is a key feature of malignant cells, it may seem contradictory that 4-OHTam, an anticancer treatment, would result in up-regulation of these processes. However, a number of recent studies from the Poirot group have shed new light on unique biological properties of the sterol metabolites involved in the cholesterol synthesis pathway which may help to explain this apparent paradox [340]. The main findings are summarised in the sections below.

6.4.5.3 Role of DHCR7

In addition to functioning as a terminal stage cholesterol synthesis enzyme (3β-hydroxysteroid-Δ7-isomerase), recent studies have demonstrated that DHCR7 also forms a hetero-oligomeric complex with another cholesterol synthesis enzyme (D8D71/EBP, 3β-hydroxysteroid-$\Delta^8\Delta^7$-isomerase). Together, these two molecules carry out a unique third enzyme activity – cholesterol-5,6-epoxide hydrolase (ChEH) activity [293, 344] (Figure 73).

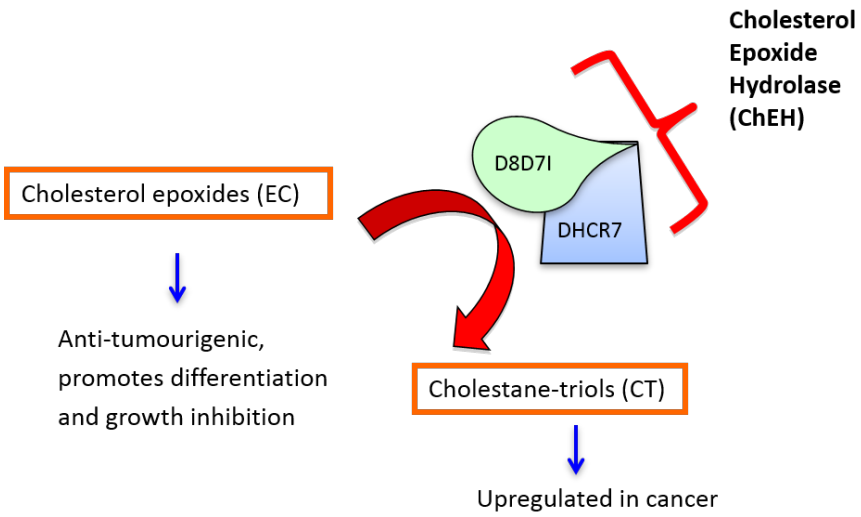

Figure 73: DHCR7 forms a hetero-oligomeric complex with D8D71 and together carry out cholesterol epoxide hydrolase (ChEH) activity.

The epoxide hydrolase family transform epoxide containing lipids via the addition of water [344, 345]. ChEH is located within the endoplasmic reticulum and is very specific for the conversion of cholesterol (5,6α,5,6β) epoxide (EC) to cholestane -3β,5α6β-triol (CT) [345]. EC have been proposed to be anti-tumourigenic metabolites and to promote the differentiation and growth inhibition of breast cancer cells, whereas CTs have been proposed to be up-regulated in cancer [340].

6.4.5.4 Modulation of ChEH activity by 4-OHTam and SERMS

Intriguingly, modulation of ChEH activity has been reported with a number of clinically prescribed drugs, of which one of the major groups are the SERMs including tamoxifen and 4-OHTam (Figure 74) [264, 345].

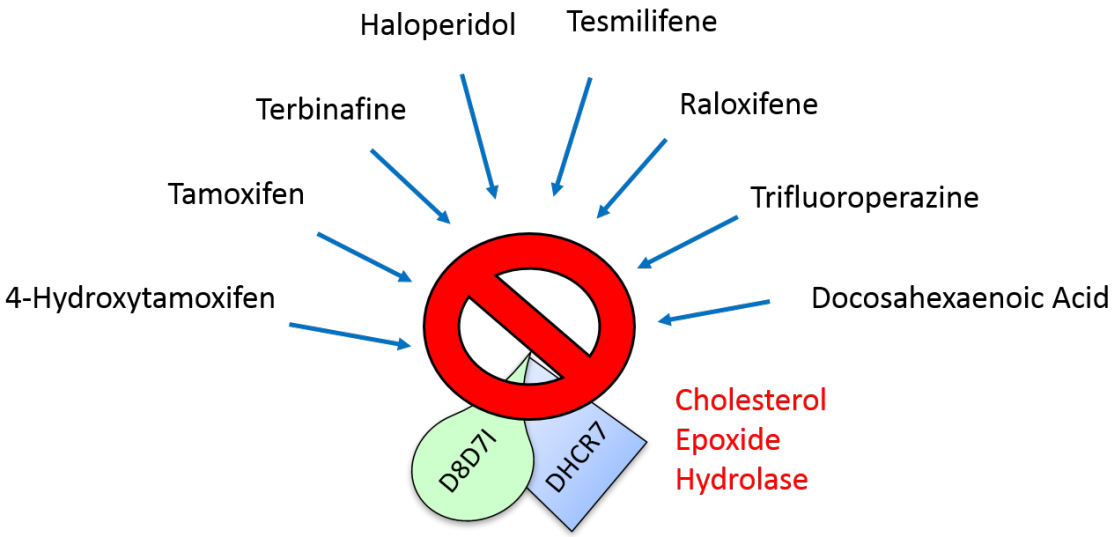

Figure 74: Drugs known to modulate the activity of cholesterol epoxide hydrolase, adapted from Poirot and Silvente-Poirot [345]. One of the most potent inhibitors of ChEH activity are the SERMs.

It has been proposed that the binding of these drugs to ChEH inhibits its activity and results in the accumulation of ECs (Figure 75) [345].

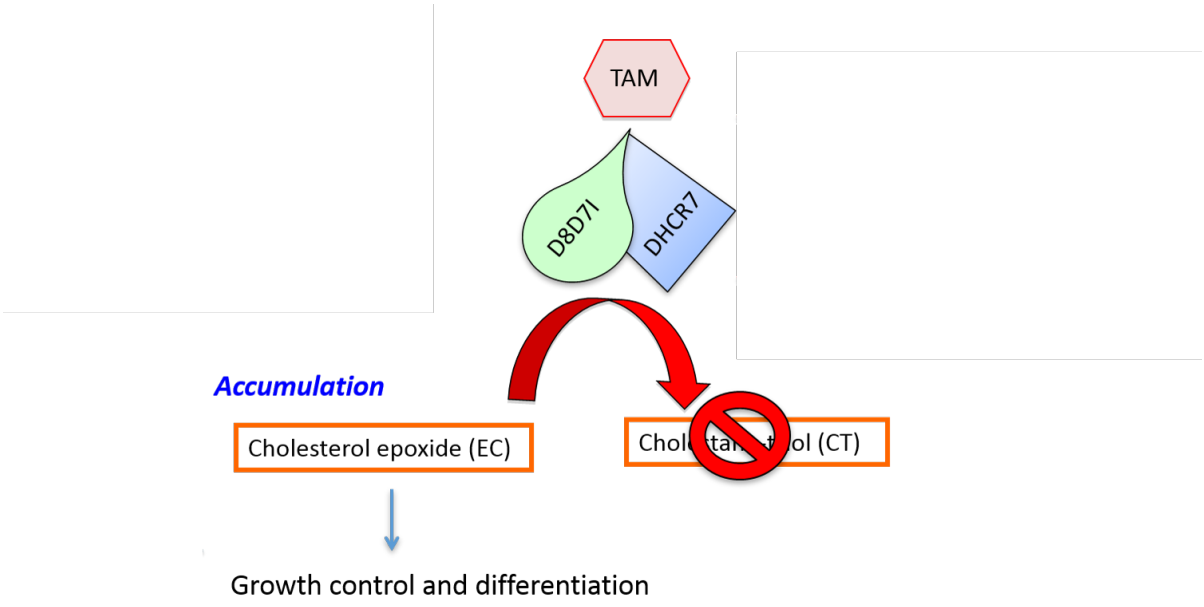

Figure 75: Tamoxifen (TAM) binds to the cholesterol epoxide hydrolase (ChEH) complex and inhibits its activity, resulting in the accumulation of antitumourigenic cholesterol epoxides (EC)[340].

The ability of tamoxifen and 4-OHTam to modulate ChEH activity reported by the Poirot group highlights the complex pharmacology of tamoxifen and suggests that the drug may have significant ER-independent mechanisms of action.

6.4.5.5 The microsomal anti-oestrogen binding site (AEBS)

Sutherland and colleagues first reported the existence of a high affinity binding site for tamoxifen within the endoplasmic reticulum in 1980 [346]. This binding site has been designated the microsomal anti-oestrogen binding site (AEBS) and significant progress in understanding the molecular identity and biology of the AEBS has recently been made by the Poirot group [264, 292, 293]. Significantly, they observed that the AEBS was capable of ChEH enzyme activity, suggesting that the AEBS and ChEH are in fact the same entity [264, 293]. They suggest the binding of tamoxifen and other SERMs to the AEBS results in inhibition of ChEH activity [264].

6.4.5.6 Consequences of ChEH inhibition by tamoxifen

The binding of tamoxifen to the AEBS, and subsequent inhibition of ChEH activity, has been proposed to result in the growth control and differentiation of human breast cancer cells due to the accumulation of cholesterol epoxides [295]. The potential mechanisms by which the cholesterol epoxides exert their re-differentiating effects have recently been explored by the Poirot group [347].

The proposed pathway involves further metabolism of the 5,6α cholesterol epoxide isomer by histamine to form a key tumour inhibitory molecule - dendrogenin A (DDA) [347].

6.4.5.7 Biological properties of dendrogenin A (DDA)

DDA is a steroidal alkaloid which has been proposed to have potent re-differentiating effects on a number of tumour cell types in-vitro including breast, melanoma and

glioblastoma [347, 348]. Furthermore, when breast and melanoma cell lines were injected into immunocompetent mice, administration of low dose DDA reduced tumour size and prolonged survival [347]. DDA treatment stimulated T lymphocyte and dendritic cell infiltration into the engrafted tumours, suggesting there may be a significant immunomodulatory role in the observed anti-tumour effects [347]. This hypothesis was supported by the observation that DDA showed no effect on tumour size or survival in immunodeficient mice [347].

DDA was also quantified in human breast tissue and was found in fivefold lower concentration in cancer tissue compared to adjacent uninvolved breast tissue, suggesting deregulation of DDA metabolism in cancer [347].

DDA itself has been proposed to be a very potent and selective inhibitor of ChEH activity, more efficacious than the SERMs [294, 347]. This suggests that DDA may further potentiate the inhibition of ChEH activity and promote the formation of cholesterol epoxides. In addition, 5,6α cholesterol epoxides have been reported to be a direct modulator of liver X receptor (LXR) signalling [349]. 5-6α cholesterol epoxides are also the substrate of cholesterol sulphotransferase SULT2B1b [350], and the resulting product of this reaction is 5,6α-EC-3-sulphate – another known modulator of LXR signalling [351]. Human and mouse tumours have been observed to produce LXR agonists which impair the ability of dendritic cells to initiate an immune response against the tumour [352]. Significantly, modulation of LXR agonist activity via the addition of SULT2B1b resulted in tumour growth control by preventing evasion from the immune system [352]. Therefore modulation of LXR signalling could potentially be a key mechanism by which DDA (and inhibition of ChEH activity by tamoxifen) exert their anti-tumour effects. Alteration of the immune cell content of the mammary stroma by tamoxifen has been observed in animal models [115].

The inhibition of ChEH activity by tamoxifen has been proposed by the Poirot group to contribute to the overall anti-cancer effect of tamoxifen in the adjuvant treatment setting of breast cancer patients, in addition to the classical mechanism of action as a competitive ER antagonist [296].

Whilst this pathway highlights an intriguing potential mechanism independent of the ER by which SERMs could exert anti-tumour effects, there are a number of other important factors to consider. Firstly, the vast majority of the data supporting the anti-tumour properties of this pathway has originated from a single laboratory and has yet to be widely replicated and validated by others. In addition, all the previous studies have focused on tumour cells and, to date, there is no evidence that ChEH is present in fibroblasts, or that inhibition of ChEH activity and accumulation of cholesterol metabolites in stromal cells would result in similar anti-tumour effects to those described in malignant epithelial cells. Furthermore, both the differential gene expression and pathway analyses show up-regulation of many genes across the entire cholesterol metabolism pathway (Appendices 2 - 6). Thus, the findings may simply reflect a generalised up-regulation of cholesterol biosynthesis. Notably, the sterol regulatory element binding protein 1 and 2 (SREBP 1/2) genes both show significantly up-regulated expression (Appendices 2 - 4). These genes encode proteins which act as transcription factors for numerous genes involved in sterol metabolism [353].

6.4.5.8 Up-regulation of DHCR7 expression may be a consequence of a feedback loop

In this study DHCR7, one of the two components of the AEBS/ChEH, showed significantly up-regulated gene expression ($p = <0.001$, Appendix 4) in the 4-OHTam treated fibroblasts compared to those treated with vehicle control. This result initially appears to contradict the data from the Poirot group suggesting that 4-OHTam inhibits the activity of ChEH, as it might be expected that increased gene expressed would enhance ChEH activity.

These conflicting results could potentially be explained by a feedback loop driven by the binding of 4-OHTam to the AEBS. The resulting inhibition of ChEH activity and accumulation of cholesterol epoxides could drive enhanced transcription of the DHCR7 gene (Figure 76). It may also be plausible that there is an increase in the translation of the DHCR7 enzyme product, but it is rendered functionally inactive due to the binding of 4-OHTam, and possibly DDA. Thus, the overall activity of ChEH could remain impaired.

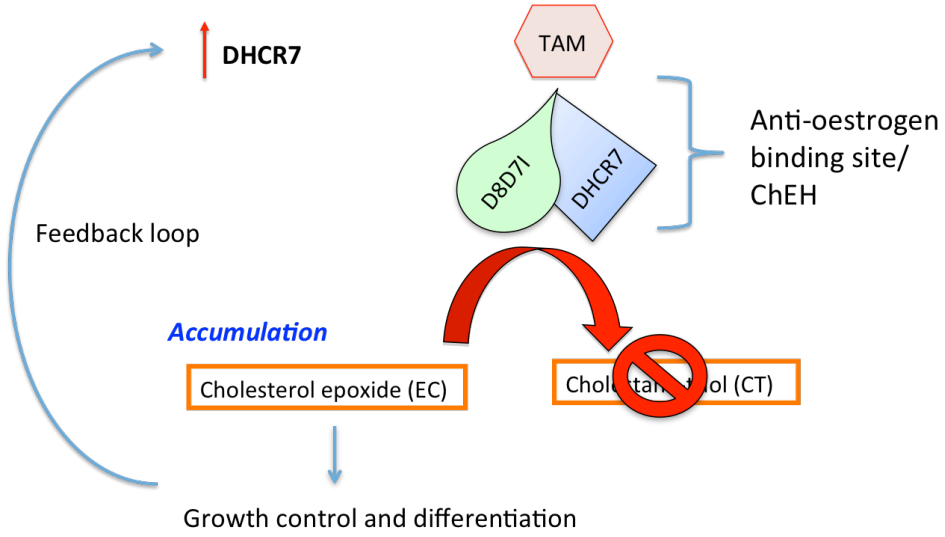

Figure 76: Increased DHCR7 gene expression was identified in the 4-OHTam treated fibroblasts. This could potentially be explained by a feedback loop driving increased expression of DHCR7 in response to 4-OHTam binding to the AEBS, inhibiting the activity of ChEH and the accumulation of cholesterol epoxides. However, there is limited data to support his hypothesis and increased DHCR7 expression may also simply reflect a generalised up-regulation of many genes in the cholesterol biosynthesis pathway.

Up-regulation of DHCR7 gene expression was only noted in the higher dose (5μM) 4-OHTam treated samples (Figure 62), suggesting there might be a critical threshold concentration at which inhibition of ChEH activity by 4-OHTam occurs. The Poirot group report threshold concentrations for inhibition of ChEH activity of 140nM for 4-OHTam and 34nM for tamoxifen [345]. These data correlate well with the findings of

this study where the lower dose (100nM) 4-OHTam treatment showed little effect on fibroblast gene expression compared to the higher dose (5μM).

Accumulation of the anti-tumorigenic cholesterol epoxides within the fibroblasts could potentially contribute to a tumour-inhibitory breast microenvironment, and may contribute to the breast cancer preventing properties of tamoxifen in high risk individuals [113], and the tumour-inhibitory phenotype of tamoxifen treated stroma observed in animal models [115].

There is, however, limited evidence to support this hypothesis and it is also possible that the up-regulated expression of DHCR7 simply reflects the generalised up-regulation of many genes involved in the cholesterol biosynthesis pathway. In addition, the other component of the AEBS (D8D71) does not feature in the top differentially expressed genes (Appendices 2 - 4) and one might expect to see a similar level of up-regulated expression as with DHCR7. Further work is required in order to demonstrate that ChEH activity is inhibited by 4-OHTam in fibroblasts.

6.4.5.9 Inhibition of ChEH activity could contribute to the anti-proliferative and de-activating effect of 4-OHTam on fibroblasts

The inhibition of ChEH activity could potentially explain the observed response of primary breast fibroblasts to 4-OHTam. A consistent, dose dependent negative effect on fibroblast proliferation was observed (Figures 23 + 24). This is consistent with the reported growth inhibitory properties of cholesterol epoxide accumulation due to ChEH inhibition [295]. In addition, concentrations of > 6μM were observed to be toxic to the fibroblasts (Figures 23, 24 + 32). Cholesterol epoxides have been reported to induce apoptosis and autophagy when present in sufficient concentrations within cells [344]. Thus both the growth inhibitory and toxic properties of 4-OHTam may be attributable to ChEH inhibition and cholesterol epoxide accumulation. However, at present there is limited evidence to support the presence of cholesterol epoxides within the 4-OHTam

treated fibroblasts. Thus, the anti-proliferative and toxic properties may also be due to alternative effects of 4-OHTam on the fibroblasts, unrelated to cholesterol metabolism.

The characteristic 4-OHTam-treated fibroblast phenotype (Figure 33) might also be related to inhibition of ChEH activity. The accumulation of perinuclear cytoplasmic vesicles may reflect the accumulation of cholesterol epoxides and other cholesterol precursors due to the inhibition of ChEH, DHCR7 and DHCR24 enzyme activity. This hypothesis is supported by observations from the Poirot group that breast cancer cell lines treated with commercially available specific inhibitors of ChEH demonstrate a similar accumulation of small vesicles in the cell cytoplasm [296]. These findings need to be interpreted with caution as the presence of cholesterol epoxides within the 4-OHTam treated fibroblasts has not been confirmed. Future work to identify to content of these vesicles is required. Interestingly the pathway analysis revealed significant up-regulation of the trans-golgi network vesicle budding pathway using the REACTOME pathway gene sets (NOM p = 0, FDR q = 0.025, Appendix 5). Up-regulation of this pathway could explain the accumulation of vesicles within the 4-OHTam treated fibroblasts. It is possible that 4-OHTam is able to stimulate this pathway via mechanisms unrelated to cholesterol biosynthesis.

6.4.5.10 Relationship to a reduction in mammographic density

The attenuation of ChEH activity in fibroblasts could potentially help to contribute to a tumour-inhibitory stromal phenotype, but it is less clear how this may contribute to the reduction in MD observed clinically in patients treated with tamoxifen [110]. The possible mechanisms that may be involved are discussed below. Other potentially contributory pathways unrelated to cholesterol metabolism are discussed in Section 6.4.6.

6.4.5.11 Does 4-OHTam treatment of fibroblasts stimulate their differentiation?

Given the observations by the Poirot group that ChEH enzyme inhibition and cholesterol epoxide accumulation in a variety of different tumour cell types can promote their differentiation [347], it is possible that cholesterol epoxide accumulation may promote fibroblast differentiation from an activated 'myofibroblast like' phenotype to a more quiescent state, and potentially towards adipogenic differentiation. Stimulating the fibroblasts towards adipogenic differentiation could gradually increase the fatty content of the breast and thus reduce the overall MD.

The differentiation of the fibroblasts to a more quiescent state is consistent with the observed reduction in SMA expression (Figure 48) and inhibition of non-canonical TGF-β signalling (Figure 56) with 4-OHTam treatment.

There is limited evidence from the RNA Seq differential gene expression and pathway analysis to support fibroblasts being pushed towards adipogenic differentiation by 4-OHTam. Firstly, there are some key markers of early stage adipogenic differentiation that are up-regulated in the differential gene expression analysis. Figure 77 below (adapted from Cristancho et al [354]) shows key genes involved with early adipogenic differentiation.

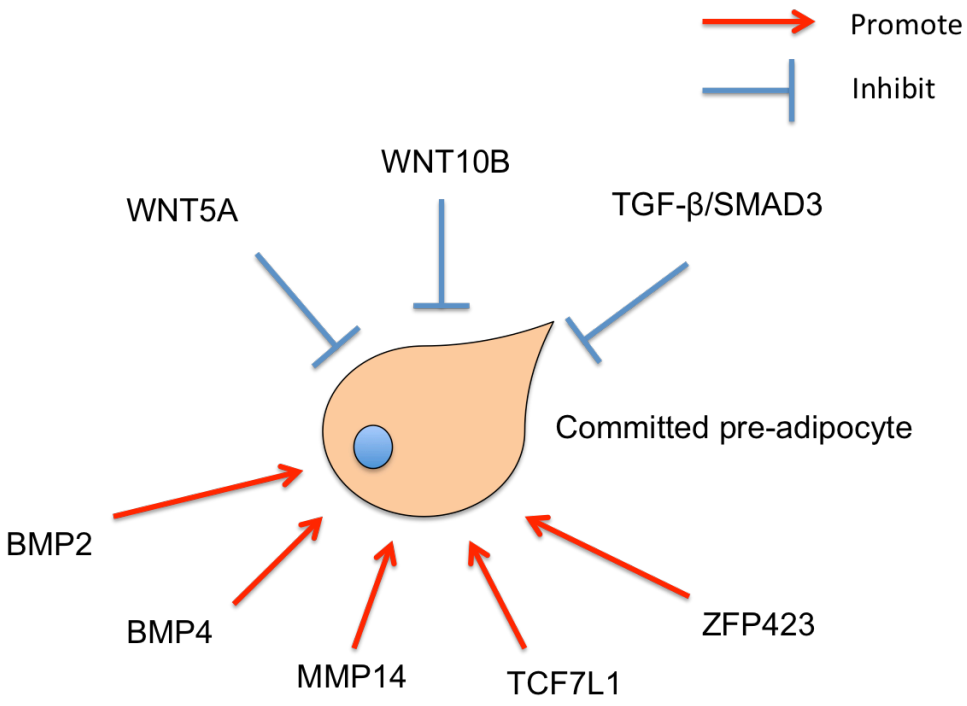

Figure 77. Genes involved in early stage adipogenesis, adapted from Cristancho et al [354].

Canonical Wnt signalling is a potent inhibitor of adipogenesis [354]. Significant down-regulation of Wnt signalling was observed in the pathway analysis (NOM p = 0, FDR q = 0.009) and DKK1, a potent inhibitor of Wnt signalling, was significantly up-regulated (p = <0.001) in the differential gene expression analysis. In addition, up-regulation of BMP2 (p = <0.001) and MMP14 (p = <0.001), genes associated with early stage adipogenesis [354], was also observed.

Peroxisome proliferator-activated receptor - gamma (PPARγ), a key mediator of adipogenesis [354], was also up-regulated in our differential gene expression analysis (p = <0.001). In addition, PPAR signalling was identified using the KEGG biological pathways resource (Appendix 6) as being significantly up-regulated (NOM p = 0.004, FDR q = 0.028) in the 4-OHTam treated fibroblasts.

Despite the up-regulation of the pathways described above, the evidence to support adipogenic differentiation of the fibroblasts by 4-OHTam is limited. An alternative explanation is that the cells simply synthesise and accumulate lipid in response to 4-OHTam treatment, without any differentiation. Furthermore, the pathway analysis (Appendices 5 + 6) shows a number of pathways related to lipid metabolism are up-regulated. This again may simply indicate a generalised increased in lipid synthesis, in parallel with cholesterol synthesis, within the treated cells, rather than differentiation.

A key observation from the differential gene expression analysis that conflicts with the hypothesis that 4-OHTam may promote adipogenic differentiation, is that leptin – a key gene involved in the terminal stages of adipogenesis [354] – shows significantly down-regulated expression (p = <0.001) in the 4-OHTam treated fibroblasts. This finding emphasises that the 4-OHTam treated cells are not undergoing full adipogenic differentiation. It is possible that 4-OHTam treatment may simply ‘deactivate’ the fibroblasts to a more quiescent ‘pre-adipocyte-like’ state. In the context of the correct

biochemical and biophysical cues these deactivated 'pre-adipocyte – like' fibroblasts might then progress on to full adipogenic differentiation. The fact that the 4-OHTam treated fibroblasts do not resemble adipocytes (Figure 33) also supports this modified hypothesis, summarised in Figure 78.

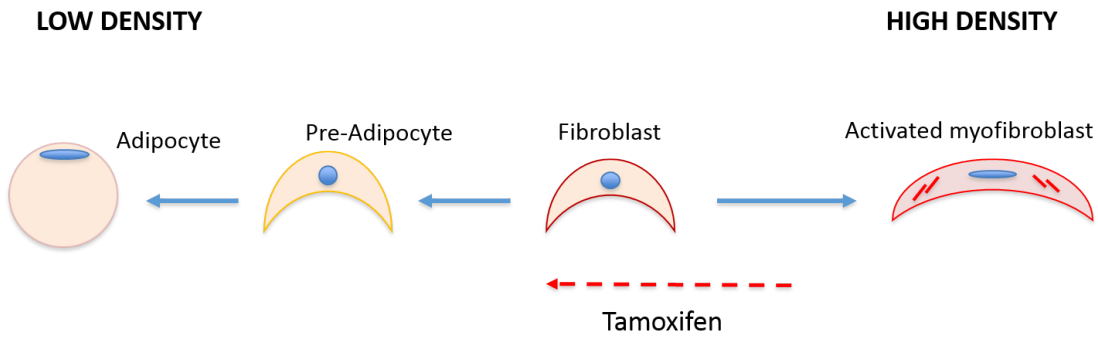

Figure 78: Tamoxifen may promote 'deactivation' of fibroblasts to more quiescent pre-adipocyte like cells, which may undergo further adipogenic differentiation. Increasing the fatty content of the breast would reduce the overall breast density. This proposed mechanism could explain the observed reduction in MD with tamoxifen treatment in high risk women [109]. It is important to note that the evidence to support differentiation of the fibroblasts by 4-OHTam is very limited and an alternative explanation may be that the fibroblasts simply synthesise more lipid in response to 4-OHTam treatment.

The down-regulation of leptin gene expression in the 4-OHTam treated fibroblasts is also intriguing as, in addition to its role in the terminal stages of adipocyte differentiation, leptin has also been implicated in contributing to a pro-tumourigenic breast microenvironment [355]. Ando and colleagues have recently reviewed the literature and suggest that leptin may act in an autocrine, endocrine and paracrine manner to enhance tumour cell proliferation, acquisition of mesenchymal phenotype, migration and invasion [355]. Thus, down-regulation of leptin gene expression in the 4-OHTam treated fibroblasts may contribute to a stroma less permissive to tumour formation.

6.4.5.12 Up-regulation of DHCR24

In addition to *DHCR7*, gene expression of *DHCR24*, another enzyme involved in the terminal stages of cholesterol synthesis, was significantly up-regulated in the 4-OHTam treated fibroblasts ($p = <0.001$, Appendix 4). DHCR24 enzyme activity has been observed by the Poirot group to be inhibited by 4-OHTam [293]. This supports the hypothesis that up-regulated expression may be due a compensatory feedback loop due to inhibition of enzyme activity. In addition, DHCR24 is known to be a co-factor of DHCR7 and the two enzymes interact physically to enhance each other's activity [356]. Thus it is possible that *DHCR24* gene expression is also up-regulated in an attempt to improve the functional activity of DHCR7. However, it is also possible that the up-regulated expression may simply be part of a generalised increased in the whole cholesterol biosynthesis pathway.

6.4.6 Down-regulated pathways in 4-OHTam treated fibroblasts

A more diverse array of pathways were observed to be down-regulated with 4-OHTam treatment compared to the up-regulated pathways which predominantly involved cholesterol and lipid synthesis and metabolism. Many of these down-regulated pathways may also contribute to the generation of an anti-tumour breast microenvironment and the reduction in MD observed clinically with tamoxifen treatment.

6.4.6.1 Cell cycle and DNA replication

Down-regulation of many pathways related to cell cycle and DNA replication were identified using both the REACTOME and KEGG biological pathway resources (Appendices 7 + 8). These data are consistent with the experimental findings of reduced fibroblast proliferation with 4-OHTam treatment (Figures 23 + 24). Pathways involving mRNA processing, homologous recombination, mismatch repair were also significantly down-regulated (Appendices 7 + 8), further highlighting the growth inhibitory properties of 4-OHTam treatment. The *Ki67* gene showed significantly

reduced expression in the 4-OHTam fibroblasts ($p = <0.001$), consistent with the experimental findings described in Chapter 4 of reduced Ki67 immunocytochemical staining in the 4-OHTam treated fibroblasts compared to those treated with vehicle control (Figure 30).

6.4.6.2 Wnt and Hedgehog signalling

The down-regulation of Wnt and Hedgehog signalling pathways was identified using the KEGG biological pathway resource (Appendix 8). These data are intriguing as both Wnt and Hedgehog are established pro-tumourigenic and pro-fibrogenic pathways [357-360]. Therefore down-regulation of these pathways could contribute to a more quiescent, less fibrotic and less 'dense' breast microenvironment.

Wnt signalling has recently been proposed to be a key mediator of stromal-epithelial cell cross talk in the breast microenvironment by Isacke and colleagues, who observed Wnt7a modulated TGF-β signalling in stromal fibroblasts [169]. Experimental results from this study showed inhibition of non-canonical TGF-β signalling through ERK1/2 (Figure 56) in 4-OHTam treated fibroblasts. Thus, this attenuation of TGF-β signalling could potentially be related to a corresponding down-regulation of Wnt signalling.

Intriguingly, Hedgehog signalling has also been shown to overlap with TGF-β signalling at the level of the GLI transcription factors [361, 362]. Furthermore, inhibition of Hedgehog signalling by DHCR7 has been reported [363], and modulation of Hedgehog signalling has also been observed in patients treated with Haloperidol – another drug known to alter ChEH activity [364]. Thus, the Hedgehog signalling pathway may also potentially contribute to the observed inhibition of non-canonical TGF-β signalling in 4-OHTam treated fibroblasts (Figure 56).

Modulation of the TGF-β-Wnt-Hedgehog signalling axis by tamoxifen may contribute to the remodelling of the mammary stroma to a tumour-inhibitory phenotype. Due to the

pro-fibrotic properties of the Wnt and Hedgehog signalling pathways, their down-regulation by tamoxifen may also contribute to the reduction in MD observed in high risk women treated with the drug [110]. Tamoxifen induced down-regulation of Wnt and hedgehog signalling may also contribute to the anti-fibrotic effects of tamoxifen observed in a variety of other organ systems [315-318], and thus may be of value in developing targeted therapies for pro-fibrogenic disorders.

6.4.6.3 ECM protein synthesis, remodelling and mechanotransduction

Down-regulation of collagen formation in the 4-OHTam treated fibroblasts was identified using the REACTOME biological pathway resource (Appendix 7). These data are in keeping with the experimental findings of reduced collagen I protein expression in 4-OHTam treated fibroblasts (Figure 42) and reduced soluble collagen in the conditioned media from 4-OHTam treated fibroblasts (Figure 43). Increased stromal collagen density increased tumour burden in a mouse model of high MD [206], therefore a reduction in fibroblast collagen I expression with 4-OHTam treatment is consistent with a stromal phenotype less permissive to tumour formation.

Modulation of collagen expression by tamoxifen has been reported in a number of studies with conflicting observations [115, 314]. Kim and colleagues found reduced collagen expression with tamoxifen treatment in a mouse model of renal fibrosis [314], whereas Hattar and colleagues found increased total collagen in the ECM of rats treated with tamoxifen [115]. Increased total collagen expression has been reported in a mammary stroma less permissive to tumour formation due to the collagen being less organised and fibrillar in nature [212].

The ability of tamoxifen to alter the biophysical properties of the breast ECM is further suggested by the down-regulation of ECM-receptor interaction, focal adhesion and integrin signalling pathways identified using both KEGG and REACTOME (Appendices 7 + 8). Weaver and colleagues observed increased ECM stiffness was associated with

increased focal adhesion and integrin signalling and pro-tumourigenic PI3 kinase activity [213]. Thus tamoxifen may be able to attenuate pro-tumourigenic signalling pathways by remodelling the ECM to a more quiescent phenotype with less mammary epithelial cell mechanotransduction. Remodelling of the breast ECM could also potentially contribute to the decrease in MD observed clinically with tamoxifen treatment.

6.4.6.4 Immune cell signalling

CTLA4 inhibitory signalling was identified to be significantly down-regulated in the 4-OHTam treated fibroblasts using the REACTOME biological pathway resource (Appendix 7). This suggests that tamoxifen may also be able to influence the interaction of fibroblasts with immune cells within the breast microenvironment. Hattar and colleagues observed changes in the immune cell content in the mammary ECM of tamoxifen treated rats [115]. In addition, cholesterol epoxides generated via the inhibition of ChEH activity by tamoxifen are known to modulate LXR signalling [351]. Modulation of LXR signalling has been suggested to influence immune cell behaviour within the tumour microenvironment [352].

Thus, tamoxifen may be acting via down-regulating multiple, diverse pathways to generate a tumour-inhibitory and less ‘dense’, breast microenvironment (summarised in Figure 79).

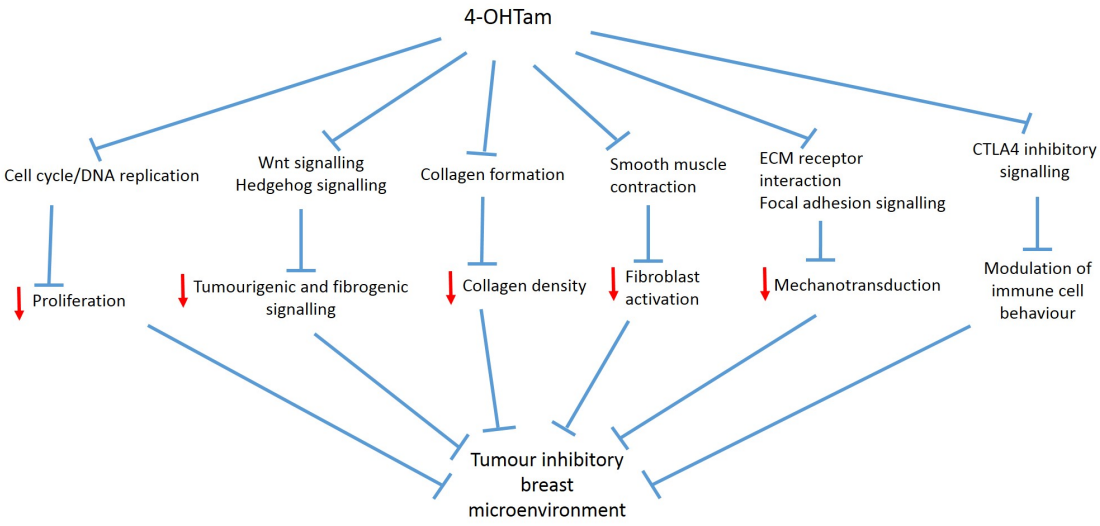

Figure 79: Summary of down-regulated pathways in fibroblasts with 4-OHTam treatment identified using RNA Seq and potential contributions of these to a tumour inhibitory breast microenvironment.

6.4.7 Expression of lysyl oxidase (LOX)

LOX, LOX like 1 (LOXL1) and LOX like 4 (LOXL4) showed reduced expression in 4-OHTam treated fibroblasts in the differential gene expression analysis (adjusted p-values 0.0033, <0.001 respectively). This contrasts with the experimental findings of no significant alteration in LOX protein expression with 4-OHTam treatment (Figure 41). It is possible that a longer treatment time may be required for the reduction in LOX gene expression to be translated into a significant reduction in protein expression.

6.4.8 Expression of FN

Interestingly, significant differential expression of fibronectin 1 (*FN1*) gene was not observed in the RNA Seq analysis, in contrast to the observed reduction of FN protein expression in a proportion of the primary fibroblast cohort (Figure 39). This could be explained by 4-OHTam promoting degradation of existing FN molecules with no effect on overall gene expression. Alternatively 4-OHTam may inhibit translation of the FN mRNA transcript, thus resulting in lower protein expression levels. 4-OHTam may also influence splicing of the FN mRNA transcript, resulting in the translation of different

isoforms of the protein which may not be recognised by the antibody used in western blotting. Thus the protein expression would appear to decrease whilst the mRNA levels remain constant. Another important consideration is that FN is a highly insoluble protein and the changes in protein expression detected with 4-OHTam treatment via western blotting may be artefactual and thus may not accurately represent the FN protein content pre- and post-treatment. This could also potentially account for the discrepancy observed between the RNA Seq and western blotting results.

6.4.9 RNA Seq experimental design considerations

The RNA Seq analysis highlighted a plethora of diverse pathways by which tamoxifen may be acting to generate a breast microenvironment less permissive to tumour formation, and which may contribute to a reduction in MD. It is not clear whether some of the pathways identified, such as increased cholesterol biosynthesis (Appendix 5), may simply be generalised effects seen in any cell treated with 4-OHTam rather than pathways which are driving the anti-tumour and density lowering effects of the drug.

One way in which the design of the RNA Seq analysis could be repeated to try and delineate the key pathways involved would be to compare the differentially expressed genes between a group of patients' fibroblasts who showed a reduction in FN expression with 4-OHTam treatment (responders) and a group of those who did not (non-responders). Pathways and genes significantly differentially expressed in the responders compared to the non-responders may highlight some of the crucial mechanisms by which tamoxifen exerts the density lowering and tumour-inhibitory effects. Only a single non-responder was included in this RNA Seq study, thus any such analysis would lack sufficient statistical power.

7 Investigation of RNA Seq findings and proposed ER-independent mechanism of 4-OHTam action on fibroblast function

7.1 Introduction

The RNA Seq data from this study showed marked up-regulation of pathways involved in cholesterol metabolism in 4-OHTam treated fibroblasts, including components of the microsomal AEBS (Appendix 4). Binding to the AEBS and inhibition of ChEH activity by SERMs has been proposed by the Poirot group to be anti-tumourigenic and to promote differentiation of tumour cells [347]. Thus, this pathway could contribute to an antitumourigenic breast microenvironment and promote differentiation of fibroblasts to a less activated stat, and potentially towards adipogenic differentiation. Increased adipogenic differentiation of the breast stroma could result in a reduction in MD.

In order to test this hypothesis, fibroblasts were treated with tamoxifen (another SERM) and a commercially available inhibitor of ChEH – tesmilifene (DPPE), to determine if these drugs modulated fibroblast function in a similar manner to 4-OHTam. Analysis of the cholesterol metabolite content of fibroblasts treated with these drug regimens was also performed to investigate potential deregulation of cholesterol metabolism.

7.2 Methods and materials

7.2.1 Quantitative reverse transcription and real time polymerase chain reaction (qRT-PCR)

7.2.1.1 RNA extraction and quantification

RNA was extracted from cultured cells using the QuickPrep miniprep kit (Zymo Research, R1054) according to manufacturer's instructions. Briefly, culture media was removed and cells washed in PBS. 400µl of lysis buffer was added to the plate and cells scraped before transferring the lysate to a 1.5ml eppendorf tube and briefly centrifuging at 12000 rpm for 30 seconds. The supernatant was then transferred to a DNA eliminating spin column and briefly centrifuged at 10000 rpm for 1 minute. 320µl of absolute ethanol (Fisher Scientific, E/0650DF/17) was mixed with the flow through and the entire amount transferred to another spin column. The column was centrifuged at 10,000 rpm for 1 minute before discarding the flow through and adding 400µl RNA Prep buffer and centrifuging in the same manner. The samples were then centrifuged with 800µl and 400µl RNA wash buffer in succession before centrifuging the spin column for 2 minutes in an empty collection tube to remove all wash buffer. The column was then transferred to a 1.5ml eppendorf tube and 25µl RNase free water added directly onto the column membrane. The tube was left to stand for 1 minute before centrifuging at 12000 rpm for 30 seconds to elute the RNA.

The RNA was quantified (ng/µl) using the Nanodrop system (Thermo Scientific) and then diluted to a concentration of 50ng/µl using RNAse-free water.

7.2.1.2 cDNA synthesis

cDNA synthesis was carried out as a two-step process using 50ng RNA per reaction. The first step involved adding 50ng of RNA (1µl) to a PCR eppendorf along with 1µl random hexamer primers (Sigma, H0268), 1µl dNTPs (10mM, Sigma, GE28-4065 57)

and 7µl RNAse free water (Fisher, 11506281). The samples were then incubated for 10 minutes at 70°C and 5 minutes at 4°C using a pre-set program on a PCR machine (Eppendorf).

The second step involved adding 2µl of reverse transcriptase enzyme buffer (Sigma, M1302-40KU), 1µl of reverse transcriptase enzyme (Sigma, M1302-40KU) and a further 7µl of RNAse free water to each reaction. The samples were then incubated at 22°C for 10 minutes, 37°C for 50 minutes and 90°C for 10 minutes. cDNA samples were stored at 4°C until required.

7.2.1.3 Quantitative real time PCR

Real time PCR was carried out using SYBR Green (Applied Biosystems, 4367659) according to manufacturer's instructions. 1µl of cDNA was used per reaction. Primers (Integrated DNA technologies) were stored as a 100µM stock and used at 0.3mM final concentration, the sequences are listed below in Table 15. 18S was used as a housekeeping gene. A PCR master mix was prepared for each reaction including; 5µl SYBR Green, 1µl forward primer, 1µl reverse primer and 2µl RNAse free water to give a 10µl total reaction volume per tube. Each reaction was perfomed in triplicate within the same plate for each all genes. Reactions were run using a Step One Plus instrument (Applied Biosystems) using the following conditions: for one cycle 95°C for 20 minutes, followed by 95°C for 1 minute and 60°C for 2 minutes for 40 cycles.

Gene	*Forward Primer Sequence 5'-3'*	*Reverse Primer Sequence 5'-3'*
DHCR7	GACAACTGGATCCCACTGCTG	CAGGTTGATGAGGGTCCAGGC
DHCR24	GGCTCATACCTGGCTTGC	CCAGAGGCCAAATGGGTAG
CD36	GGCTGTGACCGGAACTGTG	TTCTGTGCCTGTTTTAACCCAA
Leptin	CTGTGCCCATCCAAAAAGTCC	AGGAGACTGACTGCGTGTGT
18S	CAGGGGAAACCTCACCCGGC	AACGGCCATGCACCACCACC

Table 15: Primer sequences used in qRT-PCR

7.2.1.3.1 Determining relative expression level

Relative changes in gene expression were determined using the comparative cycle threshold method. The cycle threshold level (Ct) is the point at which fluorescence can be detected. The average Ct value for the sample triplicates (vehicle control and drug treated) and housekeeping gene samples (18S) was determined. The change in cycle threshold (ΔCt) was then calculated by subtracting the average Ct for the housekeeping gene from the average Ct of the target gene. The ΔCt of the vehicle control was then subtracted from the ΔCt of the drug treated sample to give a ΔΔCt value. The relative change in gene expression was then calculated using the arithmetic formula $2^{-(\Delta\Delta Ct)}$ where 2 is a constant that assumes 100% efficiency.

7.2.2 Oil Red O staining

7.2.2.1 Preparation of stock and working solutions

Oil Red O stock solution was prepared by dissolving 0.5g Oil Red O (Sigma, O-0625) in 100ml isopropanol (Acros Organics, 38971002S).

A working solution was prepared fresh prior to staining. 6ml of stock solution was mixed with 4ml distilled water and left to sit at room temperature for 1 hour. The solution was then filtered through Whatmann paper to remove any undissolved granules.

7.2.2.2 Staining procedure

Fibroblasts were seeded into triplicate wells on a 12 well plate (5 x 10^4 cells per well), hormone deprived for 24 hours and then treated for 1 week with vehicle control, tamoxifen (5μM), 4-OHTam (5μM), tesmilifene (20μM), fulvestrant (5μM) or E2 (10nM).

Culture media was removed and cells were washed with PBS before fixing in 10% NBF for 10 minutes. The cells were washed twice with PBS for 1 minute and then 1ml of Oil Red O working solution added to each well for 1 hour at room temperature. The working solution was then removed and the cells washed three times with distilled water. The cells were then counterstained with Mayer's haematoxylin for 2 minutes before washing a further five times with distilled water.

7.2.2.3 Quantification

Oil Red O staining was quantified by adding 500µl of isopropanol to each well to solubilise Oil Red O bound to lipid. The optical density of the isopropanol solution was then measured on a plate reader at 510nm.

7.2.3 Filipin staining

8 well chamber slides were pre-treated with 0.2% gelatin for 1 hour at 37^{o}C before seeding 1 x 10^4 fibroblasts into each chamber. The cells were hormone deprived for 24 hours and then treated for 1 week with either vehicle control, tamoxifen (5µM), 4-OHTam (5µM) or tesmilifene (20µM).

Filipin complex (Sigma, F9765) working solution was prepared (0.05mg/ml in PBS/10% FBS) and stored protected from light.

The culture media was removed and cells washed twice with PBS before fixing in 10% NBF for 10 minutes. The cells were washed with PBS three times before incubating with 1ml glycine (1.5mg/ml in PBS) for 2 hours at room temperature. The glycine was removed and the cells incubated with 1ml of filipin working solution for 2 hours at room temperature protected from light. The filipin was then removed and the cells washed three times in PBS before mounting a coverslip with Prolong Gold with DAPI (Life Technologies, P36931).

Images were acquired on confocal microscope LSM510. Filipin was excited using the UV laser at 350nm. Images were captured at 1024 x 1024 resolution.

7.2.4 Mass spectrometry

7.2.4.1 Treatment conditions

The sterol content of primary fibroblasts (one normal reduction mammoplasty patient 2585) treated with the following treatment conditions was determined by mass spectrometry:

- Vehicle control
- Tamoxifen (5μM)
- 4-OHTam (5μM)
- Tamoxifen (2.5μM) and 4-OHTam (2.5μM)
- Tesmilifene (20μM)
- Fulvestrant (5μM)

7.2.4.2 Sample Preparation

Fibroblasts were seeded into T175 flasks, grown to 70% confluence and hormone deprived for 24 hours. 6 flasks were prepared for each fibroblast treatment condition. A minimum of 10 x 10^6 cells was required for the analysis.

The cells were treated for 48 hours then trypsinised and counted using a haemocytometer. After counting, the cells were centrifuged at 12000 rpm for 2 minutes and the cell pellets immediately frozen at -80^{o}C.

7.2.4.3 Mass spectrometry analysis

The sterol profiling was performed by Dr Marc Poirot and Dr Sandrine Silvente-Poirot, Toulouse Centre for Cancer Research, Toulouse, France in collaboration with Dr

Antonin Lamaziere, Sorbonne Universités- Université Pierre et Marie Curie, Paris, France.

Sterols in cell homogenates were extracted with a solvent mixture containing chloroform/methanol 2/1 (v/v) spiked with epicoprostanol as an internal standard. Lipids were partitioned in chloroform after addition of saline, saponified by methanolic potassium hydroxide (0.5 N, 60^{o}C, 15 minutes). The fatty acids released were methylated with BF3-methanol (12%, 60^{o}C, 15 minutes) in order not to interfere with the chromatography of sterols. The sterols were re-extracted in hexane and silylated as described previously [365]. The trimethylsilylether derivatives of the sterols were separated by gas chromatography (GC, Hewlett–Packard 6890 series) in a medium polarity capillary column RTX-65, (65% diphenyl 35% dimethyl polysiloxane, length 30 m, diameter 0.32 mm, film thickness 0.25 µm (Restesk, Evry, France)). The mass spectrometer (Agilent 5975 inert XL) in series with the GC was set up for detection of positive ions. Ions were produced in the electron impact mode at 70 eV. The sterols were identified by the fragmentogram in the scanning mode and quantified by selective monitoring of the specific ions after normalisation with the internal standard epicoprostanol and calibration with weighed standards.

7.2.5 Electron microscopy

7.2.5.1 Preparation of fixation solution

Primary fibroblasts were fixed prior to transmission electron microscopy (TEM) using a freshly prepared gluteraldehyde (2%, Sigma, G6257) / Sorensen's buffer (0.1M, pH7.4) fixation solution.

0.1M pH 7.4 Sorensen's buffer was prepared as follows:

35.6g of sodium hydrogen phosphate dibasic dihydrate ($Na_2HPO_4.2H_2O$, Sigma, 30435) was dissolved in 1 litre distilled water – Solution A

27.6g of sodium phosphate monobasic monohydrate ($NaH_2PO_4.H_2O$, Sigma, S9638) was dissolved in 1 litre distilled water – Solution B

40.5ml of solution A was added to 9.5ml of solution B to give 50ml of 0.2M Sorensen's buffer. The pH was checked to ensure it was 7.4 before 50ml of this solution was diluted with 50ml of distilled water to give 100ml of 0.1M pH 7.4 Sorensen's buffer.

7.2.5.2 Sample preparation

Primary fibroblasts were seeded in T175 flasks and grown to 70% confluence, hormone deprived for 24 hours, then treated for one week with vehicle control, tamoxifen (5μM), 4-OHTam (5μM) or tesmilifene (20μM). The cells were viewed on an inverted phase contrast microscope to ensure perinuclear cytoplasmic vesicles were clearly visible before being trypsinised and centrifuged at 1500 rpm for 3 minutes. The supernatant was carefully removed and the cells were re-suspended in 1.5ml freshly prepared fixation solution before being transferred to a 1.5ml eppendorf and stored at room temperature.

7.2.5.3 Cell imaging

Cell imaging was performed by Dr Marc Poirot and Dr Sandrine Silvente-Poirot, Toulouse Centre for Cancer Research, Toulouse, France.

Following fixation with 2% glutaraldehyde in 0.1M Sorensen's phosphate buffer (pH 7.4), the cells were washed with the Sorensen's phosphate buffer (0.1 M) for 12 hours and then post-fixed with 1% OsO4 in Sorensen's phosphate buffer (Sorensen's phosphate 0.05 M, glucose 0.25 M, OsO4 1%) for 1 hour.

The cells were then washed twice with distilled water, and pre-stained with an aqueous solution of 2% uranyl acetate for 12 hours. Samples were then treated exactly as described previously [296]. Observations were performed with a Hitachi HT7700 Transmission Electron Microscope.

7.3 Results

7.3.1 Investigating differential gene expression of DHCR7 and DHCR24

qRT-PCR was performed to determine relative mRNA expression of DHCR7 and DHCR24, two cholesterol synthesis enzymes consistently highlighted to show up-regulated expression with 4-OHTam treatment in the pilot and follow up RNA Seq datasets. Three patients' primary fibroblasts were examined (1004, 2182, 2585).

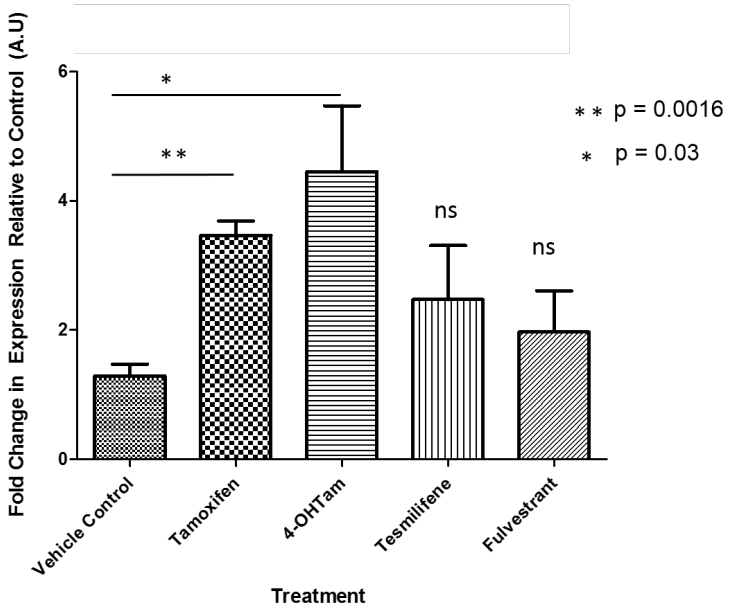

Figure 80: DHCR7 mRNA expression in fibroblasts treated with vehicle control, tamoxifen, 4-OHTam, tesmilifene and fulvestrant (n = 3). Significant up-regulation of DHCR7 was seen in three fibroblasts treated with tamoxifen (p = 0.0016) and 4-OHTam (p = 0.03).

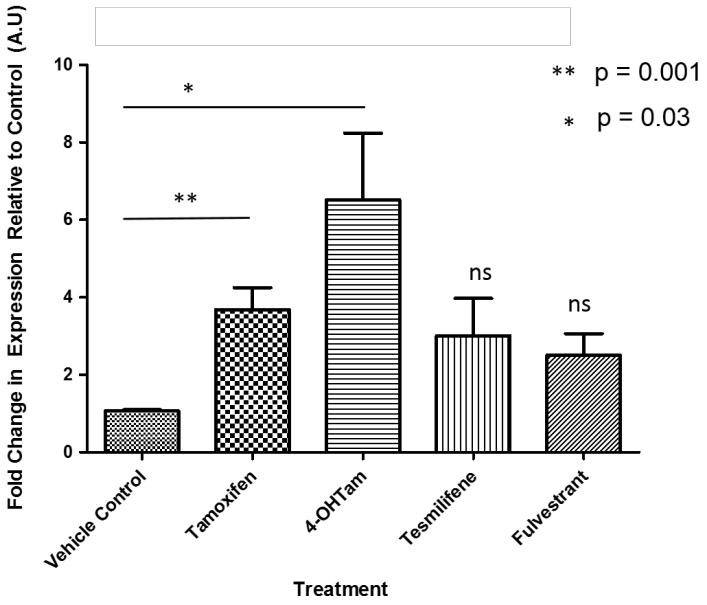

Figure 81: DHCR24 mRNA expression in fibroblasts treated with vehicle control, tamoxifen, 4-OHTam, tesmilifene and fulvestrant (n = 3). Significant up-regulation of DHCR24 was seen in fibroblasts treated with tamoxifen (p = 0.001) and 4-OHTam (p = 0.03).

Up-regulated expression of DHCR7 and DHCR24 mRNA was identified in fibroblasts treated with tamoxifen and 4-OHTam (Figure 80 + Figure 81). No significant increased expression was seen in fibroblasts treated with tesmilifene or fulvestrant.

7.3.2 Confirming lipid accumulation in 4-OHTam treated fibroblasts

Oil Red O staining was undertaken to determine if the perinuclear cytoplasmic vesicles noted in the 4-OHTam treated fibroblasts contained lipid. Fibroblasts from three patients (1004, 1890, 1923) were examined.

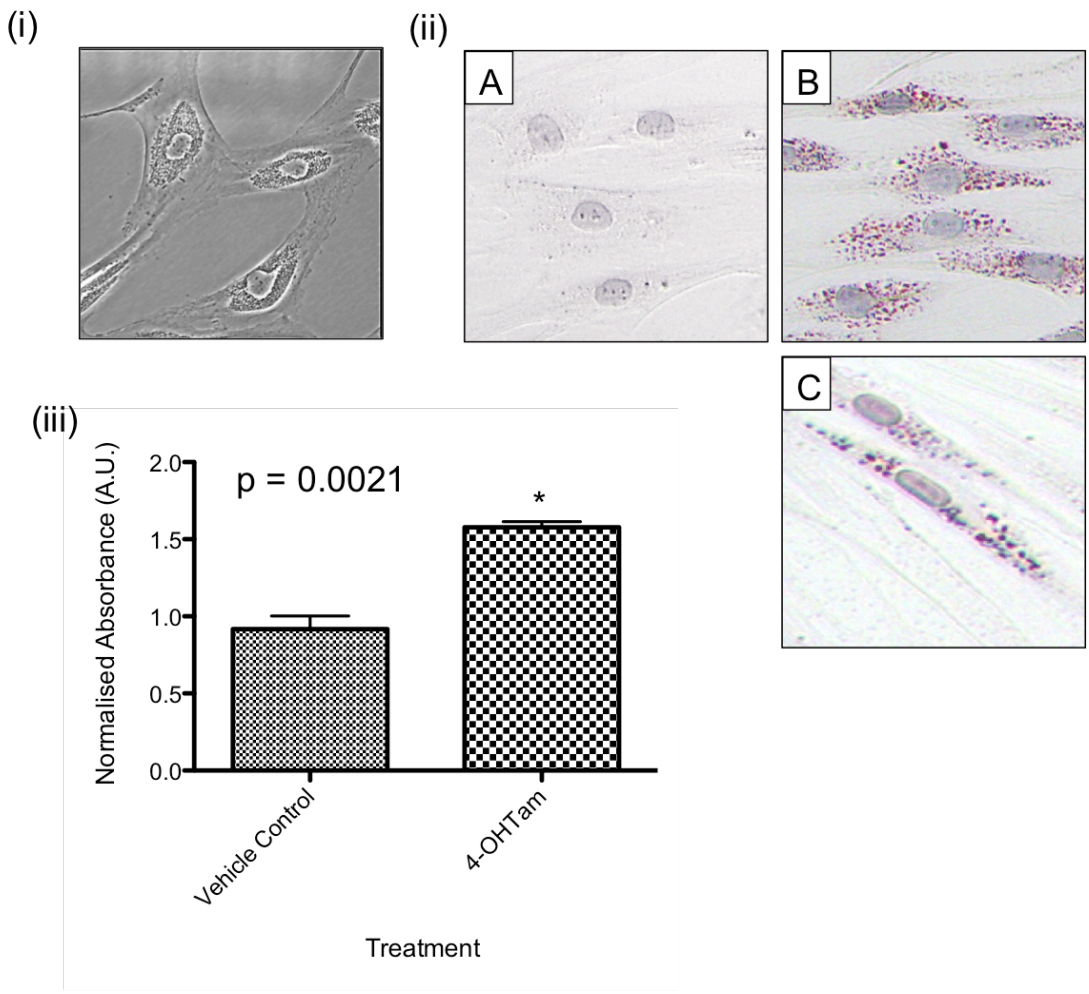

Figure 82: Lipid droplet accumulation in 4-OHTam treated fibroblasts. (i) Phase contrast image of perinuclear cytoplasmic vesicles seen in 4-OHTam treated fibroblasts (x40 objective) (ii) Oil Red O staining (A) No staining in vehicle control treated fibroblasts (x40 objective) (B) Positive Oil Red O staining in the perinuclear vesicles of 4-OHTam treated fibroblasts (x40 objective) (C) Positive Oil Red O staining in lipid droplets of all trans retinoic acid (ATRA) treated pancreatic stellate cells (positive control, x40 objective). (iii) Quantification of Oil Red staining following solubilisation in isopropanol, normalised to the vehicle control. Triplicate wells of a 24 well plate were analysed for each treatment condition in three patients' fibroblasts (n = 3). Significantly more Oil Red O is present in the 4-OHTam treated fibroblasts ($p = 0.0021$, example of patient 1004)

4-OHTam treated fibroblasts showed significantly more positive staining with Oil Red O ($p = 0.0021$, Figure 82) in the perinuclear cytoplasmic vesicles than the fibroblasts treated with vehicle control.

7.3.3 Investigating potential ER-independent effect of 4-OHTam via inhibition of ChEH activity

In order to test our hypothesis that 4-OHTam is potentially acting via ER-independent mechanisms to affect ChEH activity, fibroblasts were treated with tamoxifen (another SERM), tesmilifene (commercially available inhibitor of ChEH) and fulvestrant (Pure ER antagonist).

7.3.3.1 Effect on fibroblast proliferation

The effect of tamoxifen, tesmilifene and fulvestrant on fibroblast proliferation was assessed with the Alamar Blue assay using three patients' primary fibroblasts (1004, 2182, 2093, Figure 83)

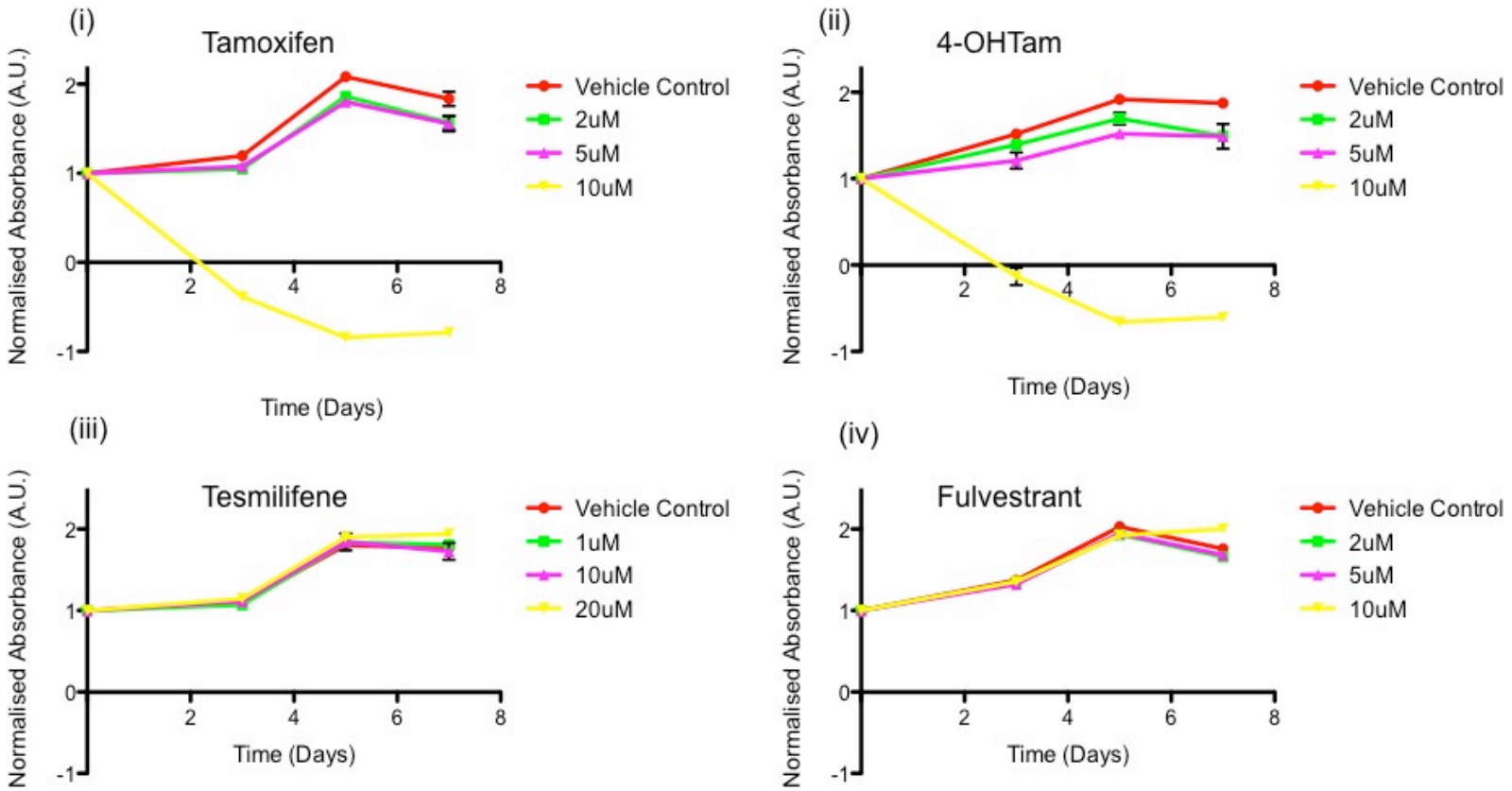

Figure 83: Effect of tamoxifen, 4-OHTam, tesmilifiene and fulvestrant on fibroblast proliferation using Alamar Blue assay. (i) Tamoxifen treated fibroblasts show a dose dependent negative effect on fibroblast proliferation, similar of the effect of 4-OHTam (ii). At high concentrations the dose of tamoxifen and 4-OHTam was toxic to the cells. Tesmilifene (iii) and Fulvestrant (iv) show no significant effect on fibroblast proliferation (n =3), example of patient 1004.

Tamoxifen showed a similar dose dependent, negative effect on fibroblast proliferation, as had been observed with 4-OHTam (Figure 83). Similarly, high concentrations of tamoxifen and 4-OHTam were toxic to the cells. Tesmilifene and fulvestrant showed no significant effect in fibroblast proliferation (Figure 83).

7.3.3.2 Effect on fibroblast activation

Protein expression of FN and SMA was assessed in primary fibroblasts from three patients (1004, 2093, 2585) treated with tamoxifen (5μM), 4-OHTam (5μM), tesmilifene (DPPE) (10μM), fulvestrant (5μM) and oestradiol (10nM).

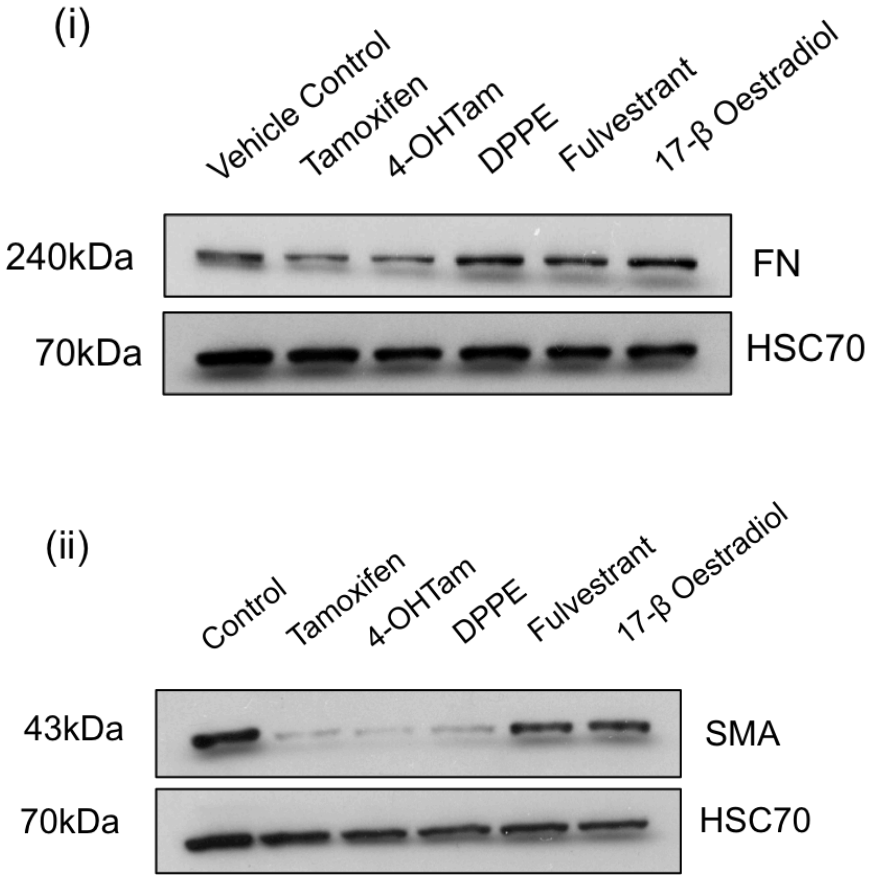

Figure 84: Expression of FN and SMA in primary fibroblasts treated with tamoxifen (5μM), 4-OHTam (5μM), tesmilifene (DPPE) (10μM), fulvestrant (5μM) and oestradiol (10nM). (i) Western blot image showing reduced FN expression in fibroblasts treated with tamoxifen and 4-OHTam. No effect on FN expression was seen with tesmilifene, fulvestrant or oestradiol (n= 3, example of patient 2093). (ii) Western blot image showing reduced expression of SMA in fibroblasts treated with tamoxifen, 4-OHTam and tesmilifene. No effect on SMA expression was seen with fulvestrant or oestradiol (n =3, example of patient 2093).

Reduced FN expression was consistently seen in fibroblasts treated with tamoxifen and 4-OHTam (Figure 84 (i)). No effect on fibroblast expression of FN was evident with tesmilifene, fulvestrant or oestradiol. Reduction in SMA expression was consistently seen in fibroblasts treated with tamoxifen, 4-OHTam and tesmilifene (Figure 84 (ii)). No effect on SMA expression as seen with fulvestrant or oestradiol.

In addition, SMA expression in three patients' primary fibroblasts (2090, 2182, 2585) was analysed following three days treatment with tamoxifen (5μM), 4-OHTam (5μM), tesmilifene (10μM) and fulvestrant (5μM) with and without TGF-β stimulation (5ng/ml).

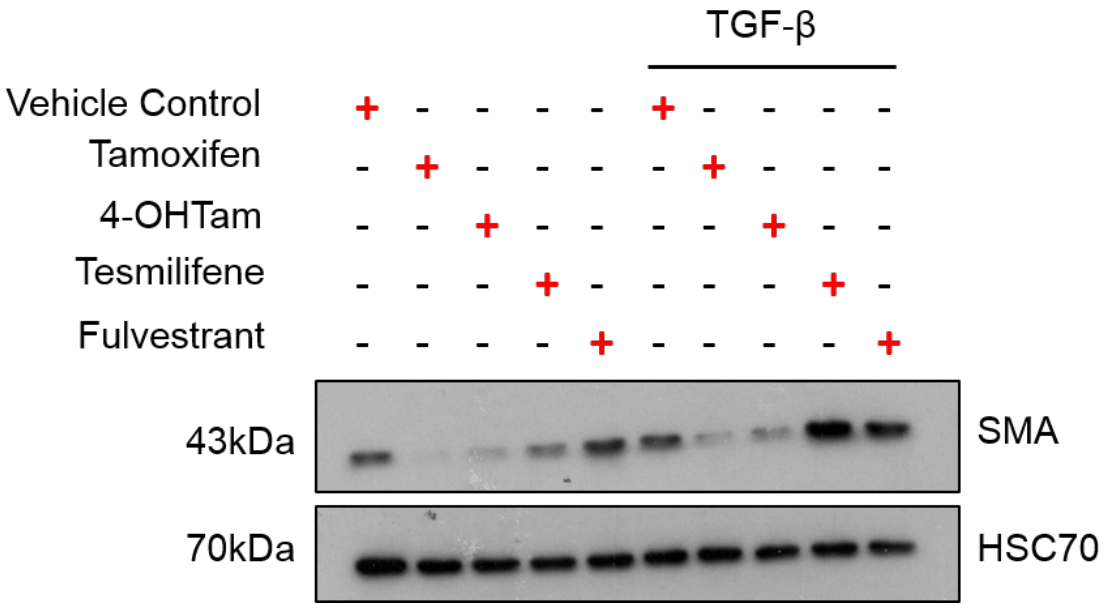

Figure 85: Fibroblast expression of SMA following treatment with vehicle control, tamoxifen (5μM), 4-OHTam (5μM), tesmilifene (10μM) and fulvestrant (5μM) with and without TGF-β stimulation (5ng/ml). Tamoxifen, 4-OHTam and tesmilifene treatment resulted in a significant reduction in SMA expression. No effect on SMA expression was seen with fulvestrant. Tamoxifen and 4-OHTam supressed SMA expression following stimulation with TGF-β. No reduced expression was seen in cells treated with tesmilifene or fulvestrant following TGF-β stimulation (n = 3, example of patient 2090).

Consistent with previous experiments, tamoxifen, 4-OHTam and tesmilifene treatment resulted in reduced expression of SMA (Figure 85). No effect was seen with fulvestrant. Following TGF-β stimulation, reduced expression of SMA was only seen in cells treated with tamoxifen and 4-OHTam, no effect was seen with tesmilifene or fulvestrant (Figure 85).

7.3.3.3 Effect on fibroblast phenotype

Primary fibroblasts from three patients (1004, 1890, 2182) were treated with vehicle control, tamoxifen (5μM), tesmilifene (10μM), fulvestrant (5μM) and oestradiol (10nM) for one week to determine if a similar phenotype to the 4-OHTam (5μM) treated fibroblasts was observed.

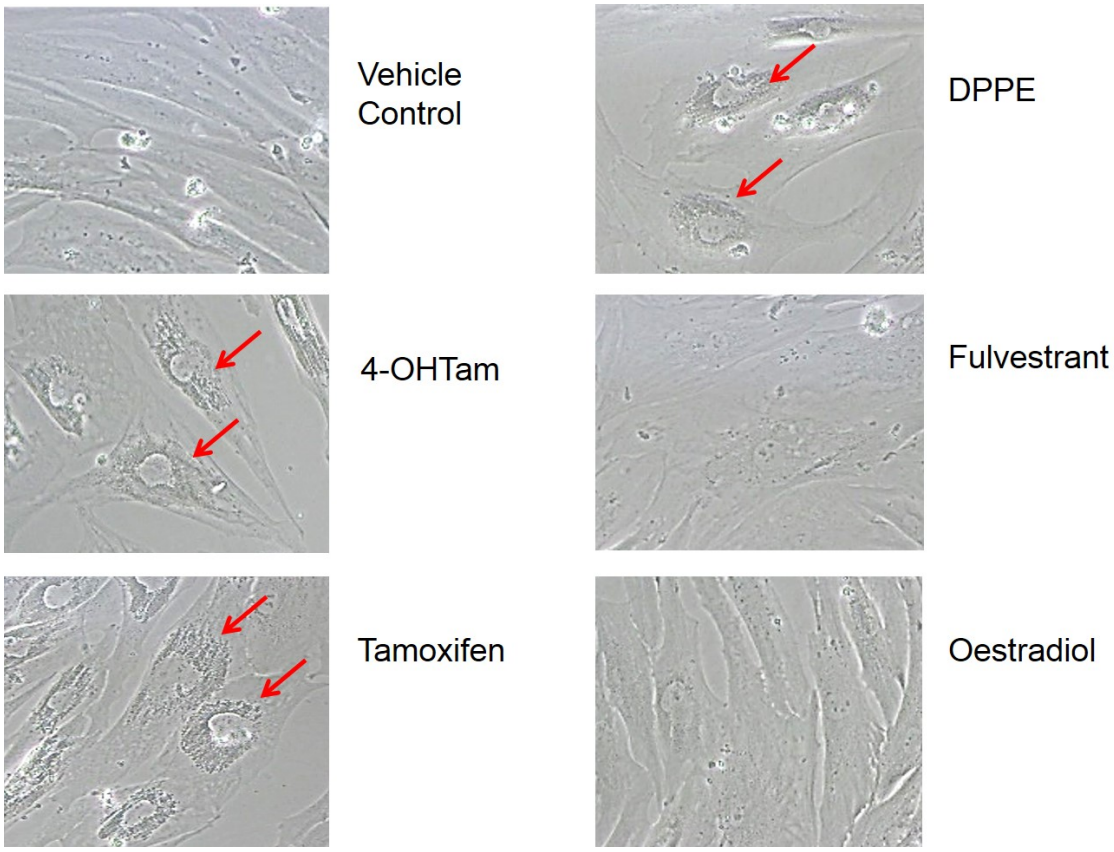

Figure 86: Effect of tamoxifen (5μM), 4-OHTam (5μM), tesmilifene (10μM), fulvestrant (5μM) and oestradiol (10nM) on primary fibroblast morphology after one week of treatment. Phase contrast images (x40 objective) showing accumulation of small perinuclear cytoplasmic vesicles (red arrows) in the fibroblasts treated with tamoxifen, 4-OHTam and tesmilifene. No vesicles were seen in the cells treated with fulvestrant and oestradiol. Example of patient 2182.

Accumulation of small perinuclear cytoplasmic vesicles was seen in the fibroblasts treated with tamoxifen, 4-OHTam and tesmilifene (Figure 86). No vesicles were identified in the cells treated with fulvestrant or oestradiol.

7.3.3.4 Effect on fibroblast accumulation of lipid droplets

Primary fibroblasts from three patients (1004, 2090, 2093) were treated with vehicle control, tamoxifen (5μM), 4-OHTam (5μM), tesmilifene (10μM), fulvestrant (5μM) and oestradiol (10nM) for one week and then stained with Oil Red O to assess lipid droplet accumulation.

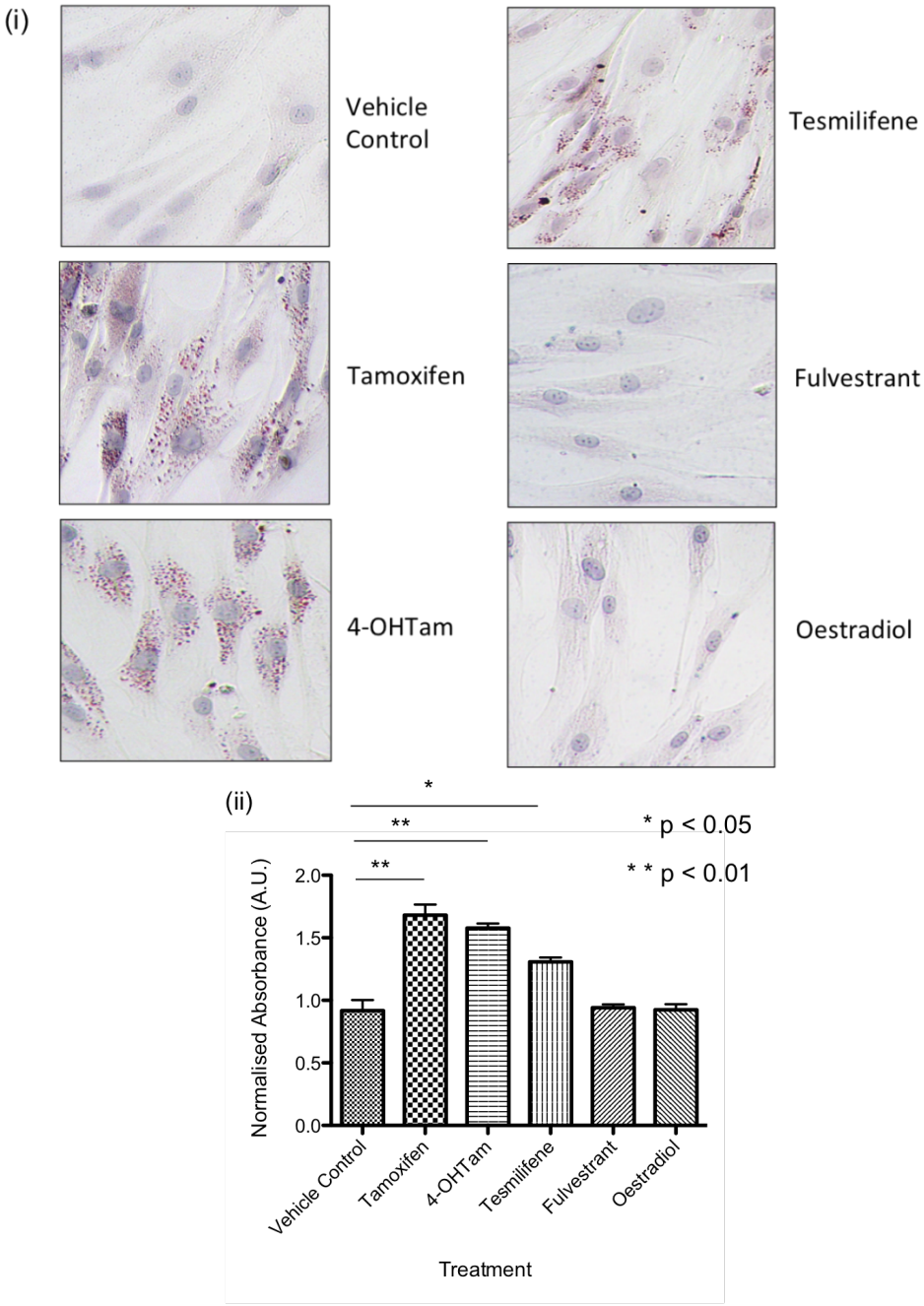

Figure 87: Oil Red O staining of fibroblasts treated with vehicle control, tamoxifen (5μM), 4-OHTam (5μM), tesmilifene (10μM), fulvestrant (5μM) and oestradiol (10nM) for one week. (i) Brightfield microscopy images (x20 objective) showing positive Oil Red O staining in cells treated with tamoxifen, 4-OHTam and tesmilifene. No significant positive staining was seen in cells treated with fulvestrant or oestradiol. (ii) Quantification of Oil Red O staining confirmed significant positive staining in the cells treated with tamoxifen (p = 0.0033), 4-OHTam (p =

0.0021) and tesmilifene (p = 0.0136), normalised to vehicle control. No significant positive staining was seen in the cells treated with fulvestrant or oestradiol. Triplicate wells of a 24 well plate were analysed for each treatment condition in three patients' fibroblasts (n = 3), example of patient 1004.

Positive Oil Red O staining was identified in the cells treated with tamoxifen, 4-OHTam and tesmilifene (Figure 87). No significant lipid droplet accumulation was identified in the cells treated with fulvestrant or oestradiol.

7.3.4 Investigating potential accumulation of cholesterol precursors (free sterols) in fibroblasts

7.3.4.1 Filipin staining for free sterols

To test the hypothesis that tamoxifen modulates cholesterol metabolism by inhibiting the activity of enzymes in the cholesterol synthesis pathway (DHCR7, DHCR24, ChEH), Filipin staining was performed to detect the presence of free sterols in two patients' fibroblasts (2090, 2585) treated with tamoxifen (5μM), 4-OHTam (5μM) and tesmilifene (10μM) for one week. Filipin is a highly fluorescent antibiotic which specifically binds cholesterol.

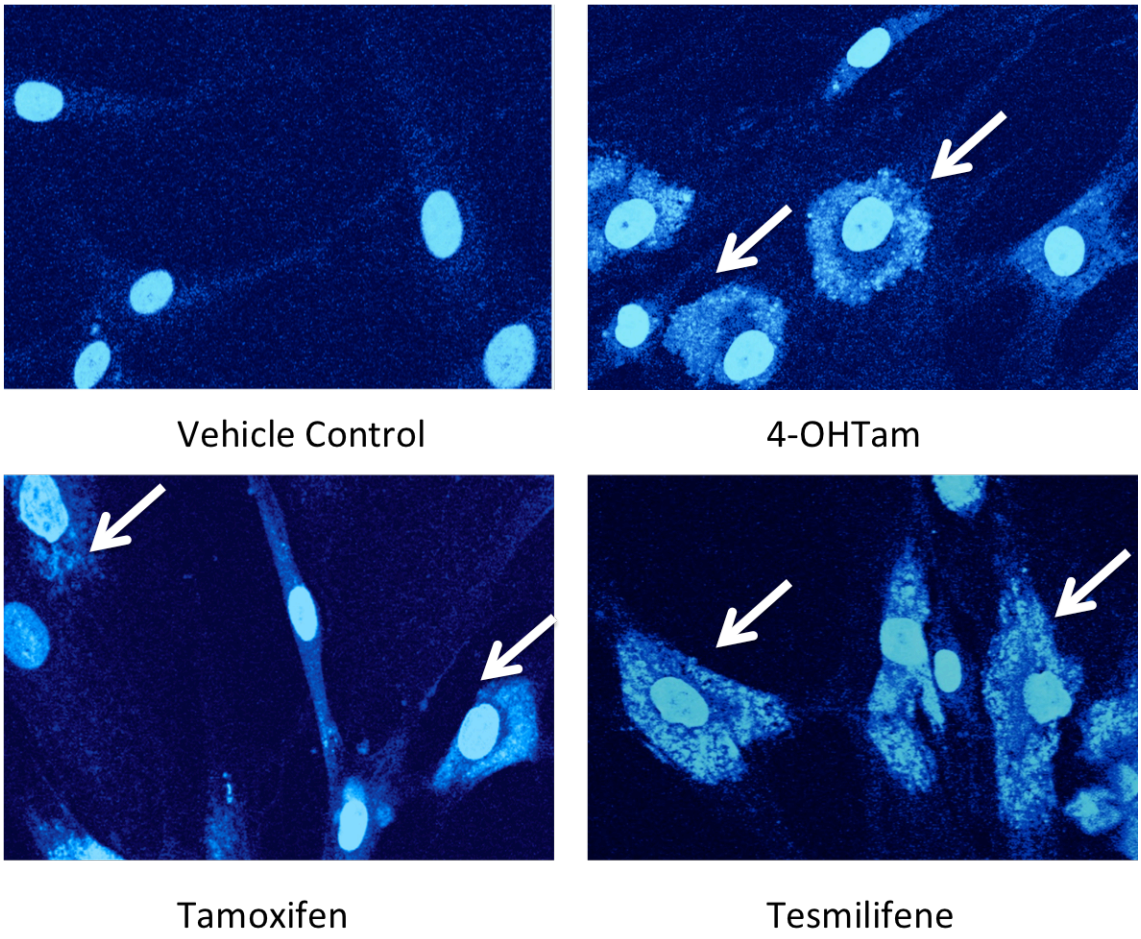

Figure 88: Filipin staining of fibroblasts treated with vehicle control, tamoxifen (5μM), 4-OHTam (5μm) and tesmilifene (10μM) for one week (x20 objective). Positive filipin staining was seen in the perinuclear cytoplasmic vesicles (white arrows) of the cells treated with tamoxifen, 4-OHTam and tesmilifene. Example of patient 2858.

Positive filipin staining was seen in the perinuclear cytoplasmic vesicles of cells treated with tamoxifen, 4-OHTam and tesmilifene (white arrows, Figure 88).

7.3.4.2 Electron microscopy for multilamellar bodies and lipid droplets

To investigate the presence of free sterols accumulating in mutlilamellar bodies within the fibroblasts (previously described in tumour cells by the Poirot group [296]), and the presence of lipid droplets, transmission electron microscopy (TEM) was undertaken on fibroblasts from one patient (2182) treated with vehicle control, tamoxifen (5μM), 4-OHTam (5μM) and tesmilifene (10μM) for 4 days. Multilamellar bodies contain unesterified sterols, which correspond to the positive perinuclear vesicles visualised by

filipin staining. Lipid droplets are amorphous organelles with no membrane containing neutral lipids (triglycerides) and correspond to the positive droplets visualised by Oil Red O staining.

(i)

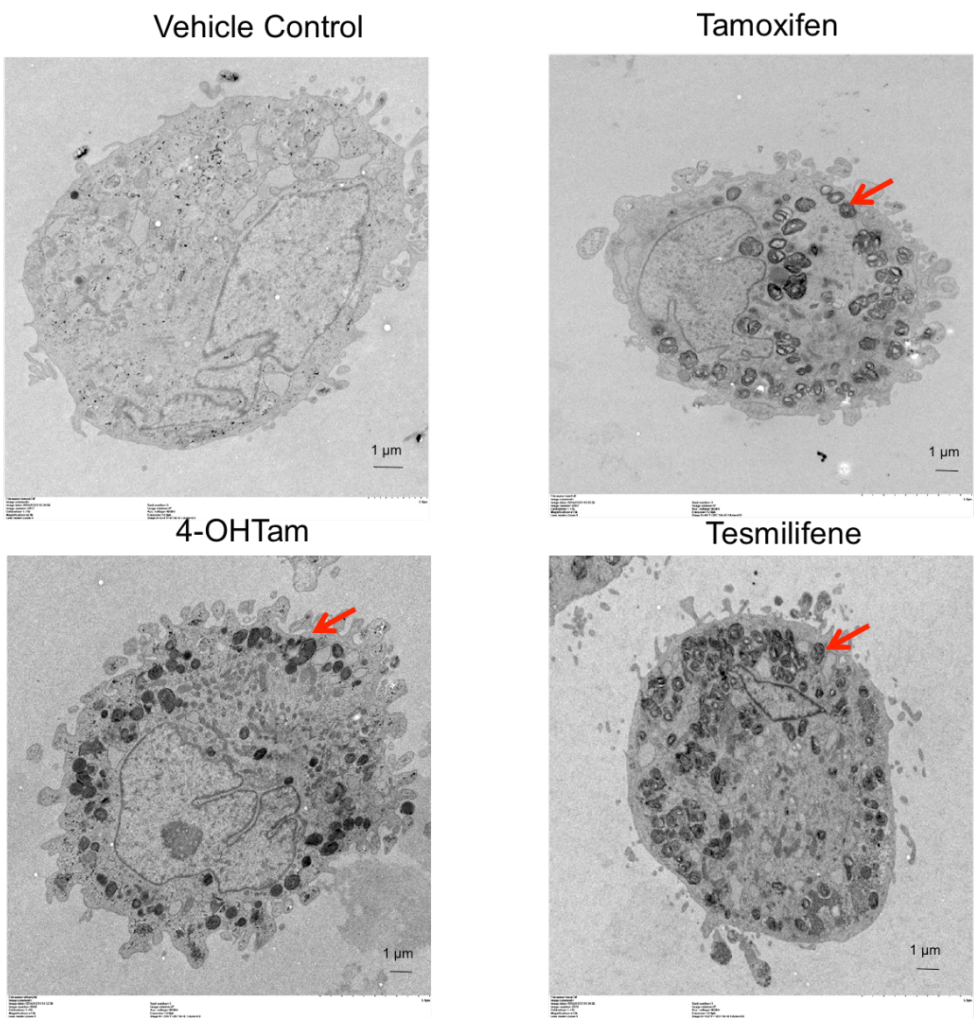

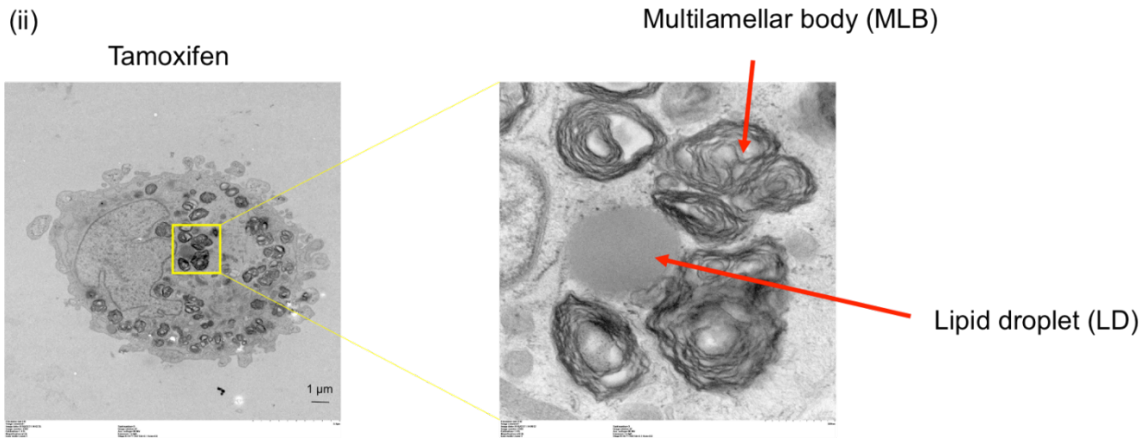

Figure 89: Transmission electron microscopy images of primary fibroblasts from one patient (2182) treated for 4 days with vehicle control, tamoxifen (5µM), 4-OHTam (5µM) and tesmilifene (20µM). (i) Whole cell images of each treatment condition. Multilamellar bodies (MLB, red arrows) are visible in 100% of cells treated with tamoxifen, 4-OHTam and tesmilifene. (ii) High magnification image of MLB and associated lipid droplet from a tamoxifen treated cell. Lipid droplets were present in 100% of cells treated with tamoxifen, 4-OHTam and tesmilifene.

Multilamellar bodies and lipid droplets were observed in 100% of the cells treated with tamoxifen, 4-OHTam and tesmilifene (Figure 89).

7.3.4.3 Mass spectrometry quantification of cholesterol metabolites

To investigate the potential accumulation of cholesterol precursors in the primary fibroblasts from one patient (2182) treated with tamoxifen, 4-OHTam, tesmilifene and fulvestrant, mass spectrometry was performed.

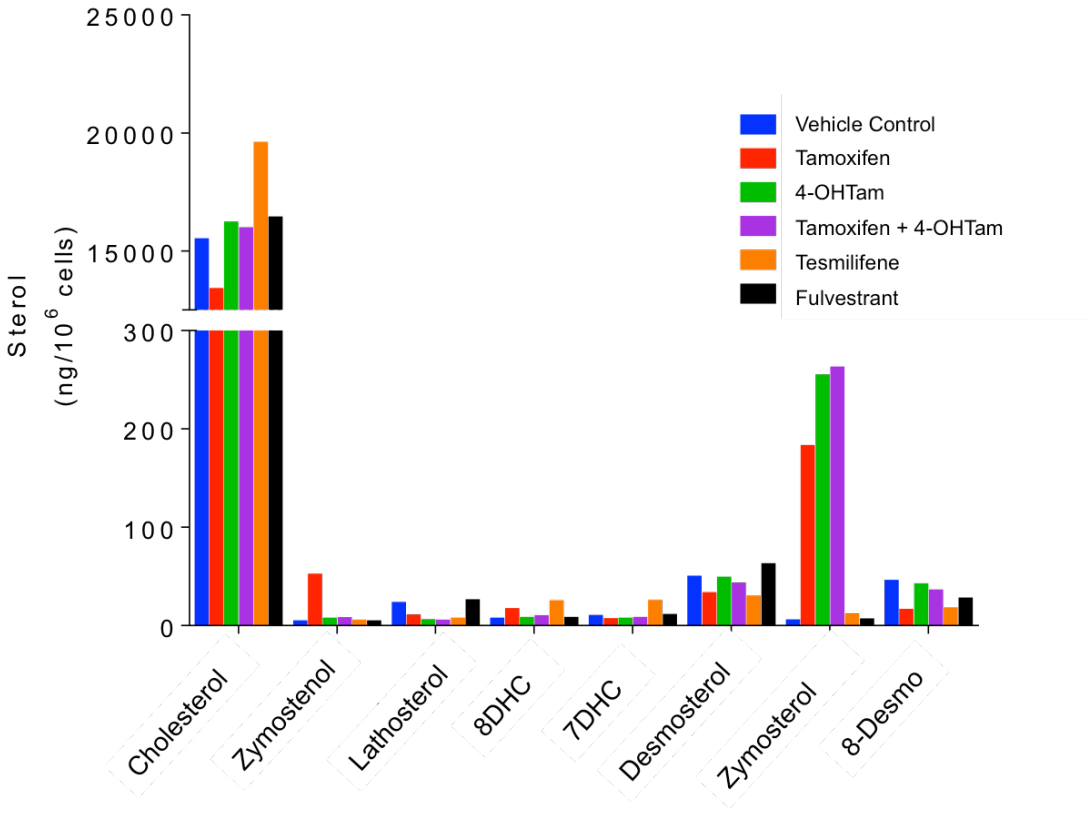

Figure 90: Mass spectrometry analysis of cholesterol precursor accumulation in primary fibroblasts from one patient (2182) treated for one week with vehicle control, tamoxifen (5µM), 4-OHTam (5µM), tamoxifen (2.5µM) and 4-OHTam (2.5µM), tesmilifene (20µM) and fulvestrant (5µM). Tamoxifen treatment resulted in increased accumulation of zymostenol and zymosterol whereas 4-OHTam treatment resulted in accumulation of zymosterol. Co-treatment with tamoxifen and 4-OHTam showed a similar pattern of precursor accumulation to 4-OHTam alone. Tesmilifene treatment resulted in accumulation of cholesterol and very mild accumulation of 8-dehydrocholesterol (8DHC) and 7-dehydrocholesterol (7DHC). Fulvestrant showed a weak accumulation of lathosterol and desmosterol (n=1).

Tamoxifen treatment resulted in increased accumulation of zymostenol and zymosterol in primary fibroblasts, whereas 4-OHTam stimulated the accumulation of zymosterol (Figure 90). Co-treatment with tamoxifen and 4-OHTam showed a similar pattern of cholesterol precursor accumulation to 4-OHTam alone (Figure 90). Tesmilifene treatment resulted in accumulation of cholesterol and a very mild accumulation of 8-dehydrocholesterol (8DHC) and 7-dehydrocholesterol (7DHC). Fulvestrant showed a weak accumulation of lathosterol and desmosterol (Figure 90).

7.3.5 Assessment of DHCR7 protein expression

DHCR7 protein expression in three patients' primary fibroblasts (1004, 2090, 2585) treated with vehicle control, tamoxifen, 4-OHTam, tesmilifene, fulvestrant and oestradiol for three days was determined, to see if the increased DHCR7 mRNA expression observed by RNA Seq and qRT-PCR in the 4-OHTam treated fibroblasts was translated into protein.

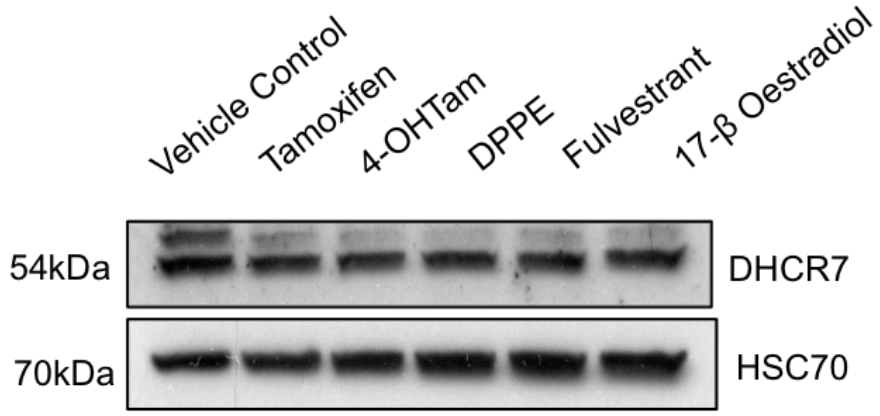

Figure 91: Protein expression of DHCR7 in primary breast fibroblasts treated with vehicle control, tamoxifen, 4-OHTam, tesmilifene, fulvestrant and oestradiol. No significant changes in protein expression were seen in any of the treatment conditions. Example of patient 2585.

No significant alteration in DHCR7 protein expression was observed in any of the treatment conditions in any of the three patients' cells (Figure 91).

7.4 Discussion

7.4.1 Investigation of differentially expressed genes (*DHCR7* and *DHCR24*) identified from RNA Seq analysis

qRT-PCR confirmed up-regulated mRNA expression of both *DHCR7* and *DHCR24* in the tamoxifen and 4-OHTam treated fibroblasts (Figure 80 + Figure 81). This suggests that both 4-OHTam and tamoxifen are acting via similar mechanisms to affect fibroblast function involving cholesterol metabolism. Notably however, up-regulated expression of *DHCR7* and *DHCR24* was not observed in the fibroblasts treated with tesmilifene. Given that tesmilifene is a commercially available inhibitor of ChEH, it might be expected that the drug would have identical effects to tamoxifen and 4-OHTam, which are also proposed to be inhibitors of ChEH by the Poirot group [345]. These data suggest that that the up-regulated expression of *DHCR7* and *DHCR24* observed with the SERMS may not be due to inhibition of ChEH activity and could represent an alternative, more generalised effect on the cholesterol biosynthesis pathway. Thus, the anti-tumourigenic and density lowering effects of tamoxifen may be due to alternative mechanisms rather than the proposed accumulation of anti-tumorigenic cholesterol epoxides resulting in fibroblast differentiation (Figure 76 + Figure 78). The RNA Seq pathway analysis has highlighted numerous other potentially contributory pathways modulated by 4-OHTam (Appendices 7 + 8).

Alternatively, the lack of significant up-regulation of DHCR7 and DSHCR24 gene expression with tesmilifene could be explained by the fact that tesmilifene is known to have a much weaker ability to inhibit ChEH activity [294] and the pathway analysis has revealed multiple effects of 4-OHTam outside of cholesterol metabolism (Appendices 7 + 8). Therefore, these combined effects may explain why an identical pattern of differential gene expression was not seen with tesmilifene and the SERMs. Thus inhibition of ChEH activity could still be a key mechanism mediating the anti-tumour and density-lowering effects.

No significant change in DHCR7 protein expression was seen with 4-OHTam or tamoxifen treatment (Figure 91), suggesting that the up-regulated mRNA expression may not be being translated into increased functional protein.

Tamoxifen is well documented to affect serum levels of cholesterol in patients receiving adjuvant therapy [366] and altered cholesterol metabolism has recently been proposed by Martin et al to be a mechanism by which resistance to anti-oestrogen therapy occurs in breast cancer patients [338]. Thus our findings are in agreement with these data that cholesterol metabolism is a crucial pathway modulated by tamoxifen that may have significant clinical implications.

Interestingly, a small but non-significant increase in *DHCR7* and *DHCR24* mRNA expression was also identified by qRT-PCR in cells treated with fulvestrant (Figure 80 + Figure 81). This is suggestive of a potential mild effect of fulvestrant on cholesterol metabolism. However, no significant differential gene expression of cholesterol metabolism enzymes were detected in the fulvestrant treated cells in the RNA Seq analysis (Figure 65 + Figure 71). Crucially, there is once again a clear difference between the effect of the SERMS and fulvestrant, supporting a mechanism of action independent of the ER.

7.4.2 Effects of SERMs, tesmilifene and fulvestrant on fibroblast proliferation and activation

To investigate the hypothesis that 4-OHTam and tamoxifen are acting via ER-independent mechanisms to alter fibroblast proliferation and activation, fibroblasts were treated with tamoxifen, 4-OHTam (SERMs), tesmilifene (selective ChEH/AEBS ligand) and fulvestrant (Pure ER-antagonist), to determine if the drugs exerted similar effects on fibroblast function.

A dose dependent, negative effect on fibroblast proliferation was observed in cells treated with tamoxifen and 4-OHTam, with no effect on proliferation demonstrated with tesmilifene and fulvestrant (Figure 83). These data further suggest that tamoxifen and 4-OHTam are acting via similar mechanisms. Once again, tesmilifene treatment resulted in different findings to the SERMs. This disparity in the effect of tesmilifene and the SERMs suggests that the effect on proliferation may not be mediated via inhibition of ChEH activity and accumulation of cholesterol precursors, and potential some of the other pathways highlighted in the RNA Seq analysis may account for the anti-proliferative effects (Figure 79). The disparity between the effect of the SERMS and tesmilifene on fibroblast proliferation is also reflected in the mass spectrometry analysis, where the cells treated with tesmilfiene show a markedly different cholesterol metabolite profile compared to the SERMS (Figure 90). It is possible that the accumulation of zymosterol in the cells treated with SERMS could exert an anti-proliferative effect.

The disparity between the effects of the SERMs and tesmilifene on fibroblast proliferation could also be due to the weak ability of tesmilifene to inhibit ChEH activity. The weak inhibitory activity of tesmilifene could be insufficient to result in sufficient cholesterol metabolite accumulation to affect proliferation. Fulvestrant had no effect on fibroblast proliferation, this further supports the hypothesis that the SERMs may affect fibroblast proliferation via ER independent mechanisms.

Reduced expression of SMA was observed in the fibroblasts treated with tamoxifen, 4-OHTam and tesmilifene, with no effect of fulvestrant or oestradiol (Figure 84). In contrast to the effects on *DHCR7/24* gene expression and fibroblast proliferation, these data support a similar mechanism of action of the SERMs and tesmilifene. This could potentially be via inhibition of ChEH or other cholesterol enzyme activity. These data suggest that inhibition of cholesterol metabolite enzyme activity may be crucial to mediating the potent ‘deactivating’ effects of tamoxifen on the mammary stroma.

However, it is also possible that the ‘deactivating’ effect may also be due to the deregulation of other pathways identified via the RNA Seq analysis (Appendices 7 + 8) which tesmilifene may also be able to influence. Overall, these data are consistent with the observations of others of the ‘deactivating’ effect of tamoxifen on fibroblast function [313, 314].

Crucially, these data also support the hypothesis that tamoxifen and 4-OHTam are acting independently of the ER to modulate fibroblast activity, as tesmilifene has purely ER-independent actions and no effect on SMA expression was observed with the pure ER antagonist fulvestrant or indeed with oestradiol itself (Figure 84).

Interestingly, when primary fibroblast SMA expression was assessed following drug treatment and stimulation with TGF-β, only the SERMs prevented TGF-β mediated up-regulation of SMA expression (Figure 85). Tesmilifene treated fibroblasts showed up-regulation of SMA following TGF-β stimulation (Figure 85).

This further highlights the differing effects on fibroblast function between the weak AEBS ligand tesmilfene and the SERMs - which have stronger affinity for the AEBS and impact on numerous other pathways (Appendices 7 + 8). The ability of the SERMs to inhibit TGF-β mediated fibroblast activation may be due to their ability to affect non-canonical TGF-β signalling (Figure 56). In addition, the RNA Seq pathway analysis revealed down-regulation of Wnt and Hedgehog signalling pathways by 4-OHTam (Appendix 8). These pathways are both known to overlap with TGF-β signalling [358, 361, 362] and thus may explain why only the SERMs, and not tesmilifene, were capable of preventing TGF-β mediated fibroblast activation. However, it also possible that this disparity in the response of the tesmilifene treated fibroblasts to TGF-β stimulation compared to the SERMs reflects an alternative mechanism of action, rather than ChEH inhibition.

The disparity between the effects of tesmilifene and the SERMs is further emphasised in the data showing down-regulation of FN expression only in the cells treated with SERMs (Figure 84). These data again suggest that there may be differing mechanisms of action between the SERMs and tesmilifene out with inhibition of ChEH activity. The complex interaction of the various pathways modulated by SERMs (Appendices 5 - 8) may account for their differing effects on FN expression compared to tesmilifene.

Overall, these data highlight that the SERMs and tesmilifene share some similarities in their effects on fibroblast function, however important differences remain. These differences could be accounted for by the interaction of multiple pathways identified in the RNA Seq analysis by which SERMs affect fibroblast function (Appendices 5 – 8). However, these data also suggest that the inhibition of ChEH activity may not be the most crucial pathway for exerting the anti-tumour and density-lowering effects of tamoxifen. Thus, future work is required to establish which of these pathways is of greatest clinical significance. In addition, the lack of effect on fulvestrant on fibroblast proliferation and expression of SMA or FN further highlights that the observed effects SERM and tesmilifene treatment may be due to ER independent mechanisms.

7.4.3 Confirming lipid droplet and cholesterol precursor accumulation in 4-OHTam treated fibroblasts

4-OHTam treated primary fibroblasts displayed a characteristic phenotype with accumulation of small perinuclear cytoplasmic vesicles (Figure 33). The RNA Seq analysis indicated that 4-OHTam treatment was profoundly influencing cholesterol and lipid metabolism (Appendices 2 - 6). Thus, it was hypothesised that the vesicles accumulating in the 4-OHTam treated fibroblasts may contain lipid or cholesterol metabolite precursors. The Poirot group have previosuly demonstrated the accumulation of both lipid droplets and free sterols (cholesterol precursors) in breast and melanoma tumour cells treated with tamoxifen [296, 347].

Oil Red O staining demonstrated significant, extensive accumulation of lipid droplets within the perinuclear cytoplasmic vesicles observed in the 4-OHTam treated cells ($p = 0.0021$, Figure 82). This demonstrates that 4-OHTam treatment of primary breast fibroblasts induces lipid accumulation. It is not possible to conclude whether the lipid accumulation is related to 'differentiation' of the fibroblasts and future work to establish the significance of the up-regulation of several key early stage adipogenic markers (Figure 77) and PPAR signalling observed in the RNA Seq analysis (Appendix 6).

To investigate if the vesicles and lipid accumulation were a result of ER-independent actions of 4-OHTam, fibroblasts were treated with tamoxifen, 4-OHTam, tesmilifene, fulvestrant and oestradiol. Accumulation of perinuclear cytoplasmic vesicles was observed in the cells treated with tamoxifen, 4-OHTam and tesmilifene. No vesicles were seen in cells treated with fulvestrant or oestradiol (Figure 86).

Furthermore, Oil Red O staining confirmed significant lipid droplet accumulation in only fibroblasts treated with tamoxifen, 4-OHTam and tesmilifene (Figure 87). The similarity of the fibroblast response to SERM and tesmilifene treatment suggests lipid droplet accumulation is a result of a similar mechanism of action, potentially via inhibition of ChEH. The lack of effect with fulvestrant and oestradiol once again suggests an ER independent mechanism of action.

In addition to the accumulation of lipid droplets, filipin antibiotic staining highlighted the accumulation of free sterols within the perinuclear cytoplasmic vesicles of fibroblasts treated with tamoxifen, 4-OHTam and tesmilfene (Figure 88). These observations suggest that both SERM and tesmilifene treatment can induce sterol accumulation in primary fibroblasts. The findings are also in keeping with the proposed ER-independent actions of tamoxifen and 4-OHTam via inhibition of ChEH activity, leading to antitumourigenic cholesterol precursor accumulation [367].

To confirm the accumulation of lipid droplets and free sterols within fibroblasts treated with SERMS and tesmilifene, suggested by the positive Oil Red O and filipin staining, transmission electron microscopy was performed. Multilamellar bodies (MLB) containing unesterified sterols and amorphous lipid droplets were clearly identified in 100% of the cells treated with tamoxifen, 4-OHTam and tesmilifene (Figure 89).

These data confirm that fibroblasts treated with SERMs and tesmilifene accumulate both cholesterol precursors and lipid droplets, corresponding to the perinuclear cytoplasmic vesicles identified in the cells treated with these drugs. The similar actions of SERMs and tesmilifene once again suggest that these effects could due to ER-independent mechanisms, potentially via inhibition of ChEH activity.

The accumulation of lipid droplets and free sterols in tumour cells treated with tamoxifen has been extensively characterised by the Poirot group [294, 295, 347]. They propose that the accumulation of cholesterol precursors within cells may stimulate their differentiation [295]. They have observed differentiating effects on a number of different tumour cells including breast, melanoma and glioma [295, 347, 348].

The appearance of lipid droplets suggests the production of cholesterol epoxides (oxysterols), which arise via the autoxidation of cholesterol precursors by reactive oxygen species (ROS) [344]. As discussed previously, cholesterol epoxides undergo further metabolism with histamine to form dendrogenin A (DDA) – a modulator of LXR signalling [347]. LXR signalling has been proposed to have potent cell differentiating capabilities [347] and is also known to stimulate the expression of lipogenic enzymes [368].

Thus, the appearance of lipid droplets within the fibroblasts treated with SERMs and tesmilifene could suggest potential inhibition of ChEH activity, cholesterol precursor

accumulation, generation of cholesterol epoxides, and modulation on LXR signalling via DDA leading to cell differentiation. However, the results may also simply indicate that fibroblasts treated with these drugs begin to accumulate lipids and sterols. Therefore future work is crucially needed to determine the effect on ChEH enzyme activity and any effect on cell differentiation.

Mass spectrometry was utilised in order to characterise and quantify the accumulation of cholesterol precursors within fibroblasts treated with SERMs, tesmilifene and fulvestrant. Each of the drugs showed a distinct profile of cholesterol metabolite accumulation (Figure 90). These data support the RNA Seq results (Appendices 2 – 8), by confirming deranged cholesterol metabolism and accumulation of metabolites within the cells.

The cells treated with a combination of tamoxifen and 4-OHTam showed a similar cholesterol metabolite profile to those treated with 4-OHTam alone (Figure 90). The variation in cholesterol precursor accumulation between drug treatments can potentially be attributed to different combinations of cholesterol enzymes inhibited by the different drugs (Figure 90/Appendix 9 – Diagram of the cholesterol metabolism pathway). It is important to note that this experiment was only carried out once and thus slight variations in fibroblast cholesterol metabolite content between drug treatments may not be significant.

These data suggest that there may be dual inhibition of both D8D71/EBP and DHCR24 by tamoxifen leading to the accumulation of zymosterol and zymostenol (Figure 90/Appendix 9). These data are entirely in keeping with the findings of the Poirot group who reported accumulation of zymostenol in cells treated with tamoxifen [295], which subsequently led to the generation of antitumourigenic cholesterol epoxides (oxysterols) via autoxidation by ROS [295]. It is, however, important to note that these observations were in tumour cells and there is currently no evidence to suggest a similar effect in fibroblasts. Furthermore, the presence of cholesterol epoxides was not

examined in the mass spectrometry analysis, therefore the accumulation of these proposed anti-tumourigenic molecules cannot be confirmed.

Interestingly, 4-OHTam treatment shows accumulation of zymosterol and no accumulation of zymostenol (Figure 90). This suggests that perhaps 4-OHTam is a slightly less potent inhibitor of D8D71/EBP than tamoxifen. This would be in keeping with observations from the Poirot group that 4-OHTam is a marginally less potent inhibitor of the AEBS/ChEH than tamoxifen [345]. 4-OHTam induces a greater accumulation of zymosterol than tamoxifen (280 vs 200 ng/10^6 cells approximately), suggesting 4-OHTam may be a more potent inhibitor of DHCR24 activity than tamoxifen. These data are also in keeping with data from the Poirot group suggesting 4-OHTam potently inhibits DHCR24 [293].

D8D71/EBP is the second component of the AEBS/ChEH (Figure 76) alongside DHCR7 – one of the top differentially expressed genes in the RNA Seq analysis. This potentially suggests that the up-regulated expression of DHCR7 may also be as a consequence of the inhibition of functional enzyme activity of its counterpart component in the AEBS. However, D8D71/EBP also functions as an enzyme alone, thus the findings may simply reflect a global effect on the cholesterol metabolism pathway.

DHCR24 was another top differentially expressed gene from the RNA Seq analysis (Appendix 4), thus the mass spectrometry data showing accumulation of cholesterol precursors specifically regulated by the DHCR24 enzyme potentially suggests that up-regulated DHCR7/24 expression could be related to inhibition of enzyme activity. Further work is needed to clarify the relationship between gene expression and enzyme activity.

The accumulation of different cholesterol precursors in the cells treated with tamoxifen and 4-OHTam is also intriguing, as it is possible that this may contribute to the variation

in clinical response to tamoxifen in the preventive setting. Data from Cuzick et al showed only approximately half of the high risk women who took tamoxifen significantly reduced their MD by ≥10% [110]. Cytochrome p450 enzymes regulate tamoxifen metabolism [271]. Thus, those individuals who extensively metabolise tamoxifen, and generate more 4-OHTam, may accumulate different cholesterol precursors. It is also possible that here may be variation in the autoxidation of the different precursors to form antitumourigenic cholesterol epoxides, and thus variation in modulation of LXR signalling and cell-differentiating capability. Future work to investigate cholesterol epoxide levels in the breast tissue of women treated with tamoxifen, and correlation with imaging and clinical outcome, is required to substantiate this hypothesis.

The difference between the cholesterol metabolites accumulating in the tesmilifene treated fibroblasts and the SERMs parallels the differences seen in proliferation and gene expression (Figure 80, Figure 81 + Figure 83). As previously discussed, these differences suggest that the effects of SERMs on fibroblast function may not be due to inhibition of ChEH activity, but potentially one of the other pathways identified in the RNA Seq analysis (Appendices 5 - 8). However, it also possible that the weaker ability of tesmilifene to inhibit ChEH activity and interacting effects from the other pathways modulated by SERMs could account for these differences. Future work to determine the clinical significance of the various pathways modulated by SERMs is required.

Fulvestrant treatment resulted in minimal variations in cholesterol metabolite levels (Figure 90) and future work is required to determine if these differences are significant. However, significant differential expression of cholesterol metabolite genes was not identified in the RNA Seq analysis with fulvestrant treatment (Figure 65 + Figure 71).

Overall these data suggest that SERMs have a profound effect on fibroblast function, including deregulation of cholesterol metabolism, resulting in the accumulation of cholesterol precursors and lipid droplets. The lack of cholesterol and lipid accumulation in cells treated with fulvestrant, suggests that these effects could potentially be

independent of the ER. In addition, there are a number of significant differences in the effect of the SERMs compared to the AEBS-ligand tesmilifene. Thus, it is not clear whether the observed effects can be attributed to inhibition of ChEH activity and fibroblast ‘differentiation’, or to one or more of the other pathways revealed in the RNA Seq analysis. Future work is therefore required to dissect which of these pathways is responsible for mediating the anti-tumourigenic and density-lowering effects of tamoxifen treatment.

8 Effect of 4-OHTam treated fibroblasts on epithelial cell behaviour

8.1 Introduction

In this study, 4-OHTam treatment of primary breast fibroblasts resulted in a variety of effects on fibroblast function including; reduced proliferation, ECM protein expression and response to the pro-fibrogenic cytokine TGF-β with inhibition of non-canonical signalling through ERK1/2. Functionally, 4-OHTam treated fibroblasts showed reduced ability to contract collagen gels and showed less migration following TGF-β stimulation.

RNA Seq analysis highlighted numerous pathways mediated by 4-OHTam, including a possible ER-independent mechanism by which 4-OHTam may modulate cholesterol metabolism and potentially promote fibroblast differentiation.

In order to evaluate the tumour inhibitory phenotype of 4-OHTam treated fibroblasts, epithelial cell lines were co-cultured with pre-treated fibroblasts in 3D collagen gels. The effect on epithelial colony size and proliferation were assessed. In addition, effect of conditioned media and FDM from 4-OHTam treated fibroblasts on epithelial cell proliferation was also assessed.

8.2 Methods and Materials

8.2.1 Cell Lines

The normal epithelial cell line HB2 and HB2 cells overexpressing Her2 protein were used as models of normal and pre-malignant epithelium for these experiments. The ER positive cell line MCF7 was used as a model of low grade ER positive breast cancer.

8.2.2 Fibroblast pre-treatment prior to 3D co-culture

Fibroblasts from patient 2585 were seeded into T175 flasks and grown until 70% confluent. The cells were hormone deprived for 24 hours then treated with vehicle control or 4-OHTam (5μM) for 48 hours. The cells were then removed from the flask using trypsin and counted using a haemocytometer prior to seeding into the collagen gels with epithelial cells.

8.2.3 Co-culture conditions

The following combinations of cells were used in the co-culture experiments:

(i) Normal HB2 cells alone

(ii) Normal HB2 cells and vehicle control pre-treated fibroblasts

(iii) Normal HB2 cells and 4-OHTam pre-treated fibroblasts

(iv) Her2 over expressing HB2 cells alone

(v) Her2 over expressing HB2 cells and vehicle control pre-treated fibroblasts

(vi) Her2 over expressing HB2 cells and 4-OHTam pre-treated fibroblasts

(vii) MCF7 cells alone

(viii) MCF7 cells and vehicle control pre-reated fibroblasts

(ix) MCF7 cells and 4-OHTam pre-treated fibroblasts

In all conditions, cells were seeded into the collagen gels at a density of approximately 350,000 cells per gel.

8.2.4 Collagen gel preparation

Gels were prepared at two densities – 1mg/ml and 3mg/ml. For three gels, a 1ml gel mixture was prepared on ice as follows:

Gel component	1mg/ml Collagen Gel	3mg/ml Collagen Gel
Rat Tail Collagen (10mg/ml, Corning, 35429)	200	600
1M HEPES (Sigma, H3375)	25	25
1M sodium hydroxide (NaOH, Sigma, S8045)	20	20
Phenol red free DMEM F12 +5% DCSS	775	375

Table 16: Collagen gel components

The 1ml gel mixture was combined with 1ml of media containing the relevant cells for the particular co-culture condition, to give a total volume of 2ml. 600µl was plated in triplicate format in the 24 well plates.

The gels were left to set at 37^{o}C for half an hour then 500µl phenol red free DMEM F12 and 5% DCSS was added on top each gel. The co-cultures were left for 5 days at 37^{o}C with media changed on day 3.

Following 5 days of co-culture, the media was removed and 1.5ml 10% neutral buffered formalin was added to each well to fix the gels. After one hour, the media was changed to sterile PBS. The gels were then carefully removed from the edge of the wells, processed and paraffin embedded for subsequent analysis.

8.2.5 Analysis of Proliferation and colony size

Cell proliferation was determined using Ki67 immunohistochemistry, as described below. Colony size was assessed by counting the mean number of cells present in each epithelial colony per H+E stained section.

8.2.6 Ki67 immunohistochemistry

8.2.6.1 Dewaxing, rehydration of sections and antigen retrieval

Unstained paraffin sections were dewaxed by warming the slides to 60^{o}C in an incubator for 10 minutes and then placing them in xylene (Fisher Scientific, X/0250/17) for 10 minutes with periodic agitation. The sections were re-hydrated through a series of graded alcohol solutions and placed in 3% hydrogen peroxide solution (Fisher Scientific, H/1750/15) for 10 minutes to block endogenous peroxidase activity. Antigen retrieval was performed by boiling the sections in citrate buffer (2.94g trisodium citrate (Sigma, S1084) in 1l dH_2O) pH 6.0 for 5 minutes twice in succession.

8.2.6.2 Blocking, antibody incubation and developing

After washing in PBS, the sections were covered in 3% BSA/5% NHS in PBS for 15 minutes at room temperature to block non-specific antibody binding. Cells were then incubated overnight at 4^{o}C with Ki67 primary antibody (Dako, M7240) diluted 1:100 in 3% BSA/5%NHS in PBS. Cells were then washed three times in PBS, incubated with biotinylated secondary anti-mouse secondary antibody (Vector Laboratories, 1:200 in 1% BSA/PBS) for 40 minutes at RT, washed in PBS a further three times before incubating with avidin-biotinylated peroxidase complex (Vectastain ABC kit, Vector Laboratories, PK 6101, 6102) for 30 minutes at RT. Cells were washed with PBS three more times before developing using a DAB kit (Vectastain, Vector Laboratories, SK 4100). Cells were then washed twice with PBS and counterstained with Haematoxylin for 2 minutes, rinsed in tap water and then dehydrated through the graded alcohol series before placing in xylene for 10 minutes. Coverslips were mounted with DPX (Sigma, 06522) mounting medium.

8.2.6.3 Quantification

10 random fields were examined at x10 objective and the number of positive cells were counted and expressed as a percentage of the total number of cells present per field.

8.2.7 Preparation of fibroblast conditioned media (FCM)

Primary fibroblasts from two patients (1923, 1989) were seeded in T175 flasks and grown to 70% confluence, hormone deprived for 24 hours and then treated with vehicle control, 5μM tamoxifen, 5μM 4-OHTam, 10μM tesmilifene or 5μM fulvestrant for 48 hours. The cells were then trypsinised off the flask and reseeded into 10cm dishes at a density of 0.8 $x10^6$ cells per flask along with 5ml serum and phenol-red free media. The cells were left to condition the media for 48 hours. The media was then harvested and centrifuged at 1500 rpm for 3 minutes to remove any dead cells and the supernatant frozen immediately at -20^oC.

8.2.8 Conditioned media proliferation assay

Epithelial cells (normal HB2, HB2 overexpressing Her2 and MCF7) were seeded in triplicate in 24 well plates at a density of $4x10^4$ cells per well, allowed to adhere to the plastic for 3 hours then serum starved overnight with phenol red free media. Triplicate wells were then treated with 0.5ml of either serum free media, FCM from vehicle control, tamoxifen, 4-OHTam, tesmilifene or fulvestrant treated fibroblasts. Proliferation was measured using the Alamar Blue assay immediately prior to treatment with FCM (time 0) and after 48 hours treatment. Absorbance values were normalised to time 0.

8.2.9 FDM proliferation assay

FDM were generated from patient 2182 in the presence of either vehicle control or 4-OHTam as described previously (section 5.2.3) in triplicate wells of a 12 well plate. Primary fibroblasts from patient 2182 (2 $x10^4$ cells per well) and MCF7 cells (5 $x10^4$ cells per well) were then seeded onto the FDM and into triplicate empty wells onto

plastic. Proliferation was measured using the Alamar Blue assay with measurements taken at time 0, 24 hours, 48 hours and 72 hours. Values were normalised to the time 0 empty well measurement.

8.3 Results

8.3.1 Fibroblast-epithelial cell 3D co-culture assays

The lower density collagen gels (1mg/ml) contracted substantially during culture, hindering assessment of colony size and proliferation. Thus these gels were not analysed further.

8.3.1.1 Comparison of epithelial cell line models

Her2 protein levels were assessed in the two HB2 cell lines to confirm overexpression of Her2 in the 'Her2 overexpressing' HB2 cell line (Figure 92).

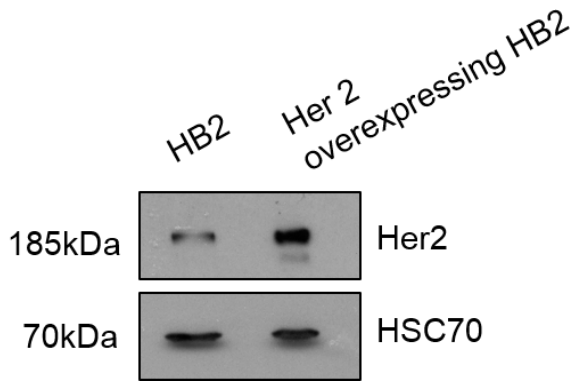

Figure 92: Western blot image confirming overexpressing of Her2 protein in the Her2 overexpressing HB2 cell line compared to the normal HB2 cells.

Each epithelial cell line was cultured alone in the collagen gels and assessed for colony size and proliferation. The normal HB2 cells formed large cohesive colonies with very few single cells. HB2 cells overexpressing Her2 formed cohesive colonies with scattered single cells (Figure 93). The colonies formed by the normal HB2 cells were significantly larger than the HB2 cells overexpressing Her2 ($p<0.0001$). The MCF7 cells formed a mixture of small cohesive colonies and numerous scattered single cells. The MC7 cell colonies were smaller than the normal HB2 and HB2 cells overexpressing Her2 (Figure 93).

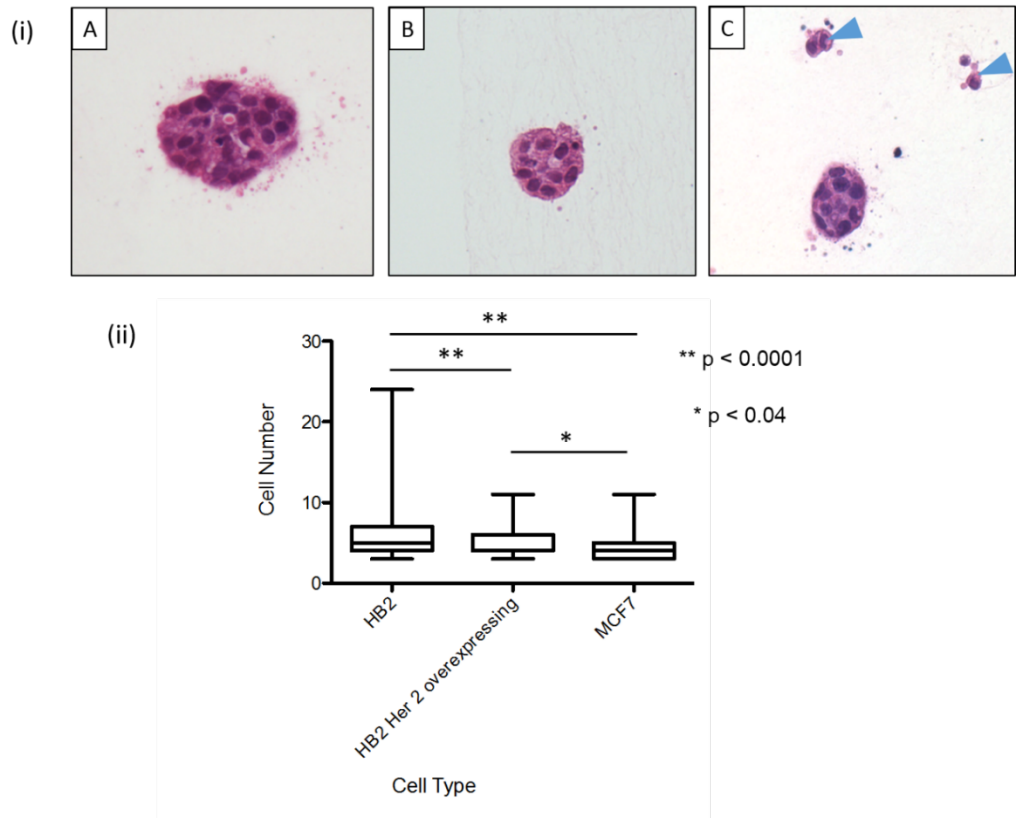

Figure 93: Epithelial cell line colony size in 3D collagen gels. (i) Representative H+E stained colony images (x20 objective). (A) Normal HB2 cells form large cohesive groups with very few single cells (B) HB2 cells overexpressing Her2 form cohesive groups with scattered single cells (C) MCF7 cells form small cohesive groups and numerous single cells (blue arrows). (ii) Graph quantifying mean colony size per cell line. Normal HB2 cell colonies are significantly larger ($p<0.0001$) than the Her2 overexpressing HB2 cells and MCF7 cells.

The normal HB2 and Her2 overexpressing HB2 cell lines showed similar levels of proliferation, assessed by Ki67 staining. MCF7 cells showed slightly higher proliferation levels than both the HB2 cell lines (Figure 94).

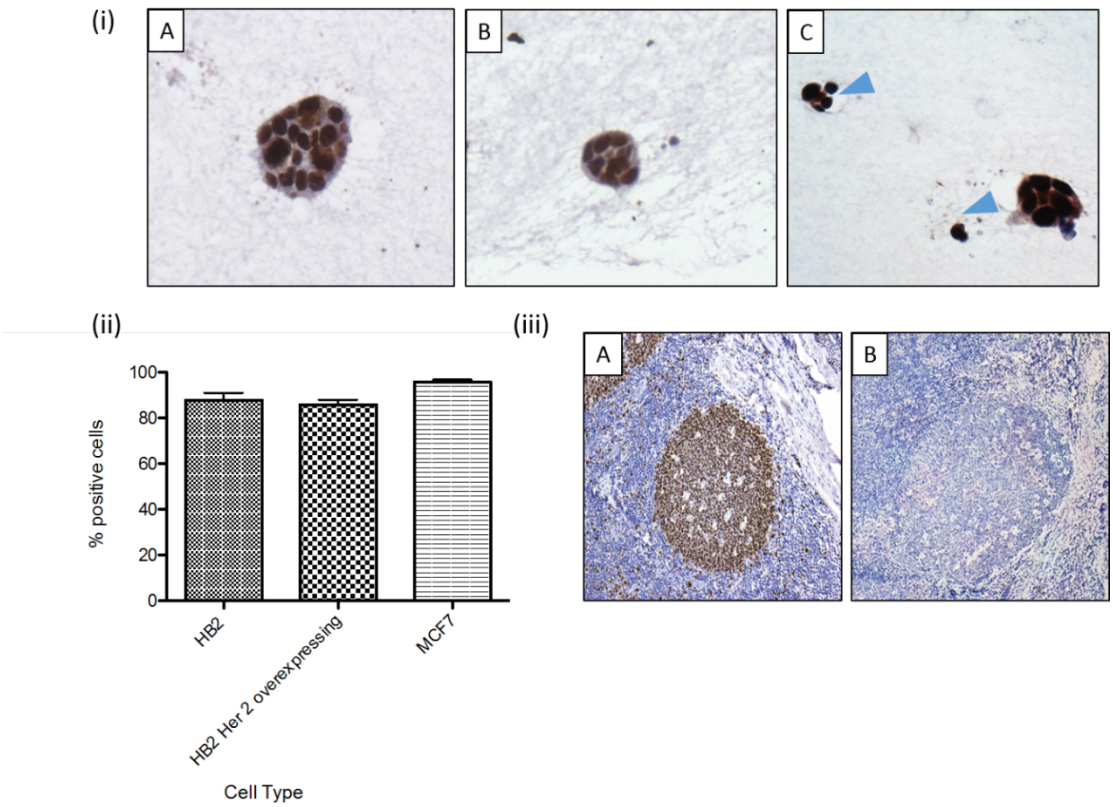

Figure 94: Proliferation of epithelial cell lines in collagen gels assessed by Ki67 immunohistochemistry. (i) Representative images of colonies showing positive staining for Ki67 (x20 objective).(A) Normal HB2 cells, (B) Her2 overexpressing HB2 cells, (C) MCF7 cells (blue arrows = single cells). (ii) Graph quantifying % Ki67 positive cells per epithelial cell line. (iii) (A) Tonsillar lymphoid tissue, x10 objective (Ki67 positive control) (B) Tonsillar lymphoid tissue, x10 objective (negative control – mouse immunoglobulin)

8.3.1.2 Co-culture of epithelial cell lines and pre-treated fibroblasts

Both the normal HB2 cells and the Her 2 overexpressing HB2 cells formed significantly smaller epithelial colonies when cultured with 4-OHTam pre-treated fibroblasts compared to those cultured with fibroblasts pre-treated with vehicle control ($p<0.0001$, (Figure 95 + Figure 96). No increase in the number of single cells was noted.

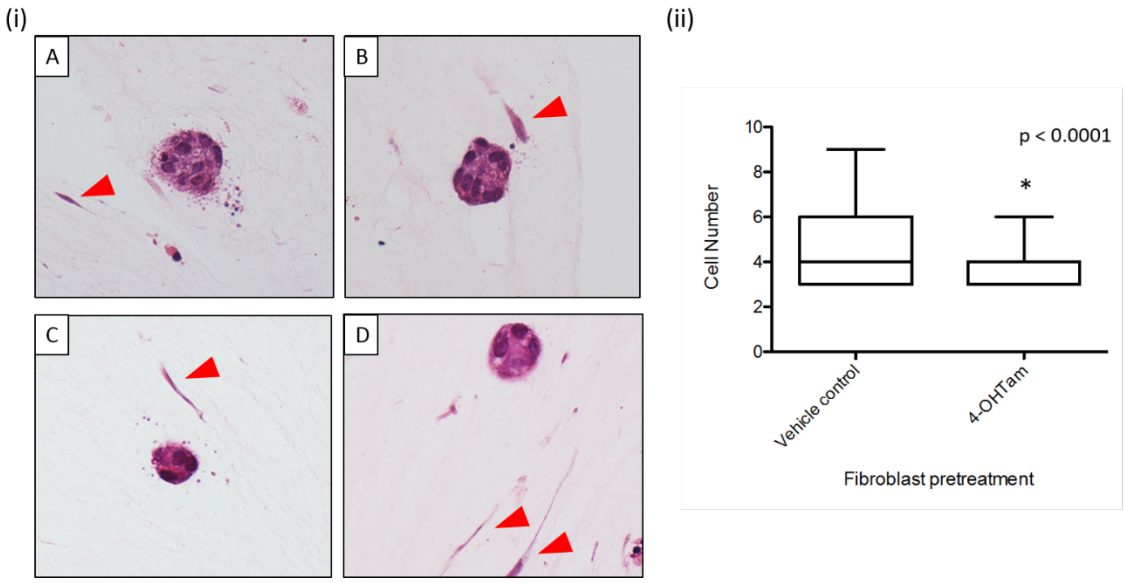

Figure 95: Effect of co-culture of normal HB2 cells with control and 4-OHTam pre-treated fibroblasts on epithelial colony size (i) Representative H+E stained images of epithelial colonies and fibroblasts (red arrows). A+B – Normal HB2 cells and vehicle control pre-treated fibroblasts, C+D – Normal HB2 cells and 4-OHTam pre-treated fibroblasts (x20 objective). (ii) Graph quantifying mean epithelial colony size. Co-culture with 4-OHTam pre-treated fibroblasts resulted in significantly smaller epithelial colony size ($p<0.0001$).

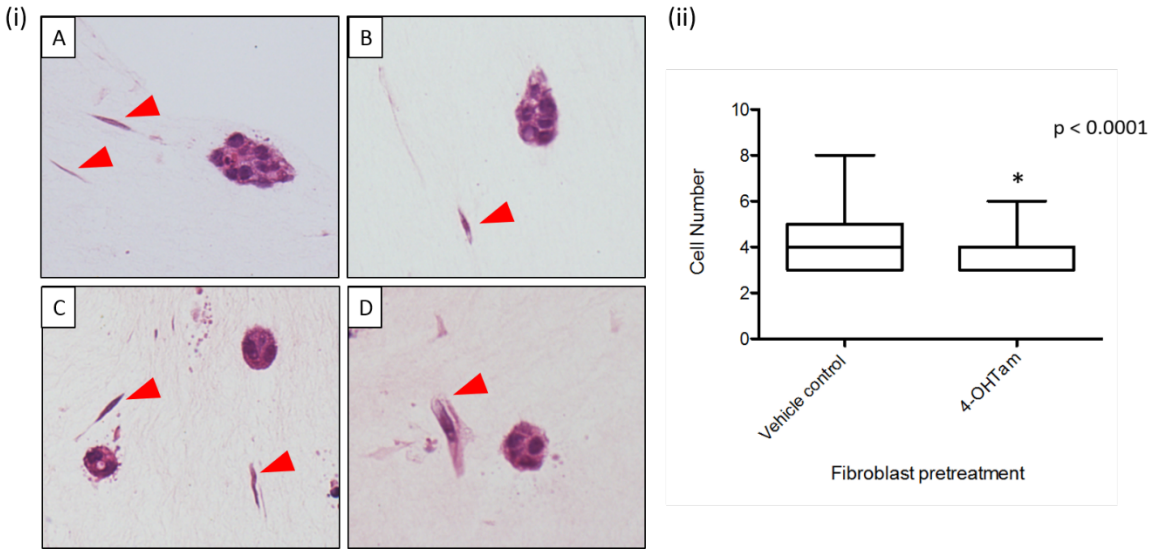

Figure 96: Effect of co-culture of Her 2 overexpressing HB2 cells with control and 4-OHTam pre-treated fibroblasts on epithelial colony size. (i) Representative H+E stained images of epithelial colonies and fibroblasts (red arrows). A+B – Her2 overexpressing HB2 cells and vehicle control pre-treated fibroblasts, C+D – Her2 overexpressing HB2 cells and 4-OHTam pre-treated fibroblasts (x20 objective). (ii) Graph quantifying mean epithelial colony size. Co-culture with 4-OHTam pre-treated fibroblasts resulted in significantly smaller epithelial colony size ($p<0.0001$).

No significant difference in MCF7 cell colony size was observed when cultured with either vehicle control or 4-OHTam pre-treated fibroblasts (Figure 97). Numerous single cells were present in both conditions.

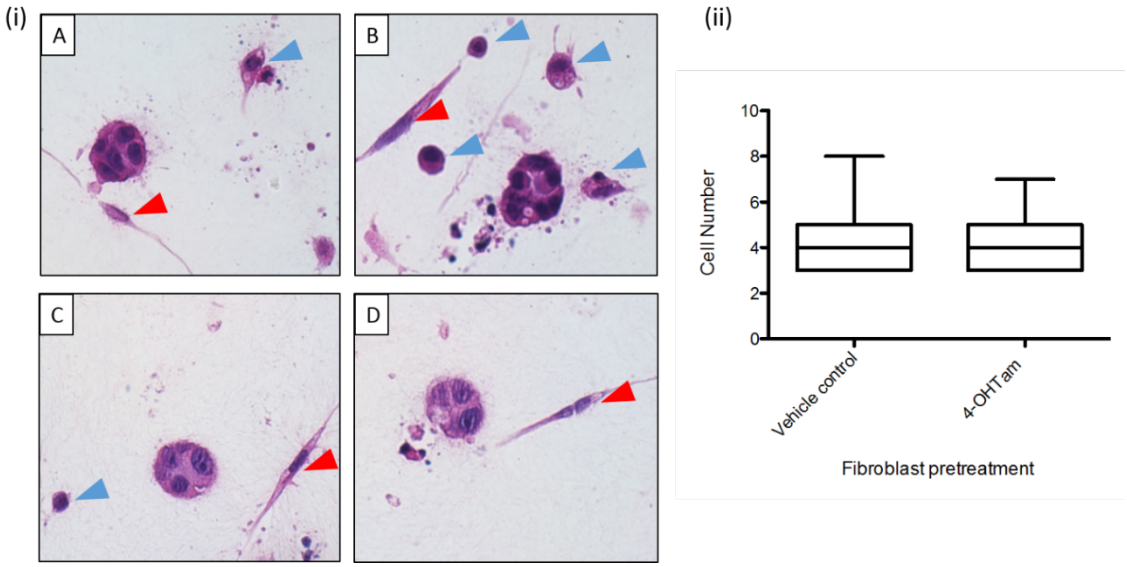

Figure 97: Effect of co-culture of MCF7 cells with control and 4-OHTam pre-treated fibroblasts on epithelial cell colony size. (i) Representative H+E stained images of epithelial colonies and fibroblasts (red arrows) with numerous single cells (blue arrows). A+B – MCF7 cells and vehicle control pre-treated fibroblasts, C+D – MCF7 cells and 4-OHTam pre-treated fibroblasts (x20 objective). (ii) Graph quantifying mean epithelial colony size. Co-culture with 4-OHTam pre-treated fibroblasts had no significant effect on epithelial colony size (p=0.1462).

No difference in the proliferation of normal HB2, Her2 overexpressing HB2 or MCF7 cells was observed between those cultured with fibroblasts pre-treated with vehicle control or 4-OHTam (Figure 98 - Figure 100).

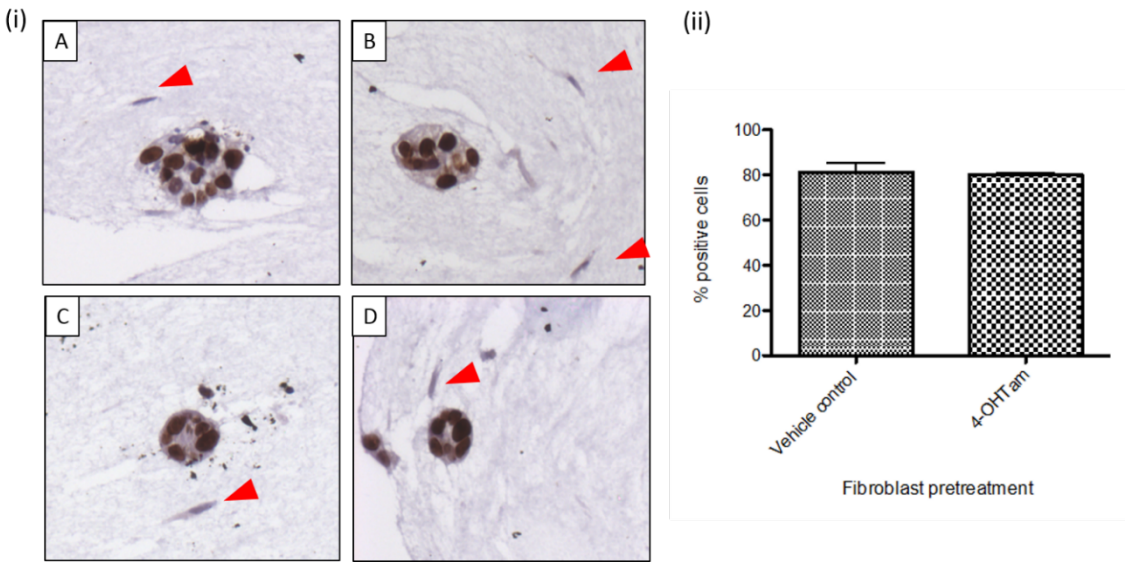

Figure 98: Effect of co-culture of normal HB2 cells with vehicle control and 4-OHTam pre-treated fibroblasts on epithelial cell proliferation (Ki67 immunohistochemistry). (i) Representative Ki67 stained images of epithelial colonies and fibroblasts (red arrows). A+B – Normal HB2 cells and vehicle control pre-treated fibroblasts, C+D – Normal HB2 cells and 4-OHTam pre-treated fibroblasts (x20 objective). (ii) Graph quantifying mean % Ki67 positive cells. No difference in epithelial cell proliferation was seen between fibroblast pre-treatment conditions.

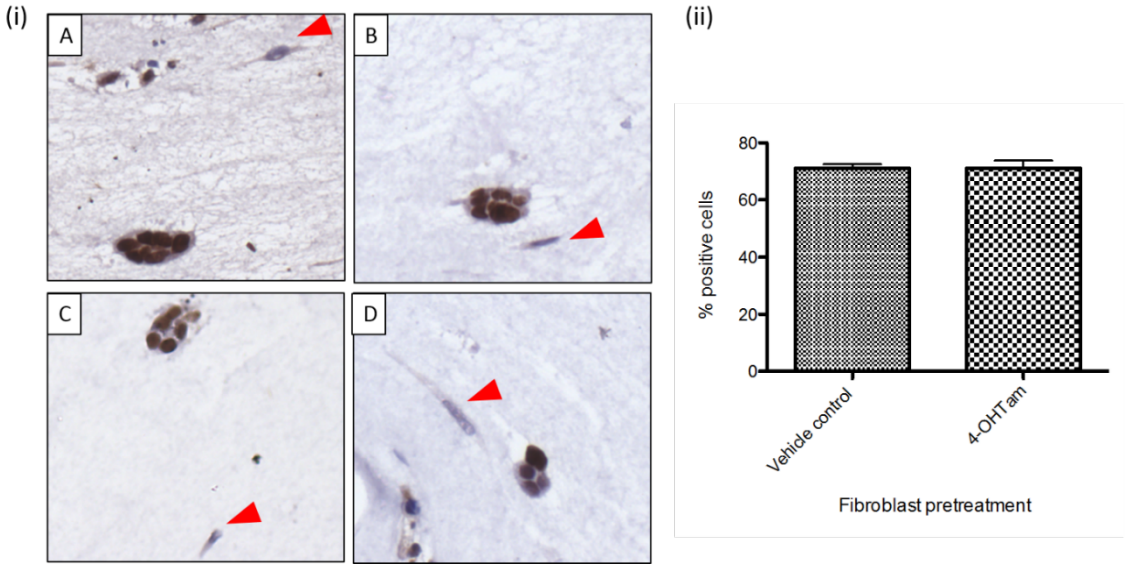

Figure 99: Effect of co-culture of Her2 overexpressing HB2 cells with vehicle control and 4-OHTam pre-treated fibroblasts on epithelial cell proliferation (Ki67 immunohistochemistry). (i) Representative Ki67 stained images of epithelial colonies and fibroblasts (red arrows). A+B – Her2 overexpressing HB2 cells and vehicle control pre-treated fibroblasts, C+D – Her2 overexpressing HB2 cells and 4-OHTam pre-treated fibroblasts (x20 objective). (ii) Graph quantifying mean % Ki67 positive cells. No difference in epithelial cell proliferation was seen between fibroblast pre-treatment conditions.

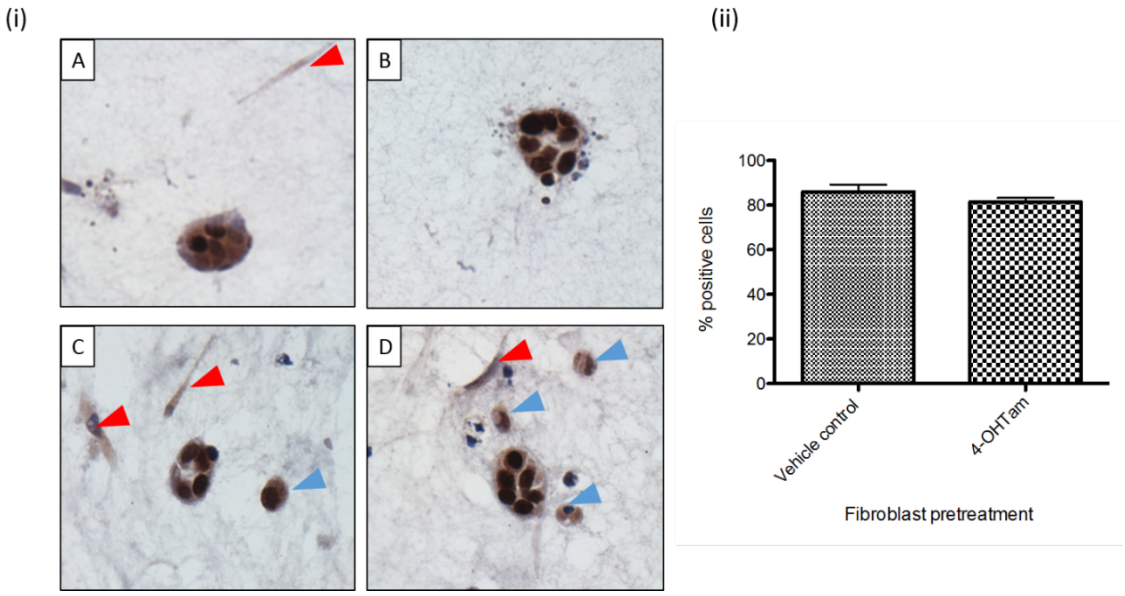

Figure 100: Effect of co-culture of MCF7 cells with vehicle control and 4-OHTam pre-treated fibroblasts on epithelial cell proliferation (Ki67 immunohistochemistry). (i) Representative Ki67 stained images of epithelial colonies and fibroblasts (red arrows) with numerous single cells (blue arrows). A+B – MCF7 cells and vehicle control pre-treated fibroblasts, C+D – MCF7 cells and 4-OHTam pre-treated fibroblasts (x20 objective). (ii) Graph quantifying mean % Ki67 positive cells. No difference in epithelial cell proliferation was seen between fibroblast pre-treatment conditions.

8.3.2 Effect of fibroblast conditioned media on epithelial cell proliferation

The normal HB2 cells did not survive 48 hours culture in FCM or serum free media. Treatment with FCM increased proliferation of both the Her2 overexpressing HB2 cells and MCF7 cells compared to treatment with serum and phenol red free media alone (negative control). No significant difference in proliferation of either epithelial cell line was observed between the different conditioned media fibroblast pre-treatment conditions (Figure 101).

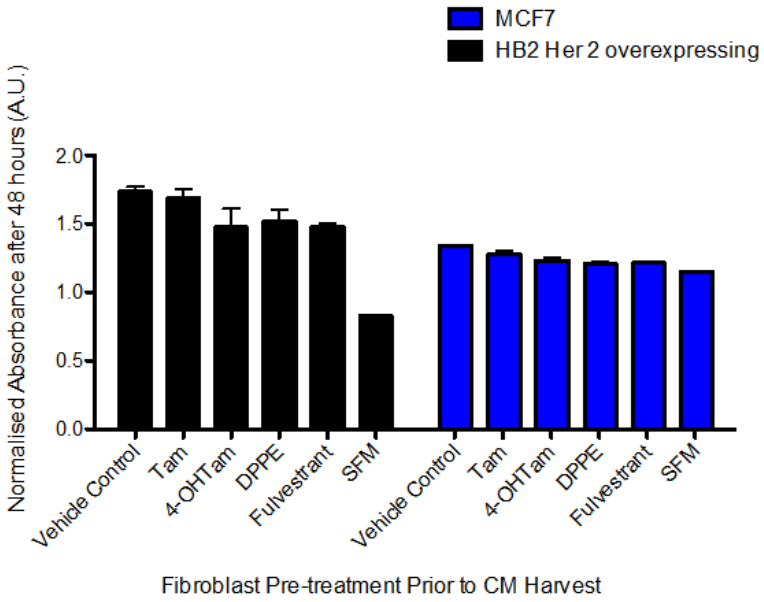

Figure 101: Effect of 48 hours treatment with FCM on the proliferation of Her2 overexpressing HB2 cells and MCF7 cells. Treatment with FCM increased epithelial cell proliferation compared to serum and phenol red free media (SFM, negative control). No significant difference in proliferation of either epithelial cell line was observed between the conditioned media fibroblast pre-treatment conditions. Example of FCM from patient 1923.

8.3.3 Effect of FDM on fibroblast and epithelial cell proliferation

Primary fibroblasts (patient 2182) seeded onto FDM showed reduced proliferation compared to those seeded onto plastic (Figure 102). Fibroblasts seeded onto FDM generated in the presence of 4-OHTam showed less proliferation than those seeded onto FDM generated in the presence of vehicle control (Figure 102).

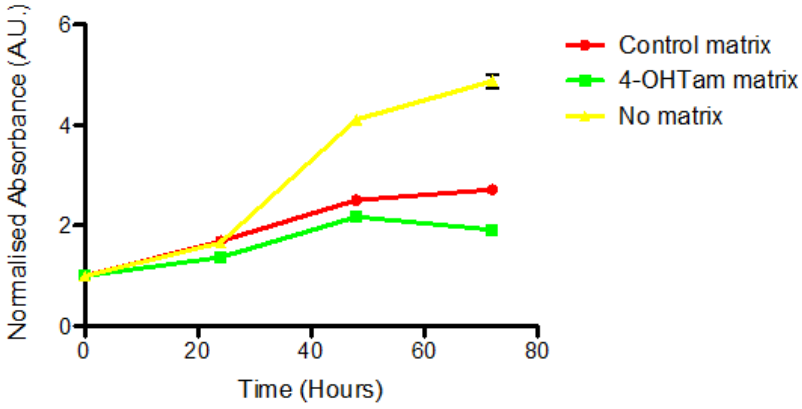

Figure 102: Effect of FDM on primary fibroblast (patient 2182) proliferation. Fibroblasts seeded onto FDM showed reduced proliferation compared to those seeded onto plastic. Fibroblasts seeded onto 4-OHTam FDM showed less proliferation than those seeded onto control FDM.

MCF7 cells seeded onto FDM showed reduced proliferation compared to those seeded onto plastic (Figure 103). There was no difference in proliferation between cells seeded onto FDM generated in the presence of either vehicle control or 4-OHTam.

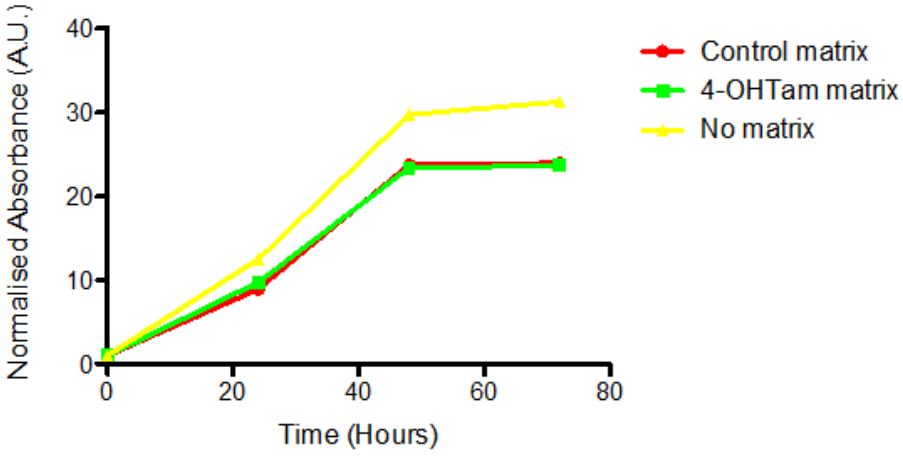

Figure 103: Effect of FDM on MCF7 cell proliferation. Cells seeded onto FDM showed reduced proliferation compared to those seeded onto plastic. There was no difference in proliferation between cells seeded on control or 4-OHTam FDM.

8.4 Discussion

8.4.1 Epithelial cell lines

Cell lines representing a spectrum of epithelial abnormality - normal (normal HB2), premalignant (Her2 overexpressing HB2) and low grade malignant (MCF7) were selected in order to detect subtle changes in behaviour following fibroblast co-culture, that may not be demonstrable if using only aggressive cancer cell lines.

The normal HB2 cells behaved in a benign manner when cultured in collagen alone, forming large cohesive colonies with very few single cells (Figure 93). The Her2 overexpressing cells showed smaller cohesive groups and scattered single cells. Whereas the MCF7 cells showed the most aggressive behaviour with only very small cohesive colonies and numerous single cells (Figure 93). It is not clear whether these individual cells represent tumour infiltration of the stroma or simply no growth of poorly cohesive individual cells.

The premalignant (Her2 overexpressing HB2) cell line showed no significant difference in proliferation than the normal HB2 cells (Figure 94). This highlights the disadvantages of using immortalised cell lines to represent normal epithelial cell behaviour, as normal epithelial cells would not demonstrate such high proliferative activity. Future work could use primary luminal epithelial cells as an alternative.

8.4.2 Fibroblast pre-treatment

8.4.2.1 Co-culture assay

Primary fibroblasts were pre-treated with vehicle control and 4-OHTam prior to adding to the collagen co-culture gels, and no drugs were present in the culture media for the gels. This ensured that the epithelial cell lines were not directly exposed to any of the drugs, therefore, any effect on epithelial cell behaviour could not be attributed to a direct effect of drug treatment.

Without additional drug dosing after the initial pre-treatment, the co-culture time was limited to 5 days, after which is was assumed that the effect of the drug pre-treatment on the fibroblasts would have worn off. This assumption was based on the reversibility of the 4-OHTam treated fibroblast phenotype observed when the drug was removed from the culture media (Section 4.3.8). After 5 days of treatment with control media, the fibroblasts had lost most of the perinuclear cytoplasmic vesicles which accumulated following 4-OHTam treatment (Figure 35).

8.4.2.2 Conditioned media assay

Primary fibroblasts were pre-treated with tamoxifen, 4-OHTam, tesmilifene and fulvestrant for 2 days prior to reseeding into a 10cm dish (0.8 x 10^6 cells/dish). The cells were allowed to adhere to the plastic, then washed with PBS twice before changing the media to serum free media to begin harvesting conditioned media. This was performed in order to ensure no drugs would be present in the conditioned media that may directly affect epithelial cell proliferation, and to ensure the same number of fibroblasts were present in each dish. 4-OHTam and tamoxifen were both observed to have negative effects on fibroblast proliferation (Figure 83), thus reseeding the pre-treated cells immediately prior to harvesting CM at a defined cell number ensured this effect on proliferation was accounted for.

8.4.3 Co-culture of fibroblasts and epithelial cells

Both the normal HB2 and Her2 overexpressing HB2 cells formed smaller colonies when co-cultured with 4-OHTam treated fibroblasts with no increase in number of single cells, suggesting that 4-OHTam treated fibroblasts may be less supportive of epithelial cell growth and proliferation (Figure 95 + Figure 96). These findings are consistent with data from Hattar and colleagues who found that cancer cell lines co-injected into mouse mammary fat pads with tamoxifen treated ECM formed smaller tumours than those co-injected with untreated ECM [115].

Despite these effects on colony size, no difference was seen in the proliferative activity of the colonies co-cultured with vehicle control or 4-OHTam pre-treated fibroblasts (Figure 98 + Figure 99). This may be due to the intrinsic proliferative activity of the cell lines used.

No difference in colony size or proliferative activity was seen with MCF7 cells (Figure 97 + Figure 100). Thus, 4-OHTam pre-treated fibroblasts may only be able to exert effects on epithelial cell behaviour at earlier stages of tumourigenesis.

The 3D co-culture model used in this study has several weaknesses. Firstly, no myoepithelial cells are present. These unique components on the breast microenvironment have been proposed to exert both tumour suppressor and tumour promoting behaviour and also synthesise basement membrane to form a physical barrier between the epithelial cells and fibroblasts [369, 370]. Thus the potential influence of the myoepithelial cells and basement membrane on epithelial-stromal crosstalk is not accounted for. In addition, many other cells present in the breast microenvironment, which may influence epithelial-stromal crosstalk, such as inflammatory cells and blood vessels, are also lacking. Furthermore, the collagen ECM that formed the 3D environment was present at a uniform density and stiffness. This is unlikely to be representative of the dynamic changes in ECM stiffness and orientation that occur during tumourigenesis. The co-culture time was also limited at only 5 days, therefore subtle changes in epithelial behaviour as a result of fibroblast-epithelial cell crosstalk may not have time to manifest within this period.

8.4.4 Effect of conditioned media on epithelial cell proliferation

Despite FCM increasing the proliferation of both the Her2 overexpressing HB2 cells and MCF7 cells compared to treatment with serum free media alone, no difference in proliferation was seen between cells treated with conditioned media from different fibroblast pre-treatment conditions (Figure 101). This lack of difference may be due to

the intrinsic proliferative activity of these cell lines. In addition, the presence of a 3D environment with multiple cell types present may be required in order to appreciate the effect of tamoxifen treated fibroblasts on epithelial cell behaviour. The assay was also only run for 48 hours which may not have sufficient time for subtle differences in proliferation between the pre-treatment conditions to be evident.

8.4.5 Effect of FDM on epithelial cell proliferation

Both fibroblasts and MCF7 cells seeded onto FDM showed less proliferation than those seeded onto plastic (Figure 102 + Figure 103). This may be due to the cells having unrestricted space to grow in the empty wells compared to the wells filled with matrix fibres. No difference in MCF7 proliferation was evident between the cells seeded on vehicle control or 4-OHTam FDM (Figure 103). These observations are consistent with the lack of difference in FDM thickness seen between the matrices generated under the different conditions – suggesting a similar ability to modulate cell behaviour. Therefore it is somewhat surprising that fibroblasts seeded onto 4-OHTam FDM show reduced proliferation compared to those seeded onto control FDM (Figure 102). However, this difference may also indicate the increased sensitivity of primary cells compared to immortalised cell lines. Thus more subtle effects of FDM on cell behaviour may be better appreciated using primary cells.

9 Final Conclusions and Future Work

The aims of this study were to:

(i) To use in-vitro models of primary human breast fibroblasts to dissect the effect of tamoxifen on stromal cell function.

(ii) To use RNA Seq to carry out a whole transcriptome analysis of the effect of tamoxifen on fibroblast gene expression.

(iii) Investigation of selected pathways modulated by tamoxifen and the role of the ER in these pathways.

(iv) To explore the impact of tamoxifen-modified fibroblasts on epithelial cell behaviour

9.1 Dissecting the effect of tamoxifen on primary breast fibroblast function

4-OHTam, the active metabolite of tamoxifen, was observed to have a profound effect on primary breast fibroblast function, acting via multiple, diverse pathways.

A direct effect of 4-OHTam on fibroblast function was initially noted after observing a consistent, dose dependent, negative effect on proliferation. In addition, 4-OHTam modulated the expression of stromal markers fibronectin and collagen I in a proportion of patients' cells. These findings were in keeping with data from animal models suggesting that tamoxifen may modify expression of stromal proteins [115, 314].

Furthermore, 4-OHTam treatment resulted in a striking, consistent reduction in expression of the key fibroblast activation marker SMA, and was able to inhibit fibroblast activation following stimulation with TGF-β. Further investigation revealed that this effect was not via inhibition of canonical SMAD signalling, instead non-canonical signalling through ERK1/2 was affected. Functionally, 4-OHTam treatment

resulted in the fibroblasts being less contractile and less migratory following TGF-β stimulation.

These observations are consistent with the anti-fibrotic effects of tamoxifen reported in the literature [313] and observations that tamoxifen treated stroma has a more quiescent phenotype [115, 313].

The differing responses of the primary fibroblasts to 4-OHTam and the pure ER antagonist fulvestrant suggest that the effects of 4-OHTam on fibroblast function may be due to ER-independent mechanisms.

RNA Seq differential gene expression and pathway analysis highlighted a plethora of pathways modulated by 4-OHTam which may contribute to the overall anti-tumour and density-lowering effects. These include a potential novel ER-independent pathway by which 4-OHTam affects fibroblast function - via modulation of cholesterol metabolism.

Significant differential expression of the cholesterol metabolite enzyme DHCR7 was consistently observed in two separate RNA Seq experiments. This enzyme is a component of the microsomal anti-oestrogen binding site (AEBS). Binding of tamoxifen, 4-OHTam and other SERMs to the AEBS has been proposed to be anti-tumourigenic [296, 347]. The proposed anti-tumour effects are mediated via inhibition of cholesterol epoxide hydrolase (ChEH) activity and accumulation of cholesterol precursors with potent cell differentiating capabilities. So far the evidence for the significance of this pathway has been limited to the work of a single laboratory and has yet to be widely replicated and validated by others. Furthermore, the effect of SERM inhibition of ChEH activity has only previously been investigated in tumour cells and there is no data regarding any effect in fibroblasts.

Nevertheless, the modulation of this pathway is an intriguing possibility and a proposed possible mechanism of action in the fibroblasts is displayed in Figure 104.

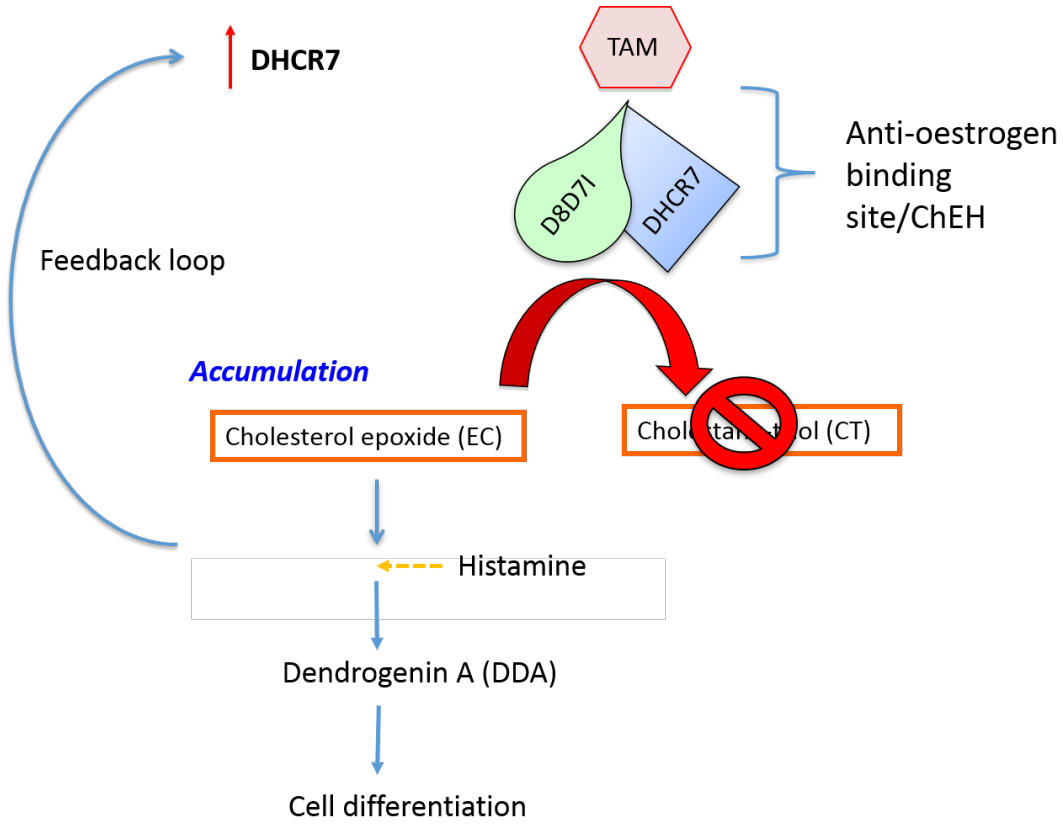

Figure 104: Summary of proposed possible ER-independent mechanism by which tamoxifen may bind to the AEBS and inhibit ChEH activity. This could result in the accumulation of anti-tumourigenic cholesterol metabolite precursors, including dendrogenin A (DDA), formed via metabolism with histamine, which may exert potent cell differentiating properties.

The inhibition of ChEH activity and accumulation of anti-tumourigenic precursors within fibroblasts could lead to the differentiation of activated fibroblasts to a more quiescent state, and potentially towards early adipogenic differentiation. Increased adipogenic differentiation of the mammary stroma could increase the fatty content of the breast and thus lower the overall mammographic density (Figure 105).

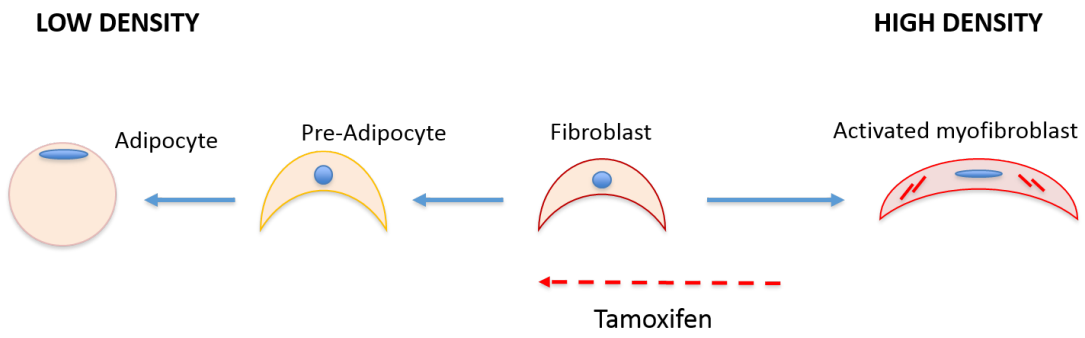

Figure 105: Possible mechanism by which tamoxifen could exert differentiating effects on fibroblasts to a more quiescent state, and possibly towards early adipogenic differentiation. Increased fatty tissue in the breast could lower the overall MD.

Despite this intriguing possible mechanism, there is limited to support that modulation of this pathway in fibroblasts could be responsible for the density-lowering and anti-tumour effects of tamoxifen.

Whilst fibroblast treatment with a commercially available inhibitor of ChEH, tesmilifene, resulted in some similar effects to those seen with SERMs, a significant number of differing effects were also seen. This suggests that other pathways modulated by tamoxifen may mediate the risk lowering effects of the drug. There are many down-regulated pathways identified in the RNA Seq analysis that could potentially modify the mammary stroma and contribute to a change in MD such as collagen formation, integrin cell surface interaction, ECM receptor interaction, Wnt and Hedgehog signalling. Future work to dissect which of these pathways are the most clinically significant is required.

Altered cholesterol metabolism and accumulation of precursors within the fibroblasts was identified with mass spectrometry, electron microscopy and filipin staining. Oil Red O staining and electron microscopy also identified accumulation of lipid droplets within the fibroblasts. Up-regulation of some early adipogenic markers was also observed in the RNA Seq analysis. The evidence in this study to support a 'differentiating' effect of 4-OHTam on fibroblasts is weak and future work is required to investigate this

hypothesis further. It is possible that SERM treatment simply induces accumulation of lipid and cholesterol metabolites within the fibroblasts without any effect on cell differentiation. Accumulation of lipids (steatosis) in liver hepatocytes is a recognised complication of tamoxifen treatment [371].

9.2 Impact of 4-OHTam treatment on fibroblast-epithelial crosstalk

Data from animal models suggest that tamoxifen treated stroma can exert tumour inhibitory effects [115]. The effect of 4-OHTam pre-treated fibroblasts on epithelial cell behaviour was investigated using 3D co-cultures, conditioned media and FDM. Co-culture with 4-OHTam pre-treated fibroblasts resulted in smaller epithelial colony sizes in normal and premalignant cells only and no significant effect on proliferation was noted. No significant effect of conditioned media from tamoxifen or 4-OHTam pre-treated fibroblasts or 4-OHTam FDM was observed.

The lack of conclusive findings in the co-culture experiments are most likely due to many key breast microenvironment components such as myoepithelial cells, immune cells and blood vessels not being present in the co-culture system. The breast microenvironment is heavily complex and epithelial-stromal crosstalk relies on interaction and coordination of multiple stromal cell types. It is likely that many autocrine and paracrine factors that control epithelial cell function are lacking in such a reductionist model.

In addition, dynamic changes in ECM stiffness and orientation could not be modelled in the co-culture system, thus the impact of tamoxifen on the biophysical properties of the mammary ECM and epithelial cell mechanotransduction could not be assessed. Furthermore, immortalised epithelial cell lines have unlimited proliferative and

replicative potential, and thus may not respond to subtle signals in the microenvironment as the normal mammary epithelial cells would.

Future work to dissect out the precise influence of tamoxifen treated stroma on epithelial-stromal crosstalk and ECM remodelling in breast tumourigenesis is required. A more sophisticated 3D model using a variety of primary cell types with an ability to modulate the biophysical properties of the ECM would be required. The Weaver group have recently described a 3D tension bioreactor platform capable of precise control of ECM stiffness [372].

The findings from the RNA Seq pathway analysis suggest that tamoxifen may modulate key signalling pathways within the ECM, which may be crucial to establish a tumour-inhibitory microenvironment. Thus, further work to fully characterise these pathways is urgently needed.

9.3 Clinical significance of findings

This study has identified novel, potentially ER-independent mechanisms of tamoxifen action in modulating the stromal microenvironment. Now future work is required to validate the clinical utility of the study findings.

A significant challenge to validating these findings in human tissue samples is obtaining matched tissue samples pre- and post- tamoxifen treatment. Given that this study is focused on the preventive setting, a tissue biopsy would need to be obtained pre- and post- tamoxifen treatment from women with no active breast disease. This is an invasive and painful procedure which many women would find unacceptable. However, a proportion of women may consent if provided with sufficient counselling over the intended benefits.

In our Breast Unit, a clinic has been established for women at moderate and high risk of breast cancer in which they are offered tamoxifen and the opportunity to donate

blood and tissue samples for research. Thus this clinic may provide an opportunity to validate the findings of this study in tissue samples from high risk women.

Another significant challenge to translational research focusing on MD relates to the heterogenous nature of MD. There may be significant local variations in density throughout an individual's breast tissue. Thus close correlation with radiology colleagues would be required when selecting a region of the breast to biopsy and obtain a tissue sample reflective of an individual's overall MD. There is currently no way of measuring MD from paraffin embedded or frozen tissue sections, thus input from radiology colleagues is essential.

Given the challenges associated with tissue validation, an alternative approach using patient serum samples could be utilised. A blood sample is much less invasive and therefore more acceptable to patients with no active breast disease than a tissue biopsy, therefore it would be expected that many more patients would consent.

The Poirot group have recently performed a proof of concept study, demonstrating that oxysterols (cholesterol precursors) can be successfully quantified in patient serum samples [373]. Therefore an important focus of future work, to evaluate the clinical significance of potential inhibition of ChEH activity by tamoxifen, will be to establish whether changes in the levels of oxysterols in patient serum samples pre- and post-tamoxifen treatment correlate with reduction in MD and protection from breast cancer. Serum samples for a pilot analysis are already being obtained through collaborations with the IBIS study, Manchester prevention study and the local high risk clinic.

Using changes in a biomarker, such as cholesterol metabolites, in the serum to predict response to tamoxifen could potentially provide a cost effective and rapid tool for predicting tamoxifen efficacy in the preventive setting. Presently change in MD after one year of treatment is the most rapid and reliable method of predicting response [247]. Changes in serum biomarker levels could be detectable much earlier, this would

allow individuals unlikely to respond to tamoxifen to be identified rapidly and offered alternative treatments. Crucially, these individuals would be spared the debilitating side effects of tamoxifen treatment.

A focus of future work could also be the development of alternative prevention strategies that target ER-independent pathways, as suggested by results from this study. This would avoid the anti-oestrogen side effects associated with tamoxifen, other SERMs and aromatase inhibitors. An alternative prevention strategy with an improved side effect profile would be invaluable to increase uptake of chemoprevention and prevent substantially more breast cancer.

Another focus of future work is to investigate the mechanism by which aromatase inhibitors prevent breast cancer, as these drugs appear to show greater efficacy than tamoxifen [122]. Understanding and comparing these preventive mechanisms would also be invaluable for the development of improved chemoprevention strategies.

A further area to be explored in future work is whether a possible ER-independent mechanism of tamoxifen action on the breast stroma observed in this study could be of clinical benefit in both the prevention and treatment of ER negative breast tumours. The epidemiological data from Cuzick and colleagues suggests that tamoxifen is effective at preventing ER positive tumours only [113]. However, given the ER-independent mechanisms of action suggested by this study, the effect on the development of ER negative tumours should also be investigated.

Reduction in MD with tamoxifen treatment of ER positive tumours in the adjuvant setting is also associated with an improved outcome [111], therefore the ER-independent actions of tamoxifen may also be of benefit in the treatment of ER negative tumours. This is an important consideration of future work as many more women may be able to benefit from the tamoxifen treatment than are currently eligible.

If tamoxifen is able to generate a microenvironment less permissive to tumour development and progression via ER-independent mechanisms, then it is possible that, in addition to ER negative breast cancer, tamoxifen may also be of benefit to tumours arising in other organ systems that have a significant stromal component. A recent study has reported that combined treatment of chemotherapy with tamoxifen was effective at overcoming resistance in an animal model of pancreatic cancer [374].

Finally, the clinical significance of the findings of this study go beyond the breast cancer field. Tamoxifen has been described in many studies to have anti-fibrotic effects and can be used to treat a number of fibrogenic disorders [315-318].

In addition to the effects on cholesterol metabolism observed in this study, many additional pathways were highlighted in the RNA Seq analysis that could contribute to these anti-fibrotic effects, such as down-regulation of Wnt and Hedgehog signalling. Therefore future work to dissect these antifibrotic mechanisms is a priority and may allow many more patients outside of the cancer research field to benefit from the findings from this study.

References

1. Hoda, S.A., *Anatomy and Physiologic Morphology*, in *Rosen's Breast Pathology*, S.A. Hoda, et al., Editors. 2014, Lippincott Williams and Wilkins. p. 1-27.
2. Lester, S.C., *The Breast*, in *Robbins and Cotran Pathologic Basis of Disease*, V. Kumar, A.K. Abbas, and N. Fausto, Editors. 2014, Elsevier: Philadelphia. p. 1043-1073.
3. Ghosh, K., et al., *Association between mammographic density and age-related lobular involution of the breast.* J Clin Oncol. **28**(13): p. 2207-12.
4. Perou, C.M., et al., *Molecular portraits of human breast tumours.* Nature, 2000. **406**(6797): p. 747-52.
5. Sorlie, T., et al., *Repeated observation of breast tumor subtypes in independent gene expression data sets.* Proc Natl Acad Sci U S A, 2003. **100**(14): p. 8418-23.
6. Sørlie, T., et al., *Gene expression patterns of breast carcinomas distinguish tumor subclasses with clinical implications.* Proc Natl Acad Sci U S A, 2001. **98**(19): p. 10869-74.
7. Aleskandarany, M.A., I.O. Ellis, and E.A. Radka, *Molecular Classification of Breast Cancer*, in *Precision Molecular Pathology of Breast Cancer*, A. Khan, et al., Editors. 2015, Springer. p. 137-157.
8. Bertucci, F., et al., *How basal are triple-negative breast cancers?* Int J Cancer, 2008. **123**(1): p. 236-40.
9. Rakha, E.A., et al., *Triple-negative breast cancer: distinguishing between basal and nonbasal subtypes.* Clin Cancer Res, 2009. **15**(7): p. 2302-10.
10. Youlden, D.R., et al., *The descriptive epidemiology of female breast cancer: an international comparison of screening, incidence, survival and mortality.* Cancer Epidemiol. **36**(3): p. 237-48.
11. *Surveillance, Epidemiology and End Results Database (SEER)*. Available from: http://seer.cancer.gov/.
12. *Cancer Research UK*. Available from: http://www.cancerresearchuk.org/.
13. Hery, C., et al., *Changes in breast cancer incidence and mortality in middle-aged and elderly women in 28 countries with Caucasian majority populations.* Ann Oncol, 2008. **19**(5): p. 1009-18.
14. Kingsmore, D., et al., *Specialisation and breast cancer survival in the screening era.* Br J Cancer, 2003. **88**(11): p. 1708-12.
15. Pisani, P., *Breast cancer: geographic variation and risk factors.* J Environ Pathol Toxicol Oncol, 1992. **11**(5-6): p. 313-6.
16. Veronesi, U., et al., *Breast Cancer.* Lancet, 2005. **365**(9472): p. 1727-41.
17. Mavaddat, N., et al., *Genetic susceptibility to breast cancer.* Mol Oncol. **4**(3): p. 174-91.
18. Ziv, E., et al., *Using Breast Cancer Risk Associated Polymorphisms to Identify Women for Breast Cancer Chemoprevention.* PLoS One, 2017. **12**(1): p. e0168601.
19. Couch, F.J., et al., *Associations Between Cancer Predisposition Testing Panel Genes and Breast Cancer.* JAMA Oncol, 2017.
20. Da Silva, L. and S.R. Lakhani, *Pathology of hereditary breast cancer.* Mod Pathol. **23 Suppl 2**: p. S46-51.
21. Cancer, C.G.o.H.F.i.B., *Menarche, menopause, and breast cancer risk: individual participant meta-analysis, including 118 964 women with breast cancer from 117 epidemiological studies.* Lancet Oncol, 2012. **13**(11): p. 1141-51.
22. Beral, V., et al., *Breast cancer and abortion: collaborative reanalysis of data from 53 epidemiological studies, including 83?000 women with breast cancer from 16 countries.* Lancet, 2004. **363**(9414): p. 1007-16.

23. Cancer, C.G.o.H.F.i.B., *Breast cancer and breastfeeding: collaborative reanalysis of individual data from 47 epidemiological studies in 30 countries, including 50302 women with breast cancer and 96973 women without the disease.* Lancet, 2002. **360**(9328): p. 187-95.
24. Lyons, T.R., P.J. Schedin, and V.F. Borges, *Pregnancy and breast cancer: when they collide.* J Mammary Gland Biol Neoplasia, 2009. **14**(2): p. 87-98.
25. Cancer, C.G.o.H.F.i.B., *Breast cancer and hormonal contraceptives: collaborative reanalysis of individual data on 53 297 women with breast cancer and 100 239 women without breast cancer from 54 epidemiological studies.* Lancet, 1996. **347**(9017): p. 1713-27.
26. *Breast cancer and hormone replacement therapy: collaborative reanalysis of data from 51 epidemiological studies of 52,705 women with breast cancer and 108,411 women without breast cancer. Collaborative Group on Hormonal Factors in Breast Cancer.* Lancet, 1997. **350**(9084): p. 1047-59.
27. Boyd, N.F., et al., *Mammographic density and the risk and detection of breast cancer.* New England Journal of Medicine, 2007. **356**(3): p. 227-36.
28. Ellis, I., *Intraductal proliferative lesions of the breast: morphology, associated risk and molecular biology.* Modern Pathology, 2010. **23**: p. S1-S7.
29. Page, D.L., et al., *Atypical hyperplastic lesions of the female breast. A long-term follow-up study.* Cancer, 1985. **55**(11): p. 2698-708.
30. Marshall, L.M., et al., *Risk of breast cancer associated with atypical hyperplasia of lobular and ductal types.* Cancer Epidemiol Biomarkers Prev, 1997. **6**(5): p. 297-301.
31. Bowen, R.L., et al., *Early onset of breast cancer in a group of British black women.* Br J Cancer, 2008. **98**(2): p. 277-81.
32. Ademuyiwa, F.O., et al., *Breast cancer racial disparities: unanswered questions.* Cancer Res, 2011. **71**(3): p. 640-4.
33. Lahmann, P.H., et al., *Body size and breast cancer risk: findings from the European Prospective Investigation into Cancer And Nutrition (EPIC).* Int J Cancer, 2004. **111**(5): p. 762-71.
34. van den Brandt, P.A., et al., *Pooled analysis of prospective cohort studies on height, weight, and breast cancer risk.* Am J Epidemiol, 2000. **152**(6): p. 514-27.
35. Chaudhry, Z.W., et al., *Comparative effectiveness of strategies to prevent weight gain among women with and at risk for breast cancer: a systematic review.* Springerplus, 2013. **2**(1): p. 277.
36. Sieri, S., et al., *High glycemic diet and breast cancer occurrence in the Italian EPIC cohort.* Nutr Metab Cardiovasc Dis, 2013. **23**(7): p. 628-34.
37. Aune, D., et al., *Fruits, vegetables and breast cancer risk: a systematic review and meta-analysis of prospective studies.* Breast Cancer Res Treat, 2012. **134**(2): p. 479-93.
38. Aune, D., et al., *Dietary fiber and breast cancer risk: a systematic review and meta-analysis of prospective studies.* Ann Oncol, 2012. **23**(6): p. 1394-402.
39. Boyd, N., *Mammographic Density*, in *Encyclopaedia of Cancer*, M. Schwab, Editor. 2009, Springer: Berlin. p. 1761-1764.
40. Wolfe, J., *Breast patterns as an index of risk for developing breast cancer.* American Journal of Roentgenology, 1976. **126**(6): p. 1130-7.
41. McCormack, V.A. and I. dos Santos Silva, *Breast density and parenchymal patterns as markers of breast cancer: A meta analysis.* Cancer, Epidemiology, Biomarkers and Prevention, 2006. **15**(6): p. 1159-1169.
42. Mavaddat, N., et al., *Genetic susceptibility to breast cancer.* Mol Oncol, 2010. **4**(3): p. 174-91.
43. Boyd, N.F., et al., *Mammographic breast density as an intermediate phenotype for breast cancer.* Lancet Oncology, 2005. **6**(10): p. 798-808.

44. Brentnall, A.R., et al., *Mammographic density adds accuracy to both the Tyrer-Cuzick and Gail breast cancer risk models in a prospective UK screening cohort.* Breast Cancer Res, 2015. **17**(1): p. 147.
45. Abdolell, M., et al., *Utility of relative and absolute measures of mammographic density vs clinical risk factors in evaluating breast cancer risk at time of screening mammography.* Br J Radiol, 2016. **89**(1059): p. 20150522.
46. Cil, T., et al., *Mammographic density and the risk of breast cancer recurrence after breast-conserving surgery.* Cancer, 2009. **115**(24): p. 5780-7.
47. Buist, D.S., et al., *Diagnosis of second breast cancer events after initial diagnosis of early stage breast cancer.* Breast Cancer Res Treat, 2010. **124**(3): p. 863-73.
48. Li, T., et al., *The association of measured breast tissue characteristics with mammographic density and other risk factors for breast cancer.* Cancer Epidemiol Biomarkers Prev, 2005. **14**(2): p. 343-9.
49. Boyd, N., et al., *Relationship between mammographic and histological risk factors for breast cancer.* Journal of the National Cancer Institute, 1992. **84**(15): p. 1170-9.
50. Turashvili, G., et al., *Columnar cell lesions, mammographic density and breast cancer risk.* Breast Cancer Res Treat, 2009. **115**(3): p. 561-71.
51. Gierach, G.L., et al., *Relationship of Terminal Duct Lobular Unit Involution of the Breast with Area and Volume Mammographic Densities.* Cancer Prev Res (Phila), 2016. **9**(2): p. 149-58.
52. Ghosh, K., et al., *Independent association of lobular involution and mammographic breast density with breast cancer risk.* J Natl Cancer Inst. **102**(22): p. 1716-23.
53. Horne, H.N., et al., *Circulating insulin-like growth factor-I, insulin-like growth factor binding protein-3 and terminal duct lobular unit involution of the breast: a cross-sectional study of women with benign breast disease.* Breast Cancer Res, 2016. **18**(1): p. 24.
54. Alowami, S., et al., *Mammographic density is related to stroma and stromal proteoglycan expression.* Breast Cancer Research, 2003. **5**(5): p. R129-35.
55. Lin, S.J., et al., *Image-guided sampling reveals increased stroma and lower glandular complexity in mammographically dense breast tissue.* Breast Cancer Res Treat, 2011. **128**(2): p. 505-16.
56. Warren, R. and S.R. Lakhani, *Can the stroma provide the clue to the cellular basis for mammographic density?* Breast Cancer Research, 2003. **5**(5): p. 225-227.
57. Sun, X., et al., *Relationship of mammographic density and gene expression: analysis of normal breast tissue surrounding breast cancer.* Clin Cancer Res, 2013. **19**(18): p. 4972-82.
58. Gabrielson, M., et al., *Amount of stroma is associated with mammographic density and stromal expression of oestrogen receptor in normal breast tissues.* Breast Cancer Res Treat, 2016. **158**(2): p. 253-61.
59. Bodelon, C., et al., *Leukocyte telomere length and its association with mammographic density and proliferative diagnosis among women undergoing diagnostic image-guided breast biopsy.* BMC Cancer, 2015. **15**: p. 823.
60. Pang, J.M., et al., *Breast Tissue Composition and Immunophenotype and Its Relationship with Mammographic Density in Women at High Risk of Breast Cancer.* PLoS One, 2015. **10**(6): p. e0128861.
61. McConnell, J.C., et al., *Increased peri-ductal collagen micro-organization may contribute to raised mammographic density.* Breast Cancer Res, 2016. **18**(1): p. 5.
62. Huo, C.W., et al., *High mammographic density is associated with an increase in stromal collagen and immune cells within the mammary epithelium.* Breast Cancer Res, 2015. **17**(1): p. 79.

63. Vachon, C.M., et al., *Aromatase immunoreactivity is increased in mammographically dense regions of the breast.* Breast Cancer Res Treat, 2011. **125**(1): p. 243-52.
64. McCormack, V.A., et al., *Sex steroids, growth factors and mammographic density: a cross-sectional study of UK postmenopausal Caucasian and Afro-Caribbean women.* Breast Cancer Res, 2009. **11**(3): p. R38.
65. Woolcott, C.G., et al., *Association between sex hormones, glucose homeostasis, adipokines, and inflammatory markers and mammographic density among postmenopausal women.* Breast Cancer Res Treat, 2013. **139**(1): p. 255-65.
66. Boyd, N.F., et al., *The association of breast mitogens with mammographic densities.* Br J Cancer, 2002. **87**(8): p. 876-82.
67. Byrne, C., et al., *Plasma insulin-like growth factor (IGF) I, IGF-binding protein 3, and mammographic density.* Cancer Res, 2000. **60**(14): p. 3744-8.
68. Guo, Y.P., et al., *Growth factors and stromal matrix proteins associated with mammographic densities.* Cancer Epidemiol Biomarkers Prev, 2001. **10**(3): p. 243-8.
69. Sun, W.Y., et al., *Insulin-like growth factor 1 receptor expression in breast cancer tissue and mammographic density.* Mol Clin Oncol, 2015. **3**(3): p. 572-580.
70. Diorio, C., et al., *Genetic polymorphisms involved in insulin-like growth factor (IGF) pathway in relation to mammographic breast density and IGF levels.* Cancer Epidemiol Biomarkers Prev, 2008. **17**(4): p. 880-8.
71. Yang, W.T., et al., *Decreased TGFbeta signaling and increased COX2 expression in high risk women with increased mammographic breast density.* Breast Cancer Res Treat, 2009. **119**(2): p. 305-14.
72. Chew, G.L., et al., *Increased COX-2 expression in epithelial and stromal cells of high mammographic density tissues and in a xenograft model of mammographic density.* Breast Cancer Res Treat, 2015.
73. Shawky, M.S., et al., *Proteoglycans: Potential Agents in Mammographic Density and the Associated Breast Cancer Risk.* J Mammary Gland Biol Neoplasia, 2015. **20**(3-4): p. 121-31.
74. Gram, I.T., E. Funkhouser, and L. Tabar, *The Tabar classification of mammographic parenchymal patterns.* Eur J Radiol, 1997. **24**(2): p. 131-6.
75. Kerlikowske, K., et al., *Variability and accuracy in mammographic interpretation using the American College of Radiology Breast Imaging Reporting and Data System.* J Natl Cancer Inst, 1998. **90**(23): p. 1801-9.
76. Boyd, N.F., et al., *Quantitative classification of mammographic densities and breast cancer risk: results from the Canadian National Breast Screening Study.* J Natl Cancer Inst, 1995. **87**(9): p. 670-5.
77. Boyd, N.F., et al., *Mammographic signs as risk factors for breast cancer.* Br J Cancer, 1982. **45**(2): p. 185-93.
78. Assi, V., et al., *Clinical and epidemiological issues in mammographic density.* Nat Rev Clin Oncol. **9**(1): p. 33-40.
79. Vachon, C.M., et al., *Mammographic breast density as a general marker of breast cancer risk.* Cancer Epidemiol Biomarkers Prev, 2007. **16**(1): p. 43-9.
80. Stone, J., et al., *Using mammographic density to predict breast cancer risk: dense area or percentage dense area.* Breast Cancer Res. **12**(6): p. R97.
81. Wong, C.S., et al., *Mammographic density and its interaction with other breast cancer risk factors in an Asian population.* Br J Cancer. **104**(5): p. 871-4.
82. Pettersson, A., et al., *Mammographic density phenotypes and risk of breast cancer: a meta-analysis.* J Natl Cancer Inst, 2014. **106**(5).
83. Lokate, M., et al., *Age-related changes in mammographic density and breast cancer risk.* Am J Epidemiol, 2013. **178**(1): p. 101-9.

84. Pike, M.C., et al., *'Hormonal' risk factors, 'breast tissue age' and the age-incidence of breast cancer.* Nature, 1983. **30**(303): p. 767-70.
85. van Duijnhoven, F.J., et al., *Postmenopausal hormone therapy and changes in mammographic density.* J Clin Oncol, 2007. **25**(11): p. 1323-8.
86. Greendale, G.A., et al., *Postmenopausal hormone therapy and change in mammographic density.* J Natl Cancer Inst, 2003. **95**(1): p. 30-7.
87. Nguyen, T.L., et al., *Explaining variance in the cumulus measures that predict breast cancer risk: a twins and sisters study.* Cancer Epidemiol Biomarkers Prev, 2013. **22**(12): p. 2395-2403.
88. Boyd, N.F., et al., *A longitudinal study of the effects of menopause on mammographic features.* Cancer, Epidemiology, Biomarkers and Prevention, 2002. **11**(10 Pt 1): p. 1048-53.
89. Moseson, H., et al., *Bone mineral density and mammographic density in Mexican women.* Cancer Causes Control, 2016. **27**(1): p. 39-46.
90. Boyd, N.F., et al., *Body size, mammographic density, and breast cancer risk.* Cancer Epidemiol Biomarkers Prev, 2006. **15**(11): p. 2086-92.
91. Boyd, N.F., et al., *The relationship of anthropometric measures to radiological features of the breast in premenopausal women.* Br J Cancer, 1998. **78**(9): p. 1233-8.
92. Thomson, C.A., et al., *Pilot study of dietary influences on mammographic density in pre- and postmenopausal Hispanic and non-Hispanic white women.* Menopause, 2007. **14**(2): p. 243-50.
93. Habel, L.A., et al., *Mammographic density in a multiethnic cohort.* Menopause, 2007. **14**(5): p. 891-9.
94. Reeves, K.W., et al., *Longitudinal association of anthropometry with mammographic breast density in the Study of Women's Health Across the Nation.* Int J Cancer, 2009. **124**(5): p. 1169-77.
95. Bertrand, K.A., et al., *Body fatness during childhood and adolescence and breast density in young women: a prospective analysis.* Breast Cancer Res, 2015. **17**: p. 95.
96. Kim, B.K., et al., *Metabolic syndrome, insulin resistance, and mammographic density in pre- and postmenopausal women.* Breast Cancer Res Treat, 2015. **153**(2): p. 425-34.
97. Tamimi, R.M., et al., *Birth weight and mammographic density among postmenopausal women in Sweden.* Int J Cancer, 2010. **126**(4): p. 985-91.
98. Castelló, A., et al., *Association between the Adherence to the International Guidelines for Cancer Prevention and Mammographic Density.* PLoS One, 2015. **10**(7): p. e0132684.
99. Wu, A.H., et al., *Double-Blind Randomized 12-Month Soy Intervention Had No Effects on Breast MRI Fibroglandular Tissue Density or Mammographic Density.* Cancer Prev Res (Phila), 2015. **8**(10): p. 942-51.
100. Bertrand, K.A., et al., *Adolescent intake of animal fat and red meat in relation to premenopausal mammographic density.* Breast Cancer Res Treat, 2016. **155**(2): p. 385-93.
101. Jacobsen, K.K., et al., *Cigarette smoking and mammographic density in the Danish Diet, Cancer and Health cohort.* Cancer Causes Control, 2016. **27**(2): p. 271-80.
102. Huynh, S., et al., *Long-term exposure to air pollution and mammographic density in the Danish Diet, Cancer and Health cohort.* Environ Health, 2015. **14**: p. 31.
103. Quandt, Z., et al., *The association of alcohol consumption with mammographic density in a multiethnic urban population.* BMC Cancer, 2015. **15**: p. 1094.
104. Frydenberg, H., et al., *Alcohol consumption, endogenous estrogen and mammographic density among premenopausal women.* Breast Cancer Res, 2015. **17**: p. 103.
105. McDonald, J.A., et al., *Alcohol intake from early adulthood to midlife and mammographic density.* Cancer Causes Control, 2016. **27**(4): p. 493-502.

106. McCormack, V.A., et al., *International Consortium on Mammographic Density: Methodology and population diversity captured across 22 countries.* Cancer Epidemiol, 2016. **40**: p. 141-51.
107. Boyd, N., et al., *Mammographic denisty as a surrogate marker for the effects of hormaone therapy on risk of breast cancer.* Cancer Epidemiol Biomarkers Prev, 2006. **15**(5): p. 961-6.
108. Sala, E., et al., *High-risk mammographic parenchymal patterns, hormone replacement therapy and other risk factors: a case-control study.* Int J Epidemiol, 2000. **29**(4): p. 629-36.
109. Cuzick, J., et al., *Tamoxifen and breast density in women at increased risk of breast cancer.* J Natl Cancer Inst, 2004. **96**(8): p. 621-8.
110. Cuzick, J., et al., *Tamoxifen-induced reduction in mammographic density and breast cancer risk reduction: a nested case-control study.* J Natl Cancer Inst, 2011. **103**(9): p. 744-52.
111. Li, J., et al., *Mammographic density reduction is a prognostic marker of response to adjuvant tamoxifen therapy in postmenopausal patients with breast cancer.* J Clin Oncol, 2013. **31**(18): p. 2249-56.
112. Sandberg, M.E., et al., *Change of mammographic density predicts the risk of contralateral breast cancer--a case-control study.* Breast Cancer Res, 2013. **15**(4): p. R57.
113. Cuzick, J., et al., *Tamoxifen for prevention of breast cancer: extended long-term follow-up of the IBIS-I breast cancer prevention trial.* Lancet Oncol, 2015. **16**(1): p. 67-75.
114. Li, J., et al., *Association of CYP2D6 metabolizer status with mammographic density change in response to tamoxifen treatment.* Breast Cancer Res, 2013. **15**(5): p. R93.
115. Hattar, R., et al., *Tamoxifen induces pleiotrophic changes in mammary stroma resulting in extracellular matrix that suppresses transformed phenotypes.* Breast Cancer Res, 2009. **11**(1): p. R5.
116. Chew, G.L., et al., *Effects of Tamoxifen and oestrogen on histology and radiographic density in high and low mammographic density human breast tissues maintained in murine tissue engineering chambers.* Breast Cancer Res Treat, 2014. **148**(2): p. 303-14.
117. Vogel, V.G., et al., *Update of the National Surgical Adjuvant Breast and Bowel Project Study of Tamoxifen and Raloxifene (STAR) P-2 Trial: Preventing breast cancer.* Cancer Prev Res (Phila), 2010. **3**(6): p. 696-706.
118. Eng-Wong, J., et al., *Effect of raloxifene on mammographic density and breast magnetic resonance imaging in premenopausal women at increased risk for breast cancer.* Cancer Epidemiol Biomarkers Prev, 2008. **17**(7): p. 1696-701.
119. Freedman, M., et al., *Digitized mammography: a clinical trial of postmenopausal women randomly assigned to receive raloxifene, estrogen, or placebo.* J Natl Cancer Inst, 2001. **93**(1): p. 51-6.
120. Cuzick, J., et al., *Selective oestrogen receptor modulators in prevention of breast cancer: an updated meta-analysis of individual participant data.* Lancet, 2013. **381**(9880): p. 1827-34.
121. Evans, D.G., et al., *Familial breast cancer: summary of updated NICE guidance.* BMJ, 2013. **346**: p. f3829.
122. Cuzick, J., et al., *Anastrozole for prevention of breast cancer in high-risk postmenopausal women (IBIS-II): an international, double-blind, randomised placebo-controlled trial.* Lancet, 2014. **383**(9922): p. 1041-8.
123. Goss, P.E., et al., *Exemestane for breast-cancer prevention in postmenopausal women.* N Engl J Med, 2011. **364**(25): p. 2381-91.

124. Cigler, T., et al., *A randomized, placebo-controlled trial (NCIC CTG MAP1) examining the effects of letrozole on mammographic breast density and other end organs in postmenopausal women.* Breast Cancer Res Treat, 2009. **120**(2): p. 427-35.
125. Cigler, T., et al., *A randomized, placebo-controlled trial (NCIC CTG MAP.2) examining the effects of exemestane on mammographic breast density, bone density, markers of bone metabolism and serum lipid levels in postmenopausal women.* Breast Cancer Res Treat, 2011. **126**(2): p. 453-61.
126. Smith, J., et al., *A pilot study of letrozole for one year in women at enhanced risk of developing breast cancer: effects on mammographic density.* Anticancer Res, 2012. **32**(4): p. 1327-31.
127. Vachon, C.M., et al., *Pilot study of the impact of letrozole vs. placebo on breast density in women completing 5 years of tamoxifen.* Breast, 2007. **16**(2): p. 204-10.
128. Gatti-Mays, M.E., et al., *Exemestane Use in Postmenopausal Women at High Risk for Invasive Breast Cancer: Evaluating Biomarkers of Efficacy and Safety.* Cancer Prev Res (Phila), 2016. **9**(3): p. 225-33.
129. Spicer, D.V., et al., *Changes in mammographic densities induced by a hormonal contraceptive designed to reduce breast cancer risk.* J Natl Cancer Inst, 1994. **86**(6): p. 431-6.
130. Wu, Q.J., et al., *Statin use and breast cancer survival and risk: a systematic review and meta-analysis.* Oncotarget, 2015. **6**(40): p. 42988-3004.
131. Ji, Y., et al., *The Effect of Atorvastatin on Breast Cancer Biomarkers in High-Risk Women.* Cancer Prev Res (Phila), 2016. **9**(5): p. 379-84.
132. Boyd, N.F., et al., *Heritability of mammographic density, a risk factor for breast cancer.* N Engl J Med, 2002. **347**(12): p. 886-94.
133. Ursin, G., et al., *The relative importance of genetics and environment on mammographic density.* Cancer Epidemiol Biomarkers Prev, 2009. **18**(1): p. 102-12.
134. Stevens, K.N., et al., *Identification of a novel percent mammographic density locus at 12q24.* Hum Mol Genet, 2012. **21**(14): p. 3299-305.
135. Vachon, C.M., et al., *Common breast cancer susceptibility variants in LSP1 and RAD51L1 are associated with mammographic density measures that predict breast cancer risk.* Cancer Epidemiol Biomarkers Prev, 2012. **21**(7): p. 1156-66.
136. Lindstrom, S., et al., *Common variants in ZNF365 are associated with both mammographic density and breast cancer risk.* Nat Genet, 2011. **43**(3): p. 185-7.
137. Lindstrom, S., et al., *Genome-wide association study identifies multiple loci associated with both mammographic density and breast cancer risk.* Nat Commun. **5**: p. 5303.
138. Keller, B.M., et al., *Associations between breast density and a panel of single nucleotide polymorphisms linked to breast cancer risk: a cohort study with digital mammography.* BMC Cancer, 2015. **15**: p. 143.
139. Brand, J.S., et al., *Identification of two novel mammographic density loci at 6Q25.1.* Breast Cancer Res, 2015. **17**(1): p. 75.
140. Stone, J., et al., *Novel Associations between Common Breast Cancer Susceptibility Variants and Risk-Predicting Mammographic Density Measures.* Cancer Res, 2015. **75**(12): p. 2457-67.
141. Mariapun, S., et al., *Variants in 6q25.1 Are Associated with Mammographic Density in Malaysian Chinese Women.* Cancer Epidemiol Biomarkers Prev, 2016. **25**(2): p. 327-33.
142. Rudolph, A., et al., *A comprehensive evaluation of interaction between genetic variants and use of menopausal hormone therapy on mammographic density.* Breast Cancer Res, 2015. **17**: p. 110.
143. Atkinson, E.J., et al., *The association of copy number variation and percent mammographic density.* BMC Res Notes, 2015. **8**: p. 297.

144. Mitchell, G., et al., *Mammographic density and breast cancer risk in BRCA1 and BRCA2 mutation carriers.* Cancer Res, 2006. **66**(3): p. 1866-72.
145. Gierach, G.L., et al., *Mammographic density does not differ between unaffected BRCA1/2 mutation carriers and women at low-to-average risk of breast cancer.* Breast Cancer Res Treat, 2010. **123**(1): p. 245-55.
146. Ramón Y Cajal, T., et al., *Mammographic density and breast cancer in women from high risk families.* Breast Cancer Res, 2015. **17**: p. 93.
147. Kelemen, L.E., T.A. Sellers, and C.M. Vachon, *Can genes for mammographic density inform cancer aetiology?* Nature Reviews Cancer, 2008. **8**(10): p. 812-23.
148. Dumas, I. and C. Diorio, *Polymorphisms in genes involved in the estrogen pathway and mammographic density.* BMC Cancer, 2010. **10**: p. 636.
149. Ellingjord-Dale, M., et al., *Polymorphisms in hormone metabolism and growth factor genes and mammographic density in Norwegian postmenopausal hormone therapy users and non-users.* Breast Cancer Res. **14**(5): p. R135.
150. Lee, E., et al., *Hormone metabolism genes and mammographic density in Singapore Chinese women.* Cancer Epidemiol Biomarkers Prev.
151. Vachon, C.M., et al., *No evidence for association of inherited variation in genes involved in mitosis and percent mammographic density.* Breast Cancer Res. **14**(1): p. R7.
152. Ding, J., et al., *Mammographic density, estrogen receptor status and other breast cancer tumor characteristics.* Breast J. **16**(3): p. 279-89.
153. Conroy, S.M., et al., *Mammographic density and hormone receptor expression in breast cancer: the Multiethnic Cohort Study.* Cancer Epidemiol. **35**(5): p. 448-52.
154. Ziv, E., et al., *Mammographic density and estrogen receptor status of breast cancer.* Cancer Epidemiol Biomarkers Prev, 2004. **13**(12): p. 2090-5.
155. Ma, H., et al., *Is there a difference in the association between percent mammographic density and subtypes of breast cancer? Luminal A and triple-negative breast cancer.* Cancer Epidemiol Biomarkers Prev, 2009. **18**(2): p. 479-85.
156. Olsen, A.H., et al., *Breast density and outcome of mammography screening: a cohort study.* Br J Cancer, 2009. **100**(7): p. 1205-8.
157. Yaghjyan, L., et al., *Mammographic breast density and subsequent risk of breast cancer in postmenopausal women according to tumor characteristics.* J Natl Cancer Inst. **103**(15): p. 1179-89.
158. Eriksson, L., et al., *The influence of mammographic density on breast tumor characteristics.* Breast Cancer Res Treat. **134**(2): p. 859-66.
159. Moshina, N., et al., *Mammographic density and histopathologic characteristics of screen-detected tumors in the Norwegian Breast Cancer Screening Program.* Acta Radiol Open, 2015. **4**(9): p. 2058460115604340.
160. Antoni, S., et al., *Is mammographic density differentially associated with breast cancer according to receptor status? A meta-analysis.* Breast Cancer Res Treat. **137**(2): p. 337-47.
161. Dvorak, H.F., *Tumors: wounds that do not heal. Similarities between tumor stroma generation and wound healing.* N Engl J Med, 1986. **315**(26): p. 1650-9.
162. Paulsson, J. and P. Micke, *Prognostic relevance of cancer-associated fibroblasts in human cancer.* Semin Cancer Biol, 2014. **25**: p. 61-8.
163. Gandellini, P., et al., *Complexity in the tumour microenvironment: Cancer associated fibroblast gene expression patterns identify both common and unique features of tumour-stroma crosstalk across cancer types.* Semin Cancer Biol, 2015. **35**: p. 96-106.
164. Aboussekhra, A., *Role of cancer-associated fibroblasts in breast cancer development and prognosis.* Int J Dev Biol, 2011. **55**(7-9): p. 841-9.

165. Kojima, Y., et al., *Autocrine TGF-beta and stromal cell-derived factor-1 (SDF-1) signaling drives the evolution of tumor-promoting mammary stromal myofibroblasts.* Proc Natl Acad Sci U S A, 2010. **107**(46): p. 20009-14.
166. Shao, Z.M., M. Nguyen, and S.H. Barsky, *Human breast carcinoma desmoplasia is PDGF initiated.* Oncogene, 2000. **19**(38): p. 4337-45.
167. Strutz, F., et al., *Basic fibroblast growth factor expression is increased in human renal fibrogenesis and may mediate autocrine fibroblast proliferation.* Kidney Int, 2000. **57**(4): p. 1521-38.
168. Hugo, H.J., et al., *Contribution of Fibroblast and Mast Cell (Afferent) and Tumor (Efferent) IL-6 Effects within the Tumor Microenvironment.* Cancer Microenviron, 2012. **5**(1): p. 83-93.
169. Avgustinova, A., et al., *Tumour cell-derived Wnt7a recruits and activates fibroblasts to promote tumour aggressiveness.* Nat Commun, 2016. **7**: p. 10305.
170. Mercier, I., et al., *Human breast cancer-associated fibroblasts (CAFs) show caveolin-1 downregulation and RB tumor suppressor functional inactivation: Implications for the response to hormonal therapy.* Cancer Biol Ther, 2008. **7**(8): p. 1212-25.
171. Martinez-Outschoorn, U.E., et al., *Oxidative stress in cancer associated fibroblasts drives tumor-stroma co-evolution: A new paradigm for understanding tumor metabolism, the field effect and genomic instability in cancer cells.* Cell Cycle, 2010. **9**(16): p. 3256-76.
172. Witkiewicz, A.K., et al., *An absence of stromal caveolin-1 expression predicts early tumor recurrence and poor clinical outcome in human breast cancers.* Am J Pathol, 2009. **174**(6): p. 2023-34.
173. El-Gendi, S.M., M.F. Mostafa, and A.M. El-Gendi, *Stromal caveolin-1 expression in breast carcinoma. Correlation with early tumor recurrence and clinical outcome.* Pathol Oncol Res, 2012. **18**(2): p. 459-69.
174. Sloan, E.K., et al., *Stromal cell expression of caveolin-1 predicts outcome in breast cancer.* Am J Pathol, 2009. **174**(6): p. 2035-43.
175. Bauer, M., et al., *Heterogeneity of gene expression in stromal fibroblasts of human breast carcinomas and normal breast.* Oncogene, 2010. **29**(12): p. 1732-40.
176. Nguyen, D.H., et al., *Radiation acts on the microenvironment to affect breast carcinogenesis by distinct mechanisms that decrease cancer latency and affect tumor type.* Cancer Cell, 2011. **19**(5): p. 640-51.
177. Scherz-Shouval, R., et al., *The reprogramming of tumor stroma by HSF1 is a potent enabler of malignancy.* Cell, 2014. **158**(3): p. 564-78.
178. Luo, H., et al., *Cancer-associated fibroblasts: a multifaceted driver of breast cancer progression.* Cancer Lett, 2015. **361**(2): p. 155-63.
179. Tyan, S.W., et al., *Breast cancer cells induce cancer-associated fibroblasts to secrete hepatocyte growth factor to enhance breast tumorigenesis.* PLoS One, 2011. **6**(1): p. e15313.
180. Miki, Y., et al., *Aromatase localization in human breast cancer tissues: possible interactions between intratumoral stromal and parenchymal cells.* Cancer Res, 2007. **67**(8): p. 3945-54.
181. Gao, M.Q., et al., *Stromal fibroblasts from the interface zone of human breast carcinomas induce an epithelial-mesenchymal transition-like state in breast cancer cells in vitro.* J Cell Sci, 2010. **123**(Pt 20): p. 3507-14.
182. Kessenbrock, K., V. Plaks, and Z. Werb, *Matrix metalloproteinases: regulators of the tumor microenvironment.* Cell, 2010. **141**(1): p. 52-67.
183. Przybylo, J.A. and D.C. Radisky, *Matrix metalloproteinase-induced epithelial-mesenchymal transition: tumor progression at Snail's pace.* Int J Biochem Cell Biol, 2007. **39**(6): p. 1082-8.

184. Hu, M., et al., *Regulation of in situ to invasive breast carcinoma transition.* Cancer Cell, 2008. **13**(5): p. 394-406.
185. Hu, M., et al., *Role of COX-2 in epithelial-stromal cell interactions and progression of ductal carcinoma in situ of the breast.* Proc Natl Acad Sci U S A, 2009. **106**(9): p. 3372-7.
186. Lu, P., V.M. Weaver, and Z. Werb, *The extracellular matrix: a dynamic niche in cancer progression.* J Cell Biol, 2012. **196**(4): p. 395-406.
187. Yang, N., et al., *Syndecan-1 in breast cancer stroma fibroblasts regulates extracellular matrix fiber organization and carcinoma cell motility.* Am J Pathol, 2011. **178**(1): p. 325-35.
188. Galdiero, M.R., et al., *Tumor associated macrophages and neutrophils in tumor progression.* J Cell Physiol, 2013. **228**(7): p. 1404-12.
189. Qian, B.Z., et al., *CCL2 recruits inflammatory monocytes to facilitate breast-tumour metastasis.* Nature, 2011. **475**(7355): p. 222-5.
190. Raz, Y. and N. Erez, *An inflammatory vicious cycle: Fibroblasts and immune cell recruitment in cancer.* Exp Cell Res, 2013. **319**(11): p. 1596-603.
191. Fiegl, H., et al., *Breast cancer DNA methylation profiles in cancer cells and tumor stroma: association with HER-2/neu status in primary breast cancer.* Cancer Res, 2006. **66**(1): p. 29-33.
192. Knower, K.C., et al., *Epigenetic mechanisms regulating CYP19 transcription in human breast adipose fibroblasts.* Mol Cell Endocrinol, 2010. **321**(2): p. 123-30.
193. Tyan, S.W., et al., *Breast cancer cells induce stromal fibroblasts to secrete ADAMTS1 for cancer invasion through an epigenetic change.* PLoS One, 2012. **7**(4): p. e35128.
194. Pavlides, S., et al., *Warburg meets autophagy: cancer-associated fibroblasts accelerate tumor growth and metastasis via oxidative stress, mitophagy, and aerobic glycolysis.* Antioxid Redox Signal, 2012. **16**(11): p. 1264-84.
195. Pavlides, S., et al., *The reverse Warburg effect: aerobic glycolysis in cancer associated fibroblasts and the tumor stroma.* Cell Cycle, 2009. **8**(23): p. 3984-4001.
196. Martinez-Outschoorn, U.E., et al., *Stromal-epithelial metabolic coupling in cancer: integrating autophagy and metabolism in the tumor microenvironment.* Int J Biochem Cell Biol, 2011. **43**(7): p. 1045-51.
197. Madsen, C.D., et al., *Hypoxia and loss of PHD2 inactivate stromal fibroblasts to decrease tumour stiffness and metastasis.* EMBO Rep, 2015. **16**(10): p. 1394-408.
198. Allen, M. and J. Louise Jones, *Jekyll and Hyde: the role of the microenvironment on the progression of cancer.* J Pathol, 2010. **223**(2): p. 162-76.
199. Pickup, M.W., J.K. Mouw, and V.M. Weaver, *The extracellular matrix modulates the hallmarks of cancer.* EMBO Rep, 2014. **15**(12): p. 1243-53.
200. Bergamaschi, A., et al., *Extracellular matrix signature identifies breast cancer subgroups with different clinical outcome.* J Pathol, 2008. **214**(3): p. 357-67.
201. Farmer, P., et al., *A stroma-related gene signature predicts resistance to neoadjuvant chemotherapy in breast cancer.* Nat Med, 2009. **15**(1): p. 68-74.
202. Helleman, J., et al., *Association of an extracellular matrix gene cluster with breast cancer prognosis and endocrine therapy response.* Clin Cancer Res, 2008. **14**(17): p. 5555-64.
203. Bremnes, Y., et al., *Endogenous sex hormones, prolactin and mammographic density in postmenopausal Norwegian women.* Int J Cancer, 2007. **121**(11): p. 2506-11.
204. Ghosh, S., et al., *Mechanical phenotype is important for stromal aromatase expression.* Steroids, 2011. **76**(8): p. 797-801.
205. Conklin, M.W. and P.J. Keely, *Why the stroma matters in breast cancer: insights into breast cancer patient outcomes through the examination of stromal biomarkers.* Cell Adh Migr, 2012. **6**(3): p. 249-60.

206. Provenzano, P.P., et al., *Collagen density promotes mammary tumor initiation and progression.* BMC Med, 2008. **6**: p. 11.
207. Provenzano, P.P., et al., *Matrix density-induced mechanoregulation of breast cell phenotype, signaling and gene expression through a FAK-ERK linkage.* Oncogene, 2009. **28**(49): p. 4326-43.
208. Samuel, M.S., et al., *Actomyosin-mediated cellular tension drives increased tissue stiffness and β-catenin activation to induce epidermal hyperplasia and tumor growth.* Cancer Cell, 2011. **19**(6): p. 776-91.
209. Raviraj, V., et al., *Regulation of ROCK1 via Notch1 during breast cancer cell migration into dense matrices.* BMC Cell Biol, 2012. **13**: p. 12.
210. Provenzano, P.P., et al., *Collagen reorganization at the tumor-stromal interface facilitates local invasion.* BMC Med, 2006. **4**(1): p. 38.
211. Conklin, M.W., et al., *Aligned collagen is a prognostic signature for survival in human breast carcinoma.* Am J Pathol. **178**(3): p. 1221-32.
212. Maller, O., et al., *Collagen architecture in pregnancy-induced protection from breast cancer.* J Cell Sci, 2013. **126**(Pt 18): p. 4108-10.
213. Levental, K.R., et al., *Matrix crosslinking forces tumor progression by enhancing integrin signaling.* Cell, 2009. **139**(5): p. 891-906.
214. Webster, M.A., et al., *Requirement for both Shc and phosphatidylinositol 3' kinase signaling pathways in polyomavirus middle T-mediated mammary tumorigenesis.* Mol Cell Biol, 1998. **18**(4): p. 2344-59.
215. Erler, J.T. and V.M. Weaver, *Three-dimensional context regulation of metastasis.* Clin Exp Metastasis, 2009. **26**(1): p. 35-49.
216. Barker, H.E., T.R. Cox, and J.T. Erler, *The rationale for targeting the LOX family in cancer.* Nat Rev Cancer, 2012. **12**(8): p. 540-52.
217. Erler, J.T., et al., *Lysyl oxidase is essential for hypoxia-induced metastasis.* Nature, 2006. **440**(7088): p. 1222-6.
218. Acerbi, I., et al., *Human breast cancer invasion and aggression correlates with ECM stiffening and immune cell infiltration.* Integr Biol (Camb), 2015. **7**(10): p. 1120-34.
219. Rubashkin, M.G., et al., *Force engages vinculin and promotes tumor progression by enhancing PI3K activation of phosphatidylinositol (3,4,5)-triphosphate.* Cancer Res, 2014. **74**(17): p. 4597-611.
220. Mouw, J.K., et al., *Tissue mechanics modulate microRNA-dependent PTEN expression to regulate malignant progression.* Nat Med, 2014. **20**(4): p. 360-7.
221. Trimboli, A.J., et al., *Pten in stromal fibroblasts suppresses mammary epithelial tumours.* Nature, 2009. **461**(7267): p. 1084-91.
222. Bronisz, A., et al., *Reprogramming of the tumour microenvironment by stromal PTEN-regulated miR-320.* Nat Cell Biol, 2012. **14**(2): p. 159-67.
223. DeFilippis, R.A., et al., *CD36 repression activates a multicellular stromal program shared by high mammographic density and tumor tissues.* Cancer Discov. **2**(9): p. 826-39.
224. DeFilippis, R.A., et al., *Stress signaling from human mammary epithelial cells contributes to phenotypes of mammographic density.* Cancer Res, 2014. **74**(18): p. 5032-44.
225. Lisanti, M.P., et al., *JNK1 stress signaling is hyper-activated in high breast density and the tumor stroma: connecting fibrosis, inflammation, and stemness for cancer prevention.* Cell Cycle, 2014. **13**(4): p. 580-99.
226. Martin, L.J. and N.F. Boyd, *Mammographic density. Potential mechanisms of breast cancer risk associated with mammographic density: hypotheses based on epidemiological evidence.* Breast Cancer Res, 2008. **10**(1): p. 201.

227. Studer, R.K. and C.R. Chu, *p38 MAPK and COX2 inhibition modulate human chondrocyte response to TGF-beta.* J Orthop Res, 2005. **23**(2): p. 454-61.
228. Aiello, E.J., et al., *Association between mammographic breast density and breast cancer tumor characteristics.* Cancer Epidemiol Biomarkers Prev, 2005. **14**(3): p. 662-8.
229. Khan, Q.J., et al., *Mammographic density does not correlate with Ki-67 expression or cytomorphology in benign breast cells obtained by random periareolar fine needle aspiration from women at high risk for breast cancer.* Breast Cancer Res, 2007. **9**(3): p. R35.
230. Esbona, K., et al., *COX-2 modulates mammary tumor progression in response to collagen density.* Breast Cancer Res, 2016. **18**(1): p. 35.
231. García-Mendoza, M.G., et al., *Neutrophils drive accelerated tumor progression in the collagen-dense mammary tumor microenvironment.* Breast Cancer Res, 2016. **18**(1): p. 49.
232. Chen, J., et al., *Projecting absolute invasive breast cancer risk in white women with a model that includes mammographic density.* J Natl Cancer Inst, 2006. **98**(17): p. 1215-26.
233. Tice, J.A., et al., *Using clinical factors and mammographic breast density to estimate breast cancer risk: development and validation of a new predictive model.* Ann Intern Med, 2008. **148**(5): p. 337-47.
234. Tice, J.A., et al., *Mammographic breast density and the Gail model for breast cancer risk prediction in a screening population.* Breast Cancer Res Treat, 2005. **94**(2): p. 115-22.
235. Barlow, W.E., et al., *Prospective breast cancer risk prediction model for women undergoing screening mammography.* J Natl Cancer Inst, 2006. **98**(17): p. 1204-14.
236. Lee, C.P., et al., *Mammographic Breast Density and Common Genetic Variants in Breast Cancer Risk Prediction.* PLoS One, 2015. **10**(9): p. e0136650.
237. Schousboe, J.T., et al., *Personalizing mammography by breast density and other risk factors for breast cancer: analysis of health benefits and cost-effectiveness.* Ann Intern Med, 2011. **155**(1): p. 10-20.
238. Evans, D.G. and A. Howell, *Can the breast screening appointment be used to provide risk assessment and prevention advice?* Breast Cancer Res, 2015. **17**: p. 84.
239. Evans, D.G., et al., *Breast cancer risk feedback to women in the UK NHS breast screening population.* Br J Cancer, 2016. **114**(9): p. 1045-52.
240. Donnelly, L.S., et al., *Uptake of tamoxifen in consecutive premenopausal women under surveillance in a high-risk breast cancer clinic.* Br J Cancer, 2014. **110**(7): p. 1681-7.
241. Lorizio, W., et al., *Clinical and biomarker predictors of side effects from tamoxifen.* Breast Cancer Res Treat, 2012. **132**(3): p. 1107-18.
242. Ropka, M.E., J. Keim, and J.T. Philbrick, *Patient decisions about breast cancer chemoprevention: a systematic review and meta-analysis.* J Clin Oncol, 2010. **28**(18): p. 3090-5.
243. Howell, A., et al., *Risk determination and prevention of breast cancer.* Breast Cancer Res, 2014. **16**(5): p. 446.
244. Boyd, N.F., et al., *Mammographic density and breast cancer risk: current understanding and future prospects.* Breast Cancer Res, 2011. **13**(6): p. 223.
245. Ko, K.L., et al., *Adjuvant tamoxifen-induced mammographic breast density reduction as a predictor for recurrence in estrogen receptor-positive premenopausal breast cancer patients.* Breast Cancer Res Treat, 2013. **142**(3): p. 559-67.
246. Nyante, S.J., et al., *Prognostic significance of mammographic density change after initiation of tamoxifen for ER-positive breast cancer.* J Natl Cancer Inst, 2015. **107**(3).

247. Nyante, S.J., et al., *Longitudinal Change in Mammographic Density among ER-Positive Breast Cancer Patients Using Tamoxifen.* Cancer Epidemiol Biomarkers Prev, 2016. **25**(1): p. 212-6.
248. Mullooly, M., et al., *Mammographic Density as a Biosensor of Tamoxifen Effectiveness in Adjuvant Endocrine Treatment of Breast Cancer: Opportunities and Implications.* J Clin Oncol, 2016.
249. Brentnall, A.R., et al., *Relationship of ZNF423 and CTSO with breast cancer risk in two randomised tamoxifen prevention trials.* Breast Cancer Res Treat, 2016. **158**(3): p. 591-6.
250. Zhou, J., et al., *The role of the tumor microenvironment in hematological malignancies and implication for therapy.* Front Biosci, 2005. **10**: p. 1581-96.
251. Fang, H. and Y.A. Declerck, *Targeting the tumor microenvironment: from understanding pathways to effective clinical trials.* Cancer Res, 2013. **73**(16): p. 4965-77.
252. Rini, B.I. and M.B. Atkins, *Resistance to targeted therapy in renal-cell carcinoma.* Lancet Oncol, 2009. **10**(10): p. 992-1000.
253. Lieu, C., et al., *Beyond VEGF: inhibition of the fibroblast growth factor pathway and antiangiogenesis.* Clin Cancer Res, 2011. **17**(19): p. 6130-9.
254. Xiong, H.Q., et al., *A phase I surrogate endpoint study of SU6668 in patients with solid tumors.* Invest New Drugs, 2004. **22**(4): p. 459-66.
255. Rossi, J.F., et al., *A phase I/II study of siltuximab (CNTO 328), an anti-interleukin-6 monoclonal antibody, in metastatic renal cell cancer.* Br J Cancer, 2010. **103**(8): p. 1154-62.
256. Zollo, M., et al., *Targeting monocyte chemotactic protein-1 synthesis with bindarit induces tumor regression in prostate and breast cancer animal models.* Clin Exp Metastasis, 2012. **29**(6): p. 585-601.
257. O'Day, S., et al., *A randomised, phase II study of intetumumab, an anti-αv-integrin mAb, alone and with dacarbazine in stage IV melanoma.* Br J Cancer, 2011. **105**(3): p. 346-52.
258. Hersey, P., et al., *A randomized phase 2 study of etaracizumab, a monoclonal antibody against integrin alpha(v)beta(3), + or - dacarbazine in patients with stage IV metastatic melanoma.* Cancer, 2010. **116**(6): p. 1526-34.
259. Ostermann, E., et al., *Effective immunoconjugate therapy in cancer models targeting a serine protease of tumor fibroblasts.* Clin Cancer Res, 2008. **14**(14): p. 4584-92.
260. LeBeau, A.M., et al., *Targeting the cancer stroma with a fibroblast activation protein-activated promelittin protoxin.* Mol Cancer Ther, 2009. **8**(5): p. 1378-86.
261. Loeffler, M., et al., *Targeting tumor-associated fibroblasts improves cancer chemotherapy by increasing intratumoral drug uptake.* J Clin Invest, 2006. **116**(7): p. 1955-62.
262. Lonard, D.M. and C.L. Smith, *Molecular perspectives on selective estrogen receptor modulators (SERMs): progress in understanding their tissue-specific agonist and antagonist actions.* Steroids, 2002. **67**(1): p. 15-24.
263. Dutertre, M. and C.L. Smith, *Molecular mechanisms of selective estrogen receptor modulator (SERM) action.* J Pharmacol Exp Ther, 2000. **295**(2): p. 431-7.
264. de Medina, P., et al., *Identification and pharmacological characterization of cholesterol-5,6-epoxide hydrolase as a target for tamoxifen and AEBS ligands.* Proc Natl Acad Sci U S A, 2010. **107**(30): p. 13520-5.
265. Coezy, E., J.L. Borgna, and H. Rochefort, *Tamoxifen and metabolites in MCF7 cells: correlation between binding to estrogen receptor and inhibition of cell growth.* Cancer Res, 1982. **42**(1): p. 317-23.

266. Johnston, S.R., et al., *Changes in estrogen receptor, progesterone receptor, and pS2 expression in tamoxifen-resistant human breast cancer.* Cancer Res, 1995. **55**(15): p. 3331-8.
267. Rochefort, H., *Oestrogen- and anti-oestrogen-regulated genes in human breast cancer.* Ciba Found Symp, 1995. **191**: p. 254-65; discussion 265-8.
268. Jensen, E.V. and V.C. Jordan, *The estrogen receptor: a model for molecular medicine.* Clin Cancer Res, 2003. **9**(6): p. 1980-9.
269. Nilsson, S., et al., *Mechanisms of estrogen action.* Physiol Rev, 2001. **81**(4): p. 1535-65.
270. Markiewicz, M., et al., *A role for estrogen receptor-α and estrogen receptor-β in collagen biosynthesis in mouse skin.* J Invest Dermatol, 2013. **133**(1): p. 120-7.
271. Higgins, M.J. and V. Stearns, *CYP2D6 polymorphisms and tamoxifen metabolism: clinical relevance.* Curr Oncol Rep, 2010. **12**(1): p. 7-15.
272. Coller, J.K., et al., *The influence of CYP2B6, CYP2C9 and CYP2D6 genotypes on the formation of the potent antioestrogen Z-4-hydroxy-tamoxifen in human liver.* Br J Clin Pharmacol, 2002. **54**(2): p. 157-67.
273. Brauch, H., et al., *Tamoxifen use in postmenopausal breast cancer: CYP2D6 matters.* J Clin Oncol, 2013. **31**(2): p. 176-80.
274. Lum, D.W., et al., *CYP2D6 genotype and tamoxifen response for breast cancer: a systematic review and meta-analysis.* PLoS One, 2013. **8**(10): p. e76648.
275. Langan-Fahey, S.M., D.C. Tormey, and V.C. Jordan, *Tamoxifen metabolites in patients on long-term adjuvant therapy for breast cancer.* Eur J Cancer, 1990. **26**(8): p. 883-8.
276. Lien, E.A., E. Solheim, and P.M. Ueland, *Distribution of tamoxifen and its metabolites in rat and human tissues during steady-state treatment.* Cancer Res, 1991. **51**(18): p. 4837-44.
277. Johnston, S.R., et al., *Effect of oestrogen receptor status and time on the intra-tumoural accumulation of tamoxifen and N-desmethyltamoxifen following short-term therapy in human primary breast cancer.* Breast Cancer Res Treat, 1993. **28**(3): p. 241-50.
278. Kisanga, E.R., et al., *Tamoxifen and metabolite concentrations in serum and breast cancer tissue during three dose regimens in a randomized preoperative trial.* Clin Cancer Res, 2004. **10**(7): p. 2336-43.
279. Davies, C., et al., *Relevance of breast cancer hormone receptors and other factors to the efficacy of adjuvant tamoxifen: patient-level meta-analysis of randomised trials.* Lancet, 2011. **378**(9793): p. 771-84.
280. Pagano, G., et al., *The role of oxidative stress in developmental and reproductive toxicity of tamoxifen.* Life Sci, 2001. **68**(15): p. 1735-49.
281. Viedma-Rodríguez, R., et al., *Mechanisms associated with resistance to tamoxifen in estrogen receptor-positive breast cancer (review).* Oncol Rep, 2014. **32**(1): p. 3-15.
282. Cuzick, J., et al., *First results from the International Breast Cancer Intervention Study (IBIS-I): a randomised prevention trial.* Lancet, 2002. **360**(9336): p. 817-24.
283. Cuzick, J., et al., *Effect of tamoxifen and radiotherapy in women with locally excised ductal carcinoma in situ: long-term results from the UK/ANZ DCIS trial.* Lancet Oncol, 2011. **12**(1): p. 21-9.
284. Yang, G., et al., *Toxicity and adverse effects of Tamoxifen and other anti-estrogen drugs.* Pharmacol Ther, 2013. **139**(3): p. 392-404.
285. von Maillot, K., H.H. Gentsch, and W. Gunselmann, *Steroid receptors and response to endocrine treatment and chemotherapy of advanced breast cancer.* J Cancer Res Clin Oncol, 1980. **98**(3): p. 301-13.
286. Johnston, S.R., M. Dowsett, and I.E. Smith, *Towards a molecular basis for tamoxifen resistance in breast cancer.* Ann Oncol, 1992. **3**(7): p. 503-11.

287. Gruvberger-Saal, S.K., et al., *Estrogen receptor beta expression is associated with tamoxifen response in ERalpha-negative breast carcinoma.* Clin Cancer Res, 2007. **13**(7): p. 1987-94.
288. Reese, J.M., et al., *ERβ1: characterization, prognosis, and evaluation of treatment strategies in ERα-positive and -negative breast cancer.* BMC Cancer, 2014. **14**: p. 749.
289. Yan, Y., et al., *Expression of both estrogen receptor-beta 1 (ER-β1) and its co-regulator steroid receptor RNA activator protein (SRAP) are predictive for benefit from tamoxifen therapy in patients with estrogen receptor-alpha (ER-α)-negative early breast cancer (EBC).* Ann Oncol, 2013. **24**(8): p. 1986-93.
290. Manna, S. and M.K. Holz, *Tamoxifen Action in ER-Negative Breast Cancer.* Sign Transduct Insights, 2016. **5**: p. 1-7.
291. Radin, D.P. and P. Patel, *Delineating the molecular mechanisms of tamoxifen's oncolytic actions in estrogen receptor-negative cancers.* Eur J Pharmacol, 2016. **781**: p. 173-80.
292. de Médina, P., G. Favre, and M. Poirot, *Multiple targeting by the antitumor drug tamoxifen: a structure-activity study.* Curr Med Chem Anticancer Agents, 2004. **4**(6): p. 491-508.
293. Kedjouar, B., et al., *Molecular characterization of the microsomal tamoxifen binding site.* J Biol Chem, 2004. **279**(32): p. 34048-61.
294. de Medina, P., et al., *Importance of cholesterol and oxysterols metabolism in the pharmacology of tamoxifen and other AEBS ligands.* Chem Phys Lipids, 2011. **164**(6): p. 432-7.
295. Payré, B., et al., *Microsomal antiestrogen-binding site ligands induce growth control and differentiation of human breast cancer cells through the modulation of cholesterol metabolism.* Mol Cancer Ther, 2008. **7**(12): p. 3707-18.
296. Segala, G., et al., *5,6-Epoxy-cholesterols contribute to the anticancer pharmacology of tamoxifen in breast cancer cells.* Biochem Pharmacol, 2013. **86**(1): p. 175-89.
297. Morad, S.A. and M.C. Cabot, *Tamoxifen regulation of sphingolipid metabolism--Therapeutic implications.* Biochim Biophys Acta, 2015. **1851**(9): p. 1134-45.
298. Corriden, R., et al., *Tamoxifen augments the innate immune function of neutrophils through modulation of intracellular ceramide.* Nat Commun, 2015. **6**: p. 8369.
299. Reddel, R.R., et al., *Differential sensitivity of human breast cancer cell lines to the growth-inhibitory effects of tamoxifen.* Cancer Res, 1985. **45**(4): p. 1525-31.
300. Zhang, W., et al., *Tamoxifen-induced enhancement of calcium signaling in glioma and MCF-7 breast cancer cells.* Cancer Res, 2000. **60**(19): p. 5395-400.
301. Lee, Y.S., et al., *Role of NAD(P)H oxidase in the tamoxifen-induced generation of reactive oxygen species and apoptosis in HepG2 human hepatoblastoma cells.* Cell Death Differ, 2000. **7**(10): p. 925-32.
302. Kim, J.A., et al., *Involvement of Ca2+ influx in the mechanism of tamoxifen-induced apoptosis in HepG2 human hepatoblastoma cells.* Cancer Lett, 1999. **147**(1-2): p. 115-23.
303. Prather, P.L., et al., *CB1 and CB2 receptors are novel molecular targets for Tamoxifen and 4OH-Tamoxifen.* Biochem Biophys Res Commun, 2013. **441**(2): p. 339-43.
304. Mato, S., et al., *CB1 cannabinoid receptor-dependent and -independent inhibition of depolarization-induced calcium influx in oligodendrocytes.* Glia, 2009. **57**(3): p. 295-306.
305. Mandlekar, S., et al., *Activation of caspase-3 and c-Jun NH2-terminal kinase-1 signaling pathways in tamoxifen-induced apoptosis of human breast cancer cells.* Cancer Res, 2000. **60**(21): p. 5995-6000.

306. Nagarkatti, N. and B.A. Davis, *Tamoxifen induces apoptosis in Fas+ tumor cells by upregulating the expression of Fas ligand.* Cancer Chemother Pharmacol, 2003. **51**(4): p. 284-90.
307. Weng, S.C., et al., *Sensitizing estrogen receptor-negative breast cancer cells to tamoxifen with OSU-03012, a novel celecoxib-derived phosphoinositide-dependent protein kinase-1/Akt signaling inhibitor.* Mol Cancer Ther, 2008. **7**(4): p. 800-8.
308. Hinz, B., et al., *The myofibroblast: one function, multiple origins.* Am J Pathol, 2007. **170**(6): p. 1807-16.
309. Pickup, M., S. Novitskiy, and H.L. Moses, *The roles of TGFβ in the tumour microenvironment.* Nat Rev Cancer, 2013. **13**(11): p. 788-99.
310. Horbelt, D., A. Denkis, and P. Knaus, *A portrait of Transforming Growth Factor β superfamily signalling: Background matters.* Int J Biochem Cell Biol, 2012. **44**(3): p. 469-74.
311. Shi, Y. and J. Massagué, *Mechanisms of TGF-beta signaling from cell membrane to the nucleus.* Cell, 2003. **113**(6): p. 685-700.
312. Mu, Y., S.K. Gudey, and M. Landström, *Non-Smad signaling pathways.* Cell Tissue Res, 2012. **347**(1): p. 11-20.
313. Carthy, J.M., et al., *Tamoxifen Inhibits TGF-β-Mediated Activation of Myofibroblasts by Blocking Non-Smad Signaling Through ERK1/2.* J Cell Physiol, 2015. **230**(12): p. 3084-92.
314. Kim, D., et al., *Tamoxifen ameliorates renal tubulointerstitial fibrosis by modulation of estrogen receptor α-mediated transforming growth factor-β1/Smad signaling pathway.* Nephrol Dial Transplant, 2014. **29**(11): p. 2043-53.
315. Dellê, H., et al., *Antifibrotic effect of tamoxifen in a model of progressive renal disease.* J Am Soc Nephrol, 2012. **23**(1): p. 37-48.
316. Degreef, I., et al., *High-dosage tamoxifen as neoadjuvant treatment in minimally invasive surgery for Dupuytren disease in patients with a strong predisposition toward fibrosis: a randomized controlled trial.* J Bone Joint Surg Am, 2014. **96**(8): p. 655-62.
317. Bocale, D., et al., *Anti-oestrogen therapy in the treatment of desmoid tumours: a systematic review.* Colorectal Dis, 2011. **13**(12): p. e388-95.
318. Brandt, A.S., et al., *Tamoxifen monotherapy in the treatment of retroperitoneal fibrosis.* Urol Int, 2014. **93**(3): p. 320-5.
319. Shim, J.S., et al., *Inhibition of angiogenesis by selective estrogen receptor modulators through blockade of cholesterol trafficking rather than estrogen receptor antagonism.* Cancer Lett, 2015. **362**(1): p. 106-15.
320. Blackwell, K.L., et al., *Tamoxifen inhibits angiogenesis in estrogen receptor-negative animal models.* Clin Cancer Res, 2000. **6**(11): p. 4359-64.
321. Kuhn, M.A., et al., *Tamoxifen decreases fibroblast function and downregulates TGF(beta2) in dupuytren's affected palmar fascia.* J Surg Res, 2002. **103**(2): p. 146-52.
322. Gomm, J.J., et al., *Isolation of pure populations of epithelial and myoepithelial cells from the normal human mammary gland using immunomagnetic separation with Dynabeads.* Anal Biochem, 1995. **226**(1): p. 91-9.
323. Katzenellenbogen, B.S., et al., *Proliferation, hormonal responsiveness, and estrogen receptor content of MCF-7 human breast cancer cells grown in the short-term and long-term absence of estrogens.* Cancer Res, 1987. **47**(16): p. 4355-60.
324. Berthois, Y., J.A. Katzenellenbogen, and B.S. Katzenellenbogen, *Phenol red in tissue culture media is a weak estrogen: implications concerning the study of estrogen-responsive cells in culture.* Proc Natl Acad Sci U S A, 1986. **83**(8): p. 2496-500.
325. Aakvaag, A., et al., *Growth control of human mammary cancer cells (MCF-7 cells) in culture: effect of estradiol and growth factors in serum-containing medium.* Cancer Res, 1990. **50**(24): p. 7806-10.

326. Jain, P.T. and J.T. Pento, *Growth medium for the evaluation of antiestrogenic compounds in MCF-7 cell culture.* Methods Find Exp Clin Pharmacol, 1991. **13**(9): p. 595-8.
327. Aida-Yasuoka, K., et al., *Estradiol promotes the development of a fibrotic phenotype and is increased in the serum of patients with systemic sclerosis.* Arthritis Res Ther, 2013. **15**(1): p. R10.
328. Palmieri, C., et al., *The expression of oestrogen receptor (ER)-beta and its variants, but not ERalpha, in adult human mammary fibroblasts.* J Mol Endocrinol, 2004. **33**(1): p. 35-50.
329. McDonnell, D.P. and S.E. Wardell, *The molecular mechanisms underlying the pharmacological actions of ER modulators: implications for new drug discovery in breast cancer.* Curr Opin Pharmacol, 2010. **10**(6): p. 620-8.
330. Peekhaus, N.T., et al., *Distinct effects of the antiestrogen Faslodex on the stability of estrogen receptors-alpha and -beta in the breast cancer cell line MCF-7.* J Mol Endocrinol, 2004. **32**(3): p. 987-95.
331. Raza, S., et al., *The cholesterol metabolite 27-hydroxycholesterol stimulates cell proliferation via ERβ in prostate cancer cells.* Cancer Cell Int, 2017. **17**: p. 52.
332. Fan, S., et al., *Estrogen promotes tumor metastasis via estrogen receptor beta-mediated regulation of matrix-metalloproteinase-2 in non-small cell lung cancer.* Oncotarget, 2017.
333. Wang, Z., et al., *ERβ localization influenced outcomes of EGFR-TKI treatment in NSCLC patients with EGFR mutations.* Sci Rep, 2015. **5**: p. 11392.
334. Mishra, A.K., A. Abrahamsson, and C. Dabrosin, *Fulvestrant inhibits growth of triple negative breast cancer and synergizes with tamoxifen in ERα positive breast cancer by up-regulation of ERβ.* Oncotarget, 2016. **7**(35): p. 56876-56888.
335. Ivanova, M.M., et al., *Estradiol and tamoxifen regulate NRF-1 and mitochondrial function in mouse mammary gland and uterus.* J Mol Endocrinol, 2013. **51**(2): p. 233-46.
336. Salem, A.F., et al., *Downregulation of stromal BRCA1 drives breast cancer tumor growth via upregulation of HIF-1α, autophagy and ketone body production.* Cell Cycle, 2012. **11**(22): p. 4167-73.
337. Morad, S.A., et al., *Novel off-target effect of tamoxifen--inhibition of acid ceramidase activity in cancer cells.* Biochim Biophys Acta, 2013. **1831**(12): p. 1657-64.
338. Simigdala, N., et al., *Cholesterol biosynthesis pathway as a novel mechanism of resistance to estrogen deprivation in estrogen receptor-positive breast cancer.* Breast Cancer Res, 2016. **18**(1): p. 58.
339. Brown, A.J., E. Ikonen, and V.M. Olkkonen, *Cholesterol precursors: more than mere markers of biosynthesis.* Curr Opin Lipidol, 2014. **25**(2): p. 133-9.
340. Gabitova, L., A. Gorin, and I. Astsaturov, *Molecular pathways: sterols and receptor signaling in cancer.* Clin Cancer Res, 2014. **20**(1): p. 28-34.
341. Moiseeva, O.M., et al., *Effect of pravastatin on phenotypical transformation of fibroblasts and hypertrophy of cardiomyocytes in culture.* Bull Exp Biol Med, 2007. **143**(1): p. 54-7.
342. He, Y.P., et al., *Involvement of ERK and AKT signaling in the growth effect of arginine vasopressin on adult rat cardiac fibroblast and the modulation by simvastatin.* Mol Cell Biochem, 2008. **317**(1-2): p. 33-41.
343. Martin, J., et al., *In vitro inhibitory effects of atorvastatin on cardiac fibroblasts: implications for ventricular remodelling.* Clin Exp Pharmacol Physiol, 2005. **32**(9): p. 697-701.
344. Poirot, M. and S. Silvente-Poirot, *Cholesterol-5,6-epoxides: chemistry, biochemistry, metabolic fate and cancer.* Biochimie, 2013. **95**(3): p. 622-31.

345. Silvente-Poirot, S. and M. Poirot, *Cholesterol epoxide hydrolase and cancer.* Curr Opin Pharmacol, 2012. **12**(6): p. 696-703.
346. Sutherland, R.L., et al., *High-affinity anti-oestrogen binding site distinct from the oestrogen receptor.* Nature, 1980. **288**(5788): p. 273-5.
347. de Medina, P., et al., *Dendrogenin A arises from cholesterol and histamine metabolism and shows cell differentiation and anti-tumour properties.* Nat Commun, 2013. **4**: p. 1840.
348. de Medina, P., et al., *Synthesis of new alkylaminooxysterols with potent cell differentiating activities: identification of leads for the treatment of cancer and neurodegenerative diseases.* J Med Chem, 2009. **52**(23): p. 7765-77.
349. Berrodin, T.J., et al., *Identification of 5α, 6α-epoxycholesterol as a novel modulator of liver X receptor activity.* Mol Pharmacol, 2010. **78**(6): p. 1046-58.
350. Fuda, H., et al., *Oxysterols are substrates for cholesterol sulfotransferase.* J Lipid Res, 2007. **48**(6): p. 1343-52.
351. Song, C., R.A. Hiipakka, and S. Liao, *Auto-oxidized cholesterol sulfates are antagonistic ligands of liver X receptors: implications for the development and treatment of atherosclerosis.* Steroids, 2001. **66**(6): p. 473-9.
352. Villablanca, E.J., et al., *Tumor-mediated liver X receptor-alpha activation inhibits CC chemokine receptor-7 expression on dendritic cells and dampens antitumor responses.* Nat Med, 2010. **16**(1): p. 98-105.
353. Guo, D., et al., *Targeting SREBP-1-driven lipid metabolism to treat cancer.* Curr Pharm Des, 2014. **20**(15): p. 2619-26.
354. Cristancho, A.G. and M.A. Lazar, *Forming functional fat: a growing understanding of adipocyte differentiation.* Nat Rev Mol Cell Biol, 2011. **12**(11): p. 722-34.
355. Andò, S., et al., *The Multifaceted Mechanism of Leptin Signaling within Tumor Microenvironment in Driving Breast Cancer Growth and Progression.* Front Oncol, 2014. **4**: p. 340.
356. Luu, W., et al., *The terminal enzymes of cholesterol synthesis, DHCR24 and DHCR7, interact physically and functionally.* J Lipid Res, 2015. **56**(4): p. 888-97.
357. Loh, Y.N., et al., *The Wnt signalling pathway is upregulated in an in vitro model of acquired tamoxifen resistant breast cancer.* BMC Cancer, 2013. **13**: p. 174.
358. Dees, C. and J.H. Distler, *Canonical Wnt signalling as a key regulator of fibrogenesis - implications for targeted therapies?* Exp Dermatol, 2013. **22**(11): p. 710-3.
359. Hanna, A. and L.A. Shevde, *Hedgehog signaling: modulation of cancer properies and tumor mircroenvironment.* Mol Cancer, 2016. **15**: p. 24.
360. Hu, L., et al., *An overview of hedgehog signaling in fibrosis.* Mol Pharmacol, 2015. **87**(2): p. 174-82.
361. Javelaud, D., et al., *TGF-β/SMAD/GLI2 signaling axis in cancer progression and metastasis.* Cancer Res, 2011. **71**(17): p. 5606-10.
362. Javelaud, D., M.J. Pierrat, and A. Mauviel, *Crosstalk between TGF-β and hedgehog signaling in cancer.* FEBS Lett, 2012. **586**(14): p. 2016-25.
363. Koide, T., T. Hayata, and K.W. Cho, *Negative regulation of Hedgehog signaling by the cholesterogenic enzyme 7-dehydrocholesterol reductase.* Development, 2006. **133**(12): p. 2395-405.
364. Lauth, M., et al., *Antipsychotic drugs regulate hedgehog signaling by modulation of 7-dehydrocholesterol reductase levels.* Mol Pharmacol, 2010. **78**(3): p. 486-96.
365. Chevy, F., L. Humbert, and C. Wolf, *Sterol profiling of amniotic fluid: a routine method for the detection of distal cholesterol synthesis deficit.* Prenat Diagn, 2005. **25**(11): p. 1000-6.
366. Lin, C., et al., *Adjuvant tamoxifen influences the lipid profile in breast cancer patients.* Breast Care (Basel), 2014. **9**(1): p. 35-9.

367. Silvente-Poirot, S., et al., *From tamoxifen to dendrogenin A: The discovery of a mammalian tumor suppressor and cholesterol metabolite.* Biochimie, 2016.
368. Schroepfer, G.J., *Oxysterols: modulators of cholesterol metabolism and other processes.* Physiol Rev, 2000. **80**(1): p. 361-554.
369. Barsky, S.H. and N.J. Karlin, *Myoepithelial cells: autocrine and paracrine suppressors of breast cancer progression.* J Mammary Gland Biol Neoplasia, 2005. **10**(3): p. 249-60.
370. Barsky, S.H. and N.J. Karlin, *Mechanisms of disease: breast tumor pathogenesis and the role of the myoepithelial cell.* Nat Clin Pract Oncol, 2006. **3**(3): p. 138-51.
371. Yang, Y.J., et al., *Clinical significance of fatty liver disease induced by tamoxifen and toremifene in breast cancer patients.* Breast, 2016. **28**: p. 67-72.
372. Cassereau, L., et al., *A 3D tension bioreactor platform to study the interplay between ECM stiffness and tumor phenotype.* J Biotechnol, 2015. **193**: p. 66-9.
373. Dalenc, F., et al., *Circulating oxysterol metabolites as potential new surrogate markers in patients with hormone receptor-positive breast cancer: Results of the OXYTAM study.* J Steroid Biochem Mol Biol, 2016.
374. Miyake, T., et al., *Combined treatment with tamoxifen and a fusicoccin derivative (ISIR-042) to overcome resistance to therapy and to enhance the antitumor activity of 5-fluorouracil and gemcitabine in pancreatic cancer cells.* Int J Oncol, 2015. **47**(1): p. 315-24.

Appendix 1: Sequence alignment data for all samples used in the RNA Seq pilot and follow up batches (P = Pilot batch, F = Follow up batch)

Sample ID and batch	Treatment	Total paired-end read counts	Uniquely aligned paired-end reads	Paired end reads with no gene features	Paired end reads with ambiguous features	Paired end reads aligned to multiple loci	% paired end reads used in the analysis
1004 P	Control 1	49812192	23256317	22537318	1417166	2601391	46.69%
1004 P	Control 2	52193855	27590213	20317021	1593375	2693246	52.86%
1004 P	Control 3	51047351	26117505	20762493	1512038	2655315	51.16%
1004 P	Tamoxifen (low) 1	56579414	29239825	22672281	1706634	2960674	51.68%
1004 P	Tamoxifen (low) 2	45786985	25340910	16670387	1475440	2300248	55.35%
1004 P	Tamoxifen (low) 3	69700261	39118083	24834516	2218173	3529489	56.12%
1004 P	Tamoxifen 1	50665774	26691372	19572427	1640373	2761602	52.68%
1004 P	Tamoxifen 2	55812238	32593446	18047157	2094356	3077279	58.40%
1004 P	Tamoxifen 3	30901029	18233015	9830853	1185842	1651319	59.00%
3078 P	Control 1	49613970	28748424	16091988	1943477	2830081	57.94%
3078 P	Control 2	52370040	31080622	16066074	2047255	3176089	59.35%
3078 P	Control 3	51954877	31463724	15551013	2054315	2885825	60.56%
3078 P	Tamoxifen (low) 1	52248496	28750171	18347529	1992928	3157868	55.03%
3078 P	Tamoxifen (low) 2	46010089	26634870	14943004	1771163	2661052	57.89%
3078 P	Tamoxifen (low) 3	50806631	28336338	17843236	1900832	2726225	55.77%
3078 P	Tamoxifen 1	52003924	30141436	16407265	2155413	3299810	57.96%
3078 P	Tamoxifen 2	44785891	25595618	14573007	1888238	2729028	57.15%
3078 P	Tamoxifen 3	51791718	28173414	18394273	1994421	3229610	54.40%
3137 F	Control 1	61007667	45057463	7580260	2004370	6365574	73.86%
3137 F	Control 2	60057274	43047234	7586746	1653640	7769654	71.68%
3137 F	Control 3	61741102	45945653	7843009	1857273	6095167	74.42%
3137 F	Tamoxifen 1	62790155	44837388	10048984	1698534	6205249	71.41%
3137 F	Tamoxifen 2	70574527	50750566	10105473	1775713	7942775	71.91%
3137 F	Tamoxifen 3	73116122	47647753	14894465	1821705	8752199	65.17%
3137 F	Fulvestrant 1	68103001	50797362	8024760	2029768	7251111	74.59%
3137 F	Fulvestrant 2	67491290	50069973	8552568	1616881	7251868	74.19%
3137 F	Fulvestrant 3	65597477	48140997	8732503	1998018	6725959	73.39%
2182 F	Control 1	67292791	52403702	6624517	1777909	6486663	77.87%
2182 F	Control 2	66298517	51466997	6537484	1681878	6612158	77.63%
2182 F	Control 3	71183621	50962142	8799133	2019723	9402623	71.59%

2182 F	Tamoxifen 1	62758311	46395403	8462253	1902874	5997781	73.93%
2182 F	Tamoxifen 2	80753089	52629857	14629380	1855127	11638725	65.17%
2182 F	Tamoxifen 3	68990566	46248885	12042623	2149983	8549075	67.04%
2093 F	Control 1	62750752	47154311	7742534	1753985	6099922	75.15%
2093 F	Control 2	67702432	45326146	10935391	2614244	8826651	66.95%
2093 F	Control 3	70671437	48617923	11148584	2064471	8840459	68.79%
2093 F	Tamoxifen 1	64801725	44930919	10916063	1990804	6963939	69.34%
2093 F	Tamoxifen 2	68346102	49886834	8783707	2378905	7296656	72.99%
2093 F	Tamoxifen 3	67530857	49717254	8056751	2441902	7314950	73.62%
2585 F	Control 1	60196080	45196111	7426754	1453479	6119736	75.08%
2585 F	Control 2	59901293	44203147	7321873	2125376	6250897	73.79%
2585 F	Control 3	76145088	54916405	9941469	2037355	9249859	72.12%
2585 F	Tamoxifen 1	80739568	56090866	13100987	2063977	9483738	69.47%
2585 F	Tamoxifen 2	66761513	52593443	5745927	1694683	6727460	78.78%
2585 F	Tamoxifen 3	73770650	55965842	6827047	2748775	8228986	75.86%
2585 F	Fulvestrant 1	61162571	42039938	8933301	1439671	8749661	68.73%
2585 F	Fulvestrant 2	70401756	48324104	10832858	1934188	9310606	68.64%
2585 F	Fulvestrant 3	67475392	50496037	7454634	1879601	7645120	74.84%

Appendix 2: Most significantly differentially expressed genes identified by ANOVA between high dose 4-OHTam treated samples and vehicle control treated samples.

Name	Description	logFC. LowT	logFC HighT	logCPM	p-Value	FDR
DHCR24	24-dehydrocholesterol reductase	-0.363	1.625	6.313	1.04E-53	1.39E-49
DHCR7	7-dehydrocholesterol reductase	-0.116	1.765	5.812	2.58E-51	1.73E-47
FASN	fatty acid synthase	-0.168	1.611	5.476	2.94E-37	1.31E-33
FADS2	fatty acid desaturase 2	-0.259	1.285	6.930	8.54E-35	2.86E-31
RSPO3	R-spondin 3	-0.426	1.410	5.752	1.33E-31	3.56E-28
HMGCR	3-hydroxy-3-methylglutaryl-CoA reductase	-0.295	1.075	6.933	4.80E-31	1.07E-27
DMKN	dermokine	-0.770	2.069	2.651	9.20E-31	1.76E-27
HMOX1	heme oxygenase (decycling) 1	-0.317	1.605	4.760	5.00E-30	8.37E-27
NPC1	Niemann-Pick disease, type C1	-0.334	0.922	6.627	2.12E-29	3.15E-26
INSIG1	insulin induced gene 1	-0.222	1.743	6.765	4.57E-29	6.13E-26
ACACA	acetyl-CoA carboxylase alpha	-0.151	0.736	7.930	3.27E-26	3.98E-23
C1orf85	chromosome 1 open reading frame 85	0.034	1.265	4.520	1.60E-25	1.79E-22
SREBF2	sterol regulatory element binding transcription factor 2	-0.145	0.985	6.332	8.97E-25	9.24E-22
SCD	stearoyl-CoA desaturase (delta-9-desaturase)	-0.490	1.868	8.869	1.25E-24	1.20E-21
GPNMB	glycoprotein (transmembrane) nmb	-0.605	1.610	9.292	1.42E-24	1.27E-21
CLCN7	chloride channel, voltage-sensitive 7	0.013	1.387	2.271	3.79E-24	3.17E-21
SHC3	SHC (Src homology 2 domain containing) transforming protein 3	0.050	1.131	3.272	9.05E-24	7.13E-21
LDLR	low density lipoprotein receptor	-0.261	1.175	7.174	1.68E-23	1.25E-20
SC5D	sterol-C5-desaturase	-0.063	1.010	5.317	9.13E-23	6.44E-20
NCR3LG1	natural killer cell cytotoxicity receptor 3 ligand 1	-0.166	1.027	4.742	2.56E-22	1.71E-19
FADS1	fatty acid desaturase 1	-0.191	1.125	8.155	2.96E-22	1.89E-19
FTH1	ferritin, heavy polypeptide 1	0.035	1.095	4.231	1.51E-21	9.17E-19
NPC2	Niemann-Pick disease, type C2	-0.262	1.121	5.728	7.19E-21	4.19E-18

LINC00906	long intergenic non-protein coding RNA 906	-0.414	2.541	-0.475	7.70E-21	4.30E-18
OSBPL8	oxysterol binding protein-like 8	-0.308	0.847	11.072	3.26E-20	1.75E-17
VAT1	vesicle amine transport 1]	-0.080	0.755	7.688	3.62E-20	1.86E-17
HMGCS1	3-hydroxy-3-methylglutaryl-CoA synthase 1 (soluble)	-0.319	1.604	5.881	4.04E-20	2.01E-17
SQSTM1	sequestosome 1	-0.302	1.401	5.920	8.06E-20	3.86E-17
TNFSF4	tumor necrosis factor (ligand) superfamily, member 4	-0.357	-1.663	6.541	8.84E-20	4.08E-17
GRN	granulin	-0.095	0.790	6.297	1.49E-19	6.67E-17
PCSK9	proprotein convertase subtilisin/kexin type 9	-0.889	1.669	2.698	2.14E-19	9.23E-17

Appendix 3: Top differentially expressed genes across the four patients from the RNA Seq follow up batch identified by ANOVA using FDR<0.05 and absolute fold change >2.

Name	Description	LogFC (tamoxifen vs control)	Log CPM	LR	p-value	FDR
LEP	leptin	-2.264	2.039	354.014	5.66E-79	8.10E-75
GPNMB	glycoprotein (transmembrane) nmb	1.429	9.216	339.982	6.44E-76	4.61E-72
PCSK9	proprotein convertase subtilisin/kexin type 9	2.376	3.614	338.827	1.15E-75	5.48E-72
QPRT	quinolinate phosphoribosyltransferase	1.770	4.712	279.452	9.89E-63	2.83E-59
MCTP1	multiple C2 domains, transmembrane 1	1.451	2.581	276.128	5.24E-62	1.25E-58
HSD17B14	hydroxysteroid (17-beta) dehydrogenase 14	1.219	2.947	260.159	1.58E-58	3.24E-55
EVI2B	ecotropic viral integration site 2B	1.287	2.411	235.990	2.95E-53	5.27E-50
C5orf46	chromosome 5 open reading frame 46	-2.329	1.379	233.170	1.21E-52	1.93E-49
PDK4	pyruvate dehydrogenase kinase, isozyme 4	-2.837	4.275	222.450	2.64E-50	3.78E-47
WNT4	wingless-type MMTV integration site family, member 4	-2.603	0.081	218.023	2.44E-49	3.18E-46
KLF15	Kruppel-like factor 15	1.472	1.294	211.881	5.34E-48	6.37E-45
NEDD9	neural precursor cell expressed, developmentally down-regulated 9	-1.263	5.498	194.831	2.81E-44	3.09E-41
DMKN	dermokine	2.266	5.385	190.988	1.93E-43	1.98E-40
SREBF1	sterol regulatory element binding transcription factor 1	1.423	5.394	178.250	1.17E-40	1.04E-37
ANGPTL	angiopoietin-like 4	-4.067	5.659	173.427	1.32E-39	1.11E-36

4						
CTSK	cathepsin K	1.421	9.942	167.970	2.05E-38	1.63E-35
SCD	stearoyl-CoA desaturase (delta-9-desaturase)	2.267	7.562	166.491	4.32E-38	3.25E-35
FHL1	four and a half LIM domains 1	-1.371	6.582	158.729	2.15E-36	1.40E-33
PLIN2	perilipin 2	-1.145	7.982	154.119	2.18E-35	1.25E-32
MLPH	melanophilin	1.231	2.136	149.382	2.37E-34	1.25E-31
TNFSF13B	tumor necrosis factor (ligand) superfamily, member 13b	1.255	1.998	143.375	4.87E-33	2.32E-30
WFDC1	WAP four-disulfide core domain 1	-2.426	-0.720	137.839	7.90E-32	3.53E-29
SCUBE3	signal peptide, CUB domain, EGF-like 3	-1.499	3.031	129.386	5.58E-30	2.22E-27
ACP5	acid phosphatase 5, tartrate resistant	1.558	1.684	128.098	1.07E-29	4.03E-27
DRD1	dopamine receptor D1	-2.365	0.570	124.731	5.83E-29	1.90E-26
GDF7	growth differentiation factor 7	-2.450	0.612	124.138	7.86E-29	2.50E-26
ART5	ADP-ribosyltransferase 5	1.700	0.081	117.257	2.52E-27	7.22E-25
AC144652.1		1.294	0.811	116.171	4.36E-27	1.22E-24
SHROOM3	shroom family member 3	-1.158	5.333	108.443	2.15E-25	5.49E-23
NPPB	natriuretic peptide B	-3.008	-1.427	107.763	3.03E-25	7.48E-23

Appendix 4: Top differentially expressed genes across all six patients between higher dose 4-OHTam and vehicle control treated samples.

Name	Description	logFC (4-OHTam vs control)	p -value	Adjusted p-value
QPRT	quinolinate phosphoribosyltransferase	1.6843	2.97E-19	2.23E-15
DMKN	dermokine	2.213	1.24E-18	6.18E-15
GPNMB	glycoprotein (transmembrane) nmb	1.533	3.43E-18	1.28E-14
NEDD9	neural precursor cell expressed, developmentally down-regulated 9	-1.206	2.28E-17	5.68E-14
DRD1	dopamine receptor D1	-2.749	6.35E-17	1.28E-13
DHCR7	7-dehydrocholesterol reductase	1.239	1.05E-16	1.75E-13
HSD17B14	hydroxysteroid (17-beta) dehydrogenase 14	1.351	1.42E-16	2.12E-13
PCSK9	proprotein convertase subtilisin/kexin type 9	2.016	2.14E-16	2.92E-13
DHCR24	24-dehydrocholesterol reductase	1.128	6.37E-16	7.33E-13
FADS2	fatty acid desaturase 2	1.192	7.86E-16	8.39E-13
SCD	stearoyl-CoA desaturase (delta-9-desaturase)	2.046	2.65E-15	1.98E-12
FHL1	four and a half LIM domains 1	-1.389	1.77E-14	9.45E-12
INSIG1	insulin induced gene 1	1.460	1.85E-14	9.55E-12
LDLR	low density lipoprotein receptor	1.009	4.89E-14	2.17E-11

Appendix 5: Significantly up-regulated pathways from the merged dataset using the GSEA tool and REACTOME pathway resource.

NAME	SIZE	ES	NES	NOM p-val	FDR q-val	FWER p-val
REACTOME_CHOLESTEROL_BIOSYNTHESIS	20	0.889	2.484	0	0	0
REACTOME_GLYCOSPHINGOLIPID_METABOLISM	28	0.745	2.292	0	0	0
REACTOME_IRON_UPTAKE_AND_TRANSPORT	28	0.714	2.256	0	0	0
REACTOME_METABOLISM_OF_LIPIDS_AND_LIPOPROTEINS	365	0.477	2.246	0	0	0
REACTOME_SPHINGOLIPID_METABOLISM	54	0.614	2.211	0	0	0
REACTOME_PHOSPHOLIPID_METABOLISM	157	0.496	2.121	0	8.40 E-05	0.001
REACTOME_INSULIN_RECEPTOR_RECYCLING	16	0.747	2.048	0	8.53 E-04	0.012
REACTOME_TRANSFERRIN_ENDOCYTOSIS_AND_RECYCLING	18	0.702	1.989	0.002	0.002	0.036
REACTOME_LATENT_INFECTION_OF_HOMO_SAPIENS_WITH_MYCOBACTERIUM_TUBERCULOSIS	17	0.715	1.981	0	0.002	0.04
REACTOME_TRIGLYCERIDE_BIOSYNTHESIS	34	0.600	1.959	0	0.003	0.053
REACTOME_NUCLEAR_RECEPTOR_TRANSCRIPTION_PATHWAY	33	0.593	1.913	0	0.005	0.1
REACTOME_TRANS_GOLGI_NETWORK_VESICLE_BUDDING	53	0.495	1.775	0	0.025	0.458
REACTOME_FATTY_ACYL_COA_BIOSYNTHESIS	15	0.637	1.702	0.004	0.050	0.752
REACTOME_SYNTHESIS_OF_PIPS_AT_THE_GOLGI_MEMBRANE	15	0.643	1.701	0.008	0.048	0.76

Appendix 6: Significantly up-regulated pathways from the merged dataset identified using GSEA and the KEGG biological pathways resource.

NAME	SIZE	ES	NES	NOM p-val	FDR q-val	FWER p-val
KEGG_LYSOSOME	106	0.679	2.735	0	0	0
KEGG_GLYCOSAMINOGLYCAN_DEGRADATION	18	0.722	2.026	0	0.003	0.008
KEGG_DRUG_METABOLISM_CYTOCHROME_P450	33	0.611	2.023	0.002	0.002	0.008
KEGG_METABOLISM_OF_XENOBIOTICS_BY_CYTOCHROME_P450	31	0.596	1.937	0	0.003	0.019
KEGG_SPHINGOLIPID_METABOLISM	30	0.573	1.791	0.002	0.017	0.127
KEGG_PPAR_SIGNALING_PATHWAY	43	0.503	1.729	0.004	0.028	0.233
KEGG_PENTOSE_PHOSPHATE_PATHWAY	20	0.592	1.717	0.002	0.027	0.261

Appendix 7: Selected significantly down-regulated pathways identified from the merged dataset using GSEA and the REACTOME biological pathways resource.

NAME	SIZE	ES	NES	NOM p-val	FDR q-val	FWER p-val
REACTOME_DNA_REPLICATION	182	-0.646	-3.012	0	0	0
REACTOME_MITOTIC_M_M_G1_PHASES	162	-0.639	-2.947	0	0	0
REACTOME_CELL_CYCLE_MITOTIC	300	-0.576	-2.888	0	0	0
REACTOME_MITOTIC_PROMETAPHASE	82	-0.704	-2.877	0	0	0
REACTOME_CELL_CYCLE	379	-0.553	-2.808	0	0	0
REACTOME_CHROMOSOME_MAINTENANCE	105	-0.625	-2.681	0	0	0
REACTOME_MUSCLE_CONTRACTION	33	-0.639	-2.223	0	5.94E-05	0.001
REACTOME_TRANSCRIPTION	190	-0.473	-2.221	0	1.19E-04	0.002
REACTOME_PROCESSING_OF_CAPPED_INTRON_CONTAINING_PRE_MRNA	134	-0.467	-2.084	0	5.33E-04	0.011
REACTOME_REGULATION_OF_MITOTIC_CELL_CYCLE	76	-0.506	-2.083	0	5.19E-04	0.011
REACTOME_TRANSPORT_OF_MATURE_TRANSCRIPT_TO_CYTOPLASM	51	-0.533	-2.004	0	0.002	0.043
REACTOME_SMOOTH_MUSCLE_CONTRACTION	23	-0.627	-1.979	0	0.002	0.057
REACTOME_MRNA_SPLICING	106	-0.458	-1.974	0	0.002	0.061
REACTOME_MITOTIC_G2_G2_M_PHASES	77	-0.481	-1.972	0	0.003	0.063
REACTOME_MRNA_PROCESSING	151	-0.425	-1.966	0	0.003	0.068
REACTOME_COLLAGEN_FORMATION	46	-0.513	-1.868	0	0.007	0.202
REACTOME_INTEGRIN_CELL_SURFACE_INTERACTIONS	61	-0.478	-1.858	0	0.008	0.218
REACTOME_GRB2_EVENTS_IN_ERBB2_SIGNALING	21	-0.594	-1.846	0.002	0.009	0.238
REACTOME_CLEAVAGE_OF_GROWING_TRANSCRIPT_IN_THE_TERMINATION_REGION_	42	-0.512	-1.820	0	0.011	0.307
REACTOME_FORMATION_OF_TUBULIN_FOLDING_INTERMEDIATES_BY_CCT_TRIC	17	-0.601	-1.753	0.002	0.020	0.512
REACTOME_DARPP_32_EVENTS	21	-0.574	-1.752	0.005	0.020	0.514
REACTOME_APC_C_CDH1_MEDIATED_DEGRADATION_OF_CDC20_AND_OTHER_APC_C_CDH1_TARGETED_PROTEINS_IN_LATE_MITOSIS_EARLY_G1	63	-0.440	-1.747	0.003	0.020	0.522
REACTOME_NCAM_SIGNALING_FOR_NEURITE_OUT_GROWTH	50	-0.466	-1.747	0.002	0.020	0.522
REACTOME_APOPTOTIC_EXECUTION_PHASE	46	-0.478	-1.746	0.005	0.020	0.523

REACTOME_CTLA4_INHIBITORY_SIGNALING	17	-0.608	-1.719	0.021	0.024	0.612
REACTOME_APC_CDC20_MEDIATED_DEGRADATION_OF_NEK2A	21	-0.563	-1.715	0.002	0.024	0.622
REACTOME_GLUCONEOGENESIS	23	-0.516	-1.651	0.016	0.039	0.828
REACTOME_HS_GAG_BIOSYNTHESIS	18	-0.542	-1.628	0.014	0.042	0.892
REACTOME_G_ALPHA_S_SIGNALLING_EVENTS	49	-0.430	-1.622	0.006	0.044	0.901
REACTOME_INTEGRIN_ALPHAIIB_BETA3_SIGNALING	21	-0.528	-1.613	0.020	0.046	0.913

Appendix 8: Significantly down-regulated signalling pathways identified from the merged dataset using GSEA and the KEGG biological pathways resource.

NAME	SIZE	ES	NES	NOM p-val	FDR q-val	FWER p-val
KEGG_SYSTEMIC_LUPUS_ERYTHEMATOSUS	81	-0.587	-2.443	0	0	0
KEGG_CELL_CYCLE	118	-0.549	-2.434	0	0	0
KEGG_DNA_REPLICATION	35	-0.679	-2.332	0	0	0
KEGG_OOCYTE_MEIOSIS	95	-0.554	-2.323	0	0	0
KEGG_HYPERTROPHIC_CARDIOMYOPATHY_HCM	59	-0.560	-2.158	0	0	0
KEGG_DILATED_CARDIOMYOPATHY	64	-0.528	-2.039	0	0.002	0.009
KEGG_PROGESTERONE_MEDIATED_OOCYTE_MATURATION	75	-0.491	-2.011	0	0.002	0.009
KEGG_WNT_SIGNALING_PATHWAY	116	-0.424	-1.880	0	0.009	0.049
KEGG_VIRAL_MYOCARDITIS	48	-0.492	-1.863	0	0.010	0.059
KEGG_HOMOLOGOUS_RECOMBINATION	27	-0.544	-1.801	0.005	0.017	0.105
KEGG_ARRHYTHMOGENIC_RIGHT_VENTRICULAR_CARDIOMYOPATHY_ARVC	54	-0.477	-1.793	0	0.016	0.114
KEGG_LONG_TERM_POTENTIATION	50	-0.476	-1.786	0.002	0.016	0.124
KEGG_MISMATCH_REPAIR	22	-0.580	-1.780	0.004	0.016	0.133
KEGG_REGULATION_OF_ACTIN_CYTOSKELETON	156	-0.388	-1.776	0	0.015	0.138
KEGG_ACUTE_MYELOID_LEUKEMIA	50	-0.468	-1.750	0	0.020	0.187
KEGG_ECM_RECEPTOR_INTERACTION	64	-0.438	-1.723	0	0.024	0.228
KEGG_RENAL_CELL_CARCINOMA	64	-0.438	-1.720	0	0.023	0.24
KEGG_ENDOMETRIAL_CANCER	46	-0.463	-1.709	0.007	0.023	0.25
KEGG_TIGHT_JUNCTION	91	-0.394	-1.665	0.003	0.032	0.341
KEGG_CELL_ADHESION_MOLECULES_CAMS	69	-0.415	-1.659	0.005	0.033	0.361
KEGG_PATHOGENIC_ESCHERICHIA_COLI_INFECTION	46	-0.450	-1.655	0.007	0.032	0.371
KEGG_HEDGEHOG_SIGNALING_PATHWAY	33	-0.477	-1.631	0.003	0.038	0.439
KEGG_MELANOGENESIS	71	-0.400	-1.628	0.003	0.037	0.445
KEGG_FOCAL_ADHESION	164	-0.358	-1.627	0	0.036	0.447
KEGG_VASCULAR_SMOOTH_MUSCLE_CONTRACTION	80	-0.397	-1.622	0	0.036	0.463
KEGG_SPLICEOSOME	124	-0.371	-1.619	0	0.036	0.476
KEGG_BASE_EXCISION_REPAIR	33	-0.469	-1.587	0.013	0.044	0.549
KEGG_ADHERENS_JUNCTION	66	-0.395	-1.576	0.010	0.047	0.579
KEGG_P53_SIGNALING_PATHWAY	60	-0.398	-1.567	0.005	0.048	0.597

Appendix 9: Cholesterol biosynthesis pathway from zymosterol